UNIVERSITY OF LIVERPOOL

Intraocular Lenses and Their Potential to Prohibit Posterior Capsule Opacification

Thesis submitted in accordance with the requirements of the University of Liverpool for the degree of Doctor in Philosophy

By

Rebecca Lace

March 2013

Acknowledgments

This work was financially supported by EPSRC and BioInteractions Ltd. case studentship.

Firstly I would like to thank my supervisors Rachel Williams and Carl Sheridan. Rachel, for your wide knowledge and understanding of biomaterials and for putting up with all my “Becky-isms”, and Carl for your expertise within ophthalmology and cell biology. Thank you both for your support, encouragement and friendship over the past four years, it has been immeasurable and I could not have done this without you both.

I would like to thank all those at BioInteractions Ltd. for providing the materials for this PhD project, their much appreciated time and technical expertise with this project. Special thanks to Simon Onis for demonstrating material coating techniques, Fanny Raisin-Dadre for her zwitterionic materials, along with Alan Rhodes, and Ajay Luthra for their technical support. Additionally I would like to thank Dr John Reddan for providing FHL124 and N/N1003A lens epithelial cell lines, and Dr Barbara Pierscionek for providing B3 lens epithelial cell line.

Thank you to all my colleges within Eye and Vision Science, for your scientific advice, answering my many “stupid questions”, moral support, and generally making this PhD very enjoyable. This would have been a lot harder without you.

Special thanks to: Stuart Marshall-Clarke for his assistance with flow cytometry, Kyle Doherty for teaching me contact angle analysis and proof reading many drafts of my thesis, Sandra Fawcett for training me on the scanning electron microscope, Dan Jones for instruction with white light interferometry. Victoria Kearns for her much appreciated scientific guidance and putting up with my constant barrage of questions and Rosalind Stewart for demonstrating dissection techniques.

Finally thank you to my Mum, Dad, James, Fran and my beautiful little niece, Allegra, for your endless love, encouragement and for believing in me through all these years of study.

Outputs

Academic Conferences

1. Oral presentation at UK Society for Biomaterials, Glasgow, July 2010.
2. Oral presentation at UK Society for Biomaterials, London, June 2011.
3. Oral presentation at Postgraduate Researchers in Science & Medicine, Liverpool, July 2011.
4. Poster presentation at the 24th European Society for Biomaterials, Dublin, September 2011.
5. Poster presentation at Surface Science of Biologically Important Interfaces, Liverpool, October 2011.
6. Oral presentation at 1st Biofuture - young European biomaterial scientists, Ghent, November 2011.
7. Oral Presentation at Roy Mapstone Research, Liverpool, November 2011 (3rd place).
8. Poster presentation at International Society for Eye Research, Berlin, July 2012.

Scheduled papers

1. Zwitterionic coating chapter 2.5 – Can the ratio of zwitterionic:monomer polymer control lens epithelial cell attachment?
2. Dedifferentiation model chapter 2.6 – Transforming Growth Factor beta 2 and 3 and their role in lens epithelial cell dedifferentiation

Abstract

Cataracts are the commonest cause of preventable blindness in the world. During surgery the natural lens is replaced with a polymeric intraocular lens (IOL), leaving the capsular bag in situ. The most common postoperative complication is scarring which is known as posterior capsule opacification (PCO). PCO occurs when residual lens epithelial cells (LECs) dedifferentiate and migrate onto the previously cell free posterior capsule. By modifying the IOL surface properties we can manipulate the cellular response. BioInteractions Ltd. is an innovative supplier of biomaterials, which aim to minimise, the host response, and provided the materials for this study. The aim of this study was to evaluate potential IOL coatings to reduce PCO. This can either be achieved by enabling a monolayer of LECs to attach to the posterior surface of the IOL, thus sandwiching the IOL to the capsular bag, or prohibiting cell attachment to the IOL entirely.

Materials and Methods

Various coatings were investigated incorporating: functional groups of poly ethylene glycol (PEG), sulphates, sulfonates, glycosaminoglycans (Heparin, (HEP) hyaluronic aid, (HA) and chondroitin sulphate (CS)) and zwitterionic monomers (10-30%). Ways to prevent dedifferentiation was also evaluated. LECs were seeded onto all coatings and monitored for a period of 7 – 14 days in cell culture. LECs were examined morphologically, cell nuclei were counted and growth curves were plotted. Water contact angle (CA) measurements were taken to measure the wettability of the coatings. Scanning electron microscope (SEM) analysis was performed to examine the topography of the coating. White light interferometry (WLI) analysis was conducted to analysis the surface roughness. Dedifferentiation of LECs and the use of TGFβ3 to neutralise or prevent dedifferentiation were also investigated.

Results and Discussions

Coatings with a greater number of water-based layers were the most hydrophilic, and did not offer the appropriate cell binding sites required to promote cell attachment. In general, little cell attachment was observed on HEP and HA coatings provided by

BioInteractions Ltd., cell attachment varied on CS coatings provided by BioInteractions Ltd. When HA and CS were covalently bound onto amine coated coverslips a reduction in cell attachment was observed. The LEC response varied across different ratios of zwitterionic monomer within the coatings. Zwitterionic coatings were not cytotoxic to LECs and surface analysis demonstrated no clear link between wettability and roughness compared to cell attachment. Addition of transforming growth factor beta 2 (TGFβ2) was chosen as a successful dedifferentiation model. Addition of TGFβ3 had little influence at reversing dedifferentiation however it may offer some protection against differentiation. PCR analysis showed a change in regulation of collagens, integrins, matrix metallopeptidase and fibronectin 1 genes, when LECs were incubated with TGFβ2, TGFβ3 or untreated (control LECs). These genes may play important roles in PCO.

Conclusions

Incorporation of functional groups influenced the cellular response, however the coatings with more water-based layers prohibit cell attachment. The cellular response varied depending on GAG type and the conformation of GAG on the surface coating. HA and CS bound to amine-coated coverslips prohibited cell attachment at higher concentrations, indicating their potential to prohibit LEC attachment. There was no clear link between wettability and cell attachment on the novel zwitterionic coatings. The ratio of zwitterionic-component:arylic-based monomer(s) influenced cell attachment. TGFβ2 successfully dedifferentiated LECs. Further work is required to understand the influence of TGFβ3 on dedifferentiation.

Contents

List of Figures

Chapter 1: Introduction

List of Tables

Glossary

αSMA – Alpha Smooth Muscle Actin

AC – Anterior Chamber

APTES – 3-aminopropyl-triethoxysilane

B3 – Human Lens Epithelial Cell Line

BSA – Bovine Serum Albumin

C4S – Chondroitin-4-Sulfate

C6S – Chondroitin-6-Sulfate

CA – Contact Angle

CCC – Continuous Curvilinear Capsulorhexis

CDI – 1,1'Carbonyldiimidazole

cDNA – Complimentary Deoxyribonucleic Acid

CK – Cytokeratin

CS – Chondroitin Sulphate

DAPI – 4',6-Diamidino-2-phenylindole Dihydrochloride

DCI – Direct Covalent Immobilisation

DMSO – Dimethyl Sulphoxide

DS – Dematin Sulphate

DSC – N,N'-disuccinimidyl Carbonate

ECM – Extracellular Matrix

EDC – 1-ethyl-3-(3-dimethylaminopropyl) Carbodiimide

EDTA – Ethylenediaminetetraacetic Acid

FCS – Fetal Calf Serum

FHL124 – Human Lens Epithelial Cell Line

FN1 – Fibronectin-1

GAG – Glycosaminoglycans

HA – Hyaluronic Acid

HCASM – Human Coronary Artery Smooth Muscle cells

HEP – Heparin

ICB – Immobilisation (followed by) Covalent Binding

ICCE – Intracapsular Cataract Extraction

IOL – Intraocular Lens

ISO – International Organisation for Standardisation

L-Glut – L-Glutamine

LAM – Laminin

LEC – Lens Epithelial Cells

LTBP – Latent TGFβ Binding Protein

MEME – Minimum Essential Medium Eagles

MES – 2-(N-morpholino)ethanesulfonic Acid

MMP – Matrix Metallopeptidase

MPC – Methacryloyloxyethyl Phosphorylcholine

MSC – Mesenchymal Stem Cell

N/N1003A – Rabbit Lens Epithelial Cell Line

NBF – Neutral Buffered Formaldehyde

Nd:YAG – Neodymium-Doped Yttrium Aluminium Garnet

NHS – N-hydroxysuccinimide

PBS – Phosphate Buffered Saline

PC – Posterior Chamber

PCO – Posterior Capsule Opacification

PCR – Polymerase Chain Reaction

PDMS – Poly Dimethyl Siloxane

PEG – Polyethylene Glycol

PEI – Polyethylenimine

PEA – Phenylethyl Acrylate

PEG – Polyethylene Gylcol

PEMA – Phenylethyl Methacrylate

Pen Strep – Penicillin Streptomycin

pHEMA – Poly 2-Hydroxyethyl Methacrylate

PI – Propidium Iodide

PMMA – Poly Methyl Methacrylate

PPI – Polypropyleneimine

PPPD – Poly P-Phenylenediamine

PPy – Polypyrrole

PS – Polystyrene

RNA – Ribonucleic Acid

RNase – Ribonuclease

RPM – Revolutions Per/Minute

RS – Rabbit Serum

SAM – Self-Assembled Monolayer

SD – Standard Deviation

SEM – Scanning Electron Microscope

TβR-I – Type 1 TGFβ Receptor

TβR-II – Type 2 TGFβ Receptor

TCPS – Tissue Culture Polystyrene

TGFβ – Transforming Growth Factor Beta

WHO – World Health Organisation

WLI – White Light Interferometry

%w/w – Percentage Weight/Weight

% w/v – Percentage Weight/Volume

1.Introduction

This thesis is concerned with synthetic materials designed to replace the natural lens in the human eye. This is a cross-disciplinary research area requiring an understanding of materials and medical devices, the anatomy and properties of the tissues of the eye and the interactions at the material/biological environment interface.

1.1 Biomaterials

A biomaterial can be defined as, “Any substance, other than a drug, or combination of substances, synthetic or natural in origin, which can be used for any period of time, as a whole or as a part of a system which treats, augments, or replaces any tissue, organ or function of the body.” [1]

Biomaterials are used as part of medical devices and implants throughout the body, for example, hip joint replacements, heart valves replacements, vascular stent implants and ocular implants. Within the eye there are a vast number of biomaterials being used to regain or enhance vision and combat degenerative diseases associated with vision loss [2]. For these devices and implants to perform to their best they need to be biocompatible. Biocompatibility refers to, ”A material that does not lead to an acute or chronic inflammatory response and that does not prevent a proper differentiation of implant-surrounding tissue.” [1]

For implantable devices there will inevitably be some tissue reaction due to the surgery, however a biomaterial with a good biocompatibility should not elicit an adverse biological response. Key to controlling the biocompatibility of a material or device is understanding the cell surface interactions.

1.2 Cell Surface Interactions

Cell/surface interactions can be broken up into two areas, firstly proteins binding to the surface and secondary cells binding to the proteins.

When a material is implanted into the biological environment proteins (long sequences of amino acids) rapidly interact with that implant surface and will, most often, adsorb onto the surface [3-6]. Protein adsorption occurs within seconds to minutes, long before any cells arrive and settle on the surface [7]. The multitude of proteins in the biological environment competes for surface binding. This was first described by Vroman and is known as the Vroman effect. Vroman outlined that initial protein adhesion is firstly mediated by highly mobile smaller proteins, generally derived from plasma. Proteins then compete to bind to the surface and these smaller proteins are replaced by larger proteins. As the proteins adsorb to the surface conformational changes within the protein occur which result in the formation of a strong bond to the surface [8]. This adsorbed protein layer can be influenced by the surface properties of the material such as surface charge, chemistry, wettability and roughness. The cellular response to this surface, in terms of cellular attachment, proliferation, morphology and phenotypic changes, is then dependent on this folding and unfolding of proteins at the interface of an implant and the biological environment, and the interfacial forces between the two [3, 6, 9-11].

Cells bind to these proteins via specific cell surface receptors, particularly integrins [7, 12-13] (Figure 1.1). Integrin binding will only occur if the adsorbed protein layer displays the correct amino acid sequences [6-7]. Since the conformation of the adsorbed protein is directly influenced by the implant surface properties different surfaces may result in variations in protein conformation and thus different cellular responses [4, 7, 14-16]. One of the major integrins to support cells binding is α5β1, fibronectin receptor. Underwood et al demonstrated fibronectin confirmation differences between tissue culture treated polystyrene and untreated polystyrene. Treated polystyrene displayed a greater number of the arginine-glycine-aspartic acid (RGD) binding sites compared to untreated polystyrene [15]. Grinnell et al previously reported similar results with tissue culture treated polystyrene and bacteriological polystyrene. Although radiolabelling

showed there was more fibronectin binding to bacteriological polystyrene than treated polystyrene, there was more anti-fibronectin antibody on treated polystyrene, suggesting different fibronectin confirmation on each surface. Fibronectin confirmation on treated polystyrene provided binding sites enabling cellular spreading [14].

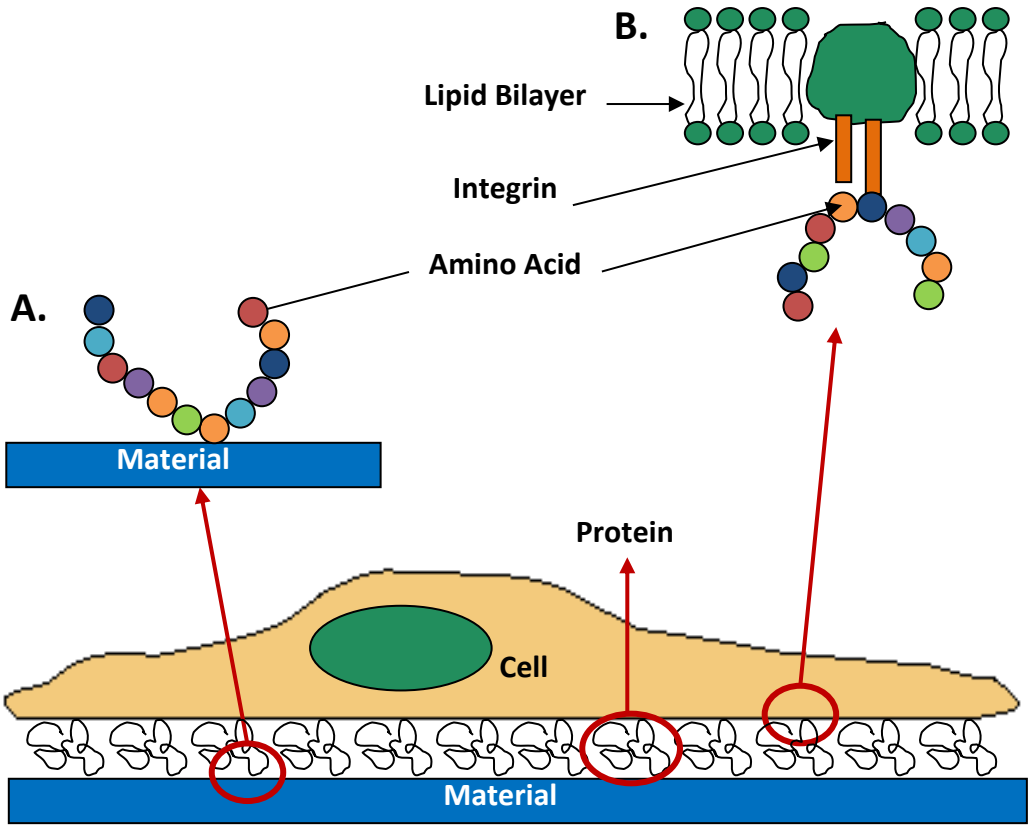

Figure 1.1: Schematic of the cell/surface interface and binding of a cell to the protein adlayer. A. Proteins adsorbed onto the surface of an implant. B. Integrin binding point. This will only occur if the correct amino acids sequence is presented to the integrin by the protein conformation. Adapted from personal communications with R.L.Williams.

These cell-surface interactions are complex and the surface properties can alter this response, this is explained in more detail throughout this chapter in the context of replacement lenses.

1.3 Anatomy of the Eye

The eye is split up into two compartments, the anterior chamber (from the lens to the cornea) which houses the aqueous humour, and the posterior segment (from the lens to the back of the eye) which houses the vitreous humour (Figure 1.2). The clear anterior surface of the eye is known as the cornea and the white of the eye is called the sclera. Light enters the eye through the cornea, which contributes to approximately 70% of the total refractive power of the eye [17]. Behind the cornea sits the coloured iris and the opening known as the pupil. Light is then refracted through the aqueous and the pupil until it meets the lens. The lens is responsible for fine focusing of light onto the retina (discussed further in section 1.6). Light continues through the vitreous and an image is formed on the retinal photoreceptors at the back of the eye. The optic nerve carries this information to the brain allowing us to see the image formed on the back of the eye [2, 18-20].

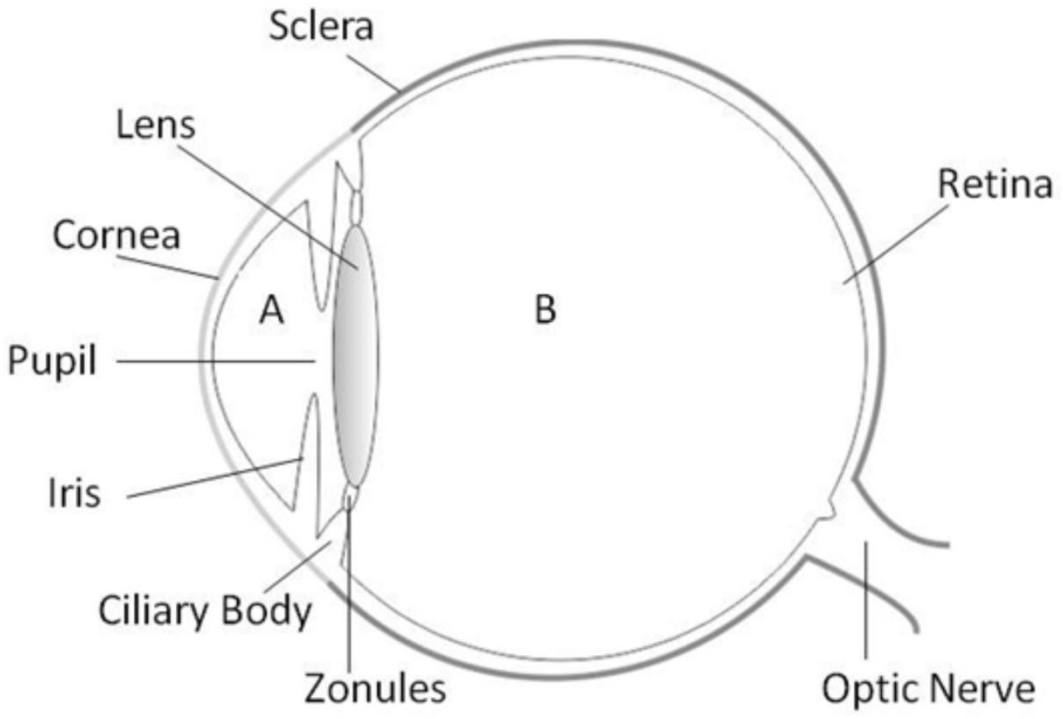

Figure 1.2: Schematic of the anatomy of the eye. Light enters the eye through the transparent anterior surface, known as the cornea. The white tissue at the periphery is known as the sclera. Light is refracted by the cornea through the aqueous humour (A) in the anterior segment. It continues through the coloured iris and the pupil until it meets the lens. Light then travels through the vitreous (B) until it reaches the retina at the back of the eye. Adapted from V.Kearns et al [21]

1.4 Anatomy of the Lens

The lens comprises of a collagen-like glycoprotein capsular bag. This collagen membrane encases the lens and is attached to the ciliary muscle via fibres called the zonules (Figure 1.3), enabling accommodation (1.6). The anterior diameter is three times the size of the anterior–posterior thickness and the anterior surface is always less curved than the posterior side. The front and back intersections are termed the poles and the edge rim is called the equator. In the developed undisturbed lens, lens epithelial cells (LECs) are arranged in a single cuboidal monolayer, and are confined to the anterior surface of the capsule bag. Mitosis of LECs occurs at the equator region where lens fibres are formed (Figure 1.3) [20, 22-23].

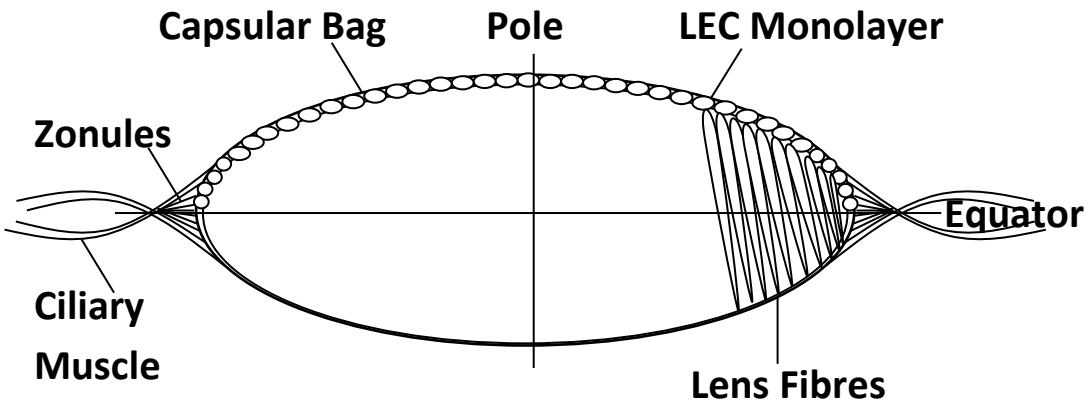

Figure 1.3: Schematic of a cross-section of the lens. The outer membrane is called the capsular bag. LECs reside on the inner anterior surface of this capsular bag and are arranged in a single cuboidal monolayer. Beneath these cells lie the lens fibres. Mitosis of LECs and fibres occurs at the equator region. Zonules are attached to the equator area of the lens and in turn are attached to the ciliary muscle, both are responsible for accommodation.

1.5 Development of the Lens

At the 4mm embryo stage in humans the lens placode is formed from the surface ectoderm, which is in direct contact with the neural ectoderm, which forms the optical vesicle. At this stage the optical vesicle is formed from a single layer of cuboidal cells. At the 5mm embryo stage invagination of the lens placode occurs to form the lens pit, the optical vesicle also invaginates to form the optical cup. By the 9mm embryo stage the lens placode has further invaginated inside the optic cup and finally separates from the surface ectoderm. After separation from the surface ectoderm the lens appears as a hollow sphere approximately 0.2mm in diameter, with a single layer of columnar cells outlining the wall. A basal wall envelops the vesicle and a thin basal lamina is synthesised that thickens to form the lens capsule.

Between the 10mm – 13mm embryo stages the lens changes from circular to an oval-like shape. Differentiation of the columnar cells on the posterior surface of the lens capsule also takes place. Cells elongate to form the first lens fibres with their nuclei nearer the anterior surface. At this point fibres are straightest and longest at the poles, they decrease in length at the equatorial region where they merge into the cuboidal cells of the anterior wall. These original fibres move towards the centre with time and are known as the nucleus. All new fibre cells are produced from the equator region and encapsulate the nucleus (original fibres), which become known as the cortex (Figure 1.4). When a cell at the equator region slowly differentiates into a fibre it elongates with the anterior stretching towards the anterior epithelium and posterior towards the posterior wall [18-19, 24-26].

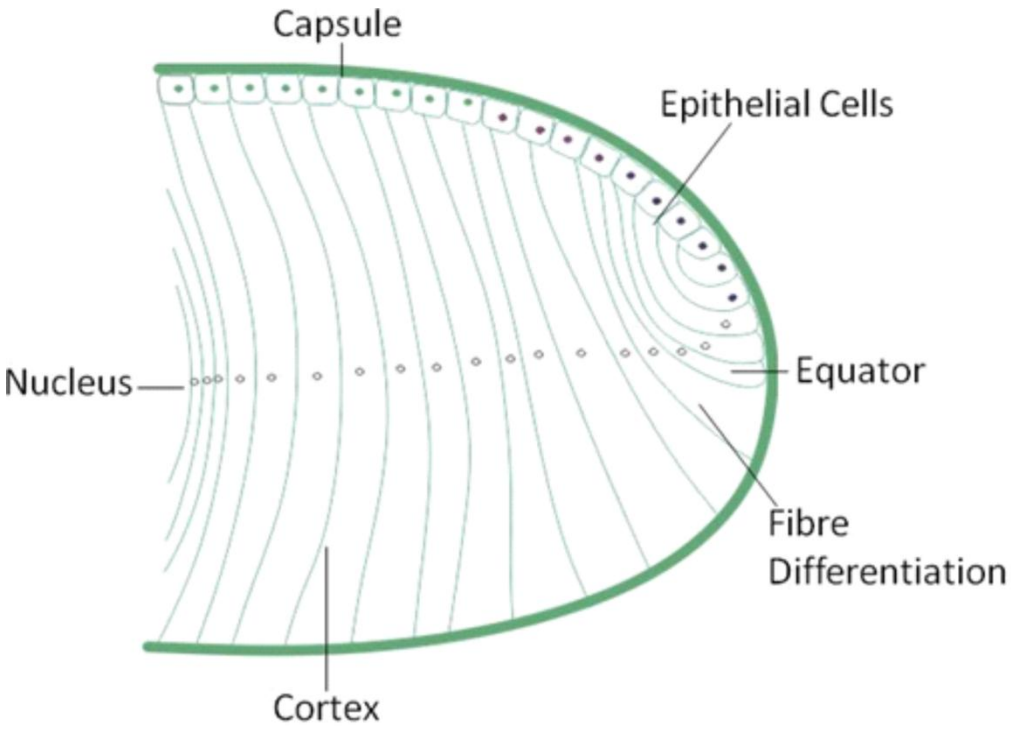

Figure 1.4: Schematic of the development of the lens fibres. A new lens cell at the equator slowly differentiates into a fibre and elongates with the anterior stretching towards the anterior epithelium and posterior towards the posterior wall until it eventually encapsulates the cortex. Adapted from V.Kearns et al [21]

This process continues throughout life meaning the lens grows with age and older fibres become compacted towards the centre, losing their nuclei (Figure 1.5). The central nucleus region becomes sclerosed and less transparent with age [18-19, 24].

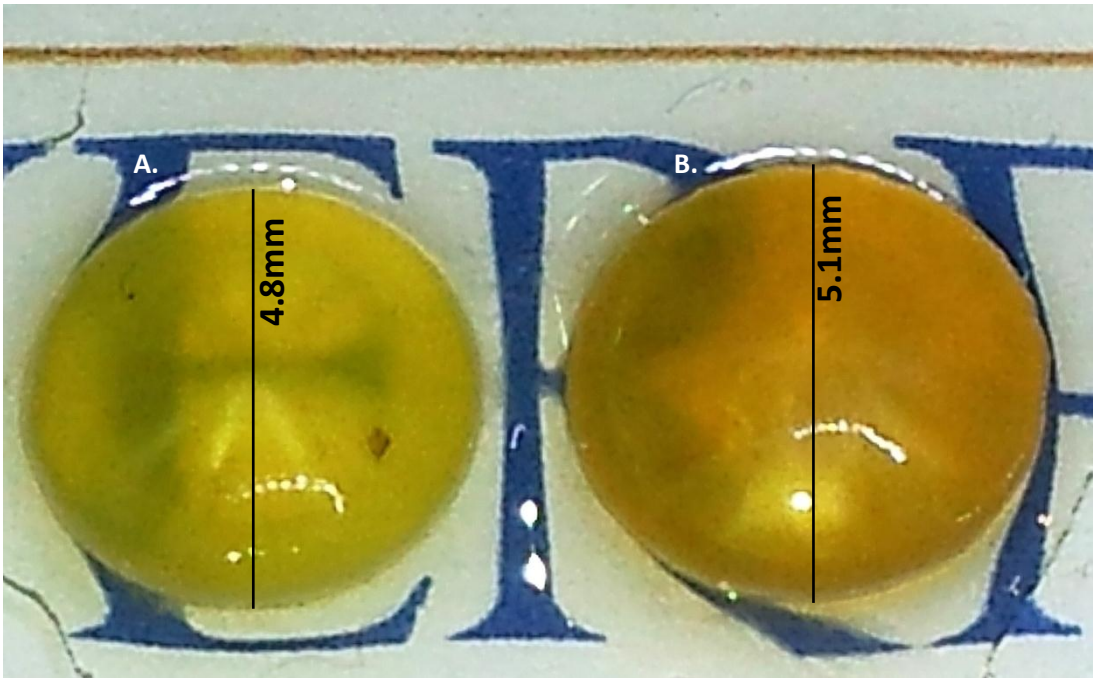

Figure 1.5: Photograph demonstrating age related differences in lenses. A. Young lens donor – Lens is smaller, more transparent and paler in colour when compared to an older lens. B. Older lens donor – Lens is bigger, less transparent and darker in colour, due to the natural aging process of the lens.

There are some physiological differences in the lens between men and women, for example a man's lens is heavier. Women seem to be less prone to cataracts (1.7) below the age of fifty compared to men, however this is reversed above the age of fifty suggesting some hormonal influence [27].

1.6 Accommodation and Disaccommodation

Objects at different distances can be focused onto the retina by changing the refractive power of the eye. To do this the geometry of the lens changes, either by increasing or decreasing its angle of curvature, known as accommodation or disaccommodation respectively. The ciliary muscle plays a key role in this process. It is attached anteriorly

to the sclera spur and posteriorly to the choroid. As previously mentioned the ciliary muscle is attached to the lens capsule via the zonules [20, 28-29].

1.6.1 Accommodation

To focus on a near object the ciliary muscle contracts, moving forward and inward. This means the zonules relax and the lens becomes more spherical. This thickens the lens axially and narrows it equatorially. Both the anterior and posterior surfaces increase in curvature, with the posterior still remaining steepest. The posterior surface is prevented from moving backwards due to the vitreous humour. The anterior surface moves forward towards the cornea. These changes contribute to increasing the refractive power of the eye (Figure 1.6) [20, 28-30].

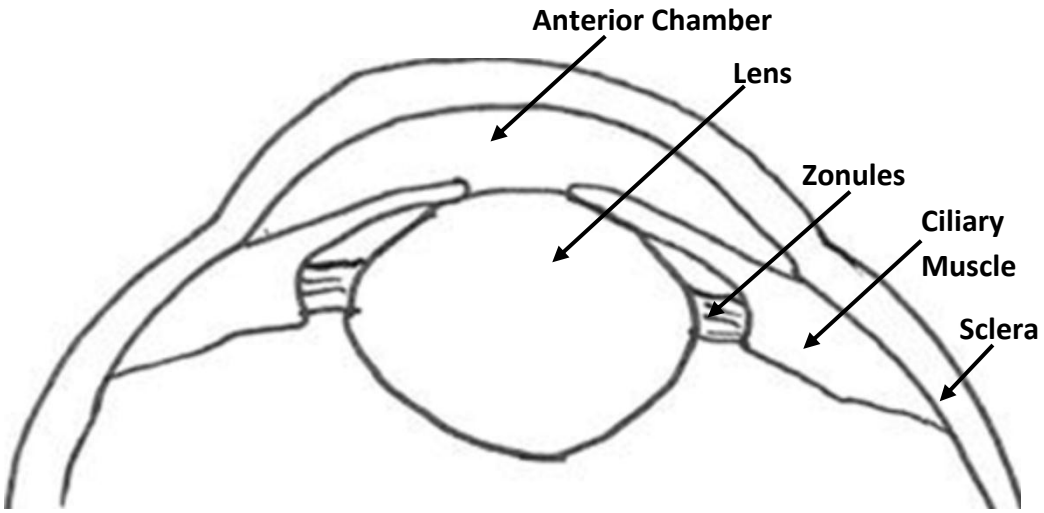

Figure 1.6: Schematic detailing the process of accommodation. The ciliary muscle contracts moving forward and inward, meaning the zonules are relaxed and the lens becomes more spherical. The anterior chamber decreases and images close up are brought into focus.

1.6.2 Disaccommodation

To focus on an object in the distance the sequence is reversed, and the ciliary muscle relaxes. The tissue to which the ciliary muscle is anchored to pulls the ciliary muscle posteriorly and outward, flattening the ciliary muscle along the scleral surface. This

means the zonules are in tension which in turn stretches and flattens the natural lens, reducing its curvature. The posterior surface remains fixed and the anterior surface retracts from the cornea. These changes contribute to decreasing the refractive power of the eye (Figure 1.7) [20, 28-30].

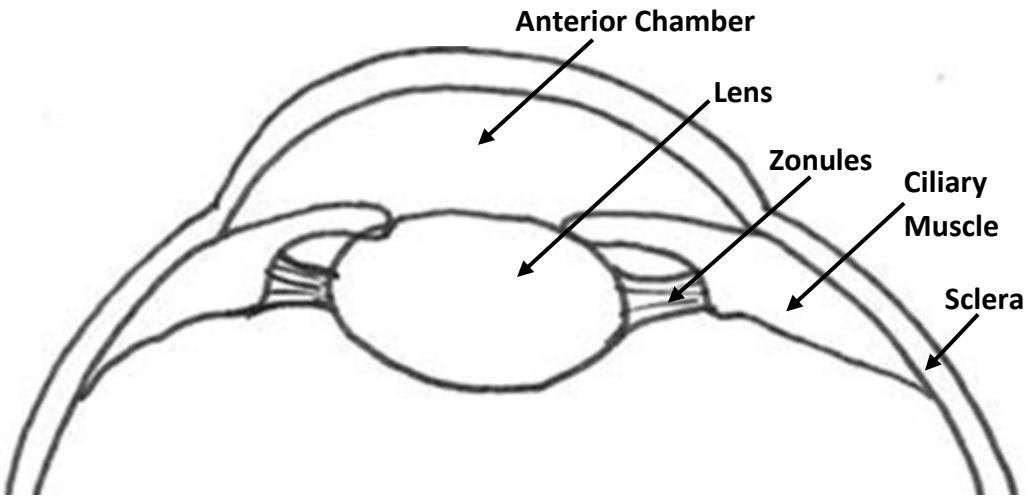

Figure 1.7: Schematic detailing the process of disaccommodation. The tissue area to which the ciliary muscle is anchored to pulls the muscle posteriorly and outward, flattening the ciliary along the sclera, meaning the zonules are in tension which in turn stretches and flattens the lens. The anterior chamber increases and images far away are brought into focus.

1.6.3 Changes with Age

The ability to change the refractive power of the natural lens by accommodation gradually diminishes with age [18-19]. This process starts to occur from as early as the second decade of life. Meaning objects must be held further away from the eye to be clearly visualised. This degradation is known as presbyopia, which means "old eye". Whilst the true reason behind this is not fully understood, several reasons have been put forward which are believed to contribute to the degeneration process. Such as alterations in the elasticity of the Bruch's membrane becoming more rigid with age, meaning the ciliary muscle cannot move forward properly when it contracts. Another proposed reason for presbyopia is that the curvature of the lens increases with age, which decreases the anterior chamber space. The lens nucleus also hardens with age.

In addition the vitreous loses its viscous properties becoming more liquid-like affecting the compression abilities it has on the posterior surface of the lens, thus allowing the lens to move posteriorly when the ciliary contracts. All of these factors have been attributed to presbyopia [18-19, 24, 30].

1.7 Cataracts

A cataract is characterised by opacification of the natural lens (Figure 1.8), which if left untreated can lead to blindness. Our most dominant sense is considered to be our vision, therefore the loss of sight can be very debilitating [31]. There are many factors that have been associated with the risk of developing cataracts, such as: UV radiation [32], smoking [33], alcohol [34], diet and diabetes [35]. Cataracts can also be congenital, caused by trauma or old age. Senile cataracts are a natural ageing process of the crystalline lens [36], and result from a change in structure of the proteins [18, 23, 28, 37-38]. The lens fibres are full of proteins and approximately one third of the lenses weight is accounted for by these proteins. One of the major proteins present within the lens is alpha crystallin, which gives the lens its clarity and refractive power [39]. These proteins, some of which are insoluble, increase in size and molecular weight with age and can aggregate together. The lens loses transparency with age as a result of these insoluble protein aggregates, increasing light scatter and glare, leading to cataract formation [20, 38, 40].

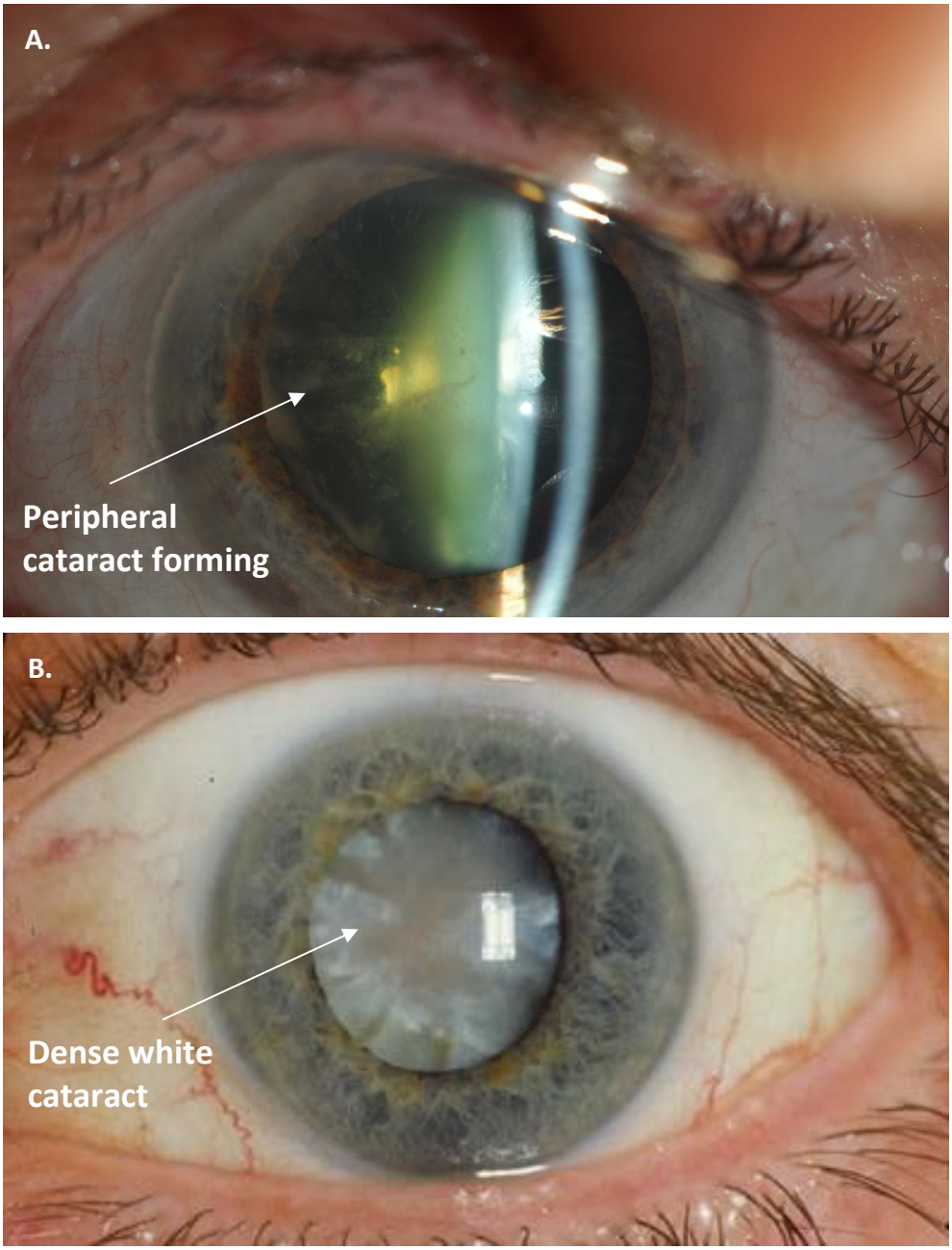

Figure 1.8: Micrographs demonstrating age related cataracts in patients whose pupils have been dilated. A. Photograph of a cataract viewed via a slit lamp in a patient at the Royal Liverpool Hospital just before theatre, their pupil has been dilated and clouding on the left-hand side of the pupil can be observed where the light is shining in. B. Photograph of a denser age-related cataract, again the patient's pupil has been dilated. In the NHS cataracts are removed much earlier (photograph A) than this late stage. National Eye Institute Reference#EDA13 [41]

Cataracts are the leading cause of preventable blindness worldwide (Figure 1.9). The most common form of cataracts is the senile cataract, which greatly reduces the quality of the patient's life. In 2000 Minassian et al constructed a model to calculate the current cataract rates and predict the backlog of cataract operations. The backlog of vision impairing cataracts was predicted at 2.36 million in England and Wales (aged 65 and older) [42]. Across the world there are an estimated 20 million people affected by cataract related blindness. The World Health Organisation (WHO) has launched a campaign, Vision 2020, to eliminate avoidable blindness. This aims to increase the volume of cataract surgery to 32 million per annum globally by 2020 [43].

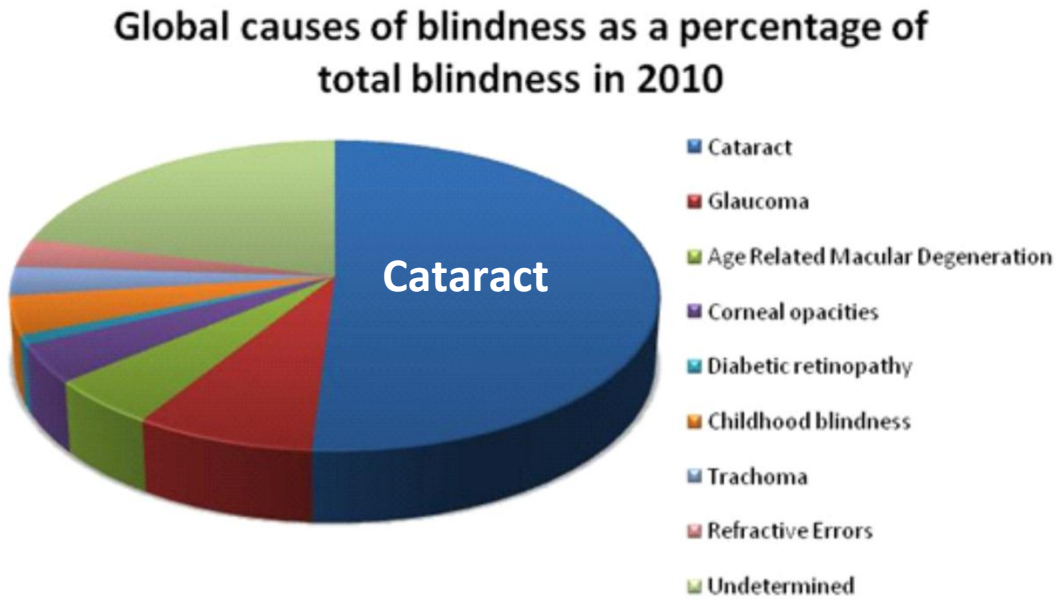

Figure 1.9: Pie-chart to demonstrate disease related blindness as a percentage of total blindness in 2002. Cataracts are the leading cause of preventable blindness worldwide, and this number is only due to increase by the year 2020, with 51% of total blindness being attributed to cataracts. Information taken from World Health Organisation – "Global data on visual impairments 2010" [44].

1.7.1 Surgical Treatment

Cataracts are treatable with a simple ophthalmic operation known as cataract surgery. In brief the cataractous lens is removed and replaced with a synthetic polymer lens to regain vision, known as an intraocular lens (IOL) (Figure 1.10). IOL's are made from a variety of materials and differ in terms of shape and design (1.9.3).

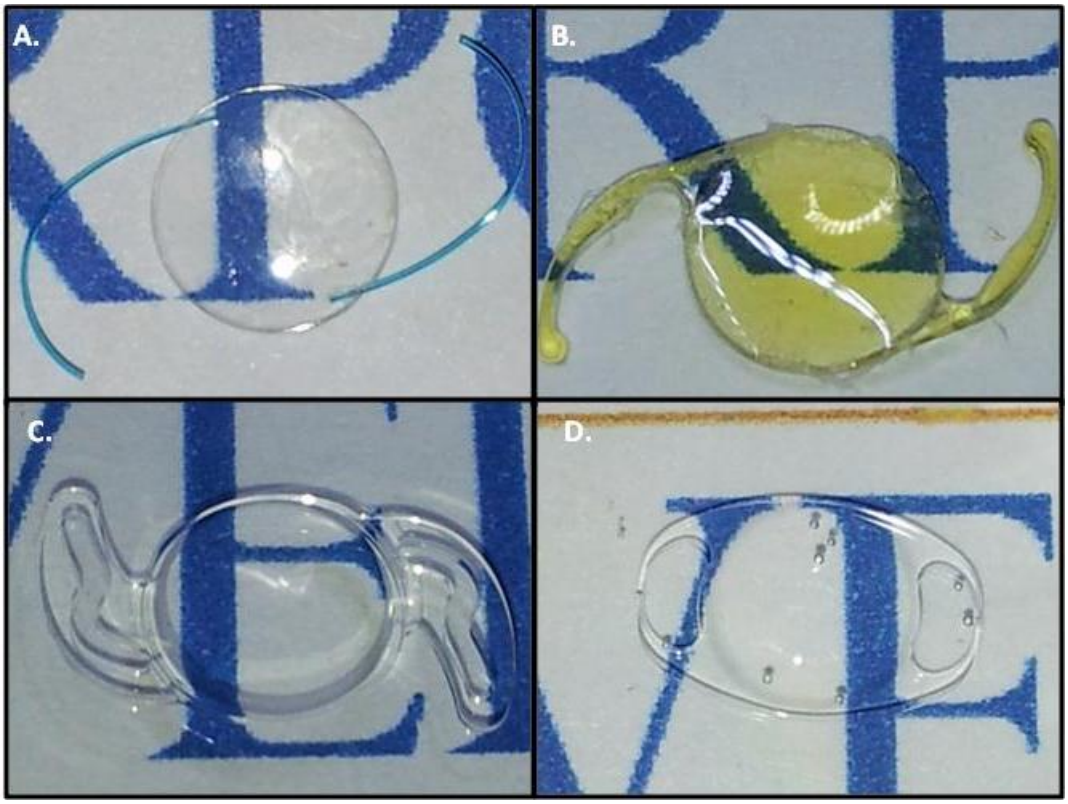

Figure 1.10: Micrographs demonstrating four types of IOL designs. IOLs vary in terms of the material, IOL shape and haptic design. A. Acrysof® IOL, B. Acrysof® IOL with UV filter, C. Rayner C-Flex® IOL and D. Artisan anterior chamber IOL.

In the developed world this surgery is performed at an earlier stage before total blindness occurs. Whereas in developing countries surgery is performed at a far later stage if resources are available. Cataract surgery is performed on an outpatient basis and takes approximately 30 minutes. It is the most commonly performed ophthalmic procedure worldwide, meaning the healthcare budget to manage this condition is significant [42, 45-47].

In cataract surgery a small incision, of approximately 3 mm, is first made in the limbal region of the eye, where the clear cornea meets the white sclera (Figure 1.11-A). This small incision allows for rapid visual recovery and minimises surgical induced astigmatism. A continuous circular capsulorhexis (CCC) is then made in the anterior capsule, allowing the surgeon access to the lens fibres. The opaque natural lens is disintegrated by phacoemulsification which uses ultrasonic waves to break up the lens matter (Figure 1.11-B). Lens fibres are removed by irrigation/aspiration leaving the capsular bag in situ, which is made up of all of the posterior capsule and most of the anterior capsule. A polymer IOL, (Figure 1.11-C) is then folded and implanted through the capsulorhexis. The IOL slowly unfolds within the capsular bag (Figure 1.11-D). The arms of the IOL, known as haptics, secure the IOL in place and allow vision to be restored [2, 25, 48]. An injected viscoelastic material aids the cataract extraction method by protecting the endothelial inner surface of the cornea, increasing the depth of the anterior chamber allowing room for instruments, and absorbing ultrasound energy [2].

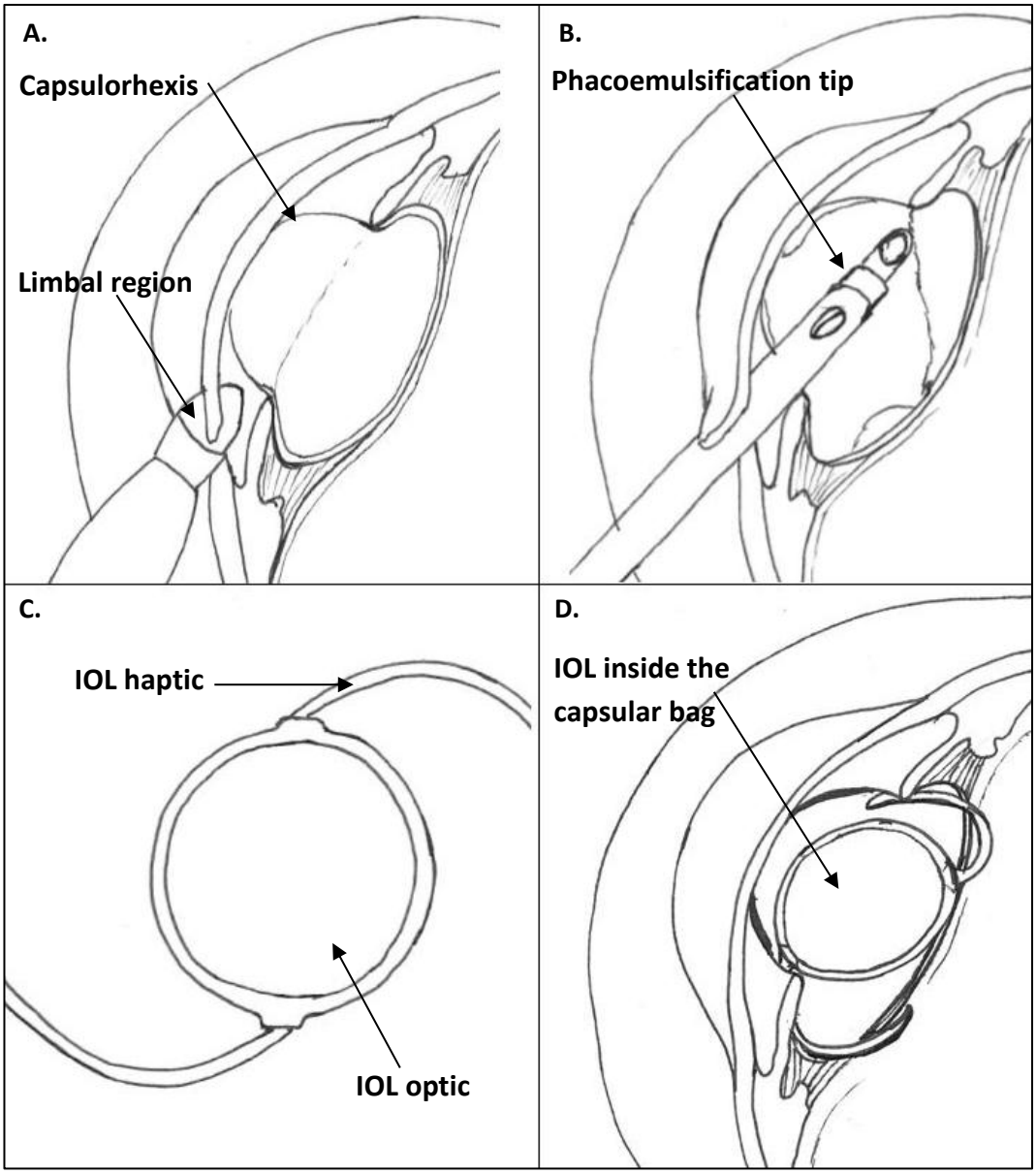

Figure 1.11: Schematic demonstrating the process of cataract removal and implantation of an IOL. A. Small incision is made in the limbal region, where the clear cornea meets the white sclera. B. Removal of the cataract by phacoemulsification, C. Polymer IOL and D. IOL unfolded inside the capsular bag to restore vision. Adapted from Healthwise Inc [49].

Prior to the use of IOLs the whole cataractous lens was removed and nothing was inserted inside the eye, therefore thick glasses were required to attempt to correct vision. Sir Harold Ridley was the first person to implant an IOL (the Ridley IOL) made from poly methyl methacrylate (PMMA), in 1950. This material was selected based on observations of pilots during World War II who got pieces of the canopy (made from

PMMA) lodged into their eye. This seemed to cause little inflammatory response and was transparent, therefore was chosen as the first IOL material. Originally the whole lens and capsular bag were removed known as intracapsular cataract extraction (ICCE), a PMMA anterior chamber (AC) fixed IOL was then implanted. Since then the surgical procedure has evolved and improved (1.9.1) [30].

The Ridley IOL was very bulky and mechanically difficult to fixate in the eye, and was eventually discontinued. This led to an influx of improvements to the PMMA IOL suggested by other surgeons at the time. PMMA remained the dominant material choice until the 1990's, when advancements in materials meant foldable IOLs emerged (Figure 1.12). These materials can be grouped into three groups, hydrophilic acrylate (predominantly poly hydroxyethyl methacrylate, pHEMA) hydrophobic acrylate (phenylethyl methacrylate PEMA and phenylethyl acrylate PEA) and silicone (poly dimethyl siloxane PDMS) [30].

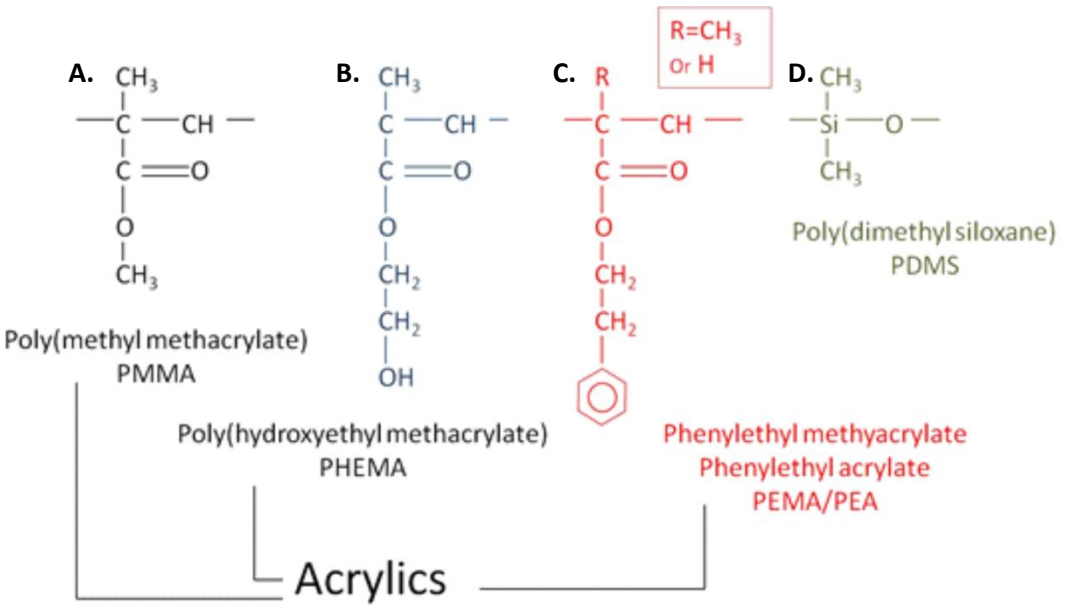

Figure 1.12: Chemical structure of available IOLs. A. PMMA, B. PHEMA, C. PEMA/PEA and D. PDMS. Diagram courtesy of R.L. Williams.

1.8 PCO

There are some postoperative complications associated with scarring after implantation of an IOL, of which posterior capsule opacification (PCO) (Figure 1.14) is the most common [50]. The usual physiological monolayer of LECs on the anterior capsule causes no clinical problem, however the capsule remains a stage for cellular adhesion and migration [51]. During cataract surgery LECs on the anterior capsule and the lens fibres are removed via phacoemulsification and irrigation/aspiration, however the nature of the surgery means it is very difficult to remove all cells [51]. PCO occurs when residual LECs, normally present on the anterior capsule, migrate onto the previously cell free posterior capsule, in response to the surgical trauma caused and implantation of an IOL [52]. These cells then dedifferentiate into fibroblast-like cells causing the posterior capsular bag to wrinkle, causing light scattering (Figure 1.13), distorting the light path to the back of the eye.

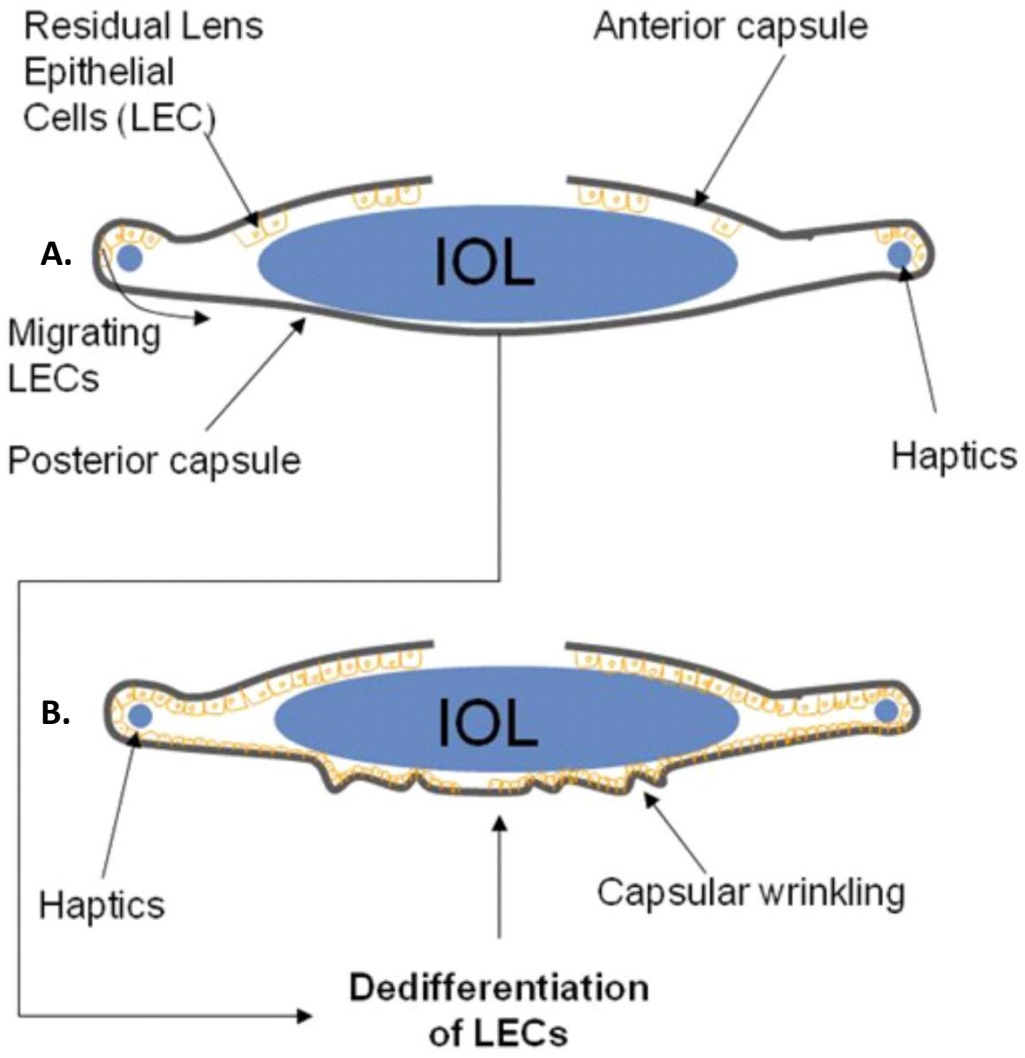

Figure 1.13: Schematic of PCO development. A. Residual LECs on the anterior capsule following surgery and IOL implantation. B. Migration of LECs onto the previously cell free posterior capsule, where cells dedifferentiate into fibroblast-like cells and cause wrinkling of the posterior capsule, which results in loss of vision. Adapted from personal communications with R.L. Williams

The trauma caused during surgery induces cytokine release such as elevated levels of transforming growth factor beta (TGFβ), causing changes in LEC phenotype and morphology [53]. TGFβ is usually present in the inactive form in aqueous humour, and is activated after surgery as part of the natural wound healing response [54-55]. The isoform most abundant in the eye is TGFβ2. It is known that LECs secrete TGFβ2 post operatively [56], causing dedifferentiation of LECs, meaning modifications in their

structure to produce different proteins, such as α smooth muscle actin (αSMA) [56-58]. αSMA is expressed by myofibroblast-like cells which are thought to be responsible for excessive contractile forces, causing capsular wrinkling [59]. The protein and morphological changes provoke repair and regeneration of LECs and fibres known as Elschnig's pearls [60-61] and Soemmering's Ring [5, 61]. As well as the surgical trauma, the degree of PCO is also affected by the material, surface properties and shape of the IOL [10, 62]. This process occurs post operatively but PCO (Figure 1.14) may take several years to develop [24, 63].

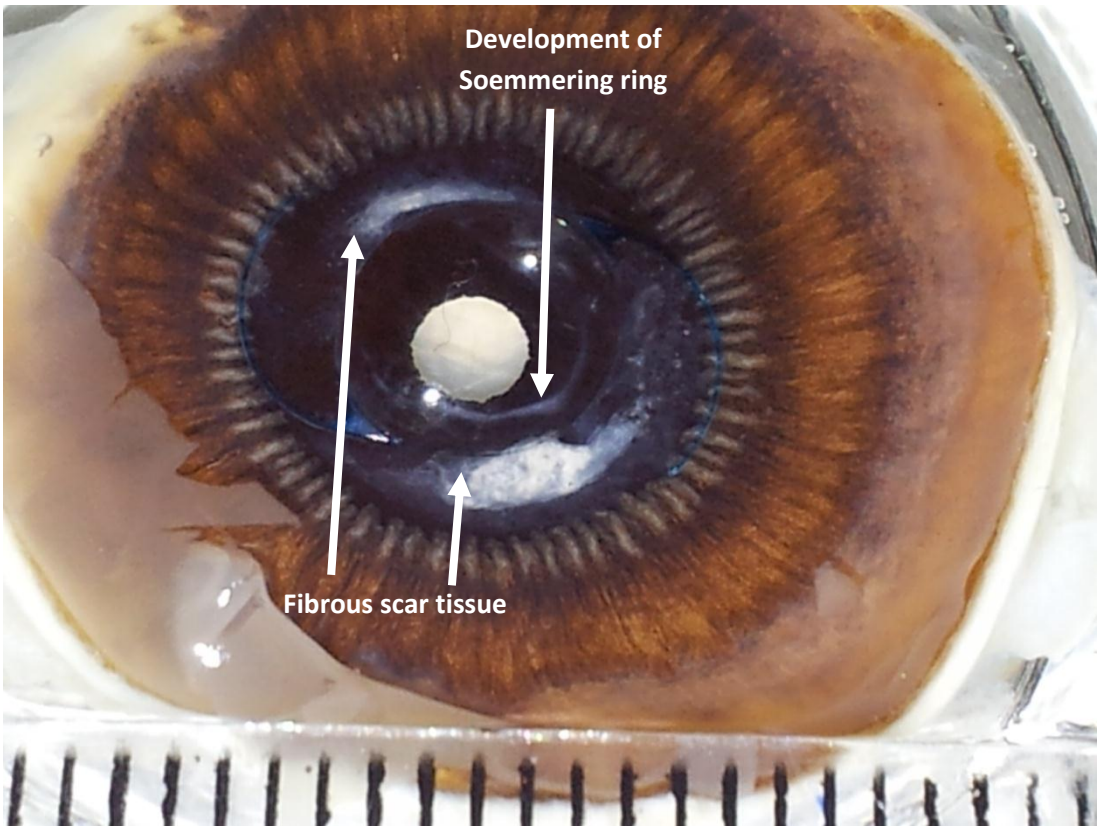

Figure 1.14: Photograph demonstrating a donor eye with IOL implant and early PCO formation. Early fibrosis was observed as scar tissue at the periphery. As well as development of Soemmering's Ring.

PCO rates vary between studies [64]. Schaumberg et al demonstrated this and pooled all published rates for PCO for different materials together. The overall (95% confidence limits) incidence of PCO rates for years 1, 3 and 5 were, 11.8% (9.3–14.3%), 20.7% (16.6–24.9%) and 28.4% (18.4–38.4%) respectively [46, 65]. Boureau et al reported a PCO

rates for three square edge design IOLs, Acrysof SA6S0 (Alcon, n=250), AR40E (Advanced medical optics, n=254) and XL-Stabi (Zeiss-loltech, n=263) in a retrospective study conducted by 10 ophthalmology centres in France. PCO occurred in 13.1% Acrysof SA6S0 IOLs, 23.3% in 4AR40E IOLs and 45.4% in XL-Stabi IOLs, three years postoperatively. Based on data from the year 2005 Boureau et al calculated the total budget for post-capsulotomy complications for all cataract interventions was €18.5 million for the Acrysof SA6S0 IOLS, €12 million for AR40E IOLs and €21.4 million XL-Stabi IOLs [66].

1.8.1 Surgical Treatment

There are no therapeutic agents available to prevent PCO, therefore a second operation is required using an Nd:YAG (neodymium doped yttrium aluminium garnet) laser, known as a capsulotomy. This procedure involves burning a hole through the posterior capsule to regain a clear light path to the back of the eye. This can lead to further complications such as retinal detachment, damage to the IOL, increase in intraocular pressure and corneal oedema. In addition to the risk factors involved with capsulotomy it also poses a significant cost factor on the healthcare system, severely limiting its use in developing countries. A better understanding is therefore required to improve the outcome of cataract surgery [25, 66-69].

1.9 Current Research to Prevent PCO

There are various routes being investigated to eliminate the clinical significance of PCO and these are all interlinked. These include surgical technique, the use of therapeutic agents and IOL design either in terms of their shape or materials (Figure 1.15).

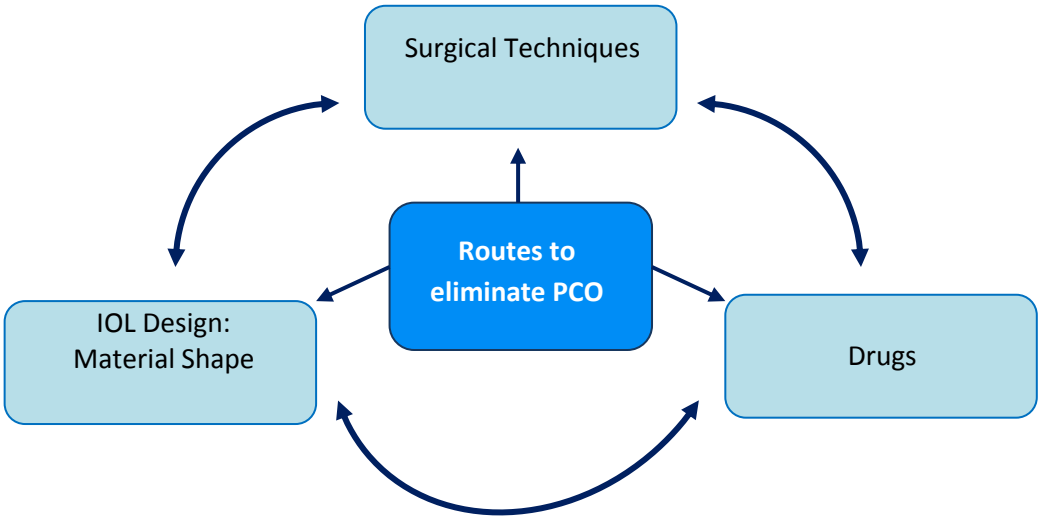

Figure 1.15: Schematic demonstrating routes being investigated to eliminate the clinical burden of PCO. Research areas are all interlinked.

1.9.1 Surgical Techniques

Initially research was undertaken to improve surgical techniques by minimising the amount of injury caused and reducing the inflammatory response [25]. Firstly, research was aimed at improving the fixation and location of the IOL. Several AC IOLs emerged between the years 1952 – 1962, however inflammation due to abrasion of the cornea and uvea meant they were abandoned. Iris supported designs soon followed in 1957 – 1973. These had round loops on the side of the IOL to suture them into place, and were made from different materials to the IOL optic. Complications occurred with these IOLs ≥6 years postoperatively, including decompensation of the cornea, as well as iris erosion and dislocation of the IOL. AC IOLs were revisited in the 1970 – 1980's with the introduction of haptics made from PMMA or other biomaterials, however the outcome was still unfavourable resulting in inflammation and glaucoma. This led to posterior

chamber (PC) fixated IOLs with "J" shaped haptics, originally being positioned behind the iris and in front of the capsule, in an area called the sulcus. These IOLs led to iris chafing, decentration of the IOL if one haptic accidently fell into the bag and PCO [30, 52]. Further improvements to "C" shaped haptics and opening the capsular bag by capsulorhexis, meant reliable implantation of PC IOLs to the current position, known as "in the bag" capsular fixation [30, 52]. Firstly this prevents irritation to other tissue and secondly it creates an IOL optic barrier, forcing the IOL and the posterior capsule together, eliminating space for cell migration. Another area of improvement has been the decrease in capsulorhexis size, to create a tight fit for the IOL and to minimise interaction with the aqueous humour [70-71].

In addition, the inflammatory response can be minimised by decreasing the incision size and taking care to enhance cortical clean-up of residual LECs. Peng et al studied the benefits of using hydrodissection, coupled with phacoemulsification and irrigation/aspiration. The process of hydrodissection requires injecting saline in-between the capsular bag and lens, creating a fluid stream around the lens making phacoemulsification quicker and easier. Peng et al proved on autopsy eyes that hydrodissection accompanies the elevation of the lens away from the capsular bag, enhancing cortical clean up. This process has also been shown to decrease surgical time [48, 70].

Improvements to surgical technique can minimise the amount of trauma caused, and inevitably the wound healing response. This is crucial as it has been shown that the wound healing response provokes changes in LEC signalling which increases proliferation rates, extracellular matrix (ECM) deposits, capsular contraction and differentiation, thus leading to PCO [60, 72]. As mentioned earlier TGFβ2 levels are elevated post operatively [56] inducing αSMA expression, causing wrinkling and distortion to the capsular bag [59]. These intracellular and extracellular changes to LECs are thought to be a cause of PCO [56, 73]. Therefore research has been carried out to reduce TGFβ2 either in terms of minimising the initial wound healing response, or by using drugs to prevent TGFβ2 secretion (1.12) [56, 74].

1.9.2 Drug Release

Drugs have been administered during and after cataract surgery with the aim of reducing inflammation and PCO. Typically inflammation is controlled by administering eye drops or injections, but some researchers have investigated the use of IOLs as a system for drug delivery [25, 75-78]. Pharmacological agents are being used to kill remaining LECs left behind after surgery, however there is a worry that any drug aiming to cause cell death could be toxic to other areas of the eye [51, 67, 71]. This is why pharmacological agents being tested have not left the laboratory stage or at most the animal testing phase [71]. Pharmacological agents currently being tested include, antimetabolites (for example methotrexate, mitomycin C and 5-FU), anti-inflammatory and immunological substances. A common problem for these pharmacological agents is the sustained release and contact of the drug to the appropriate area of the eye. Pandey et al combined the use of 5-FU with an intracapsular ring to prevent contraction and inhibit LEC proliferation. The results were mixed and indicated the intracapsular ring may prevent central PCO by inhibiting LEC growth inward, but the pharmacological effects of 5-FU were not demonstrated [72].

The drug daunorubicin has been applied to IOL's and successfully reduced PCO by 50% in an animal study, however corneal endothelial side effects were reported, indicating this antimetabolite would not be suitable for clinical use [79].

Using IOLs to minimise the post operative infection has also been studied via soaking hydrophilic acrylic IOLs in gatifloxacin and moxifloxacin antibiotics for 24 hours. IOLs were implanted into rabbits. The results showed higher concentrations of drugs were delivered for a prolonged period of time to the target area, than the amount of drug delivered with the use of antibiotic drops [80-81]. This area has potential for future IOL development [51].

The Surodex implant is a biodegradable polymer implant, inserted inside the anterior chamber at the same time as cataract extraction, and slowly releases the steroid dexamethasone to reduce to post operative inflammation [51, 82]. Tan et al showed that implantation of the Surodex decreased anterior flare, examined by flare meter, up to 30 days postoperatively when compared to conventional 0.1% dexamethasone eye

drops [76]. In another study Tan et al implanted 2 Surodex drug delivery systems per eye and found that flare was only significantly lower than 0.1% dexamethasone eye drops control until the 15 days postoperative time point. Surodex treatment did reduce ocular discomfort, photophobia and lacrimation [77]. Both studies reported that no significant difference in corneal endothelial cell loss between Surodex and dexamethasone treatment 1 year after surgery [76-77]. Wadood et al also reported that there was no difference in corneal endothelial cell numbers, however they found no difference in flare or subjective assessment of inflammation between Surodex or dexamethasone treated eyes [78].

1.9.3 IOL Design

Biocompatibility of IOLs can be broken down into two research themes, biological and mechanical compatibility. Biological compatibility can be assessed by the degree of adhesion of macrophages, giant cells and LECs to the IOL [52]. Mechanical compatibility can be determined by the fit of the IOL inside the capsular bag and influence of IOL shape has on LEC migration. Mechanical compatibility can therefore be broken down into two components, IOL material and IOL shape. Due to the overlap between the two research themes biological compatibility will be discussed in both these sections.

1.9.3.1 IOL Material

In the beginning of the 1980's Starr Inc. introduced the first foldable silicone IOL made from a proprietary poly-siloxane [52]. The formulation was then developed over the next 15 years and other companies introduced lenses with different refractive indexes, mechanical properties and UV protection. Complications with silicone IOLs arose such as unfolding rapidly in a spring like motion and adhesion of silicone oil to the back of the IOL, if it was required as a tamponade agent in the future. pHEMA has extensively been used for contact lenses due to its wettability properties, the same material was later applied to IOLs, however fixation was difficult and complications arose after capsulotomy with Nd:YAG laser. In 1994 Alcon introduced the Acrysof® IOL, a new soft hydrophobic copolymer of phenylethyl acrylate and phenylethyl methacrylate, with a UV absorbing filter. A much thinner design meant it could be inserted inside a smaller incision of just 3mm, the IOL also unfolded slowly reducing inflammation and remaining

centred. There have been several modifications from the three-piece foldable IOL with PMMA "C" shaped haptics, inserted with forceps, to the injectable one-piece IOL with integral haptics made for the same material as the optic [31].

It is known that IOL material and surface properties, such as wettability can influence the severity of the postoperative cellular response, and the development of PCO [67]. Wettability refers to the spreading of a liquid on a solid surface. If the water droplet was very rounded on a surface there would be a low interaction with the surface and it would be more hydrophobic, than if the water droplet was highly spread across the surface and would be termed hydrophilic (Figure 1.16).

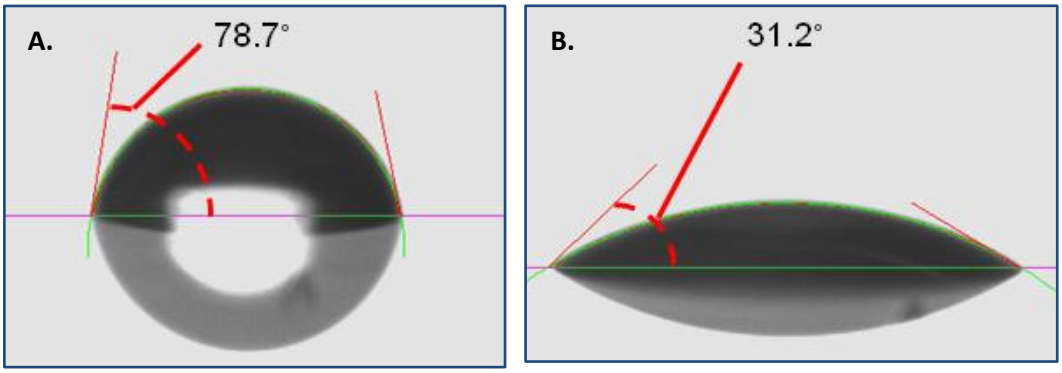

Figure 1.16: Photograph demonstrating wettability of a surface on A. A more hydrophobic surface with a higher contact angle and B. A more hydrophilic surface with a lower contact angle. Photograph courtesy of K.G. Doherty.

The wettability is influenced by the surface and interfacial tension. A high surface tension would pull the water droplet across the surface to try and reduce the tension. The surface tension is countered by the interfacial tension at the surface/liquid interface, which pulls the water droplet away from the surface. In terms of IOLs there has been much controversy over cell attachment and wettability, and the argument of hydrophobic vs. hydrophilic IOLs to prevent PCO [83]. This controversy is highlighted in the studies of Yao et al and Schroeder [84-85].

Yao et al investigated two types of silicone IOLs, one foldable IOL and one surface modified foldable IOL with phospholipid monomers, to make it more hydrophilic. The wettability of both was evaluated using contact angle analysis. This measures the angle between the water droplet and the surface, to give it a degree of wettability. LECs were also seeded onto the surfaces and the results show lower cellular attachment on the modified silicone IOLs, indicating a more hydrophilic IOL would be best suited for reduction of PCO [84]. Schroeder et al performed a similar study investigating adhesion of fibronectin on varying hydrophilic IOLs, as it is thought that fibronectin increases cellular attachment and thus PCO. Again contact angle measurements were taken. The results showed more hydrophilic IOLs had more fibronectin attached. This indicates a more hydrophobic IOL would be best suited for reducing fibronectin attachment and therefore PCO. These two studies contradict each other and add to the case that there is still no clear link between wettability and PCO [85].

Deposits on IOLs either in terms of cell type, such as fibroblasts, macrophages or LECs or ECM macromolecules can lead to an inflammatory response [86]. Lauren et al and Saika et al have examined LEC secretion of different collagen types [87] and how this is influenced by the material [86]. LECs have been shown not only to secrete their specific basement membrane protein, collagen type IV, but also type I and III in bovine LECs when left for a long period in tissue culture (up to 10 months). These results indicate that in long term culture LEC secretion of collagen changes phenotype [87]. Saika et al later found traces of type I collagen on PMMA IOLs explanted from human eyes along with cells having the appearance of macrophages and giant cells. In one particular case fibrous deposits where found encasing the lens haptics with a thin membranous deposit. This fibrotic tissue appeared to have many cellular components included cell debris and some macrophages, however no fibroblastic cells were identified. As fibrotic tissue is generally long lasting conclusions were made that fibrosis was formed immediately after surgery as a wound healing response, and by the time of the analysis the fibroblast cells were absent [86].

Mullner et al reviewed four different IOLs in terms of their inflammatory responses. LEC, Small round, fibroblast-like, epithelioid, and giant cells were all examined as these

cells play an important role in postoperative inflammation and the foreign body reaction. The four IOLs studied were, Hydroview™ (hydrophilic hydrogel IOL), AcrySof® (hydrophobic acrylic IOL), MemoryLens (hydrophilic acrylic IOL) and CeeOn 920 (hydrophobic silicone IOL). Mullner et al observed that different IOL materials alter the cellular reaction. Small round and fibroblast-like cells were seen on all IOL groups, and decreased in numbed between 7 – 30 days. These cells increased in number at 90 days in the AcrySof® (hydrophobic) and MemoryLens (hydrophilic) groups. Epithelioid and giant cells can be used as an indicator of the biocompatibility of an IOL material, due to the fact they are found in eyes with a prolonged inflammatory reaction. The number of these cells between the four groups was not significantly different. In conclusion, the Hydroview (hydrophilic acrylic) group had the highest incidence of LECs numbers but the lowest incidence of epithelioid and giant cells (after 180 days). The AcrySof® (hydrophobic acrylic) group had the lowest incidence of LEC's (after 180 days), but the highest incidence of epithelioid and giant cells (after 90 days). The CeeOn 920 (hydrophobic silicone) group had the lowest incidence of all cells after 180 days. This indicates variations in material and cellular attachment, and in particular, wettability may influence epithelioid and giant cell attachment [88].

Tognetto et al compared three different types of HEMA IOLs manufactured with different methacrylate copolymers (Hydroview H60M, ACR6D and Stabibag) in 73 patients for their biocompatibility on the anterior surface. The anterior surface was analysed for small rounded cell attachment and anterior capsule opacification, up to 180 day postoperatively. The results showed a greater percentage of Stabibag IOLs had small rounded cells adhered during the first month, however ACR6D group had the largest percentage of anterior capsule opacification during the first month and at 180 days postoperatively. Although all IOLs were based on HEMA with different methacrylate copolymers variations in terms of the wound healing response were observed, it is therefore believed that the chemical composition leads to this wound healing response [89].

As previously mentioned αSMA is expressed by myofibroblast cells and gives an indication of a wound healing and inflammatory response to implantation of an IOL.

Mahelokova et al examined the expression of αSMA on different culture substrates. LECs proliferation and αSMA expression was examined on collagen I, collagen IV, microscope glass slides and uncoated polystyrene dishes. The authors concluded that the substrate influenced attachment, proliferation and expression of αSMA in LECs [90]. Therefore αSMA could also be used to examine how substrates affect the dedifferentiation of LECs.

1.9.3.2 IOL Shape

Alcon's Acrysof® IOL was the first IOL to utilise a square edge design. This is designed to create a barrier eliminating space and applies more pressure on the posterior capsule, due to the 90^0 angle, sandwiching the posterior capsule to the IOL (Figure 1.17).

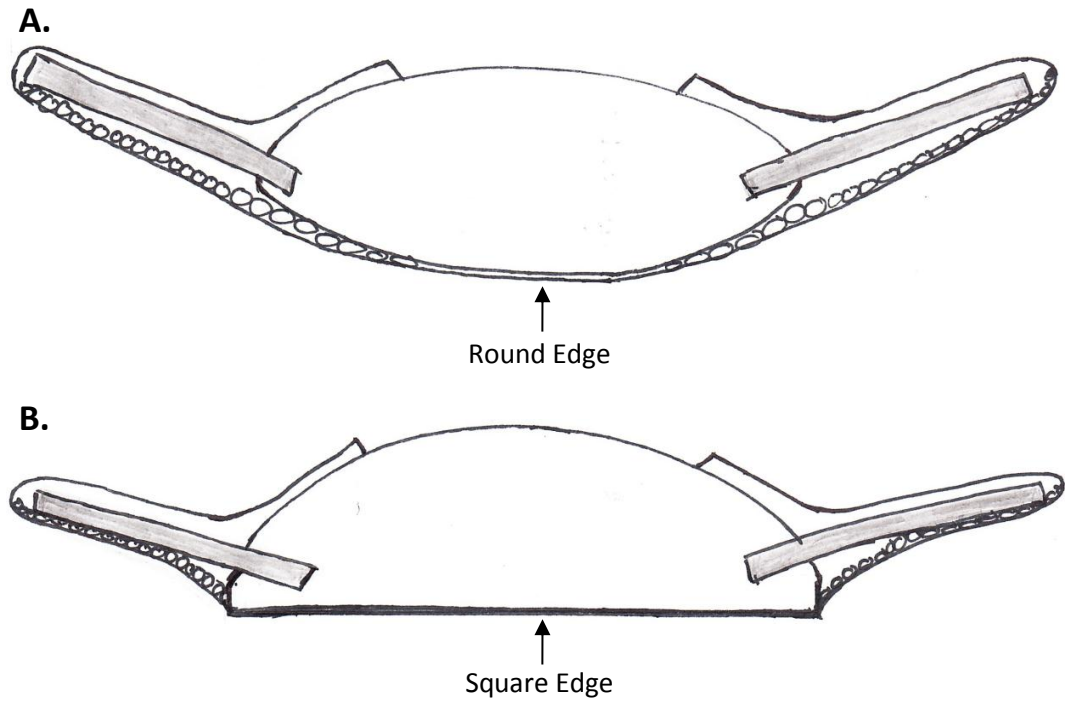

Figure 1.17: Schematic of round and square-edge designed IOLs: A. Round-edge IOL does not cause a bend in the posterior capsule so room is still available for LEC migration from the equator region onto the previously cell-free posterior capsule. B. Square-edge design IOL creating a bend in the posterior capsule and applying pressure to the posterior capsule creating a tight fit. Minimal space for LEC migration is present maintaining cell free posterior capsule.

Based on a rabbit study Nishi et al. showed that PCO levels were significantly lower in the square edge hydrophobic acrylic (AcrySof®) IOL compared to silicone and PMMA round edged IOLs. Capsular bags were examined 2, 3 and 4 weeks after implantation [91]. Oshika et al found similar inhibition of PCO with the square edge Acrysof® IOL [92]. It was later shown by Nishi and Nishi that it was the square edge design of a PMMA and an Acrysof® IOL that could prevent migration of LECs. The benefit resulting from the square edged IOL was illustrated using a rabbit model with a follow up time of 3 weeks [93]. Peng et al demonstrated this square edge barrier effect in human pseudophakic autopsy eyes. PMMA, silicone and hydrophobic acrylic (AcrySof® IOL) were studied. Square edge Acrysof® IOLs blocked LEC growth on the posterior capsule in more cases, when compared to square edge PMMA IOLs. Silicone IOLs could not hinder LEC growth [94]. Ayaki et al later showed that the finishing of experimental 3-piece hydrophobic acrylic elastomer IOLs influenced the level of PCO, in a rabbit model. When IOLs had been tumbled and polished it led to significantly more PCO due to the edge being more curved than no finishing of the edge. Ayaki et al also evaluated the level of PCO between three clinical IOLs, Acrysof® MA30BA, Sensar® AR40 and CeeOn® 911. The round edge Sensar® IOL had significantly more PCO amongst the clinically available IOLs. Supporting the theory that sharp edge acrylic IOLs are superior to round edge equivalents [95]. In a further rabbit study by Nishi et al no differences were seen in PCO rates when comparing two square edge design IOLs, the hydrophobic acrylic IOL (Alcon AcrySof® MA60BM) and the 3-piece silicone IOL (Pharmacia CeeOnTM 911) [96]. Leading them to believe the shape was key to reducing the effect of migrated LECs and PCO rather than IOL material.

The Acrysof® IOL has been shown to have some adhesive properties, which encourages LEC adhesion in a single monolayer, which bonds the IOL to the capsule [22]. Linnola et al proposed the sandwich theory as an explanation for the variable PCO formation with different IOLs. The sandwich theory was presented in 1997 and explains that during cataract surgery a CCC is performed to allow the IOL to be implanted. The remaining anterior capsule bonds to the surface of the IOL directly, or as a result of the remaining LECs. This leaves the anterior capsule clear and seals the IOL onto the capsular bag. LECs proliferate from the equator region onto the posterior capsule where they meet

the 90^0 edge of the IOL, which partly hinders and directs the proliferating cells to form a monolayer, thus creating a bond to the posterior capsule (Figure 1.17). Since only a monolayer of LECs are present on the posterior capsule the capsule remains clear, in the same way the anterior capsule does. Some of these cells later die as a result of increased pressure on the posterior capsule, ageing and poor nutrition**.** Linnola later showed that not only does the Acrysof® IOL allow LEC attachment but also ECM attachment. The adhesion of fibronectin, vitronectin, laminin and collagen type IV to Acrysof®, hydrogel, silicone and PMMA IOLs was investigated in pseudophakic human autopsy eyes. Fibronectin is a major glycoprotein and is found in the body where firm binding is required. Fibronectin was the most dominant ECM molecule present on all IOLs. Fibronectin strongly adheres to collagen, therefore the collagen capsular bag severed as a mediator to attach the IOL to the posterior capsule. Results from pseudophakic autopsy eyes showed a sandwich-like structure consisting of, the posterior capsule, fibronectin, LECs, fibronectin and IOL, or with the posterior capsule bond to the IOL directly via fibronectin. This bond prevents further in-growth of LECs onto the posterior capsule, suggesting fibronectin is produced before LECs proliferate. This was seen significantly more in the Acrysof® group than in the hydrogel, silicone or PMMA IOLs [22, 97-101]**.** Linnola et al noted that there was a greater amount of vitronectin adhered to Acrysof® than PMMA and silicone IOLs [98]. Johnson also found more fibronectin adsorbed onto Acrysof® than PMMA lenses with saturation occurring within 2 hours at 50µg/ml [5].

The IOLs described in this IOL design section have been monofocal IOLs which mean they do not correct for visual inaccuracies. There have, however, been recent developments towards toric multifocal and accommodative IOLs in the past ten years, yet these still suffer from PCO [102-104]. These can vary in terms of their design and shape [105-106]. In addition IOLs are also being used in refractive surgery to correct myopia or hyperopia in a phakic eye (with natural lens), as an alternative to laser surgery or correction via contact lenses or glasses [107-108]. Due to this the demand on IOLs as ophthalmic implants is vast, therefore complications associated with IOL shape and material and their effect on PCO, needs to be fully understood for the field to progress and advance [31].

1.10 Polymers for Controlling Cellular Response

Covalent binding allows modification of a surface without affecting the bulk materials, and achieves a stable bond between the added functional group, and the biomaterial surface. This offers a wide scope for attaching various functional groups to a surface offering chemical stability. Functional groups often employed in covalently bounding include hydroxyl (-OH), amine ($-NH_2$), amide ($-CONH_2$) and carboxyl (-COOH) groups. There has been much use of poly(ethylene glycol) (PEG) in biomaterials applications via covalent binding. PEG is hydrophilic and as a result has the ability to decrease non-specific binding of proteins and cellular adhesion. It also has non-toxic and non-immunogenicity properties, therefore has been added to several biomaterials. This can be achieved via direct covalent binding to the hydroxyl group present at either end of PEG. Covalent binding can be achieved by utilising various coupling agents such as, N-hydroxysuccinimide (NHS) and 1-ethyl-3-(3-dimethylaminopropyl) carbodiimide (EDC). NHS increases electron attraction and reacts to activate carboxylic acid groups to promote amide bonds. EDC is also used to activate carboxylic acid increasing their reactivity towards amines and hydroxyl groups, it promotes coupling reaction and therefore efficiency [109].

Danion et al bound PEG onto pHEMA contact lenses with the aim of immobilising ophthalmic drugs. Hydroxyl groups present on the surface of the contact lenses were activated via coupling reagent N,N'-disuccinimidyl carbonate (DSC). Poly-(ethylenimine) (PEI) was added to the surface of the contact lenses to encourage amine groups. PEG was grafted onto the PEI layer using NHS carbodiimide reaction. Intact liposome layers preloaded with a fluorescent dye were bound onto the anterior and posterior surface of the contact lenses, to monitor the release for the later purpose of drug delivery. Release of the fluorescent dye showed good stability of the intact liposomes when stored for up to a month at 4°C [110]. mPEG is the mono-functionalised derivative of PEG and reduces unwanted crosslinking, but still retains the beneficial properties of PEG. BioInteractions Ltd. bound mPEG onto soft contact lenses to reduce protein adhesion and spoiling via a coupling agent, 1,1'-carbonyldiimidazole (CDI). This again activates carboxylic acid groups and forms esters between carboxylic acid and PEG [109]. Various studies have investigated the potential of PEG to reduce protein adsorption and platelet

and cell adhesion [111-115]. Kim et al investigated the cellular adhesion effect on PEG grafted onto PMMA IOLs by implantation using a rabbit model. Results showed a significant reduction in cellular adhesion, indicating the potential of PEG to decrease cellular debris and formation of foreign body reaction and PCO [114].

PEI has been used for various biomaterial applications to induce cellular attachment and proliferation [116-117]. Lakard et al examined the potential of several amine-based polymers polyethyleneimine (PEI), polypropyleneimine (PPI), polypyrrole (PPy) and poly(p-phenylenediamine) (PPPD), as an alternative to poly-L-lysine, which is commonly used as an adhesive molecule. Rat neuronal cells were investigated for their adhesive, proliferative and morphological properties on the above polymers. PEI and PPI both encouraged a higher number of cellular attachment compared to PPy and PPPD, with typical morphological growth, indicating their use as an adhesion molecule for biomaterial surfaces [118]. PEI has also been shown to encourage cellular attachment in, human embryonic kidney cells, rat pheochromocytoma cells and human fibroblast cells [119].

As mentioned early the surface chemistry can control cellular adhesion via protein adsorption, however, as polymeric surfaces can undergo conformational rearrangements in responses to environmental conditions, work has been carried out to produce a defined and controlled substrates [120-122]. Cells are reported to have greater adhesion to surfaces containing COOH and NH_2 functional groups, than those with CH_3 and OH groups [122]. Amine groups have therefore been added to various substrates for the purpose of encouraging cellular attachment and growth [123-124]. Keselowsky et al demonstrated conformational differences in adsorbed fibronectin and varying cellular adhesion onto four self assembled monolayers (SAMs). Four functional end groups, CH_3 (nonpolar hydrophobic surface), OH (neutral hydrophilic surface), COOH (negatively charged surface) and NH_2 (positively charged surface) were investigated. Fibronectin was adsorbed onto the different SAMs at various concentrations and measured. More fibronectin was adsorbed onto positively charge NH_2 and least on neutrally charged OH SAMs. A centrifugation cellular adhesion assay was performed and SAMs were coated with a range of fibronectin densities. The results showed that

cells adhered strongly to OH SAMs at lower fibronectin density. NH_2 and COOH SAMs had comparable cellular adhesion at intermediate fibronectin densities and CH_3 SAMs had comparable cellular adhesion only at high fibronectin densities. These results demonstrate the surface chemistry affects the fibronectin adsorption and cellular adhesion strength between SAMs [3]. Lee et al examined human erythroleukemia (K100) cellular adhesion onto COOH, NH_2, and CH_3 SAMs. NH_2 SAMs had a significantly higher number of adhered cells compared to COOH and CH_3 [122], Indicating that properties such as the surface charge and functional group govern cellular behaviours.

1.11 Glycosaminoglycans

Glycosaminoglycans (GAGs) are long chains of polysaccharide units that are synthesised in the Golgi apparatus[125]. Their linear sugar chains can be sulphated at various points [126-127]. They are found in the ECM and on cell surfaces themselves. GAGs are known to be involved in cell cycle regulation due to their rigidity and integrity, which allows for cell migration, proliferation and differentiation, particularly with epithelial cells. They also have the ability to bind to growth factors, and can be covalently attached to a protein to form a proteoglycan. If GAG functionalised surfaces could encourage a desired protein adsorption layer they could be utilised to manipulate cell behaviour [128-130].

Heparin (HEP) is derived from heparan sulphate and is widely used in anticoagulation drugs. HEP is stored in the granules of mast cells and when realised prevents clotting. Heparin is widely used after surgery to prevent clotting especially where mobility is hindered [126].

Hyaluronic acid (HA) otherwise known as hyaluronan is the only GAG that is not sulphated, meaning it cannot be covalently bound to other proteins [9]. It is not covalently linked to a core protein unlike other GAGS and is said to be the simplest GAG [126]. Rather than being synthesized in the Golgi, HA is produced in the plasma membrane by hyaluronan synthase [126]. HA is found in the ECM and is responsible for cellular behaviours such as promoting proliferation, along with cell-cell and cell-matrix adhesion [129-133]. HA has a long mobile molecular chain with a high molecular weight and is highly negatively charged [126]. It has the capacity to bind one part HA to 100 parts water. HA takes the form of a hydrated hydrogel like substance and in the body is used as a space filler, providing structural support [126]. During embryonic development epithelial cells secrete HA to create space for new cells to proliferate [126]. It is present in the vitreous at 0.02 – 1mg/cm^3 [128, 131], the aqueous at ~1.1-1.14 µg/ml [130, 134], the lens as well as other places in the body such as synovial fluid and cartilage. HA is used in ophthalmology, as a constituent in eye drops, to promote corneal wound healing and in the viscoelastic material used in cataract surgery. The viscoelastic material protects the inner surface of the cornea, retains the cornea space

and allows the surgeon room to operate and insert instruments [9, 126, 128-133]. If immobilised in the appropriate way with the right configuration HA could be a non-fouling polymer, inhibiting protein and cellular adhesion [9].

Chondroitin sulphate (CS) is another major GAG that is present within the ECM, and has similar responsibilities for regulating cell behaviour as HA. Sulfation of CS can occur in two positions, chondroitin-4-sulfate (C4S) and/or chondroitin-6-sulfate (C6S). They both contain carboxylated and sulphated charged groups within the disaccharide unit, and can either occur separately or together depending on the tissue [126]. CS is present in the anterior capsule but diminishes with age [135]. CS is also sometimes used in these viscoelastic products to aid cataract surgery [2].

As the capsular bag has structural and physiological changes with age Winkler et al examined the basal membrane of the anterior capsule for proteoglycans, in patients that had senile cataracts. To explore these age dependent changes four removed anterior capsulorhexis explants were received from people with senile cataracts (aged between 67 – 87). Four younger donors were used as a control, two who suffered from congenital cataracts (aged one and two) and two who suffered from perforating eye injuries (both aged 20). Biochemical and immunological analysis was used to examine distribution of heparin, chondroitin-6-sulphate and dermatan sulphate across the full thickness of young and senile anterior lens capsules. This showed the capsule to have a complex composition of proteoglycans, the most dominant being heparin, but chondroitin sulphate was also present. GAGs appeared as a thin lamina layer in the control (younger) anterior capsulorhexis explants. Heparin stained very strongly. Chondroitin-6-sulphate and dermatan sulphate were also present but with a less prominent layer in the humoral surface (outer surface which is in contact with the aqueous). In senile cataract anterior capsulorhexis explants heparin appeared distorted and not heterogeneous in the humoral surfaces. In both senile and young lens capsulorhexis explants heparin was most prominent when lens epithelial cell loss had occurred (clean up of LEC during surgery). This demonstrates the changes in GAG distribution with age across the capsular bag, with the most prominent GAG being Heparin [135].

GAGs have been used with several cell types to tailor the cellular response by encouraging or preventing cellular attachment [136-138]. Heng et al characterises human umbilical vein endothelial cell (HUVEC) adhesion and proliferation on HA, HEP and CS, using either poly-L-lysine or chitosan as an underlying layer. Significant differences in the percentage of cellular adhesion were seen at early time points on the different underlying layers, however these became insignificant at later time points. HA resulted in the least amount of cell proliferation regardless of the underlying layer. HEP and CS encouraged a similar amount proliferation by day 10 with no significant different between the GAGs. These results indicate the three GAG coatings produce different cellular growth profiles with HUVEC. Coatings functionalised with HEP and CS could encourage endothelial cellular attachments [137]. Contrasting results were seen in dermal fibroblasts. Attia et al examined the cellular response on polysulfone substrates bound with HA and CS. CS did not promote cellular adhesion whereas HA encouraged cellular adhesions and supported proliferation, meaning the cellular type and underlying layer may influence cellular attachment [138].

Uygun et al investigated if GAGs on chitosan membranes could increase the growth of mesenchymal stem cells (MSC). Six GAGs, HEP sodium, heparin, CS4, CS6, HA and dermatan sulphate (DS), at six different ratios, 0.04, 0.08, 0.1, 0.2, 0.5 and 1.0mg GAG/mg chitosan, were chosen to examine their influence on MSC proliferation, spreading and differentiation. The GAGs were immobilised onto chitosan membranes in one of two ways. In the first method GAGs were added onto chitosan membranes overnight at 4°C then covalently linked to the chitosan membrane using EDC solution, for 24 hours at room temperature (referred to as immobilisation followed by covalent binding, ICB). In the second method GAGs were activated using EDC solution for 15 minutes then added to chitosan membranes for 24 hours at room temperature (referred to as direct covalent immobilisation, DCI). Presence of the GAGs on the surfaces were determined by staining with toluidine blue, the amount of GAG bound to a surface was determined by using safranin-O dye and determined indirectly by measuring the reaction solution and the wash solution. More GAGs were immobilised onto the surfaces via the ICB method than the DCI method. As the concentration of GAG increased so did the level of GAG immobilised onto a surface, there was only slight

variations between GAGs. The DCI method had more variation in terms of bound GAG ranging between 39.9 – 92.1%. The ICB method produced swollen and rough surfaces regardless of GAG type that did not allow cells to attach, whereas the DCI method produced smooth surfaces. On the DCI method for all GAG types cell growth was increased with the increasing concentration of GAG. C4S produced the highest cell density at 1 mg/mg. The morphology of the cells were examined by fluorescent staining for phalloidin and vinculin, a focal adhesion protein which if present at the ends of actin fibres suggests integrin involvement in cellular adhesion. Heparin, HS, C4S and HA showed significant levels of cell spreading from phalloidin staining and had some vinculin present inside the cell. MSCs on C6S and DS were less spread and had disorganised actin fibres. Whereas the actin fibres of HA and C4S were aligned and similar to tissue culture plastics, vinculin was also found at the end of these actin fibres indicating integrin involvement. This study gives an indication as to how cell behaviour and adhesion can be controlled with different GAG types and concentration [139].

D'Sa et al examined LECs response to HA coatings. HA was immobilised onto atmospheric pressure plasma modified polystyrene substrates. Amine groups were added to the coatings via silinisation. HA was covalently bound to the surface at 1mg/ml and 3mg/ml via carbodiimide coupling reaction using EDC/NHS agents. The results showed a significant reduction in LECs attachment at 24 hours and 48 hours post seeding, indicating HA exists in a confirmation that could provide a steric layer to inhibiting cellular attachment [9].

1.12 Transforming Growth Factor Beta

Within the lens TGFβ2 plays a role in dedifferentiation and capsular wrinkling [140-141], it is realised postoperatively as part of the natural wound healing response (Figure 1.18) [56-58]. It can also lead to the expression of ECM proteins such as fibronectin [142] which is associated with PCO [143]. There are three isoforms of the TGFβ super-family, TGFβ1, TGFβ2 and TGFβ3, they all contribute to cell proliferation, migration, differentiation and apoptosis. They share between 70 – 80% homology and signal using the same cell surface receptors, however, depending on the cell type, they display different and sometimes opposing effects in vivo. TGFβs are unable to send signals to the cell nucleus without first binding to a receptor. TGFβs are expressed in an inactive form and must attach to these receptors before a signal is passed through the cell cytoplasm to the nuclei. In detail, the inactive part contains propeptide and latent TGFβ binding protein (LTBP). Either proteolysis or pH regulation activates TGFβ, which allows it to bind to type 2 receptor (TβR-II) on the cell membrane, and recruits type 1 receptor (TβR-I) in the cell cytoplasm. Further phosphorylation of TβR-I by TβR-II activates SMAD2 and SMAD3, which transmits TGFβ signals to the nucleus (Figure 1.18) [24, 143].

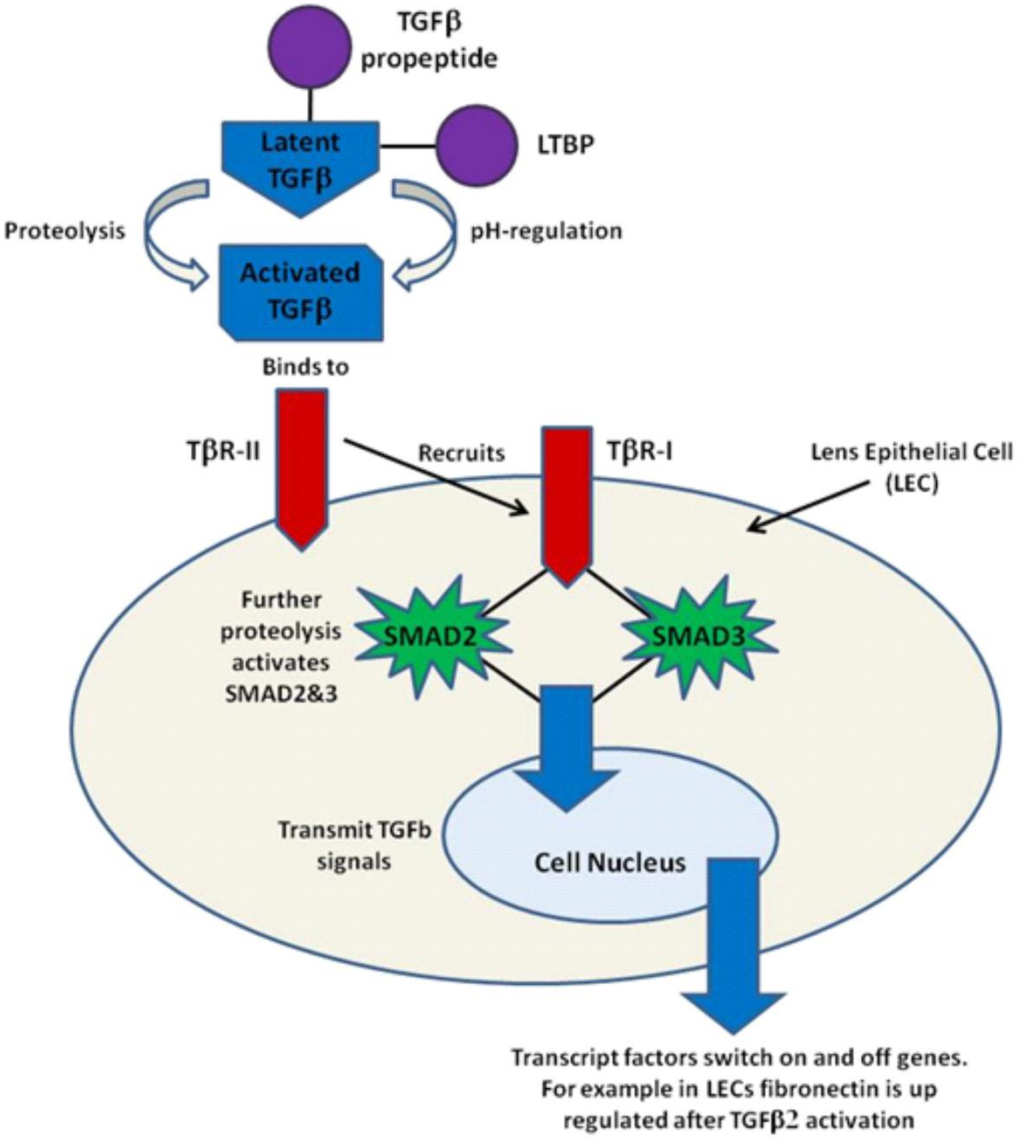

Figure 1.18: Schematic demonstrating the process of TGFβ activation and signalling (in the context here of a lens epithelial ell (LEC)). Latent TGFβ contains TGFβ propeptide and LTBP. It is activated by proteolysis or pH regulation, which allows it to bind to type 2 receptor (TβR-II) and recruits type 1 receptor (TβR-I). Further phosphorylation of TβR-I by the TβR-II activates SMAD2 and SMAD3 which transmits TGFβ signals to the nucleus. Depending on the cell type transcript factors turn genes on/off, in the example here of a LEC fibronectin is up regulated after TGFβ2 activation. Adapted from Hao et al [143].

The effect TGFβ has on LECs and fibres are distinctively different, for example, TGFβ is required to promote normal differentiation events in lens fibres, whereas in LECs TGFβ is associated with the fibrosis seen after cataract surgery [24, 142]. TGFβ1 was first studied in rat LECs in vitro by Lui at al. They showed that cultures incubated with 20ng/ml of TGFβ1 underwent rapid elongation and accumulation of ECM, capsular wrinkling and cell death. Whilst all three isoforms have the potential to cause these changes within the eye, TGFβ2 is the most abundant and the most potent [140, 144].

Hales et al reported opacities or plaques of abnormal cells across the anterior capsule when whole rat lenses were cultured with 5ng/ml of TGFβ2. Cuboidal epithelial cells usually present on the anterior capsule had been replaced with spindle shaped multilayer cells, with areas of contraction. Lenses treated with TGFβ2 had positive expression of αSMA, laminin and collagen type I, components not usually present or associated with the LECs. Control samples showed no positive staining for these molecules [141]. Lovieu et al performed a similar study where similar ECM and cytoskeleton markers were present, including the addition of collagen type III and fibronectin [145].

Wormstone et al has contributed to research on TGFβ2 secretion using a human monoclonal antibody neutralising TGFβ2, called CAT 152 [56, 74]. Wormstone found that when capsular bags from donor eyes were incubated in vitro with 10ng/ml of TGFβ2 and 10µg/ml of CAT 152 capsular bags did not show any contractile effects or light scatter. Capsules appeared severely wrinkled when CAT 152 was not present. CAT 152 suppressed TGFβ2 induced expression of αSMA and fibronectin, compared to capsular bags incubated with TGFβ2 in the absence of CAT 152 [146]. Further studies examining TGFβ2 signalling in LEC line FHL124 also supported this. LECs were cultured in 5% serum for 3 days and serum starved for 2 days before exposure to experimental conditions for 24 hours. Experimental conditions were medium supplemented with 10ng/ml TGFβ2 with and without CAT 152 (0.1-10µg/ml). CAT 152 again successfully inhibited contractile induced behaviour of TGFβ2 and αSMA expression [147]. Wormstone et al also showed that even short term exposure of LECs to TGFβ2 (2 days) induces long term morphological changes and a fibrotic response, characterised by up-

regulated expression of αSMA, 28 days later [74]. This is in agreement with Hales et al conclusions on rat LECs [58].

There has been much recent research in the role of TGFβ3 in cleft palate and wound healing. Cleft palate is the failure of palatal midline epithelial seam (MES) cells to fuse during development, meaning the epithelium never forms a single confluent palatal mesenchymal structure. TGFβ3 has been shown to regulate these interactions and is expressed abundantly by the palatal medial edge epithelial (MEE) cells [143, 148]. In cleft palate the expression of TGFβ3 is significantly reduced. In a study using TGFβ3 null mice cleft palate occurred in 100%, therefore is believed to be critical for the adhesion and fusion of the MEE cells [143]. This was also reported by other authors [148-151]. In vitro Brunet et al used neutralising TGFβ1, 2 and 3 antibodies to block their activity. This showed that by blocking TGFβ3 activity normal palate development was disrupted, and by 72 hours the MEE had not adhered and the midline seam had not fused. When antibodies specific to blocking TGFβ1 and TGFβ2 were used no effect on palate fusion was observed and cultures appeared similar to untreated controls [152]. This shows that TGFβ3 is critical in palatal fusion and therefore may play a role in epithelial monolayer formation [143].

Scar free wound healing in skin is seen in early embryos but not in adults. Cowin et al characterised TGFβ's in fetal and adult wounds. TGFβ1 and TGFβ2 were seen at low levels in fetal wounds, TGFβ3 was expressed in the epidermis of fetal skin. All three isoforms were present in adult wounds. However when adult wounds were treated with TGFβ3 there was noticeable improvements or even scar free wound healing. It was concluded that TGFβ3 produces a regenerative healing response in epithelia, potentially leading to scar free healing [153], whereas TGFβ1 and TGFβ2 have been associated with fibrotic scarring [143, 153-155].

TGFβs were also investigated by Karamichos et al, to encourage corneal fibroblasts to deposit ECM in a similar manner seen during stromal development. TGFβ1, TGFβ2 or TGFβ3 was added to the growth media at a concentration of 0.1ng/ml. All isoforms increased cell number and ECM production when compared to control (no TGFβ).

TGFβ1 and TGFβ2 caused expression of collagen III and α-smooth muscle actin, however this was not seen in TGFβ3 cultures. TGFβ3 stimulated matrix alignment and seemed to mimic the natural cornea, whereas TGFβ1 and TGFβ2 demonstrated a fibrotic response. TGFβ3 is currently being used in several studies to reduce scar tissue in skin. Shah et al showed that TGFβ3 greatly reduces scar formation. Incisions were made in the subcutaneous skin of rats. Incisions were injected with varying concentrations of TGFβ1, TGFβ2, TGFβ3, anti-TGFβ1 and anti-TGFβ2. Control wounds were either left untreated or injected with PBS 0.1% BSA. Rats injected with TGFβ1, TGFβ2 and controls had stiff white scarring four months post treatment. Rats injected with anti-TGFβ1 and anti-TGFβ2 had a marked reduction in scar formation. Rats treated with TGFβ3 had reduced deposition of collagen type I and III and fibronectin compared to controls, and wound site showed little to no scarring. This demonstrates specific isoform roles of TGFβ in scar formation [156].

There is therefore the possibility to use TGFβ3 as a tool to reduce scaring elsewhere in the body. One company called "Ronova" introduced a pharmaceutical agent containing TGFβ3 known as "Jusitva™". The aim of "Jusitva™" was to prevent and reduce scar formation. Clinical trials in over a 1000 patients have been performed. Occelston et al reported successful results for the phase I and II UK clinical trials with 34 month follow ups, no safety or tolerability issues were reported. Appearance of scar tissue was evaluated by both the surgeons and histological analysis. Scarring was significant improvement when wound margins were injected with "Jusitva™" compared to a placebo, causing a prevention and reduction of scarring and fibrotic response [157].

Further evaluation of "Jusitva™" in a phase III EU trail however proved unsuccessful when primary and secondary endpoints were not met. Primary endpoints were evaluated based on photographic assessment 12 months postoperatively. Photographs were evaluated by an independent panel and graded against the Global Scar Comparison Scale. Secondary endpoints used the same Global Scar Comparison Scale but were evaluated by the patients themselves and the clinical investigator. Over 350 patients were recruited from the EU and two concentrations of "Jusitva™" were evaluated, 200ng and 500ng/100ul/linear cm of wound margin, administered twice

following wound closure and 24 hours later [158]. These results were surprising after the success of phase I and II trails. This opens up more questions than answer, and curiosity about what is happening at the gene level and what interaction TGFβ3 has on wound healing.

1.13 Novel BioInteractions Ltd Materials

The level of PCO is dependent on the material therefore possible surface modifications can be considered to control cell attachment and aim to tailor the cellular response. As previously mentioned cells interact with the surface of the IOL, therefore the biocompatibility is primarily influenced by this surface. Characteristics such as wettability, surface chemistry and surface topography can greatly affect the biocompatibility. Modifications to the surface properties can influence the cellular response, without changing the bulk material [83]. This was the approach taken with BioInteractions Ltd. Using BioInteractions Ltd. techniques and expertise potential coatings for IOLs were developed and examined.

The materials tested in this PhD have been supplied by BioInteractions Ltd who are based at Reading University. Their focus is on producing specialised coatings for a range of cardiovascular devices and catheters, providing non-thrombogenic, anti-thrombogenic and drug delivery opportunities. These coatings aim to minimise human host response which causes protein deposits, inflammation and fibrosis, inevitably resulting in device failure and patient discomfort. Their technology uses a layer by layer technique to build up the coatings with desirable functional groups to tailor a desired cellular response for a given application. BioInteractions Ltd. wished to expand their coatings and expertise to ophthalmic implants.

1.14 Hypothesis and Aims

The hypothesis for this PhD was that PCO can be prevented by surface modified coatings for potential IOLs, to control the cell-surface interactions, without affecting the bulk material.

There are two ways that this can be approached:

1. Firstly, LECs are less likely to cause any adverse scarring if they maintain their phenotype. If a surface coating (of an IOL) could encourage a monolayer of LECs to grow that could sandwich the back of the IOL to the capsular bag, this would maintain a clear light path to the back of the eye.
2. Secondly, if a surface coating (of an IOL) could inhibit cell migration, it would prevent wrinkling and contraction of the posterior capsule, therefore maintaining a clear light path to the back of the eye.

The aims of this project were:

1. To evaluate the surface properties and LEC response to existing BioInteractions Ltd. coatings (001, 002, 003, 004 and pHEMA) and use these results to suggest new coatings that could be developed to produce the desired effect.
2. To investigate if glycosaminoglycans could be attached to a material and used as coatings for IOLs to influence the cellular response.
3. To investigate the influence of surface wettability and topography of coatings with zwitterionic characteristics on cell attachment.
4. To establish a model for dedifferentiation of LECs and, particularly, the role of TGFβ2 and TGFβ3 in LEC dedifferentiation and investigate if manipulation of the levels of these cytokines could be used to reduce the scarring response following cataract surgery.

2. Material and Methods

2.1 Material Coatings and Techniques

This section outlines the material coatings provided by BioInteractions Ltd. and the experimental techniques used to evaluate them.

2.1.1 Material Coatings

Polymer surface coatings provided by BioInteractions Ltd. were built up using a layer by layer technique. All the coatings provided by BioInteractions Ltd. are listed in the table below, grouped into experiments along with details of the cell staining method and surface analysis performed on each group (Table 2-1). Coatings and experimental procedures will be explained further in the relevant sections to follow.

Table 2-1: Coatings provided by BioInteractions Ltd., cell line used, duration and experimental procedures

Experiment Group	Coating Name	Cell Line	Duration	Staining	Surface Analysis
Group One polyethylenimine (PEI) + anticoagulation polymers 1	001	FHL124	7 days	Mayer's haematoxylin and live/dead assay	N/A
	004				
	pHEMA				
Group Two PEI + anticoagulation polymers 2	001	FHL124	14 days	Propidium Iodide (PI) and Phalloidin	Contact angle, scanning electron microscopy (SEM) and white light interferometry (WLI)
	002				
	003				
Group Three Glycosaminoglycan (GAG) polymers	Hyaluronic acid	N/N1003A	14 days	4',6-Diamidino-2-phenylindole dihydrochloride (DAPI), Phalloidin and alpha-smooth muscle actin (αSMA)	Contact angle, SEM and WLI
	Chondroitin sulphate				
	Heparin				
Group Four Zwitterionic Polymers	F	N/N1003A	7 days	DAPI, Phalloidin, αSMA and resazurin	Contact angle, SEM and WLI
	G				
	H				
	I				
	J				
	K				
	L				
	M				

Polymer coatings provided by BioInteractions Ltd. grouped into experiments 1 - 4. For each group the coating codes are present, details of what cell line was used, duration of each experiment, what staining was performed and what surface analysis techniques were used. All coatings were sterilized for 5 minutes at 150J/cm^2 using CL-1000 ultraviolet crosslinker (UVP) prior to use.

2.1.2 Cell Culture Techniques

All cell culture was carried out using a class II microbiology hood. Microbiology hoods were cleaned with virkon (Du Pont) and 70% ethanol (University of Liverpool's Chemistry Department). All cell vessels were purchased from Greiner Bio One and cells were cultured in the incubator at 37°C at 5% CO_2. All phosphate buffered solution (PBS, Oxoid) used was calcium and magnesium free. Three cell lines were used throughout this study (Table 2-2). Cells were maintained in minimum essentials medium eagles (MEME, Sigma Aldrich) supplemented with either, fetal calf serum (FCS, Biosera) or rabbit serum (RS, Sigma Aldrich) and 1 % L-Glutamine (L-Glut, 200mM, Sigma Aldrich).

Table 2-2: Details of the three cell lines used throughout this PhD project

Cell Type	Code	Origin	Culture Conditions
Human-LEC	FHL124	kindly donated by Dr John Reddan of Oakland University, MI, USA	MEME + 5% FCS + L-Glut
Human-LEC	B3	kindly donated by Barbara Pierscionek of University of Ulster, Coleraine, Northern Ireland	MEME + 10% FCS + L-Glut
Rabbit-LEC	N/N1003A	kindly donated by Dr John Reddan of Oakland University, MI, USA	MEME +8% RS + L-Glut

Table details human and rabbit LEC lines used, including code names, where they were obtained from, what culture medium was used and the concentration of serum that was used.

Cells were fed every 2 – 3 days by removing around ⅔ of medium from the flask or well and replacing with fresh medium. Cells were checked at the same time under the phase contrast microscope, Diaphot (Nikon) for abnormal growth and infections. All cell lines became confluent within a week. Once cells became confluent FHL124 LECs were passaged at a 1:3 ratio, B3 and N/N1003A LECs were passaged at a 1:5 ratio. To passage cells all culture medium was removed from the flask or well and cells were washed with PBS. A solution of 0.5mg/ml porcine trypsin and 0.2mg/ml EDTA (trypsin, Sigma Aldrich, UK) in PBS was used. Enough solution was added to cover the base of the vessel and cells were incubated for ~4 minutes at 37°C. Cells were then removed from the

incubator and viewed under the microscope to ensure all cells had dislodged. The trypsin was quenched in medium containing serum, transferred to a universal and centrifuged at 1000 RPM (180g) for 5 minutes. Once finished the supernatant was discarded (cell freezing or cell counting was performed if necessary sections 2.1.3 and 2.1.4). The pellet was resuspended in fresh medium and split at the appropriate ratios mentioned above into new flasks or wells, and placed in the incubator. FHL124's were kept to approximately passage 25, B3 and N/N1003A LECs were kept to approximately passage 45. All cells lines were stained for cytokeratin, as a marker for epithelial cells, and alpha B-crystallin to characterise their phenotype (2.1.17).

2.1.3 Freezing and Retrieval of LECs

Freezing down cells was routinely carried out to create a stock of cells that could be used at a later date. Cells were removed using trypsin and centrifuged, as detailed above. The pellet was suspended in 900µl of fresh MEME containing 20% FCS or 20% RS (depending on the cell type) and transferred to a cryovial. 100µl of cryopreservation medium, dimethyl sulphoxide (DMSO, Sigma Aldrich, UK), was added gradually in a swirling motion to mix the solution. Cryovials were labelled and then placed in the isopropanol container, "Mr Frosty®", (Nunc International, UK) and stored in a -80°C freezer. This provided a repeatable cooling rate of -1°C/minute before transferring the cyrovials into the liquid nitrogen dewar, (at -196°C) for long term storage. Cells were retrieved by warming a cryovial in the water bath (37°C) for a couple of minutes until thawed. Cell solution was then transferred into a universal containing 10 - 15ml of fresh warm medium containing serum, to dilute the DMSO. Cells were then centrifuged (2.1.2), however this time all resuspended cell solution was transferred into one flask.

2.1.4 Seeding Cells

Throughout this PhD cells were seeded at a known density per cm^2 onto tissue culture treated polystyrene (TCPS) plates and surface coatings provided by BioInteractions Ltd. and monitored for a period of days. To do this a haemocytometer was used to count the cells. Cells were lifted from the flask using trypsin (outlined above in section 2.1.2) and centrifuged. Cells were resuspended in fresh medium and 20µl of the cell solution was pipetted into the haemocytometer. Cell counts were taken from the four corner

grids of the haemocytometer chamber. The total number of cells was averaged to give the number of cells/ml. Based on the required seeding density and area of the well cells would be seeded into, the volume of cell solution per well was calculated. The remaining volume of medium needed per well was then calculated. The total volume of cell solutions needed for all wells for the experiment was calculated, and added to the correct volume of fresh medium in a glass bottle and mixed well prior to seeding. Using a multivolume dispenser pipette, 1ml of the cell/medium solution was added into each well of a 24 well plate. This volume varied slightly depending on the size of the plate used for each experiment. Plates were placed in the incubator. Representative phase contrast micrographs were taken throughout the study starting at day one and cells were fed every 2 – 3 days.

2.1.5 Seeding Density Growth Curve

A cell growth curve is a way of establishing the general growth pattern at different time intervals for a particular cell type. To determine the optimum seeding density for FHL124 LECs, a seeding density growth curve was set up in a 24 well plate. Initially three seeding densities were tested, $1x10^3/cm^2$, $1x10^4/cm^2$ and $1x10^5/cm^2$. Four wells per concentration were set up, cells were counted on days 1, 4, 7 and 10. Cells were counted using a haemocytometer. This was then repeated at seeding densities, $5x10^3/cm^2$ and $1x10^4/cm^2$, however this time cells were fixed, micrographed and cell nuclei were counted. In order to visualise the nuclei, cells were stained with 100% Mayer's haematoxylin (Leica Biosystems, UK, section 2.1.9). Three random micrographs per well were taken using the inverted phase contrast microscope, images were analysed using ImageJ cell counter plug-in, by placing a marker on each cell to count cells per field of view (2.1.7). Cells were considered to be mononuclear, therefore each nuclei counted corresponded to one cell. The chosen seeding density was used for other cell lines to compare cell growth across all surface coatings.

2.1.6 Serum Growth Curve

The optimum serum concentration was not known for FHL124 LECs therefore a serum growth curve was set up using a similar method as detailed in 2.1.5. Cells were seeded onto 24 well plates at a seeding density of $1x10^4/cm^2$. The following serum

concentrations were tested, 5%, 10% and 20% FCS. FHL124 LECs were fixed on days 1, 3 and 4 with absolute methanol (Fisher Scientific, UK) and stained with Mayer's haematoxylin (2.1.9). Again three random images were taken per well using the inverted phase contrast microscope, and cells were counted using ImageJ cell counter plug in (2.1.7).

2.1.7 Image Analysis for Coated Surfaces

In order to analyse average cell growth on coatings, cells were stained with Mayer's haematoxylin and micrographed using the Diaphot inverted phase contrast microscope (Nikon, UK), or fluorescently stained with Propidium Iodide (PI) or 4′,6-Diamidino-2-phenylindole dihydrochloride (DAPI) and micrographed using the Axiovert 200 inverted microscope (Zeiss, UK). To achieve an average cell count per field of view, three micrographs per well were taken with an x10 objective, or four micrographs with an x20 objective. For seeding density (2.1.5) and serum (2.1.6) studies random micrographs were taken. For material coating studies micrographs were taken in approximately the same area each time to compare cell growth across coatings (Figure 2.1). As the material coating should be homogenous one micrograph was taken near the centre, one to the left and one to the right. Cells were considered to be mononuclear, therefore each nuclei counted corresponded to one cell. Nuclei were counted and then averaged across all wells of the same coating for that time point.

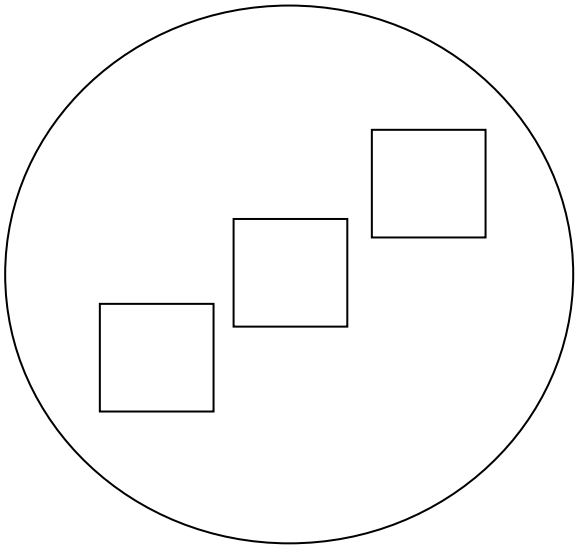

Figure 2.1: Schematic to illustrate the photographed area of each well for the purpose of cell counting. The squares represent the approximate positions of photographed area in a well of a 24-well plate. As the coating should be homogenous three micrographs were taken in approximately the same area in each well. One in the centre, one to the left hand side and one to the right hand side.

Cells were counted using ImageJ version 1.45S software package (National institute of Health, USA) in one of two ways. Either by using the cell counter plug-in to place a marker on the cell when clicked and count the total markers, or a macro configured to count cells automatically by converting the image to binary and counting the particles larger than 40 pixels.

2.1.8 Harvesting Human Primary LECs

Human donor globes were either retrieved from The Manchester Eye Bank or The Royal Liverpool University Hospital, following local ethical approval and conforming to the Human Tissue Act (2004). Donor globes reached the laboratory within 48 hours post mortem. All dissections were carried out in a class I dissection hood. The dissection hood was cleaned, along with any equipment that was needed. In order to retrieve the lens the whole globe was cut along the equator and the anterior segment removed. The zonules were careful cut and the lens, with the capsular bag intact, was lifted free and placed on a piece of filter paper (Whatman, UK). The paper allowed the lens to remain stable whilst performing a capsulorhexis. A small amount of MEME or PBS was added to stop the capsular bag from becoming tacky and sticking to the paper. A 25 gauge needle

(Sherwood Medical, UK) was attached to a 1ml syringe and was bent at 2 right angles to produce a step-shaped needle (Figure 2.2).

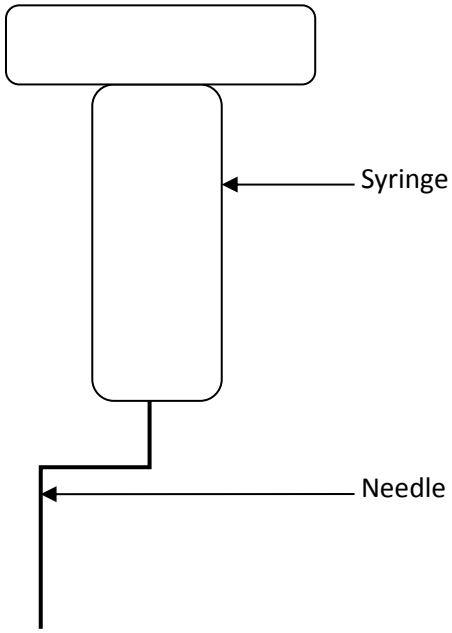

Figure 2.2: Schematic of the bent needle used to perform capsulorhexis. A 25 gauge needle attached to a 1ml syringe. The needle was bent in a step-shape to help perform a capsulorhexis on a human donor lens.

Using this needle a small nick was made in the capsule and a capsulorhexis was performed (Figure 2.3). The lens was hydrodissected away from the capsular bag with a similar procedure to cataract surgery. The remaining bag was removed from the filter paper and placed into a well of a 6 well plate epithelial side down, along with the removed anterior capsulorhexis explant. The sample was incubated at 37°C with a small amount of MEME supplemented with 20% FCS, 1% L-Glut, 1% penicillin streptomycin (Pen-Strep, 10,000 units penicillin and 10mg streptomycin/ml, Sigma Aldrich) and 1% Amphotericin B (fungizone, 250µg/ml Sigma Aldrich). More medium was added 1-2days later when the capsular bag explant had settled and adhered to the well. Cells were fed every 3 – 4 days, by removing half the medium and replacing with fresh medium.

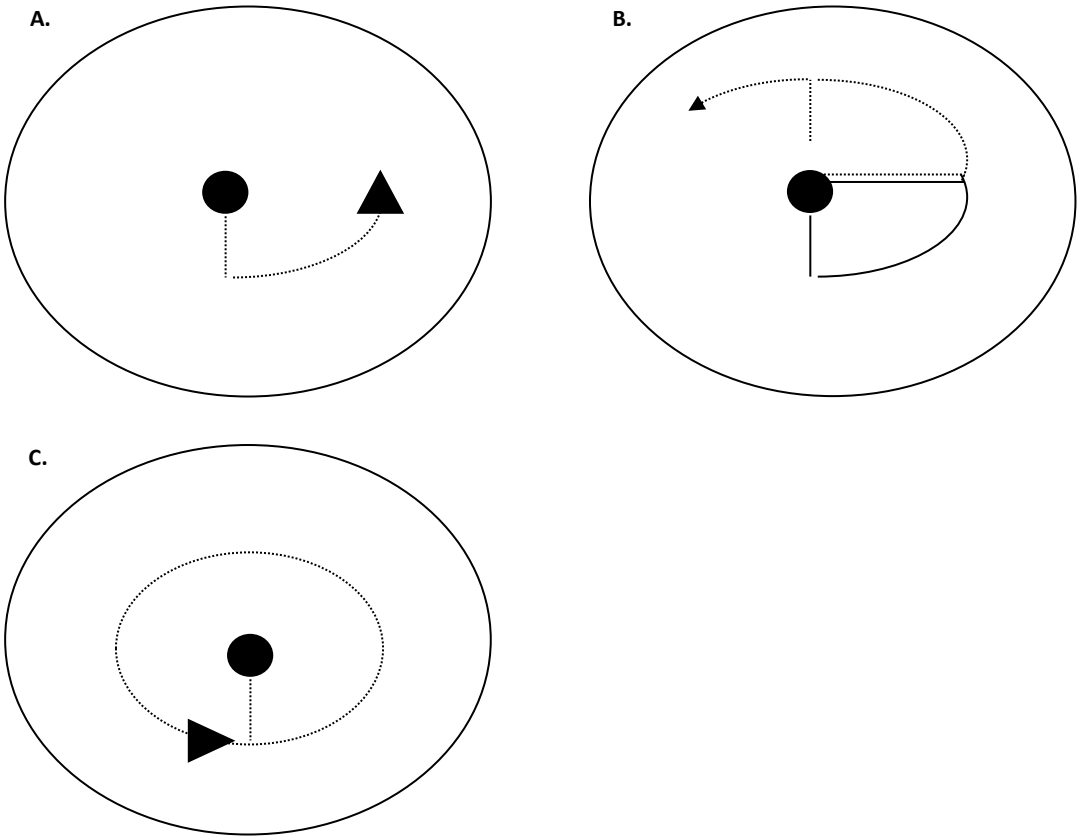

Figure 2.3: Schematic to demonstrate how a capsulorhexis was performed. A. First a nick was made in the centre of the lens capsule. This was dragged down and towards the right in an anticlockwise motion. B. The anti clockwise circular motion was continued up and round to a 12 o'clock position. C. The circular motion was followed down to meet to original 6 o'clock position, completing the capsulorhexis.

Performing the capsulorhexis and hydrodissecting the lens out of the capsular bag can be very difficult and was not always successful. As this method was inefficient a variation to the technique was made after a nick in the capsular bag had been made with the needle (Figure 2.4-A). Using this nick a small section of the anterior capsule was cut away. Using this hole in the anterior capsule, cuts were made towards the equator of the capsule using a pair of small surgical scissors (Figure 2.4-A). These cuts/flaps were peeled back with a pair of forceps to reveal a flower shape (Figure 2.4-B). The lens was hydrodissected out from the centre and the capsular bag was placed in a Petri dish as described above.

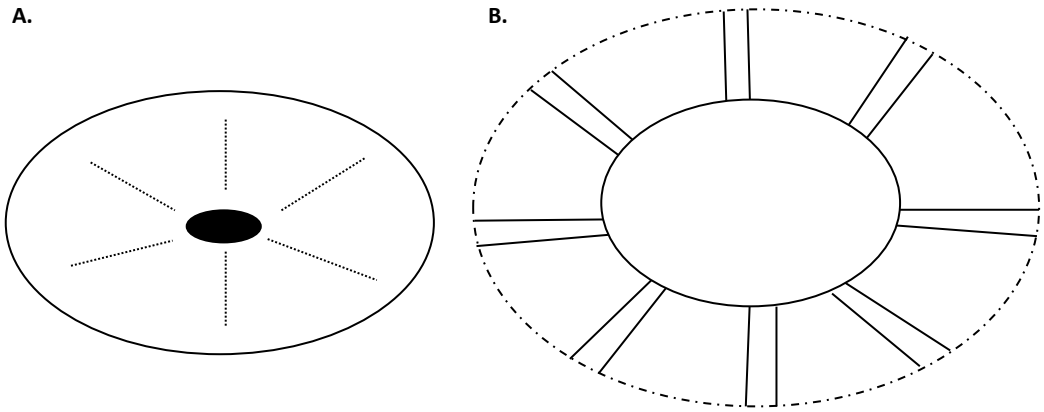

Figure 2.4: Schematic displays an alternative method performed to remove the lens from the capsular bag. A. First a nick was made in the centre of the lens capsule. A pair of scissors where then used underneath this nick and small cuts were made towards the equator. B. These cuts/flaps were peeled back to reveal a flower shape and expose the lens. Meaning the lens could be removed from the capsular bag.

2.1.9 Mayer's Haematoxylin

Cells were stained with Mayer's haematoxylin for the purpose of visualising cell nuclei, using the following protocol:

1. Removed medium from wells
2. Rinsed cells three times with PBS
3. Fixed cells with absolute methanol (Fisher Scientific, UK) for 5 minutes at 4°C
4. Removed methanol
5. Rinsed cells a further three times with PBS
6. Added Mayer's haematoxylin (1%) for 4 minutes
7. Removed Mayer's haematoxylin and rinsed cells with water for approximately a minute until the water ran clear
8. Added 250µl of PBS to each well to achieve a clearer micrograph

2.1.10 Methylene Blue

Cells were stained with methylene blue (Sigma Aldrich, UK) for the purpose of visualising cell nuclei, using the following protocol:

1. Removed medium from wells
2. Rinsed cells three times with PBS
3. Fixed cells with absolute methanol (Fisher Scientific, UK) for 5 minutes at 4°C
4. Removed methanol
5. Rinsed cells a further three times with PBS
6. Added methylene blue (0.05 wt%) for 2 minutes
7. Removed methylene blue and rinsed cells with water for approximately 1 minute until the water ran clear
8. Added 250µl of PBS to each well to achieve a clearer micrograph

2.1.11 Toluidine Blue

Toluidine blue (Sigma Aldrich, UK) was used to stain for the presence of glycosaminoglycan (GAGs) on coatings, using the following protocol:

1. Toluidine blue (0.1 w/v% in deionised water) was added to GAG coatings for 5-10 minutes
2. Removed toluidine blue and coatings were rinsed with water
3. Micrographs were taken of the stained coatings

2.1.12 Resazurin

A resazurin (Sigma Aldrich, UK) assay was used to assess the metabolic activity of LECs, using the following protocol:

1. Stock resazurin (1mg/ml) in MEME medium was made up and kept for up to six months at 4° in foil
2. Removed medium from wells
3. Make up 10% resazurin working solution in medium and add to LECs
4. Incubate for 3 hours at 37°
5. Aliquot 100µl of 10% resazurin from wells into a black 96 well plate in triplicate
6. Discard of remaining resazurin and rinse cells with PBS before adding fresh medium
7. Read plate on a fluorescence plate reader at 530 excitation/590 emission wavelengths

2.1.13 Propidium Iodine

Propidium Iodine (PI) (Sigma Aldrich, UK) is a nuclear stain which binds to the DNA inside nuclei and fluoresces red (excitation 491-496nm; emission 636-642nm). To stain with PI the following protocol was used:

1. Removed medium from wells
2. Rinsed cells three times with PBS
3. Fixed cells with either methanol or 10% neutral buffered formaldehyde (NBF, BIOS Europe ltd) at room temperature for 10 minutes
4. Removed fixative
5. Rinsed cells a further three times with PBS
6. PI solution (100µl Ribonuclease (RNase, Sigma Aldrich), 895µl PBS and 5µl PI) was added to cells (not in direct light) and left for 5 minutes at room temperature on a laboratory rocker
7. Removed PI and rinsed cells three times with PBS
8. Refilled wells with PBS so cells did not dry out

2.1.14 DAPI

DAPI (Invitrogen, UK) is another nuclei stain which fluoresces blue (excitation 350nm; emission 470nm). To stain with DAPI the following protocol was used:

1. Removed medium from wells
2. Rinsed cells three times with PBS
3. Fixed cells with either methanol or NBF
4. Removed fixative
5. Rinsed cells a further three times with PBS
6. A working stock was made (1µl of DAPI to 2999µl of PBS) and was used at a 1:10 ratio stock:PBS
7. DAPI was added (out of the light) and left for 5 minutes at room temperature on a laboratory rocker
8. Removed DAPI and rinsed cells three times with PBS
9. Refilled wells with PBS so cells did not dry out

2.1.15 Phalloidin

Phalloidin (phalloidin 488 (excitation 495nm; emission 518nm), Invitrogen, UK) is a cytoskeleton stain that stains f-actin fibres in a cell and was used to examine the cells morphology. To stain with phalloidin the following protocol was used:

1. Removed medium from wells
2. Rinsed cells three times with PBS
3. Fixed with NBF
4. Removed fixative
5. Rinsed cells a further three times with PBS
6. Permeabilised cells with 1% Triton X (Sigma Aldrich, UK, diluted in PBS) for 5 minutes at 4°C
7. Removed Triton x and rinsed cells three times with PBS
8. phalloidin was added (out of the light) at a concentration of 1:40 made up in 0.1% Tween 20 (Sigma Aldrich, UK, diluted in PBS) for 30 minutes at room temperature on the laboratory rocker.
10. Removed phalloidin and rinsed cells three times with PBS (nuclei staining was performed at this stage)
11. Refilled wells with PBS so cells did not dry out

2.1.16 Live/Dead Assay

A live dead assay (Invitrogen, UK) was used as a staining method to give an indication of how a coating or environment affected the cells. Live cells were stained green and dead cells stained red, using the following protocol:

1. Removed medium from wells
2. Rinsed cells three times with PBS
3. Live/Dead solution was made up of calcein-AM (green) at 1:500(PBS) and ethidium homodimer-1 (red) at 1:200
4. Each solution was added (out of the light) simultaneously and left for 30 minutes at 37°C
5. Live/Dead assay solution was removed and cells were rinsed three times with PBS
6. Refilled wells with PBS so cells did not dry out and imaged immediately

2.1.17 Primary and Secondary Antibody Staining

Cells have been stained with various antibodies. These include various cytokeratin as an epithelial marker to characterise the cell phenotype, alpha B-crystallin protein (Abcam) as an additional characterisation method and alpha smooth muscle actin (αSMA, Abcam, UK) as a marker for dedifferentiated LECs (
Table 2-3).

Table 2-3: Details of antibodies used throughout the PhD project

Antibody	Clone	Concentration
Mouse monoclonal pan cytokeratin (CK 4, 5, 6, 8, 10, 13 & 18) (Santa Cruz, Insight biotechnology, UK)	C11	1:100
Mouse monoclonal pan cytokeratin (CK 8 & 18) (Abcam, UK)	NCL-5D3	1:100
Mouse monoclonal cytokeratin (19) (Dako, UK)	RCK108	1:100
Mouse monoclonal pan cytokeratin (1, 2, 3, 4, 5, 6, 7, 10 ,13, 14, 15, 16 & 19) (Dako, UK)	AE1/AE3	1:100
Mouse monoclonal pan cytokeratin (5, 6 8, 17 & probable 19) (Dako, UK)	MNF116	1:100
Mouse monoclonal alpha B-crystallin (Abcam, UK)	1B6.1-3G4	1:100
Mouse monoclonal αSMA (Abcam, UK)	1A4	1:100

Table detailing primary antibodies, antibody clone and the concentrations used at.

Antibody staining was performed following the below protocol:

1. Removed medium from wells
2. Rinsed cells three times with PBS
3. Fixed with either methanol or NBF
4. Removed Fixative
5. Rinsed cells a further three times with PBS
6. Permeabilised cells with 1% Triton X (Sigma Aldrich, UK, diluted in PBS) for 5 minutes at 4°C
7. Removed Triton x and rinsed cells three times with 0.1% Tween 20
8. Blocked cells with 10% goat serum (Sigma Aldrich, UK) diluted in PBS:1% bovine serum albumin, (BSA, Sigma Aldrich, UK) for 30 minutes at 37^{o}C
9. Primary antibody and negative control mouse IgG (Dako, UK) was added at 1:100 (PBS:1%BSA) overnight on a laboratory rocker at 4^{o}C (out of light)

10. Removed antibody and rinsed cells thoroughly with 0.1% Tween 20
11. Alexa Fluor® secondary antibodies (Invitrogen, UK) were added (out of light) at 1:100 or 1:250 (PBS:1%BSA) for 1 hour at 37°C
12. Removed secondary and rinsed cells thoroughly with PBS:Tween 20
13. Performed phalloidin (2.1.15) and/or nuclei staining (2.1.13 or 2.1.14, optional)
14. Refilled wells with PBS so cells did not dry out and imaged immediately

2.1.18 Surface Analysis

Several surface analysis techniques were used throughout this PhD, including contact angle measurement (CA) analysis, scanning electron microscopy (SEM) and white light interferometry (WLI).

2.1.18.1 Contact Angle

The wettability of coatings was determined by measuring the CA at the surface/liquid interface by dispensing a small water bead onto a sample, using the DSA 100 (KRÜSS GmbH, Germany). Throughout this PhD the sessile drop technique was used for measuring static CA. This involved dispensing a drop from a syringe and using a goniometer to capture an image.

The DSA 100 has two set ups for dosing different sized water beads, a macro and a piezo-electric system, the principle is the same for each set up. Both set ups have been used during this PhD. When the macro set up was used a 2 µl drop size was chosen and nine points per sample were measured, in three rows of three across the sample, completed in triplicate. In the piezo-electric set up water was dispensed through a piezo dosing unit and the voltage and pulse width determine how much water was dispensed. A voltage of 80V and a pulse of 200µs was selected which gave roughly 720pl – 960pl drop size. Again nine readings per sample were taken in triplicate. A circle profile function was fitted to all water droplets. The CA was determined by measuring the angle of intersection between the baseline (surface of sample) and this circle profile.

2.1.18.2 Scanning Electron Microscopy

Scanning electron microscope (SEM) analysis was performed using the LEO 1550 (Zeiss, UK) to examine the topography of the coatings provided by BioInteractions Ltd. this was particularly useful in checking for homogeneous coatings. Coated coverslips were placed onto SEM stubs before chromium coating using the EMI TECH K575X (Quorum Technologies, UK) to make them conductive. Each sample was coated twice with chromium to give a coating thickness of roughly 200nm. Three to five random areas of the sample were micrographed per magnification. This was performed in triplicate.

2.1.18.3 White Light Interferometry

White light interferometry (WLI) analysis was performed using the WYKO NT3300 profilometer (VEECO, USA). Samples were chromium coated first to make them reflective. The same samples that were used for SEM were also used for WLI analysis. To examine the roughness and how uniform the coating was, 3 – 5 random areas of the sample were analysed per magnification (x50 and x100). This was performed in triplicate.

2.1.19 Statistical Analysis

All graphs are presented with mean average ± 1 standard deviation (SD). All statistical analysis was performed using IBM SPSS V.20 statistics software. One-way ANOVA was used to measure the statistical significance followed by Dunnett's T3 or Tukey's post hoc test, depending whether homogeneity of variances were significantly different or not significantly different, respectively. Statistical significance was assumed when $p<0.05$.

2.2 Anticoagulation Polymers Coatings – 1

For material coatings in group one, two and three (Table 2-1) the chemistry was quite similar and the base polymer for all was polyethylenimine (PEI). The preparation of PEI is outlined below.

All solutions were made up in ultra-pure water to an end volume of 500ml. All washes were performed using deionised water. All solutions were mixed well and the pH was checked as the pH can greatly affect the charge and amine groups present. The following mixtures were made up:

(1) PEI mixture (BioInteractions Ltd. UK) was used at 4% by adding 20g of PEI was added to 500ml of ultra-pure water (pH 10). The basic polymer absorbs carbon dioxide and reduces the pH so it was covered with foil (for approximately 15 minutes), until ready to be used.

(2) Polymer B (BioInteractions Ltd. UK) was a mixture of sulphates, sulfonates and polyethylene glycol (PEG) with no heparin. Sodium tetraborate buffer (BioInteractions Ltd. UK) was used with this polymer (pH 8.5). 1.25g of polymer B was added to 500ml of ultra-pure water.

(3) Both mixtures were crosslinked with glutaraldehyde (25% solution pH 6.5, BioInteractions Ltd. UK. 1.5ml was added to the 500ml of ultra-pure water. Once mixed the solution was stored at 4^{o}C until it was ready to use.

After all solutions were made up PEI was polymerised into 24 well plates by adding 1ml/well of solution (1) for 5 minutes at room temperature, then plates were rinsed three times with water. Followed by 1ml/well of solution (2) for 5 minutes at room temperature, and again rinsed three times. 1ml /well of cross linking agent (3) was then added for a final 5 minutes at room temperature and again rinsed three times. Wells were rinsed a final time with ultra-pure water before plates were left to dry in the oven at 40^{o}C for 1 hour. Coverslips were made in the same way for surface analysis, by submersing the coverslips in a Petri dish containing each solution for 5 minutes. Care was taken to make sure they did not overlap, to provide an even coating and reduce scratches. Coverslips were placed in clips and stacked in a rack to dry in the oven.

The additional layers on top of the PEI vary in terms of the functional groups present and end charge, dictating how the polymer interacts with the cells. Although the base chemistry for coatings in group 1 and group 2 was the same each coating has a slightly different composition. Each coating contains three components, heparin, negative charged sulphates and hydrophilic PEG chains, each of these components plays a specific role within the coating (Figure 2.5).

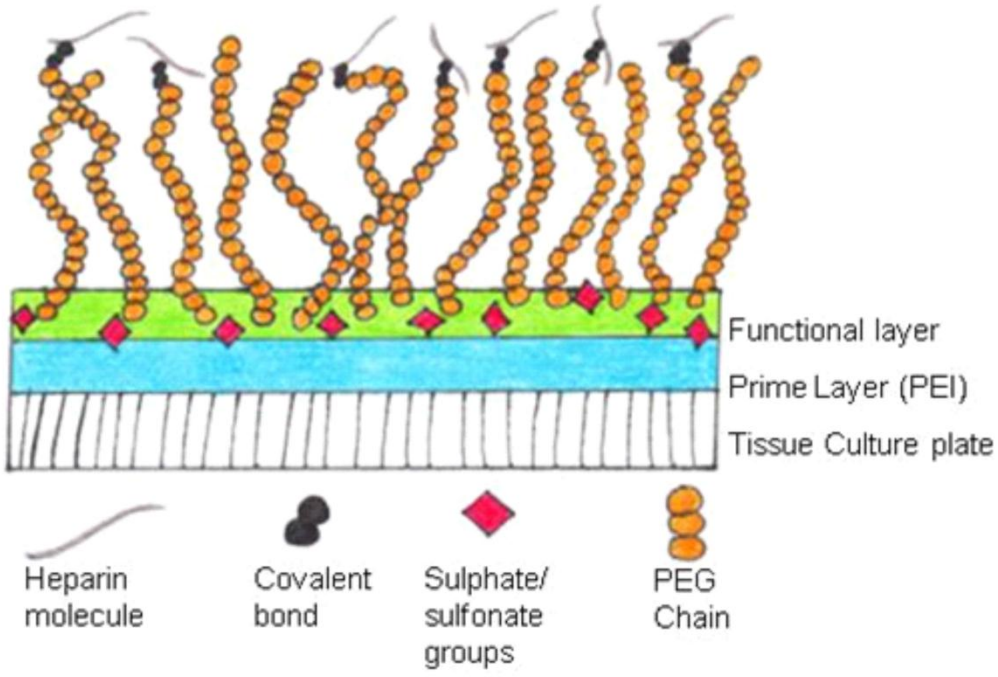

Figure 2.5: Schematic of the base chemistry for coatings 001, 002 and 003. Each coatings varies slightly in terms of the number of layers but all contain PEI base then additional PEG, sulphates, sulfonates and heparin groups which are designed to repel cell and protein attachment. Adapted from BioInteractions Ltd [159].

Coating 001 was a two layer water based polymeric coating, it has a positively charged primer layer which is PEI and can bind to both hydrophobic and hydrophilic surfaces. The second copolymer layer is negatively charged containing PEG which enhances hydrophilicity and laminar flow, sulphates and sulfonates to repel cells and heparin to confer anti-thrombogenic properties. Coating 004 is similar to 001 and only varies in terms of the number of layers and thus the amount of functional groups, PEG and heparin. Poly HEMA (pHEMA) is a 2-hydroxyethyl methacrylate which functions as a

hydrogel and has been previously used in clinic for IOL materials and therefore used as a control.

2.2.1 Cell Growth Study

Coatings were tested in a preliminary qualitative manner to optimise the coating process and cell culture techniques. Coatings 001, 004 and pHEMA were synthesized onto glass coverslips (13mm diameter) and directly into 24 well plates. FHL124 LECs were seeded on coated coverslips (13mm diameter) at $1x10^4/cm^2$. Six coverslips per coating were set up, and LEC attachment and growth was monitored for a total of 7 days. In addition LECs were seeded into a coated 24 well plate (eight wells per coating). LEC attachment and growth was evaluated whilst in culture for a total of 11 days. Uncoated TCPS wells served as a control in both studies to examine typical LEC growth and attachment in culture. For both studies representative phase contrast micrographs were taken throughout the study starting at day 1 and cells were fed every 2 – 3 days.

2.2.2 Cell Staining

Coated coverslips were fixed at day 7 with methanol for 5 minutes and stained with Mayer's haematoxylin (2.1.9), to visualise the cell nuclei and cytoplasm of the cell. Coated wells were fixed at day 11 and a live/dead assay (2.1.15) was carried out.

2.3 Anticoagulation Polymers Coatings – 2

Coating 002 has the same composition as 001 but has been lightly crosslinked using glutaraldehyde. Coating 003 is similar to coating 002 but has a total of five water based high molecular weight polymer layers. Similar to 002 more functional groups are present, when compared to 001, and it too has been lightly crosslinked with glutaraldehyde to confer stability (Figure 2.6).

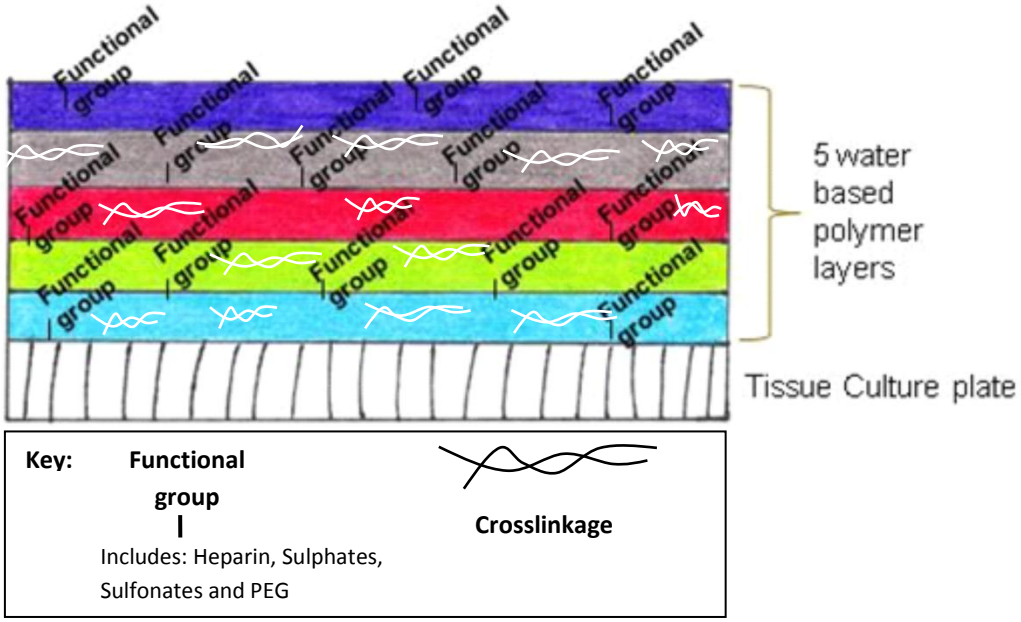

Figure 2.6: Schematic of multi-layered coating 003 provided by BioInteractions Ltd. Due to 003 having five layers more functional groups were present, including heparin, sulphates and PEG. Adapted from BioInteractions Ltd. 2010

2.3.1 Cell Growth Study

Coatings from group 2 (001, 002 and 003) were synthesized directly into 24 well plates, and examined for a longer time period of 14 days. Plates were fixed at days 1, 4, 7, 10 and 14. FHL124 LECs were seeded at $1x10^4/cm^2$ into six coated wells per coating for each time point. Uncoated TCPS wells served as a control. Representative phase contrast micrographs were taken throughout the study starting at day 1, and cells were fed every 2 – 3 days.

2.3.2 Cell Staining

At the various time points (days 1, 4, 7 10 and 14) cells were fixed with NBF and stained with PI (2.1.13) and phalloidin (2.1.15). The average cell growth on each coating per time point was calculated by counting the cell nuclei using ImageJ cell counter plug-in.

2.3.3 Surface Analysis

CA measurements were taken using the macro system (2.1.18.1). Nine CA measurements were taken across each sample, repeated in triplicate. Coatings were also examined under the SEM (2.1.18.2). A wide area of the sample was viewed and 3 – 5 representative micrographs of the coating were taken, again repeated in triplicate.

2.4 GAG Coatings

Three methods of synthesising GAG coatings were investigated to examine if the cellular response was affected by the GAG itself or how the GAG was bound to the surface. The three methods were: firstly, BioInteractions Ltd. polymer GAG coatings (2.4.1), secondly, GAGs dissolved in medium then adsorbed onto various substrates (2.4.2) and thirdly, covalently bound GAGs onto amine coated coverslips (2.4.3). Adsorbed GAG coatings and bound GAG coatings only examined hyaluronic acid (HA) and chondroitin sulphate (CS) as the response of heparin (HEP) was well established and no further evaluation was required.

2.4.1 BioInteractions Ltd. Cell Polymer Coatings

BioInteractions Ltd. synthesised HEP, HA and CS, using a proprietary method, directly into 24 well plates, each plate contained all three GAGs (eight wells per coating). An additional uncoated TCPS plate was used as a control.

2.4.1.1 Cell Growth Study

N/N1003A LECs were seeded onto GAG polymer coatings and TCPS at a seeding density of $1x10^4/cm^2$. Representative phase contrast micrographs were taken throughout the study starting at day 1 and cells were fed every 2 – 3 days. Cells were fixed at days 1, 4, and 7 with NBF.

2.4.1.2 Cell Staining

GAGs plates were fixed with NBF on days 1, 4, 7 10 and 14. Cells were stained with phalloidin (2.1.15), to examine the cytoskeleton, αSMA (2.1.17) to view myofibroblast cells and give an indication of dedifferentiation and DAPI (2.1.14) to stain the nuclei. Three micrographs per well were taken using an x10 objective. The average cell growth on each coating at each time point was measured by counting cell nuclei using a configured macro to count cells in ImageJ.

2.4.1.3 Surface Analysis

Polystyrene coverslips were coated with HEP, HA and CS for the purpose of surface analysis. The piezo-electric system was used for CA measurements (2.1.18.1), 9 points

per sample were measured, repeated in triplicate. Their topography was investigated using SEM (2.1.18.2) and WLI (2.1.18.3). Five areas per sample were analysed on WLI at x50 objective, repeated in triplicate.

2.4.1.4 Time Lapse Microscopy

GAGs coatings were also examined using the IncuCyte time lapse microscopy (Essen BioScience) for a total of 14 days, micrographs were taken every hour to build up a video of still micrographs. Micrographs were taken in the exact same location each time using a motorised stage and software.

2.4.2 Adsorbed GAG Coatings

Five variations of the adsorbed GAG assay were studied to optimise the conditions (Table 2-4). These included varying the: concentration of HA and CS (0.01mg/ml, 0.1mg/ml, 1mg/ml, 5mg/ml and 10mg/ml), incubation times (3 hours and 24 hours), temperatures (4°C and 37°C) and substrates (TCPS plastic, PEI base polymer and polystyrene coverslips (PS, Goodfellow, UK, roughly cut 10mm x 10mm). In addition HA and CS were added to the cell culture medium.

Table 2-4: To detail the various incubation times and optimisation of the soluble GAG assay.

#	Incubation Time	Concentrations	Substrates
1	3 hour incubation at 37°C – GAGs rinsed off	0mg, 0.01mg, 0.1mg, 1mg, 5mg and 10mg – 500µl p/w	Base polymer, TCPS & PS
2	3 hour incubation at 37°C – GAGs not rinsed off	0mg, 0.01mg and 0.1mg and 1mg – 500µl p/w	Base polymer, TCPS and PS
3	24 hour incubation at 37°C – GAGs not rinsed	0mg, 0.01mg and 0.1mg and 1mg – 500µl p/w	Base polymer and TCPS
4	24 hour incubation at 4°C – GAGs not rinsed off	0mg, 0.01mg and 0.1mg and 1mg – 500µl p/w	Base polymer and TCPS
5	GAG added in medium	0mg, 0.01mg and 0.1mg and 1mg – added in medium	Base polymer, TCPS and PS

The above table presents all adsorbed GAG assays tested, numbered 1-5. Various incubation times and concentrations were tested to optimise the process of binding the GAGs to the different substrates.

HA and CS were dissolved in medium and mixed well prior to adding either 500µl or 1000µl per/well to the substrates at the above concentrations, temperatures and time periods. HA and CS were removed and wells were either rinsed with fresh medium or not before seeding N/N1003A LECs. To replicate the same environment as the polymer GAG coatings provided by BioInteractions Ltd. HA and CS were adsorbed onto the base polymer, as this was the base material present in the polymer GAG coatings. LECs seeded straight onto the base polymer in the absence of any GAG served as a positive control. To confirm if the HA and CS encouraged cell growth or the base polymer, LECS were seeded onto PS coverslips either in the presence or absence of adsorbed GAG. LECs seeded onto PS in the absence of any GAG served as a negative control as PS does not encourage cell growth. LECs were also seeded onto TCPS in the presence or absence of adsorbed GAG. LECs seeded onto TCPS in the absence of any GAG served as a control.

2.4.2.1 Cell Growth Study

N/N1003A LECs were seeded onto the adsorbed coatings (4 wells per GAG concentration) at a seeding density of $1x10^4/cm^2$. Cells were fed every 2 – 3 days and monitored for a total of seven days. Base polymer, PS and TCPS wells with the absence of GAGs served as controls. Representative micrographs were taken on days 1, 4 and 7. Micrographs were taken from the same well in roughly the same area at each time point so cell growth could be monitored throughout the study.

2.4.2.2 Quantifying the Amount of GAG Present

Toluidine blue was used at 0.1% w/w in distilled water to assess whether the GAG was present (2.1.11). Toluidine blue was added to adsorbed GAG coatings for 5 minutes and then removed and rinsed with water. If HA and CS were present the coated wells or coverslips stained blue.

2.4.3 Bound GAG Coatings

HA and CS were immobilised onto modified 13mm glass coverslips (Agar Scientific, UK) coated with amine functionality by silinisation. GAGs were bound onto glass coverslips following the below protocol:

1. 10% 3-aminopropyl-triethoxysilane (APTES, Sigma Aldrich, UK) was made up in isopropanol
2. Glass coverslips were placed inside 24 well plates (4 coverslips per concentration).
3. APTES (10%) solution was mixed well then pipetted onto glass coverslips and left for 10 minutes
4. Coverslips were washed thoroughly with isopropanol
5. APTES coated coverslips were left to air dry overnight
6. 3mg/ml, 1mg/ml and 0.1mg/ml of HA and CS were dissolved in a solution of 0.01M 2-(N-morpholino)ethanesulfonic acid (MES, Sigma Aldrich, UK) buffer
7. GAGs were added to a reaction solution of 0.05M N-hydroxysuccinimide (NHS, Sigma Aldrich, UK)/0.2M 1-ethyl-3(3-dimethylaminopropyl) carbodiimide hydrochloride (EDC, Sigma Aldrich, UK) sequentially, made up in MES buffer, to activate the GAGs
8. Activated GAG solutions were stirred for 1 hour at room temperature
9. 1ml of activated GAG solution was added to amine coated coverslips overnight at room temperature on a laboratory rocker
10. The following morning bound GAG coverslips were washed with double distilled ultrapure water (Sigma Aldrich, UK) throughout 24 hours, 2 – 3 changes of water were made
11. 24 hours later the distilled water was removed and bound GAG coverslips were left to air dry for two hours in a class II biological hood
12. Bound GAG coverslips were used in cell culture the same day
13. Prior to seeding cells the coverslips were UV sterilised for 5 minutes at 1500J/cm^2

2.4.3.1 Cell Growth Study

N/N1003A LECs were seeded onto the bound GAG coatings (four wells per concentration) at a seeding density of $1x10^4/cm^2$ for a total of 7 days. Amine coated coverslips, glass coverslips and untreated TCPS wells served as controls. Representative micrographs were taken on days 1, 4 and 7. Micrographs were taken from the same well in approximately the same area at each time point so cell growth could be monitored throughout the study. On day 7 cells were fixed at methanol for 5 minutes at 4°C and stained with methylene blue (2.1.10) to visualise the LECs attachment and growth.

2.4.3.2 Quantifying the Amount of GAG Present

Additional bound GAG coverslips were synthesised and stained with toluidine blue (2.1.11) to determine the presence of HA and CS.

2.4.3.3 Surface Analysis

Additional bound GAG coverslips were synthesised for the purpose of contact angle analysis. The piezo-electric system was used for CA measurements (2.1.18.1), 9 points per sample were measured, repeated in triplicate.

2.5 Zwitterionic Polymers

Six novel zwitterionic coatings (F–K) and three control coatings (L–N) were synthesized directly onto 24 well plates at BioInteractions Ltd. (Table 2-5).

Table 2-5: Composition details of zwitterionic coatings

Coating	Novel Zwitterionic Polymer Composition
F	90% butyl methacrylate 10% novel zwitterionic monomer
G	80% butyl methacrylate 20% novel zwitterionic monomer
H	70% butyl methacrylate 30% novel zwitterionic monomer
I	58% hydroxypropyl methacrylate 31% hexyl methacrylate 11% novel zwitterionic monomer
J	50% hydroxypropyl methacrylate 30% hexyl methacrylate 20% novel zwitterionic monomer
K	50% methoxyethyl methacrylate 30% hexyl methacrylate 20% novel zwitterionic monomer
L	100% poly (butyl methacrylate)
M	90% butyl methacrylate 10% 2-methacryloyloxyethyl - phosphorylcholine (MPC)
N	70% butyl methacrylate 30% 2-methacryloyloxyethyl - phosphorylcholine (MPC)

Composition of zwitterionic coatings and ratios of zwitterionic monomer: comonomer(s) used.

2.5.1 Cell Growth Study

Four wells per coating were synthesised, F-K coatings were in one plate and L-N coatings were in an additional plate. N/N1003A LECs were seeded on coated wells at $1x10^4/cm^2$, uncoated TCPS wells served as a control. Representative phase contrast micrographs were taken throughout the study starting at day 1 and cells were fed every 2 – 3 days. Cells were fixed at days 1, 4 and 7 with NBF.

2.5.2 Cytotoxicity Assay

To test whether the coatings were prohibiting cell attachment via the chemistry and not because the coatings were leaching toxic material into the medium, a cytotoxicity assay was performed, following BS EN ISO 10993-5:2009 using the extraction method. To do this medium was added directly to coatings F-N and incubated at 37° for 48 hours. In addition medium was added to polystyrene coverslips (blank) and TCPS wells (negative control) and incubated at 37° for 48 hours. N/N1003A LECs were seeded at $5x10^4/cm^2$ onto 24 well TCPS plates for 24 hours. Medium from the sub confluent LEC monolayer was removed and replaced with medium from the coatings and control wells. 5% DMSO was added to four wells of sub confluent LECs and served as a positive control to kill the LECs. LEC metabolic activity was monitored at days 1 and 3 by a resazurin (Sigma Aldrich, UK) assay. To do this medium was removed and replaced with medium containing 10% resazurin (in the dark). Cells were incubated for 3 hours at 37°. After this time 100µl of the medium containing resazurin was aliquoted from each well into a black plate in triplicate. The plate was read on the FLx800 microplate fluorescence plate reader (Bio-Tek Instruments INC., UK) at 530 excitation/590 emission wavelengths.

2.5.3 Toxicity Assay

An additional toxicity assay was performed to observe if unattached cells from coatings F-N could be removed from the coated wells, seeded into fresh TCPS wells and attach, spread and grow as usual. LECs were seeded onto the coated wells and left for two hours to attach, TCPS served as a control. After two hours medium with floating cells were removed from coated wells and reseeded onto fresh 24 well plates. As some cells attach to coatings J, L and N the original plates were kept and these wells were refilled with fresh medium, meaning any cells that had adhered in the two hours could continue to grow. The metabolic activity was assessed using resazurin again on days 1 and 4.

2.5.4 Cell Staining

Zwitterionic plates were fixed with NBF on days 1, 4 and 7. Cells were stained with DAPI, (2.1.14) and phalloidin (2.1.15). To assess LEC growth three micrographs per well were taken and the cell nuclei was counted using a macro set up in ImageJ. The average cell growth of each coating at each time point was calculated.

2.5.5 Time Lapse Microscopy

Zwitterionic coatings were examined using the IncuCyte time lapse microscopy (Essen BioScience) for a total of 7 days. Micrographs were taken every hour to build up a video of still micrographs. Micrographs were taken in the exact same location each time.

2.5.6 Surface Analysis

Contact angle measurements were taken using the piezo-electric system (2.1.18.1), 9 points per sample were measured, repeated in triplicate. The topography of the coatings was also examined using SEM (2.1.18.2) and WLI (2.1.18.3). For WLI 4 areas per sample were analysed x50 and four at x100 magnification.

2.5.7 Bulk Materials

Coating F was copolymerised with pHEMA and synthesised as a bulk material. Contact lens moulds were used as IOL moulds were not available. The bulk material was cured using UV light. PHEMA contact lenses were used as a control. Contact lenses were placed in 13mm diameter cell crowns to hold the lens in place inside a 24 well plate. N/N1003A LECs were seeded at $1x10^4/cm^2$ for seven days. To compare the bulk material to the gold standard, LECs were also seeded onto Acrysof (Alcon) acrylic IOLs. Untreated TCPS wells served as a control. Phase contrast micrographs were taken during the seven days in culture. On day 7 cells were fixed with methanol for 5 minutes and cells were stained with methylene blue (2.1.10) to visualise the cell attachment, morphology and growth.

An additional control of C-Flex (Rayner) pHEMA IOL was separately tested to compare LEC response to bulk material pHEMA provided by BioInteractions Ltd. LECs were seeded on Acrysof IOLs to repeat and confirm cellular response. Uncoated TCPS wells were used as a control. Cells were seeded at $1x10^4/cm^2$ for 7 days. Phase contrast micrographs were taken during the 7 days in culture. On day 7 cells were fixed with methanol and cells were stained with methylene blue.

2.6 Dedifferentiation Model and TGFβ3 Assay

The effect TGFβ3 (Invitrogen, UK) had on N/N1003A LECs was examined prior to examining the effect TGFβ3 had on dedifferentiated LECs.

2.6.1 Rabbit Serum Assay

The optimum serum concentration for growing and maintaining N/N1003A rabbit LECs is 8% rabbit serum (RS). Prior to the use of TGFβ3 a serum concentration study was conducted to analyse N/N1003A LECs and establish the lowest serum concentration that would sustain proliferation. Based on the literature two approaches were taken to analyse the reduced serum concentrations. Firstly by reducing the serum concentration from the start and seeding cells at $1x10^4/cm^2$ in 2%, 0.5% and 0% RS, four wells per serum concentrations were analysed. Cells were fixed at different time points, days 1, 4 and 7. Secondly by seeding cells at $1x10^4/cm^2$ in medium containing optimum 8% RS for a period of time (either 24hours and 72 hours), serum starving the cells for 24 hours, prior to reducing the serum to 2%, 0.5% and 0%. Plates were fixed at days 1, 4 and 7 after cultured in experimental conditions. Medium supplemented with 8% rabbit serum served as a control for all studies. The nuclei were stained with PI, four micrographs per well were taken on an x20 objective, cells were counted using a macro in ImageJ.

2.6.2 Dedifferentiation Model

To test the hypothesis that TGFβ3 could reverse or prevent the effect of dedifferentiation a model to dedifferentiated LECs was investigated. To quantify dedifferentiation LECs were stained with αSMA. Optimisation of αSMA antibody was carried out on human coronary artery smooth muscle cells (HCASM, Promocell, UK). Dedifferentiating LECs were examined via culturing LECs in three different scenarios, detailed below.

2.6.2.1 PMMA

Poly methyl methacrylate (PMMA) was originally the material of choice for IOLs but has since been replaced with improved IOL materials, because LECs dedifferentiated and contracted on this material causing PCO. N/N1003A LECs were seeded at $1x10^4/cm^2$ onto PMMA (The Plastic Shop, UK) roughly cut 11mm by 11mm and placed in a 12 well

plate. Six coverslips per time point and four time points (days 1, 4, 7 and 14) were examined. At each time point cells were fixed with NBF and stained for αSMA (2.1.17).

2.6.2.2 Scratch Assay

A scratch assay was performed to try and replicate the trauma caused postoperative in cataract surgery. N/N1003A LECs were seeded at $1x10^4/cm^2$ into a 6 well plate and maintained until a monolayer of cells was formed. A scratch was made through the centre of the well with a 1ml pipette tip. Re-growth of cells in the scratched area was monitored on days 1, 4 and 7 (post scratch). At each time point cells were fixed with NBF and stained for αSMA (2.1.17).

2.6.2.3 TGFβ2 Dose Dependant Study

TGFβ2 is elevated postoperatively as part of the natural wound healing response causing dedifferentiation. This causes the posterior capsule to scar and wrinkle leading to PCO. N/N1003A LECs were seeded at $1x10^4/cm^2$ into a 24 well plates and grown for 72 hours in MEME containing 8% RS then serum starved for 24 hours before changing to experimental medium. Experimental medium was MEME (2% RS + L-glut) containing, 1.5ng/ml, 3ng/ml or 10ng/ml of TGFβ2. Six wells per concentration per time point were examined. Plates were fixed on days, 1, 4 and 7, (post experimental medium) and stained for αSMA (2.1.17).

2.6.3 Optimisation

TGFβ2 was repeated using more concentrations, 3ng, 5ng, 6.5ng, 8ng and 10ng/ml TGFβ2, following the same procedure outlined above (2.6.2).

2.6.4 TGFβ3 Dose Dependant Study

To investigate the influence TGFβ3 had on LECs morphology and phenotype a dose dependent study was evaluated for 7 days. The concentrations (10ng, 1ng, 100pg and 10pg/ml) and time exposure of TGFβ3 (1 hour, 24 hours or 7 days) were varied. N/N1003A LECs were seeded into 24 well plates at $1x10^4/cm^2$ in MEME containing 8% RS for 72 hours then serum starved for 24 hours, before removing all medium and changing to the various TGFβ3 experimental conditions. These included adding 300µl of MEME

containing 10ng, 1ng, 100pg and 10pg /ml TGFβ3 and 2% RS for 1 hour at 37°C, adding 500µl of MEME containing 10ng, 1ng, 100pg and 10pg /ml TGFβ3 and 2% RS for 24 hours, or 1ml of MEME containing 10ng, 1ng, 100pg and 10pg /ml TGFβ3 and 2% RS for 7 days. Control wells were seeded and maintained in exactly the same way but with the absence of any TGFβ3. Cells were fed every 2-3 days with the corresponding medium. Micrographs were taken during the 7 days from the same well in roughly the same area so the cell growth and morphology could be monitored. On day 7 cells were fixed with NBF and stained with αSMA (2.1.17). Dedifferentiation was semi-quantitatively analysed by measuring the area of αSMA staining as a percentage of the total field of view, this was achieved by programming a macro on ImageJ.

2.6.5 Dedifferentiation Model

The dedifferentiation model and TGFβ3 were studied in conjunction with each other to determine if TGFβ3 could reverse or prevent dedifferentiation (Figure 2.7).

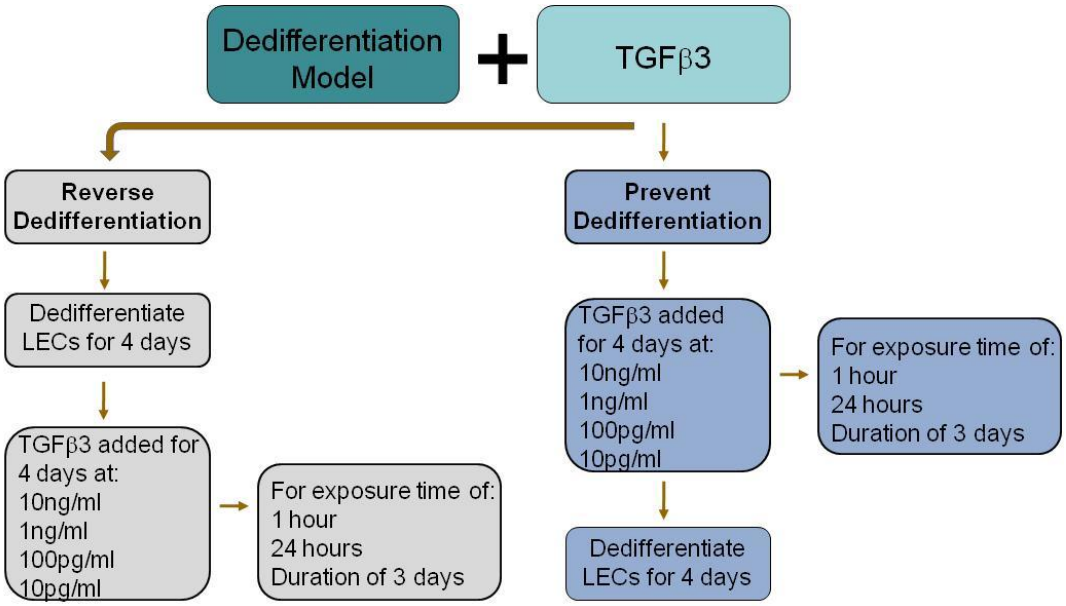

Figure 2.7: Flow chart to demonstrate the principle of using the dedifferentiation model in conjunction with TGFβ3. To test the hypothesis that TGFβ3 could either reverse dedifferentiation (left hand side) or prevent dedifferentiation (right hand side).

To test the hypothesis that TGFβ3 could reverse dedifferentiation, TGFβ3 was added to already dedifferentiated cells, following the same procedure as previously described. Briefly N/N1003A were seeded at $1x10^4/cm^2$ and cultured in MEME containing 8% RS for 72 hours, serum starved for 24 hours, before switching to MEME containing 2% RS with 5ng/ml TGFβ2 to dedifferentiate the LECs for 4 days. On day 4 MEME was changed and cells were treated with TGFβ3 at the same concentrations and time exposures as previously described (2.6.4) for a further four days. This involved either removing all medium containing TGFβ2 and adding 300µl-500µl of medium containing various concentrations of TGFβ3 for either 1 or 24 hours at 37°C, or half the medium containing TGFβ2 was removed and replaced with MEME 2% RS containing various concentrations of TGFβ3 for the remaining four days. At the end of the experiment plates were fixed with NBF and stained to examine the expression of αSMA (2.1.17). Dedifferentiation was analysed by measuring the area of αSMA staining as a percentage of the total field of view, this was achieved by programming a macro on ImageJ. To test the hypothesis that TGFβ3 could prevent dedifferentiation, TGFβ3 was added for four days prior to dedifferentiating cells with TGFβ2 for the remaining four days, following the same procedure as described above.

2.6.6 Flow Cytometry

As the method to analyse αSMA expression was semi quantitative, flow cytometry was used to determine a quantitative method to sort a population of LECs. N/N1003A LECs were seeded into three $25cm^2$ flasks at $1x10^4/cm^2$. LECs were either treated with MEME containing 2% RS with no TGFβ2, or MEME containing 8% RS for 72 hours then serum starved for 24 hours, followed by experimental conditions of MEME containing 2% RS with 5ng/ml TGFβ2 for four days. Cells were fed on day 2 with the appropriate medium. The flow cytometry was operated by Dr Stuart Marshal Clarke, University of Liverpool. To prepare the cells for flow cytometry cells were stained as described in section 2.1.17, however as a suspension of cells was required cells were fixed, washed, permeabilised and stained in suspension in 1.5ml eppendorfs. Centrifugation was performed between each step to remove supernatant and wash cells. To determine the usability of flow cytometry as a method for quantification 8 vials of LECs were prepared, 4 vials of

untreated LECs (no TGFβ2) and 4 vials of LECs treated with TGFβ2, with the following staining conditions:

1. LECs + PBS + PBS (unstained cells)
2. LECs + negative mouse IgG + secondary Alexa Fluor® 488 (negative control)
3. LECs + primary αSMA + secondary Alexa Fluor® 488 (stained cells)

Each vial contained a minimum of 500,000 cells suspended in 0.5ml PBS: 1% BSA. Cells were stained with 500µl of primary and secondary antibodies (1:100).

2.6.7 RT^2-PCR Assay

The difference in gene expression between untreated B3 LECs (no TGFβ2) and LECs treated with various TGFβ2 and TGFβ3 conditions were evaluated, using the extracellular matrix and adhesion molecules RT² profiler PCR array (QIAGEN, UK), which examined 84 genes involved in cell-cell and cell-matrix interactions (appendix 1). Housekeeping genes were incorporated onto the plate to ensure the procedure had been successful. B3 LECs were seeded at 1x10^4/cm^2 in a 24 well plate and treated with MEME 10% FCS for 72 hours, cells were then serum starved for 24 hours before changing to experimental conditions.

Experimental conditions were either:

1. MEME containing 2% FCS for four days
2. MEME containing 2% FCS with 5ng/ml TGFβ2 for four days
3. MEME containing 2% FCS with 10ng/ml TGFβ3 for four days followed by MEME containing 2% FCS with 5ng/ml TGFβ2 for the remaining four days (2.6.5)

Cells were fed every 2-3 days with the appropriate medium. RNA was extracted using RNeasy extraction kit (QIAGEN, UK). Cells were lysed using buffer RLT (10µl β-mercaptoethanol/1ml Buffer RLT). For each experimental condition four wells were pooled. Further DNA was removed following the optional DNase digestion steps. The total RNA was read using the BioPhotometer Plus (Eppendorf). A total of 1µg/ml RNA for each condition was converted into 102µl cDNA synthesis reaction following RT²

profiler PCR array protocol (Qiagen). cDNA was mixed with 1350µl SYBR green mastermix and 1248 µl RNase-free water. Using a multi channel pipette 25µl of cDNA solution was aliquoted into the PCR array 96 well plate. Plates were centrifuged for 60 seconds before reading plates on the Light Cycler 480 (Roche).

3. Results

3.1 Material Coatings and Techniques

This section will examine results from characterising LEC phenotype, seeding density growth assay, serum assay and techniques to harvest native LECs.

3.1.1 Cell Culture Techniques

Cytokeratin antibody staining was carried out to characterise the cell phenotype. Various cytokeratin antibodies were tested (Table 3-1). In addition N/N1003A's were stained for alpha B-crystallin protein (clone 1B6.1-3G4, anti-mouse, Abcam).

Table 3-1: Antibody clones used to stain FHL124, B3 and N/N1003A LECs

Cell Line	Clone	Cytokeratins
FHL124	C11 anti-mouse, Santa Cruz	4, 5, 6, 8, 10, 13 and 18
B3	C11 anti-mouse, Santa Cruz	4, 5, 6, 8, 10, 13 and 18
N/N1003A	C11 anti-mouse, Santa Cruz	4, 5, 6, 8, 10, 13 and 18
	NCL-5D3 anti-mouse, Abcam	8 and 18
	RCK108 anti-mouse, Dako	19
	AE1/AE3 anti-mouse, Dako	1, 2, 3, 4, 5, 6, 7, 10 ,13, 14, 15, 16 and 19
	MNF116 anti-mouse, Dako	5, 6 8, 17, and probably 19

Table demonstrating cytokeratin antibody clones used in immunocytochemistry, details of the supplier and specific cytokeratins to which they bind.

FHL124 LECs were stained with pan cytokeratin, clone C11. Cytokeratin staining was present illustrating positive epithelial cell expression (Figure 3.1). Intensity of stain was independent of concentration used.

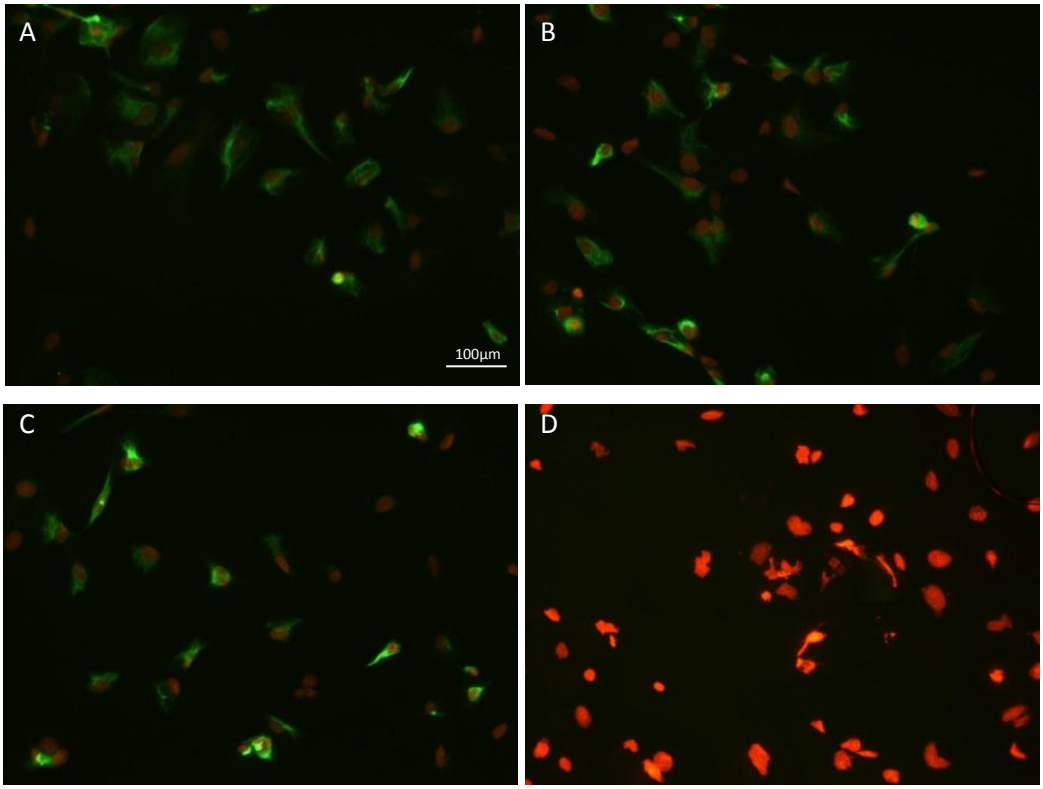

Figure 3.1: Fluorescent micrographs demonstrating cytokeratin (green, clone C11) and PI (red) staining of FHL124 LECs. At antibody concentrations of A. 1:200, B. 1:250, C. 1:400 and D. Negative mouse IgG control at a concentration of 1:100. Intensity of stain was independent of concentration of antibody used.

B3 LECs were also stained with pan cytokeratin, clone C11. Many B3 LECs stained positively for cytokeratin expression (Figure 3.2).

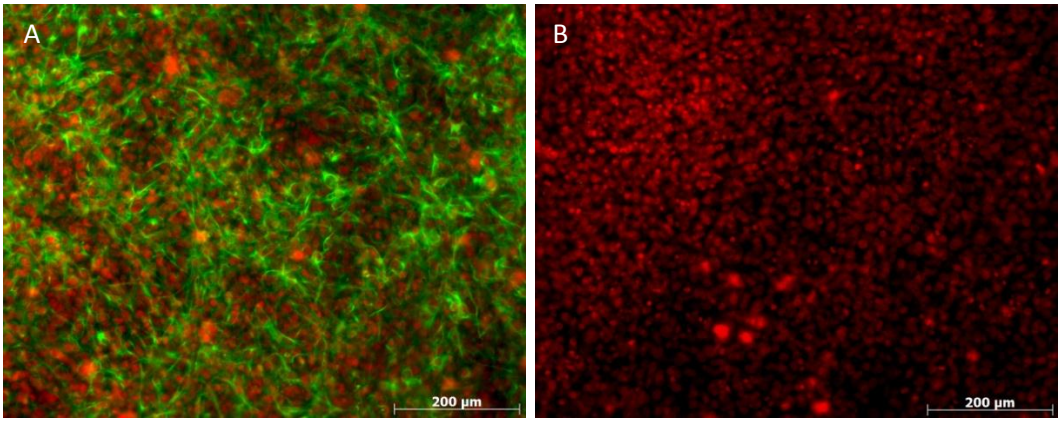

Figure 3.2: Fluorescent micrographs demonstrating positive cytokeratin staining (green, clone C11) and PI (red) of B3 LECs. At a concentration of A. 1:100 and B. Negative mouse IgG control at a concentration of 1:100.

No primary antibody was found that was specific to react with rabbit species, however several monoclonal cytokeratins specific to human were tested on N/N1003A LECs using ARPE-19 cells as a positive control. None of the cytokeratins tested proved successful in staining rabbit LECs, N/N1003A's. Crystallins have been used as a method for proving lens epithelial cell phenotype [160-166]. Based on this N/N1003A LECs were stained for alpha B-crystallin (Abcam). Rabbit LECs stained positive for alpha B-crystallin (Figure 3.3).

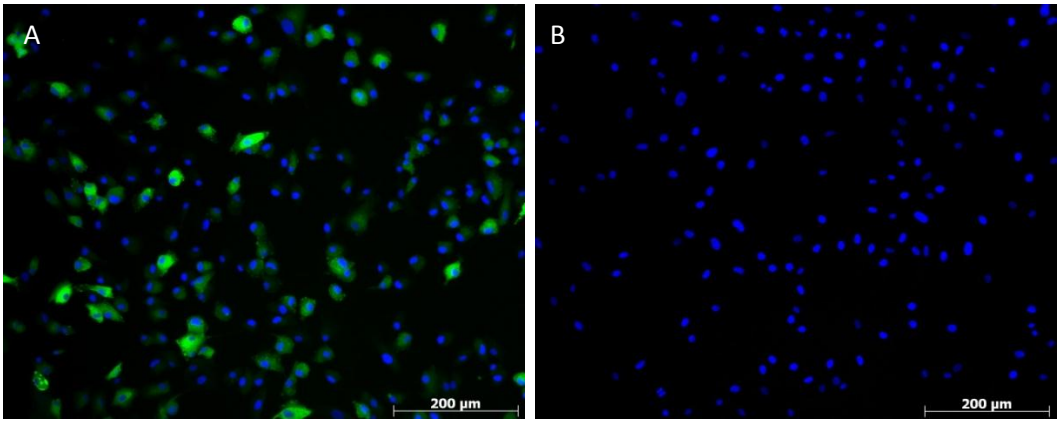

Figure 3.3: Fluorescent micrographs demonstrating positive alpha B-crystallin staining (green, clone 1B6.1-3G4) and DAPI (blue) of N/N1003A LECs. At a concentration of A. 1:100 and B. Negative mouse IgG control at a concentration of 1:100.

3.1.2 Seeding Density Growth Curve

To optimise tissue culture techniques a seeding density growth curve experiment was performed using FHl124 LECs to characterise their usual growth pattern at different seeding densities. Firstly cells were counted using a haemocytometer. Results showed that cells seeded at $1x10^3/cm^2$ did not contain enough cells to allow for accurate counting at early time points, i.e. no cells were present on the haemocytometer. Cells seeded at $1x10^5/cm^2$ became confluent by approximately day 3 – 4 with cells having to be diluted to be counted accurately. Therefore a different method for counting cells was explored. Cells were fixed at different time points and stained with Mayer's haematoxylin, for the purpose of counting cell nuclei (Figure 3.4).

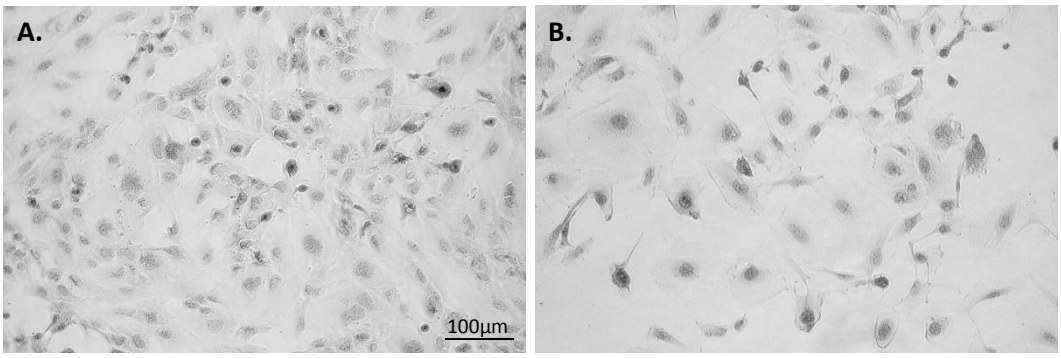

Figure 3.4: Phase contrast micrographs demonstrating FHL124 LECs stained with Mayer's haematoxylin. At seeding density of A. $1x10^4/cm^2$ day 4 and B. $5x10^3/cm^2$ day 4

For cells seeded at $1x10^4/cm^2$ there was a higher proliferation rate between days 1 – 4 whereas most proliferation occurred between days 4 – 7 at $5x10^3/cm^2$ (Figure 3.5). The number of cells began to plateau by day 7 for $1x10^4/cm^2$ seeded density. Cells seeded at $5x10^3/cm^2$ continue to divide at day 7 but at a slower rate. Based on this a seeding density of $1x10^4/cm^2$ was chosen for FHL124, B3 and N/N1003A cell lines to observe cell growth on all coatings and any additional cell growth assays.

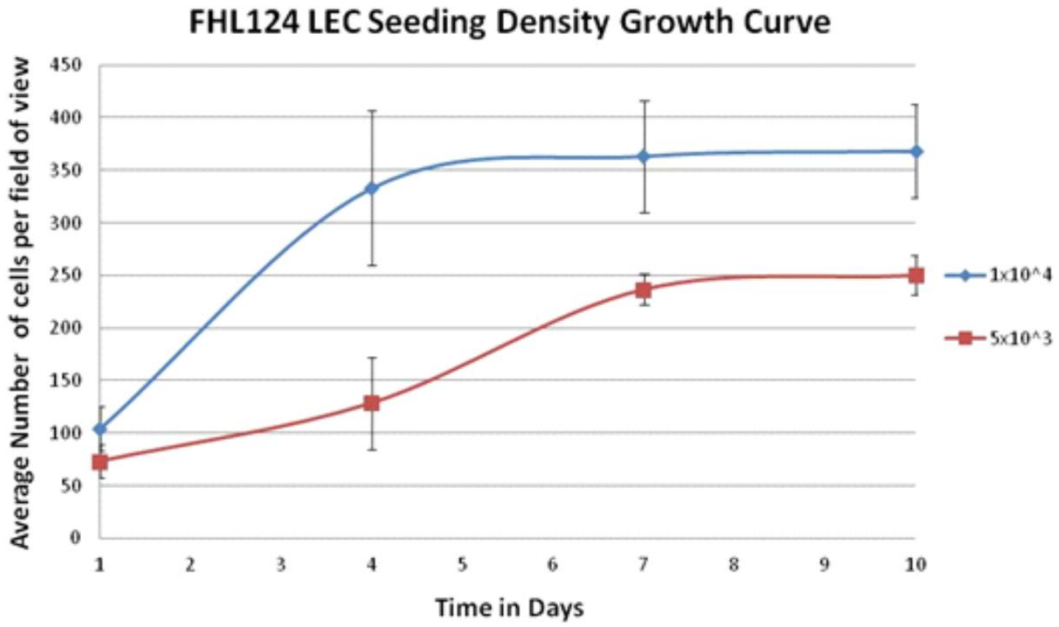

Figure 3.5: Graph demonstrating FHL124 LEC seeding density growth curve of $1x10^4/cm^2$ and $5x10^3/cm^2$ seeding densities. Error bars equal ± 1 standard deviations. $1x10^4/cm^2$ seeding density reached confluency by approximately day 4, whereas $5x10^3/cm^2$ took approximately 7 – 10 days to reach confluency.

3.1.3 Serum Growth Curve

A short experiment was set up to optimise the FCS concentration used with FHL124 cell line as this was not previously known. From the previous study it was shown that the area of exponential growth for LEC seeded at $1x10^4/cm^2$ was between days 1 – 4 (Figure 3.5), therefore cells were analysed on day 1, 3 and 4. Little difference in cell growth between the FCS concentrations was observed, 5% FCS had a slight increase between days 3 – 4 (Figure 3.6). All serum concentrations produced a similar growth curve. At each time point there was no significant difference in cell numbers between serum concentrations, analysed by a one-way ANOVA Tukey's post hoc test ($p>0.05$). A serum concentration of 5% FCS was chosen for FHL124 LECs as it was the lowest level of serum FHL124 LECs needed to sustain proliferation and retain epithelial morphology.

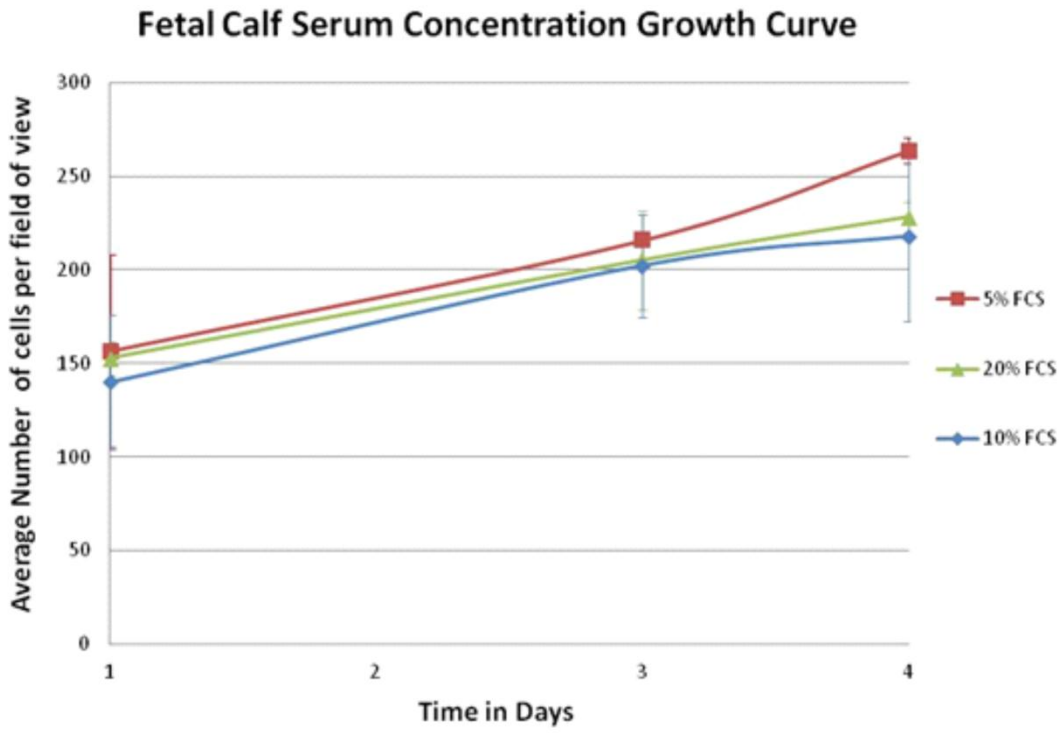

Figure 3.6: Graph demonstrates FHL124 LEC line serum (fetal calf serum, FCS) growth curve of 5% FCS, 10% FCS and 20% FCS serum concentration. Error bars equal ± 1 standard deviations. All serum concentrations produced roughly the same amount of cell attachment per field of view by 4 days and were not significantly different (analysed using one way ANOVA with Tukey's post hoc test).

The recommended serum concentration for B3 LECs was 10% FCS. The optimum serum concentration for N/N1003A was known to be 8% RS [167-168].

3.1.4 Harvesting Native Human LECs

Harvesting native LECs from donor eyes was difficult, both in terms of availability of the eyes and the technique. Cells grew at a slow rate and became difficult to dislodge with trypsin, resulting in fewer LECs than expected, even when wells were pooled together. Due to this experiments were not be repeated with native LECs as was desired. Instead all experiments were carried out using cell lines.

3.2 Anticoagulation Polymers Coatings – 1

Coatings from group 1 (001, 004 and pHEMA), were tested in a qualitative manner to optimise the process of the coatings and tissue culture techniques. 001, 004 and pHEMA coatings were synthesised onto glass coverslips (13mm diameter, Agar Scientific) and directly into 24 well plates.

3.2.1 Cell Growth Study

FHL124's were seeded onto coated coverslips for a total of 7 days, and coated plates for a total of 11 days. Phase contrast micrographs were taken of LECs on the different coatings whilst they were in culture (Figure 3.7), uncoated TCPS wells served as a control. Most LECs on 001 and 004 were rounded with poor attachment. Some attached cells had an elongated morphology. Some defects with 004 were noted around the edges of the coated coverslips especially at later time points. Some cells initially attached to the pHEMA coating however at later time points the cells had become rounded. When FHL124 LECs were seeded onto coated wells micrographs showed a similar attachment and growth profile so data is not presented here.

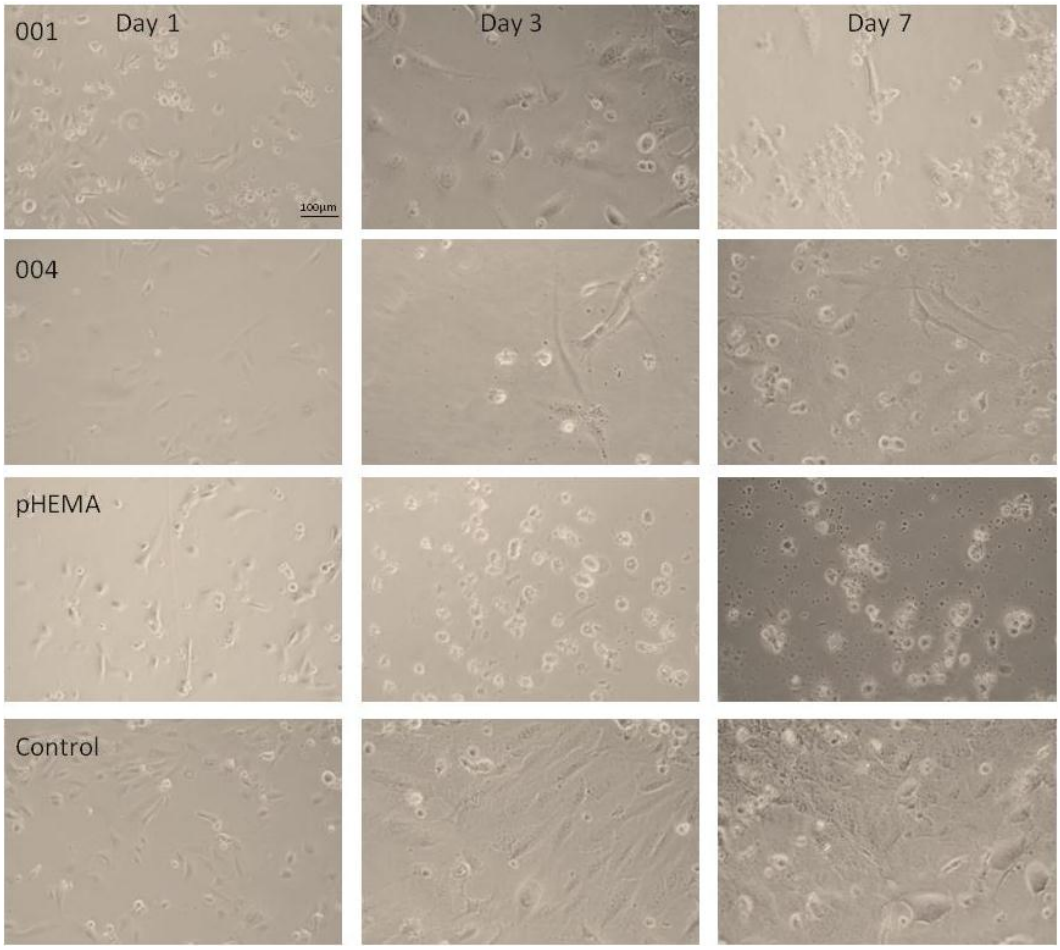

Figure 3.7: Phase contrast micrographs demonstrating FHL124 LECs seeded onto coated coverslips from polymer group 1 (001, 004 and poly (hydroxyethyl methacrylate) (pHEMA)) and tissue culture polystyrene (TCPS) control at days 1, 3 and 7. LECs on 001 were attached but were either elongated or rounded. LECs observed on 004 were similar to 001. LECs initially attached to pHEMA on day 1, but become rounded and loosely attached by day 3. LECs attached and proliferated on TCPS control, with typical epithelial morphology and started to become confluent by day 7.

3.2.2 Cell Staining

At day 7 samples were fixed with methanol for 5 minutes. Methylene blue staining was performed on the coated coverslips and the wells the coverslips had been in and phase contrast micrographs were taken. As the coated coverslips had hydrophilic gel-like properties 001, 004 and pHEMA absorbed the methylene blue, therefore visualising the cells proved difficult. Nearly all cells had either detached or were washed off during fixation, cells that remained were rounded (Figure 3.8).

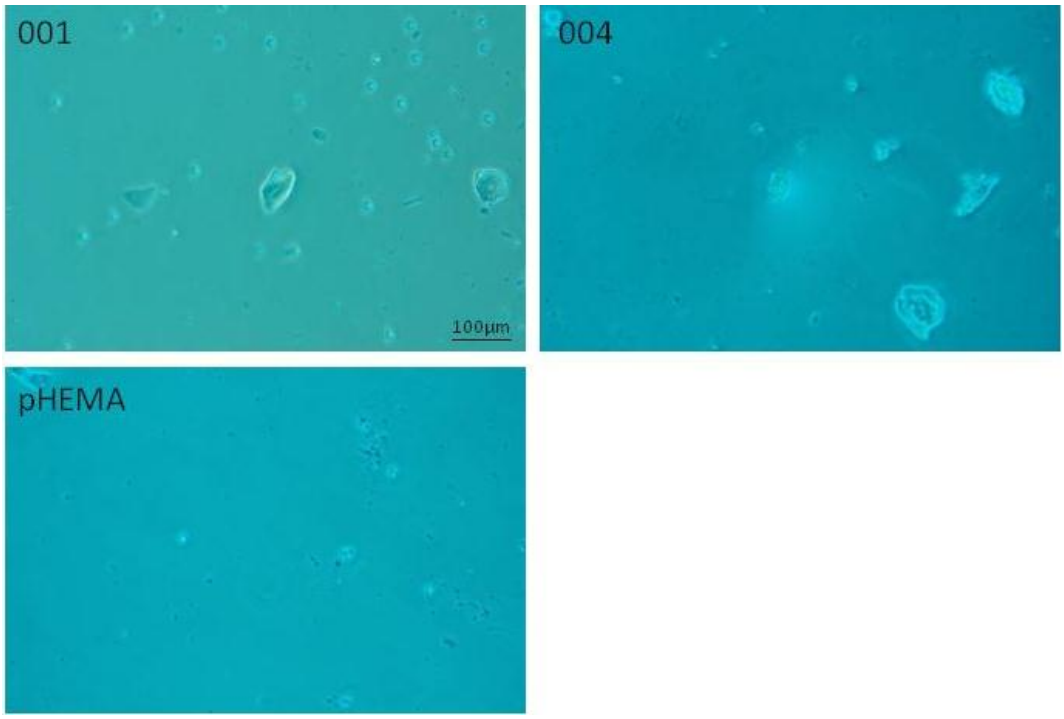

Figure 3.8: Phase contrast micrographs demonstrating methylene blue staining of FHL124 LECs seeded onto coated coverslips from polymer group 1 (001, 004 and poly (hydroxyethyl methacrylate) (pHEMA)) at day 7. Coatings 001, 004 and pHEMA were a hydrophilic gel-like coatings which absorbed the dye, therefore visualising cells was difficult. Cells that remained after washing and fixing were rounded on all three coatings.

The wells the coverslips had been in were also micrographed to examine if any cells had adhered to the well. These gave an indication as to whether the coatings were cytotoxic, or leach toxic material into the medium. FHL124 LECs adhered to the wells 001 and 004 coverslips had been in (Figure 3.9), indicating the coatings were not cytotoxic to the cells. LECs were well spread, produced small patches of cell growth and

appeared epithelial in morphology, similar to the TCPS control. Coating 001 coverslips adhered to the plate which was a result of the material becoming tacky, due to the hydrogel-like nature of the coating. A few LECs had attached around the edge of the well pHEMA coverslips had been in. This was probably due to the fact that initially all LECs seemed to adhere to the pHEMA coverslips on day one, before becoming round and lifting off at later time points. The cells that adhered to the TCPS control wells appeared epithelial in morphology and by day 7 were starting to produce a monolayer of LEC growth.

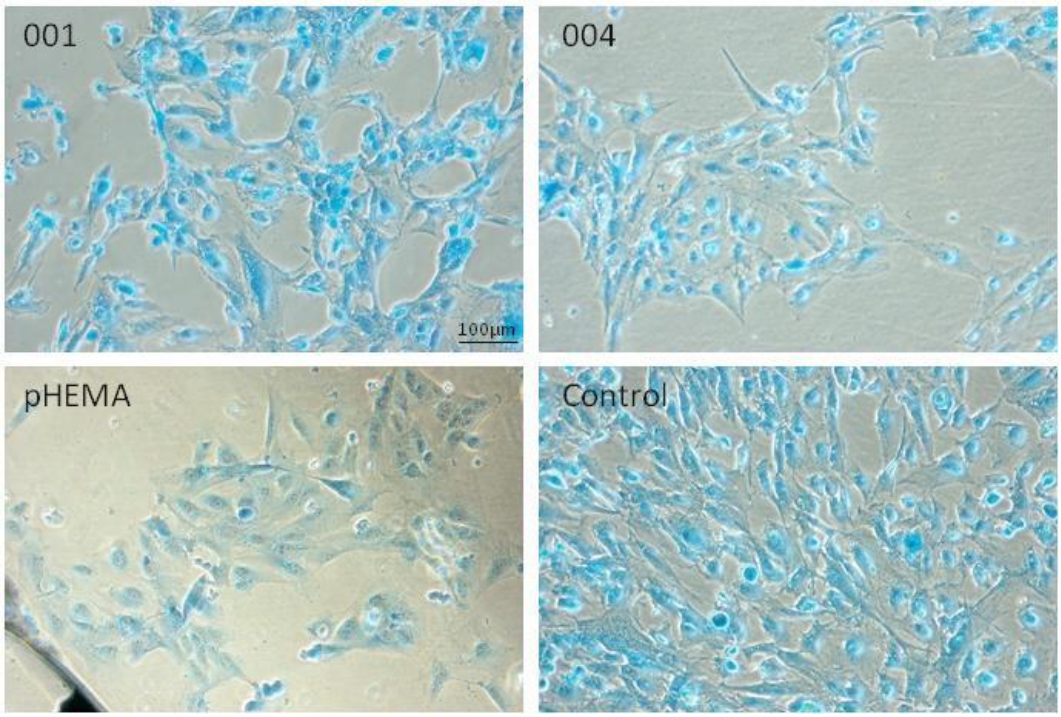

Figure 3.9: Phase contrast micrographs demonstrating methylene blue staining of FHL124 LECs adhered to wells that contained 001, 004 and poly (hydroxyethyl methacrylate) (pHEMA) coated coverslips and tissue culture polystyrene (TCPS) at day 7. LECs adhered to all wells indicating the coatings were not cytotoxic to the LECs. Wells that previously contained 001, pHEMA and 004 showed confluent small patches of cell growth with epithelial morphology similar to the control.

LECs seeded onto coated wells were left in culture for 11 days and a live/dead assay was performed. LECs on the coated wells appeared to have a slightly more rounded morphology than on the coverslips. By day 11 cells had attached and formed a confluent monolayer of live (green) cells with only few dead (red) cells on the TCPS control (Figure 3.10). Coating 001 showed a mix of live and dead cells, however the majority were dead. Coating 004 and pHEMA absorbed the dye due to their surface properties, so there was a lot of background stain, making live/dead analysis difficult. When comparing coating 004 live/dead images to the phase contrast micrograph almost all LECs were rounded and dead. Coatings 004 and pHEMA did not support cell attachment, the lack of attachment may be due to the coatings surface properties.

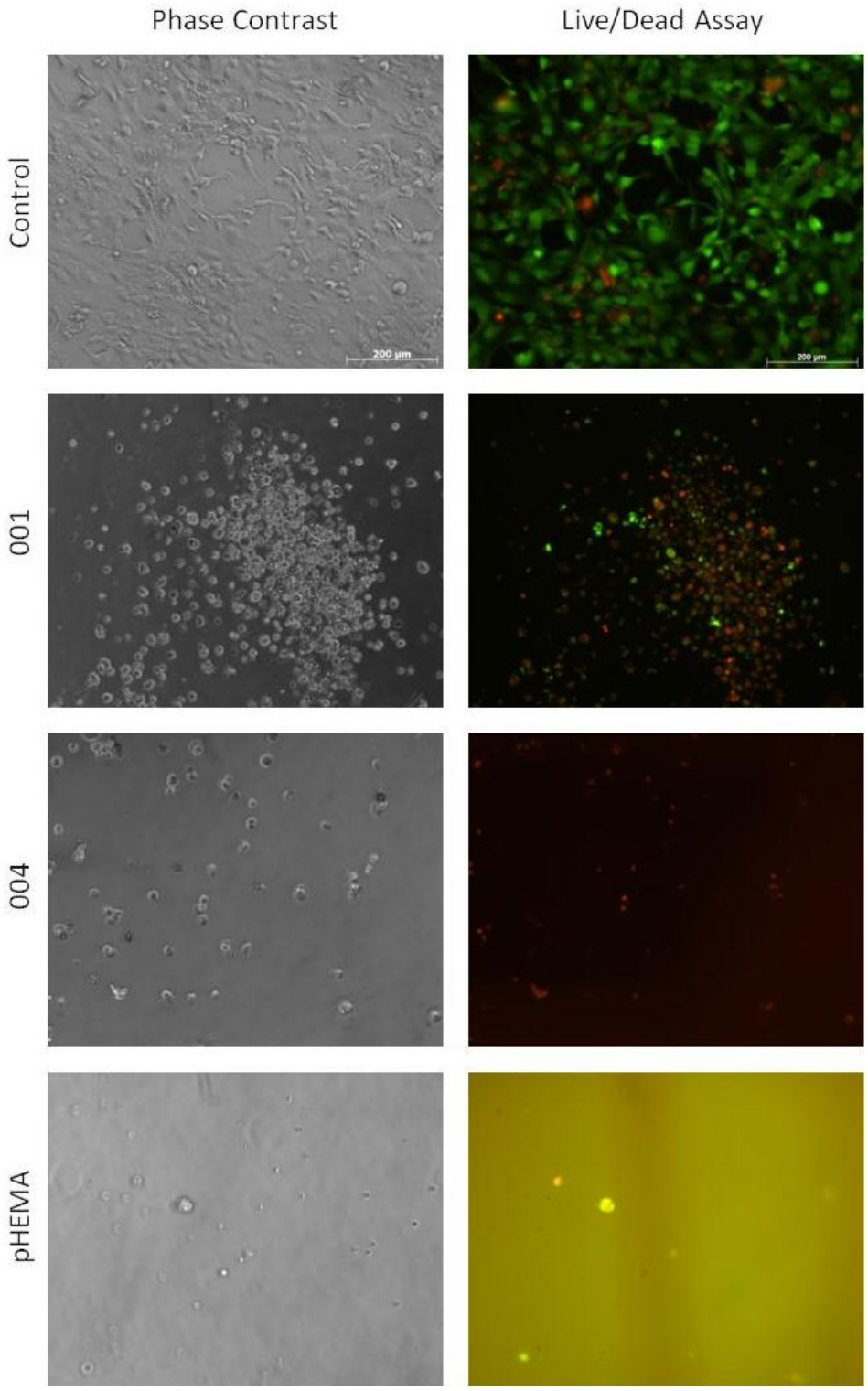

Figure 3.10: Fluorescent micrographs demonstrating Live/Dead assay of FHL124 LECs on control (tissue culture polystyrene (TCPS)) and 001, 004 and poly (hydroxyethyl methacrylate) (pHEMA) at day 11. The control shows a confluent monolayer of live cells. 001 showed a mix of live (green) and dead (red) cells, however the majority were dead. pHEMA and 004 absorbed the dye as they were both hydrogel-like coatings, the majority of cells were dead.

3.3 Anticoagulation Polymers Coatings – 2

From this point on coatings were synthesised directly onto 24 well plates. Coatings in group 2 were examined for a longer time period of 14 days.

3.3.1 Cell Growth Study

LECs were studied whilst in cell culture by taking phase contrast micrographs at each time point (Figure 3.11). LECs responded differently to the various coatings shown via the amount of attachment and growth on 001, 002 and 003. Interestingly, coatings 001 produced more cell attachment and growth than in group 1 experiments, this may be due to improvements in the coating process and cell culture technique. By day 14 small semi-confluent patches were observed on coating 001. Coating 002 encouraged more LEC attachment and growth compared to 001. Few LECs adhered and spread on coating 003. In general LECs attached to coating 003 were mainly rounded and not strongly adhered, however when cells did attach they were more elongated in morphology and did not look epithelial-like. LECs grown on the TCPS control wells represented the typical growth pattern for this cell line. LECs adhered to TCPS became confluent by around day 7 after this point some LECs rounded up due to lack of space.

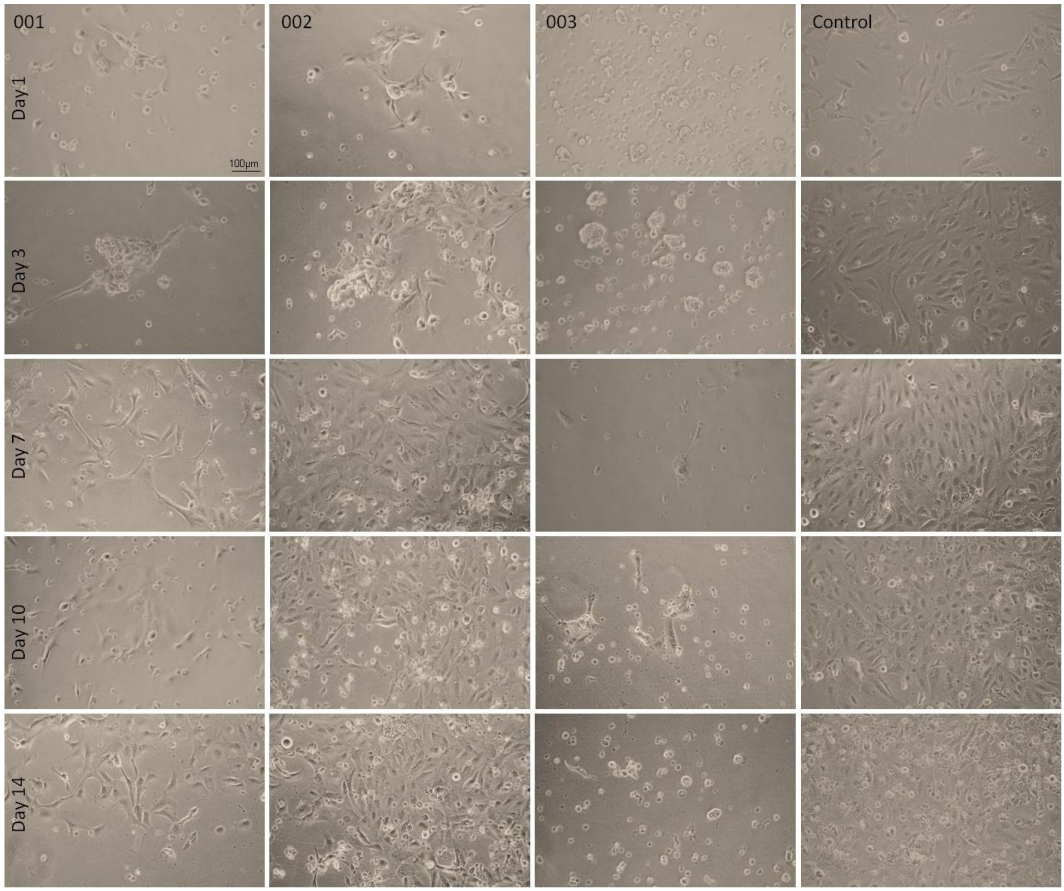

Figure 3.11: Phase contrast micrographs demonstrate FHL124 LECs seeding onto coatings 001, 002, 003 and control (tissue culture polystyrene (TCPS)) during cell culture at days 1, 3, 7, 10 and 14. Cell attachment and growth varies on the various substrates. Coating 001 allows some cell attachment and growth but not as much as coating 002. By day 14 small patches of confluent cell growth were visualised on coating 002. Coating 003 repelled cell attachment and the majority of cells were rounded on this coating, the cells that did attach do not appear epithelial-like and are elongated. Cells seeded onto control TCPS showed typical LEC attachment and supported a monolayer of LECs by day 14.

3.3.2 Cell Staining

Cells were stained with phalloidin-FITC (green) to view the f-actin filaments within the cytoskeleton and PI (red) to visualise the nuclei. Coatings 001 and 002 had some cell attachment and were reasonably well spread, whereas 003 had few cells attached throughout the time in cell culture (Figure 3.12). TCPS control was confluent by day 10 and cells had become tightly packed, phalloidin staining demonstrated cells had an epithelial morphology.

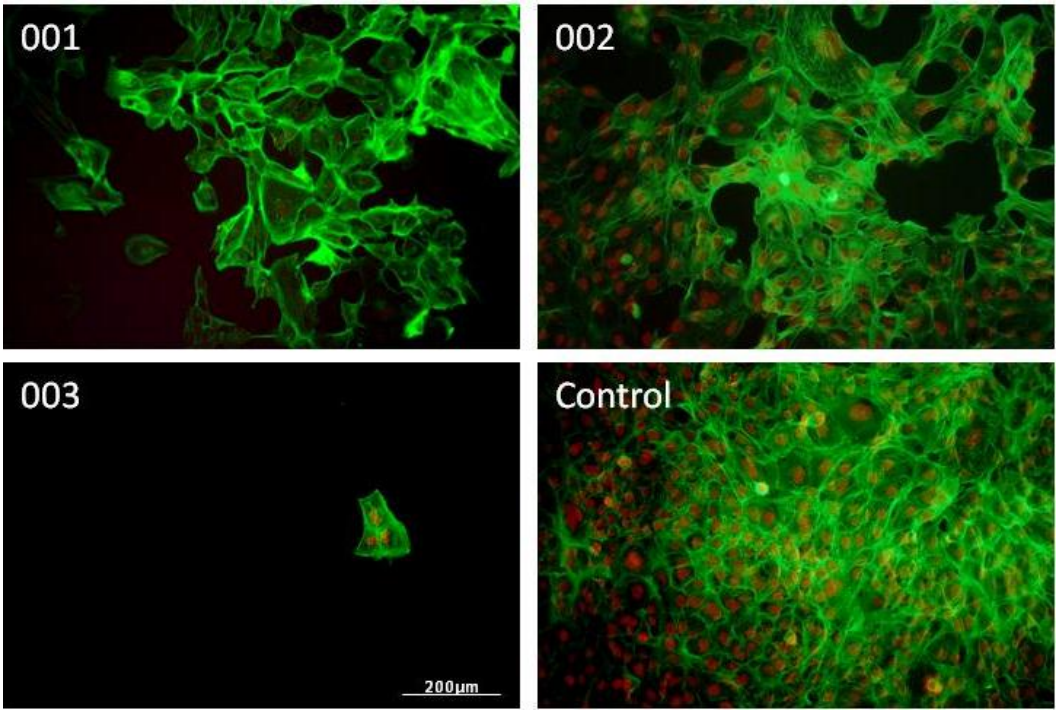

Figure 3.12: Fluorescent micrographs demonstrating immunocytochemical staining of f-actin fibres (green) and nuclei (red) of FHL124 LECs seeded onto coatings 001, 002, 003 and control (tissue culture polystyrene (TCPS)) at day 10. LECs at day 10 on 001 and 002 are reasonably well spread, with 002 having more cell attachment. Coating 003 had few cells if any attached by day 10. TCPS control was confluent by day 10, cells were tightly packed and epithelial in morphology shown through F-actin fibre

After all micrographs were taken cell nuclei were counted using ImageJ and a cell growth curve was plotted (Figure 3.13). An area of exponential cell growth was observed between days 7 – 10 on TCPS, cell proliferation began to plateau after day 10. Cell attachment and growth on coatings 001 and 002 were not significantly different ($p>0.05$). Coatings did not produce a monolayer of cells in the time frame, however by

day 10 cell numbers started to increase, indicating LECs may have carried on proliferating if they were left in cell culture for longer. Coating 003 had few cells attached if any during the 14 days in cell culture and was significantly different from all other coatings ($p<0.05$).

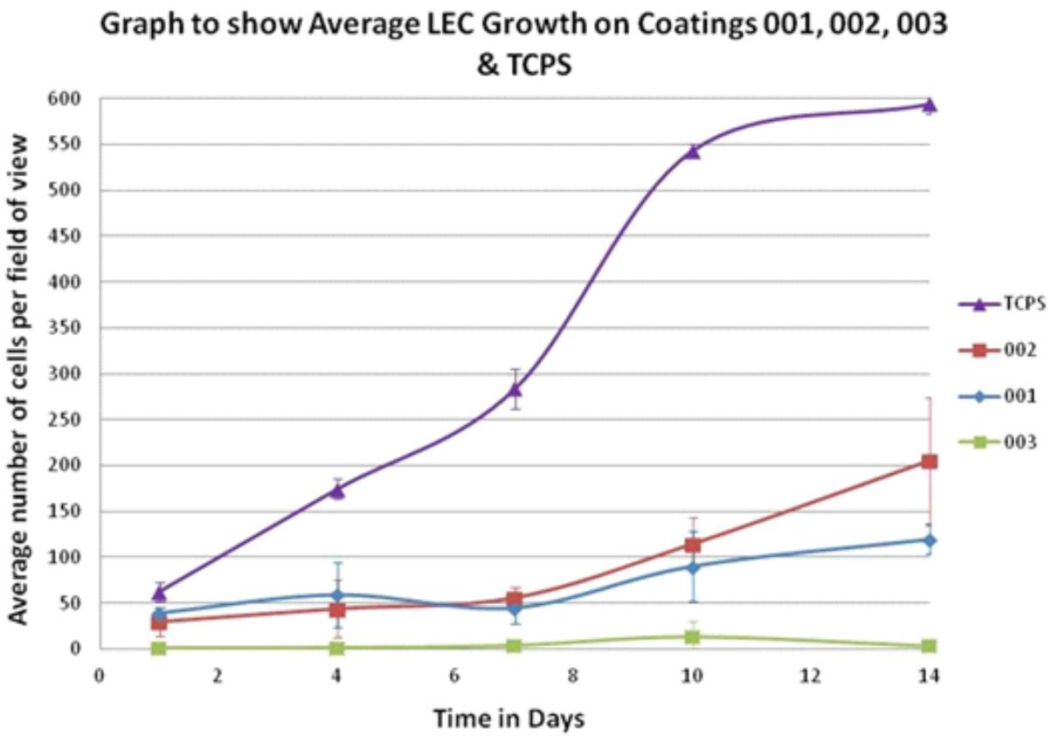

Figure 3.13: Graph demonstrating LEC attachment and growth on 001, 002, 003 and tissue culture polystyrene control (TCPS) coatings during 14 days in cell culture. Error bars equal ± 1 standard deviations. TCPS wells represent the standard growth for this cell line, cells became confluent by day 10. Coatings 001 and 002 were similar to each other and produced a similar growth curve with large standard deviations. Cell growth did increase from day 10, however a monolayer was not formed in this time period. Coating 003 did not support cells attachment during the 14 days in cell culture.

3.3.3 Surface Analysis

As the surface chemistry and properties are proprietary to BioInteractions Ltd. CA measurements were taken (Table 3-2) and coatings were analysed using SEM (Figure 3.14). The CA between all three coatings and PEI control was significantly different, ranging from an average of 29° to 68°. Coating 003 had the lowest CA from

BioInteractions coatings with a CA of approximately 35° and was more hydrophilic than coatings 001 (68°) and 002 (62°).

Table 3-2: Demonstrates average contact angle (CA) measurements of coatings 001, 002, 003 and poly ethylinimine (PEI) base substrate.

Coating	Sample 1	Sample 2	Sample 3	Average	
001	71.1 ± 5.0	61.7 ± 5.5	70.1 ± 8.1	67.6±5.2	*
002	59.9 ± 4.9	62.4 ± 3.2	63.4 ± 5.8	61.9±1.8	*
003	31.9 ± 11.5	36.8 ± 6.1	36.8 ± 6.8	35.2±2.8	*
PEI	29.3± 1.3	27.4± 4.1	31.3± 2.2	29.3± 3.1	*

CA measurements of coatings 001 and 002 were similar, however all coatings were significantly different. Error bars equal ± 1 standard deviations. * denotes significant difference were $p<0.05$. Coatings 003 had a total of 5 water based layers and the CA measurement was more hydrophilic than 001 and 002. PEI had the lowest CA.

SEM analysis showed all three coatings to be featureless up to x400 magnification (Figure 3.14). Some small particles were observed on the surface of a few samples, however this was most likely to be dust due to their size and distribution.

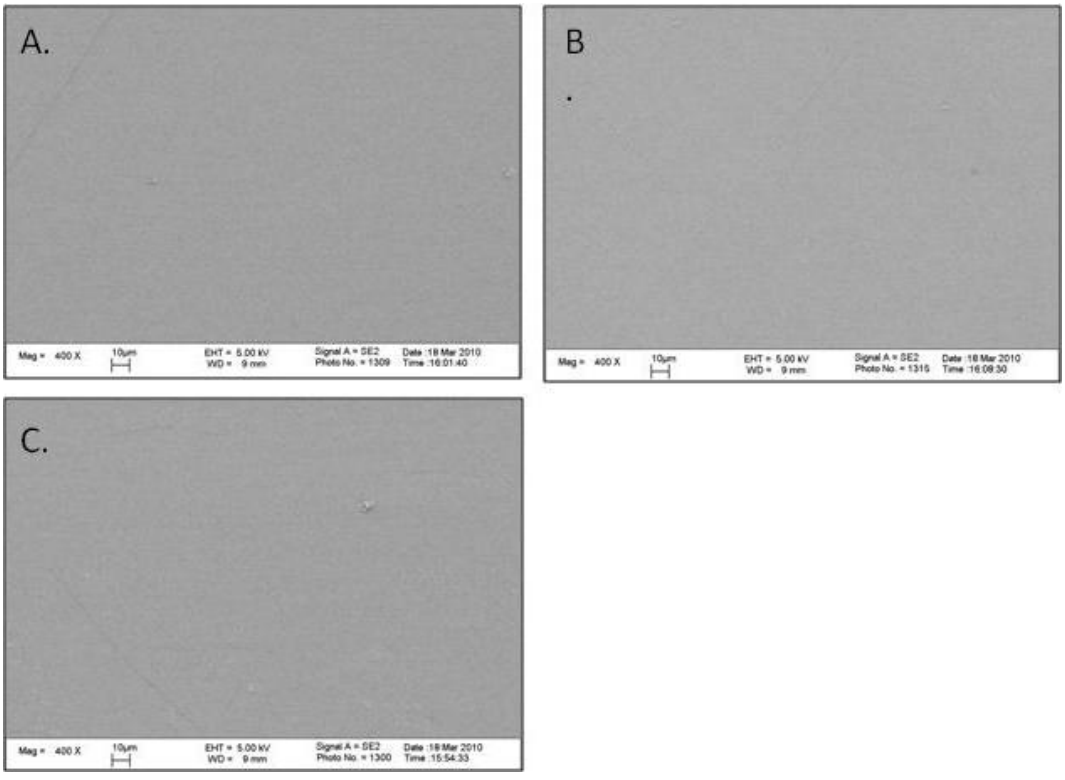

Figure 3.14: Representative scanning electron microscopy (SEM) micrographs of A. Coating 001. B. Coating 002 and C. Coating 003. All coatings appeared featureless and uniformly coated.

3.4 GAG Coatings

BioInteractions Ltd. provided GAG polymer coatings containing heparin (HEP), Hyaluronic acid (HA) and chondroitin sulphate (CS). Additionally GAG coatings were synthesised in house to examine if the cellular response was affected by the GAG itself or how it was present and bound to the surface.

3.4.1 BioInteractions Ltd. Polymer Coatings

Hep, HA and CS were synthesized directly in 24 well plates, an additional untreated TCPS plate was used as a control.

3.4.1.1 Cell Growth Study

HEP did not encourage cell attachment during the 14 day period (Figure 3.15). HA produced a similar response however, small areas of cell attachment were observed randomly throughout some wells during the 14 days in cell culture. CS encouraged a greater number of LECs attachment and growth than HEP and HA, however this was not equivalent to TCPS control. By day 14 a monolayer of LECs was observed on TCPS.

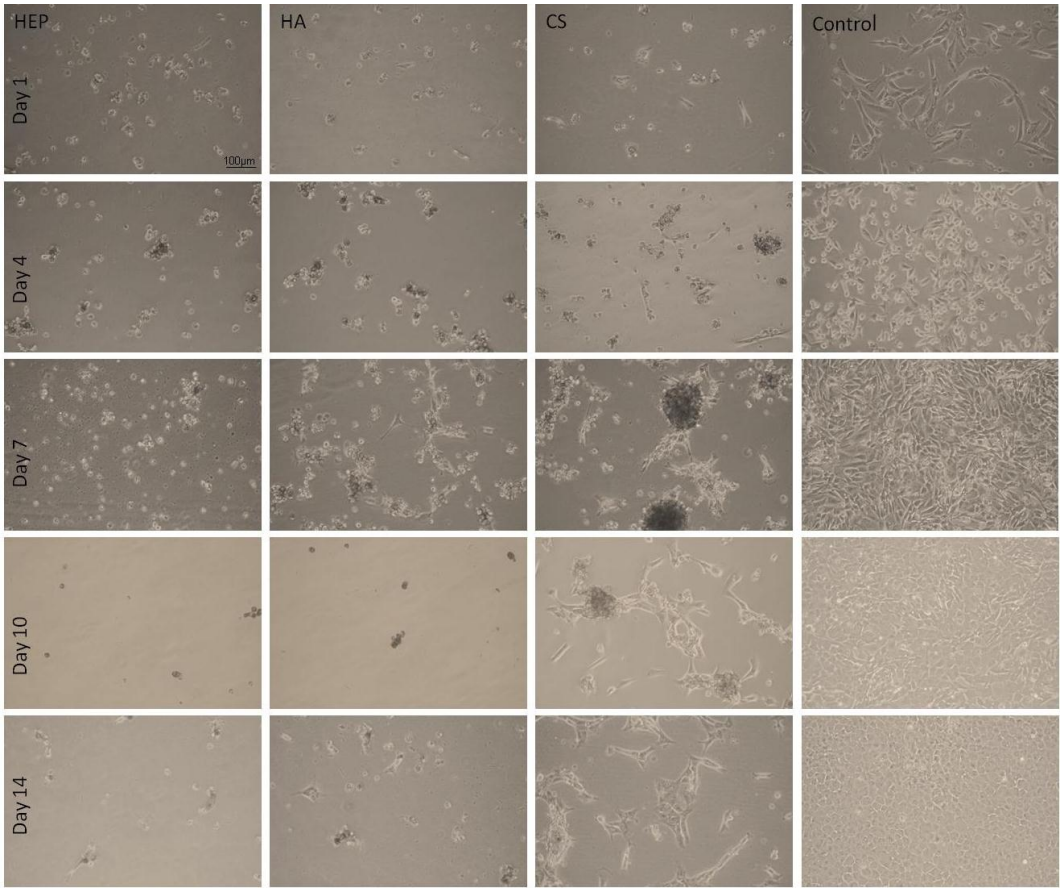

Figure 3.15: Phase contrast micrographs demonstrating N/N1003A LECs attachment and growth on GAG polymer coatings, heparin (HEP), hyaluronic acid (HA), chondroitin sulphate (CS) and tissue culture polystyrene (TCPS) control, during the 14 days in cell culture. HEP did not encourage cell attachment, HA produced a similar response however in some areas small patches of cells were observed. CS encouraged LEC attachment and growth to a certain degree and TCPS enabled LECs to adhere and proliferate to achieve a confluent monolayer by day 14.

3.4.1.2 Cell Staining

LECs were fixed and stained for αSMA to visualise myofibroblast-like cells, with phalloidin-FITC to visualise the f-actin fibres of the cytoskeleton and DAPI to visualise the nuclei (Figure 3.16). No positive expression of αSMA was observed in LECs seeded onto HEP, HA, and CS, similar to TCPS control. This indicates polymer GAG coatings do not encourage dedifferentiation into myofibroblast-like cells. No cells were observed on HEP at day 14 (Figure 3.16-A). Cells appeared rounded onto HA coatings (Figure 3.16-B). More cells were present on CS coating compared to HEP and HA coatings. F-actin fibres were present in most cells seeded onto CS coating, however some cells had a rounded morphology (Figure 3.16-C). LECs seeded onto TCPS control wells appeared to have a typical cobble-stone epithelial morphology with actin bands present around the periphery of the cells (Figure 3.16-D).

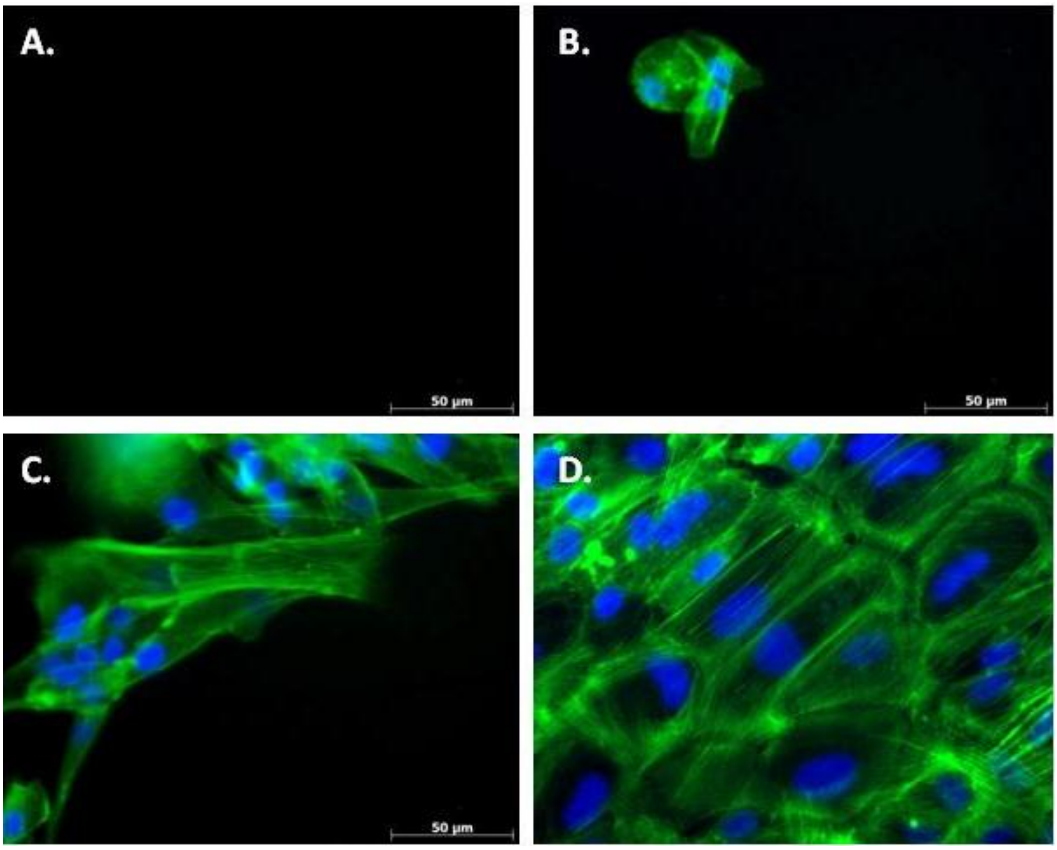

Figure 3.16: Fluorescent micrographs demonstrating immunocytochemical staining of phalloidin (green) and DAPI (blue) of N/N1003A LECs on GAG polymer coatings A. heparin (HEP), B. hyaluronic acid (HA), C. chondroitin sulphate (CS) and D. tissue culture polystyrene (TCPS) control at day 14. No cells were observed on HEP. Few cells, if any, were attached to HA coating, cells had a rounded morphology. More cells were observed on CS coatings, F-actin fibres were present in most cells. TCPS wells enabled cell attachment with epithelial morphology and actin rings around the periphery on the cells.

Cell nuclei were counted and a growth curve was plotted (Figure 3.17). Cells seeded onto TCPS became confluent by approximately day 7. Cell growth on CS plateaued by day 10 however a monolayer of cell growth was not observed. HA and HEP did not enable cell attachment during the 14 days in cell culture. Significant difference was observed between all coatings on day 14.

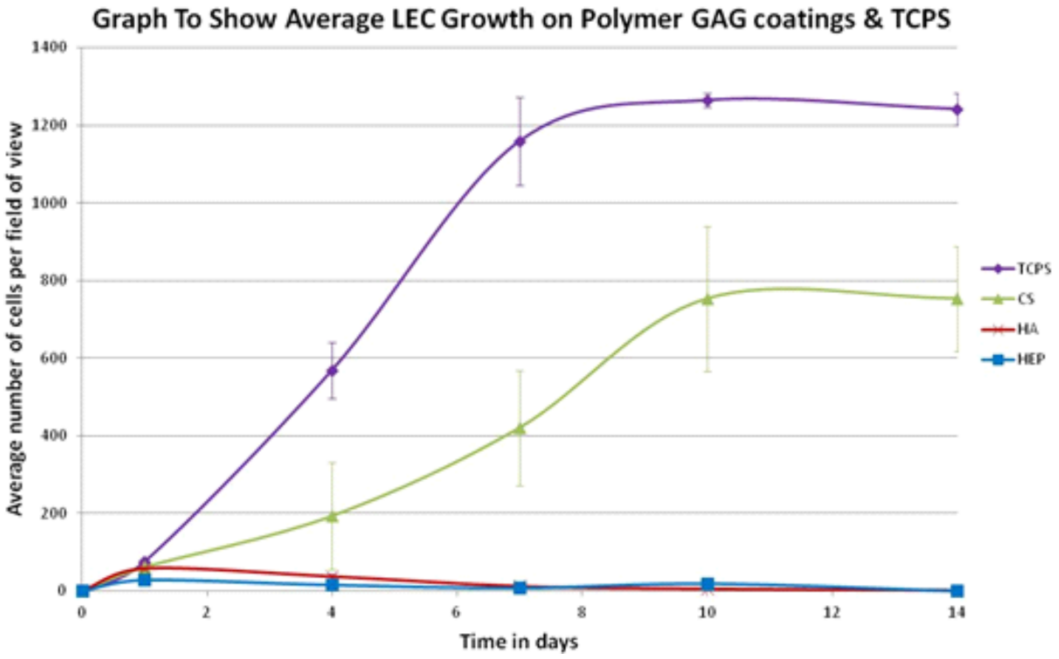

Figure 3.17: Graph demonstrating N/N1003A LEC growth GAG polymer coatings, heparin (HEP), hyaluronic acid (HA), chondroitin sulphate (CS) and tissue culture polystyrene (TCPS) control, during the 14 days in cell culture. Error bars equal ± 1 standard deviations. Results showed that HEP and HA did not enable LEC attachment and growth, CS promoted some attachment and growth at a slower rate compared to TCPS control.

3.4.1.3 Surface Analysis

TCPS and PEI had a significantly higher CA than the GAG coatings (Figure 3.18). CAs for HEP, HA and CS were similar to each other and ranged between 23 – 25°, however the CA for CS was significantly lower than HEP (p=0.006). Data were analysed using Dunnett's T3 post hoc test.

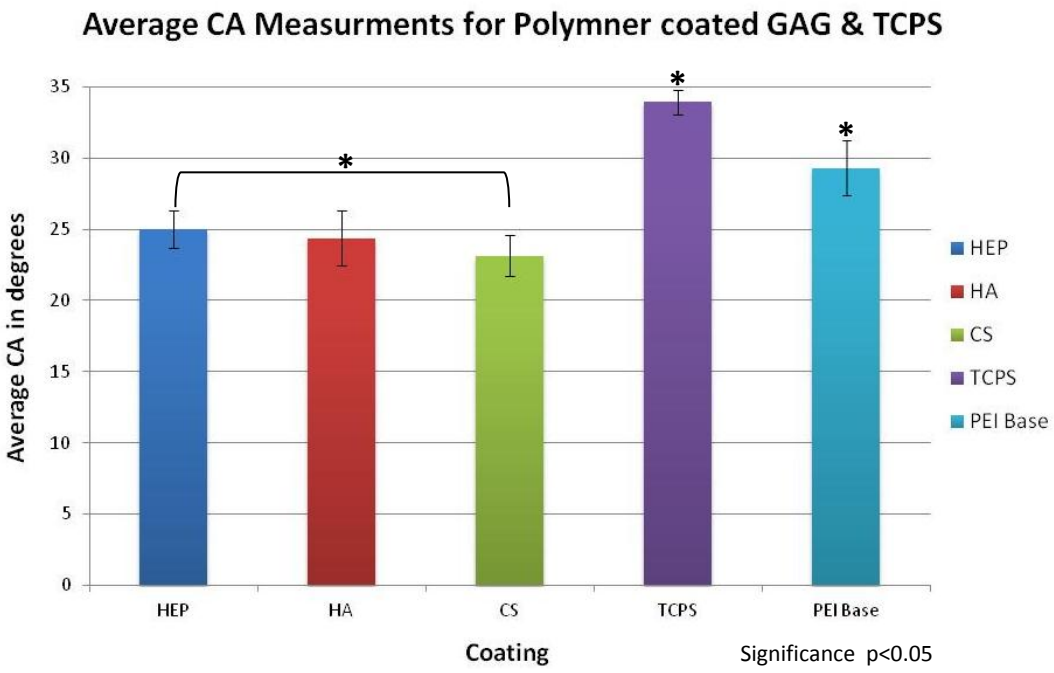

Figure 3.18: Contact angle measurements (CA) of polymer GAG coatings, heparin (HEP), hyaluronic acid (HA), chondroitin sulphate (CS), tissue culture polystyrene (TCPS) and poly ethylenimine (PEI). Error bars equal ± 1 standard deviations. * denotes significant difference were p<0.05. HEP, HA and CS had similar CA ranging from 23-25°, meaning they had similar wettability properties, however HEP and CS were significantly different from each other. TCPS and PEI control were slightly more hydrophobic and both were significantly different from all other coatings.

When coatings were viewed under the SEM, coatings appeared smooth and homogenous, at x5000 magnification (Figure 3.19). Higher magnifications of x10000 were taken but did not show anything different.

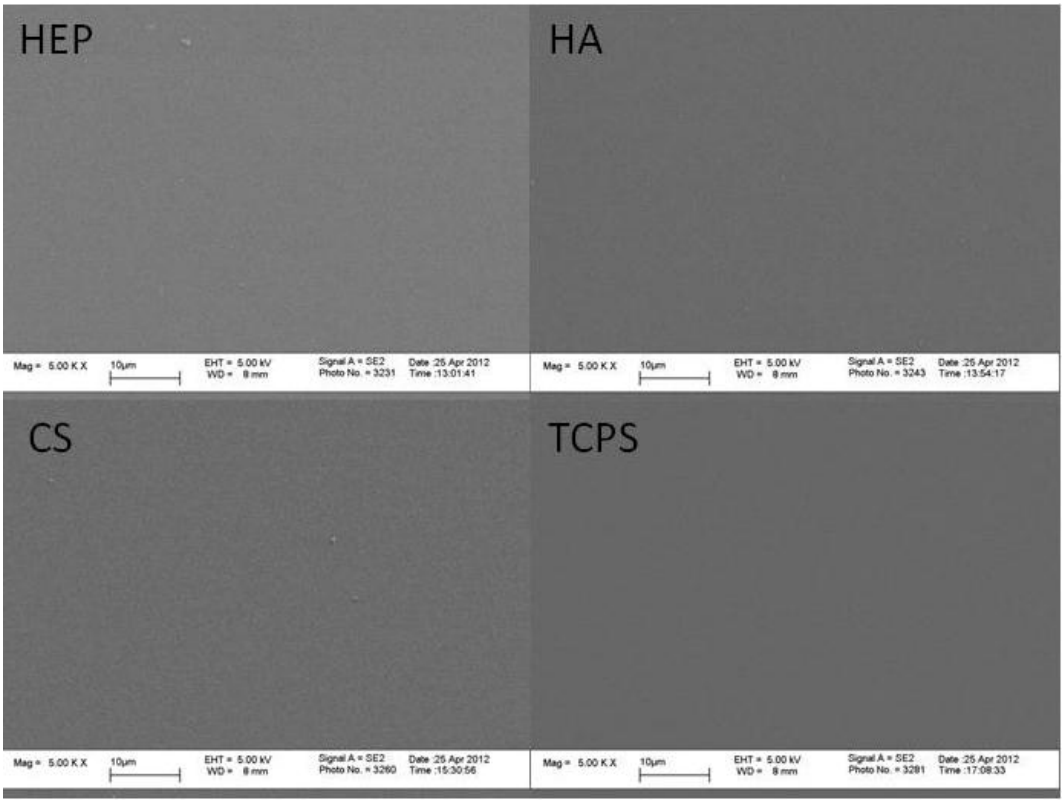

Figure 3.19: Representative scanning electron microscopy (SEM) micrographs of heparin (HEP), hyaluronic acid (HA), chondroitin sulphate (CS) and tissue culture polystyrene (TCPS). All coatings appeared smooth and featureless.

To evaluate the topography of the coatings further WLI was performed to measure the surface roughness of the coating. The roughness of all GAG coatings were relatively flat compared to TCPS and ranged from 10 – 12 nm (Figure 3.20). TCPS and CS coatings were similar (p=1), as were HEP and HA (p=1), however, HEP and HA had a significantly lower roughness than both TCPS and CS. Data were analysed using Dunnett's T3 post hoc test.

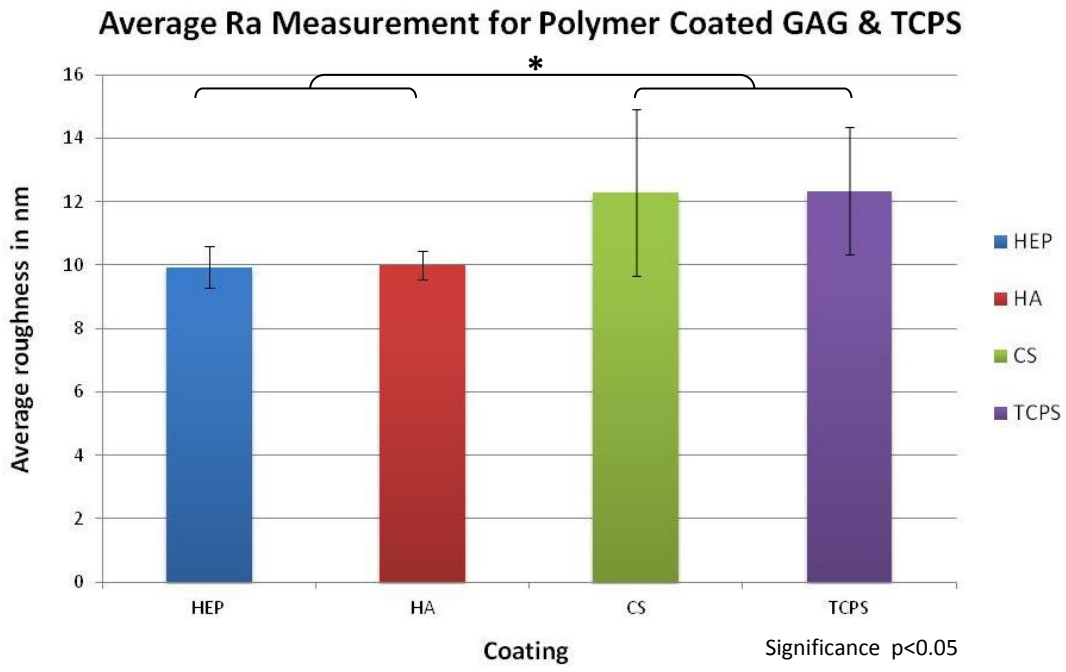

Figure 3.20: Graph demonstrating average roughness (Ra) values for polymer GAG coatings, heparin (HEP), hyaluronic acid (HA), chondroitin sulphate (CS) and tissue culture polystyrene (TCPS). Error bars equal ± 1 standard deviations. * denotes significant difference were P<0.05. All coatings were relatively flat and smooth with similar Ra values in the range of 10 – 12 Ra, however HEP and HA were significantly different to CS and TCPS.

3.4.1.4 Time Lapse Microscopy

Time lapse microscopy analysis was performed on the coated GAG plates provided by BioInteractions Ltd (Appendix A). HEP gave a different LEC response when monitored with time lapse microscopy. Cells settled on HEP polymer coating between 3 – 4 hours. A high proportion of cells attached appeared to be rounded, this was more noticeable between day 0 – day 7 (approximately). By day 14 a near confluent monolayer was reached, however cell morphology was elongated and not typical of LEC morphology. HA encouraged areas of cell attachment and growth, LECs proliferated during the 14 days in cell culture. LECs settled within 3 hours on CS polymer coating, small areas of cell growth were observed with some cells remaining rounded during the 14 days. LECs settled within 30 minutes on TCPS control, cells spread and proliferated to form a confluent monolayer by day 14.

3.4.2 Adsorbed GAGs Coatings

Five variations of the adsorbed GAG experiments were studied:

1. 3 hour incubation at 37°C – followed by a rinsing step
2. 3 hour incubation at 37°C – without a rinsing step
3. 24 hour incubation at 37°C – without a rinsing step
4. 24 hour incubation at 4°C – without a rinsing step
5. GAG added to cell culture medium

3.4.2.1 3 Hour Incubation at 37°C Followed by a Rinsing Step

LECs were monitored in cell culture for a total of seven days and phase contrast micrographs were taken.

When CS was adsorbed onto PEI base polymer for "3 hour incubation at 37°C followed by a rinsing step" cells attached and spread across all GAG concentrations during the seven days, similar to the PEI control (Figure 3.21). There was a reduction in LEC attachment across all CS concentrations when compared to the PEI control on day 4, however by day 7 the majority of concentrations had produced a monolayer, similar to the PEI control. 10mg/ml CS had fewer cells attached by day 7 when compared to other concentrations. When HA was adsorbed for "3 hour incubation at 37°C followed by a rinsing step" a similar LECs response was observed therefore the micrographs are not shown.

LECs attached and spread to CS adsorbed coatings onto TCPS wells for "3 hour incubation at 37°C followed by a rinsing step", regardless of concentration. LECs attachment to CS coatings was similar to TCPS control (Figure 3.22). A decrease in cell attachment was observed on day 4 at 10mg/ml CS. By day 7 typical epithelial cobblestone morphology was observed on TCPS control and all CS adsorbed coatings.

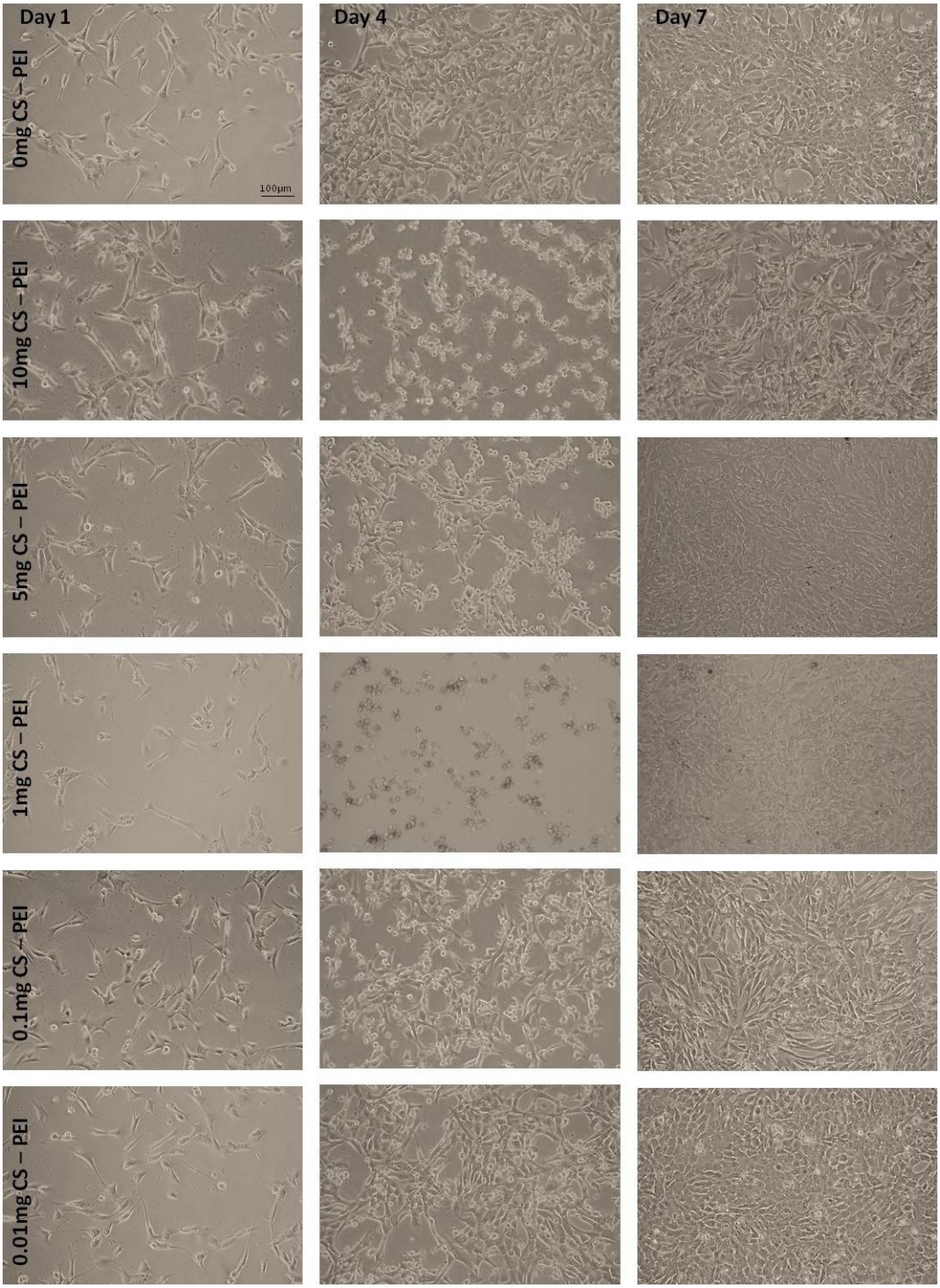

Figure 3.21: Phase contrast micrographs of cells on adsorbed chondroitin sulphate (CS) on polyethylenimine (PEI) base polymer for 3 hours incubation at 37°C followed by a rinsing step. There was a reduction in LEC attachment across all CS concentrations at day 4 when compared to untreated PEI control. However by day 7 monolayers had formed across most concentrations, similar to the control. 10mg/ml had a slight decrease in LEC attachment by day 7.

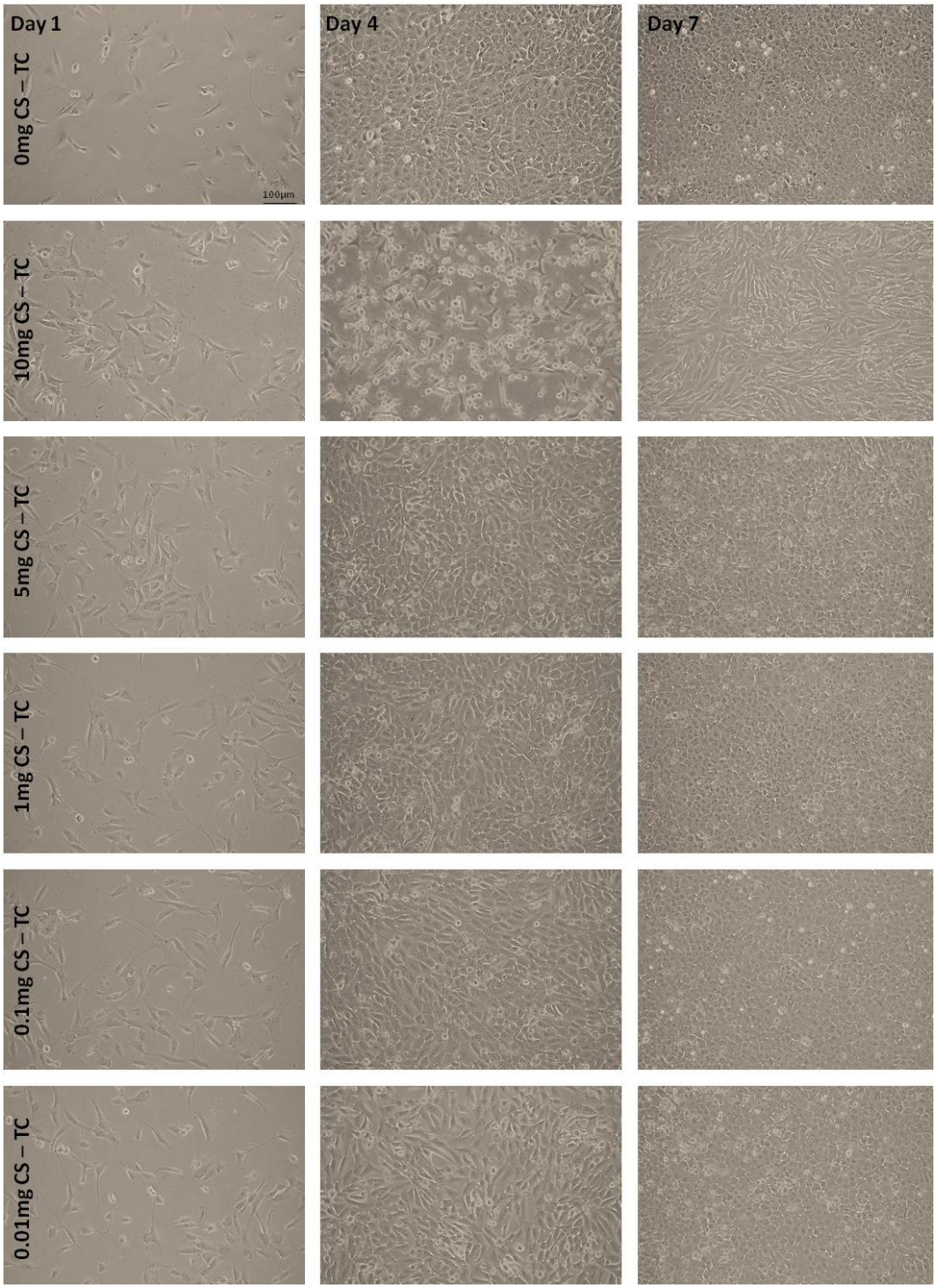

Figure 3.22: Phase contract micrographs demonstrating cell attachment on chondroitin sulphate (CS) adsorbed onto tissue culture polystyrene (TCPS) for 3 hours incubation at 37°C followed by a rinsing step. All CS concentrations produced a monolayer of LEC by day 7, similar to untreated TCPS control. By day 4 10ng/ml CS had less cell attachment, but this had recovered by day 7.

CS did not encourage LEC attachment when adsorbed onto PS coverslips for "3 hour incubation at 37°C followed by a rinsing step", regardless of concentrations, similar to PS coverslips control (Figure 3.23).

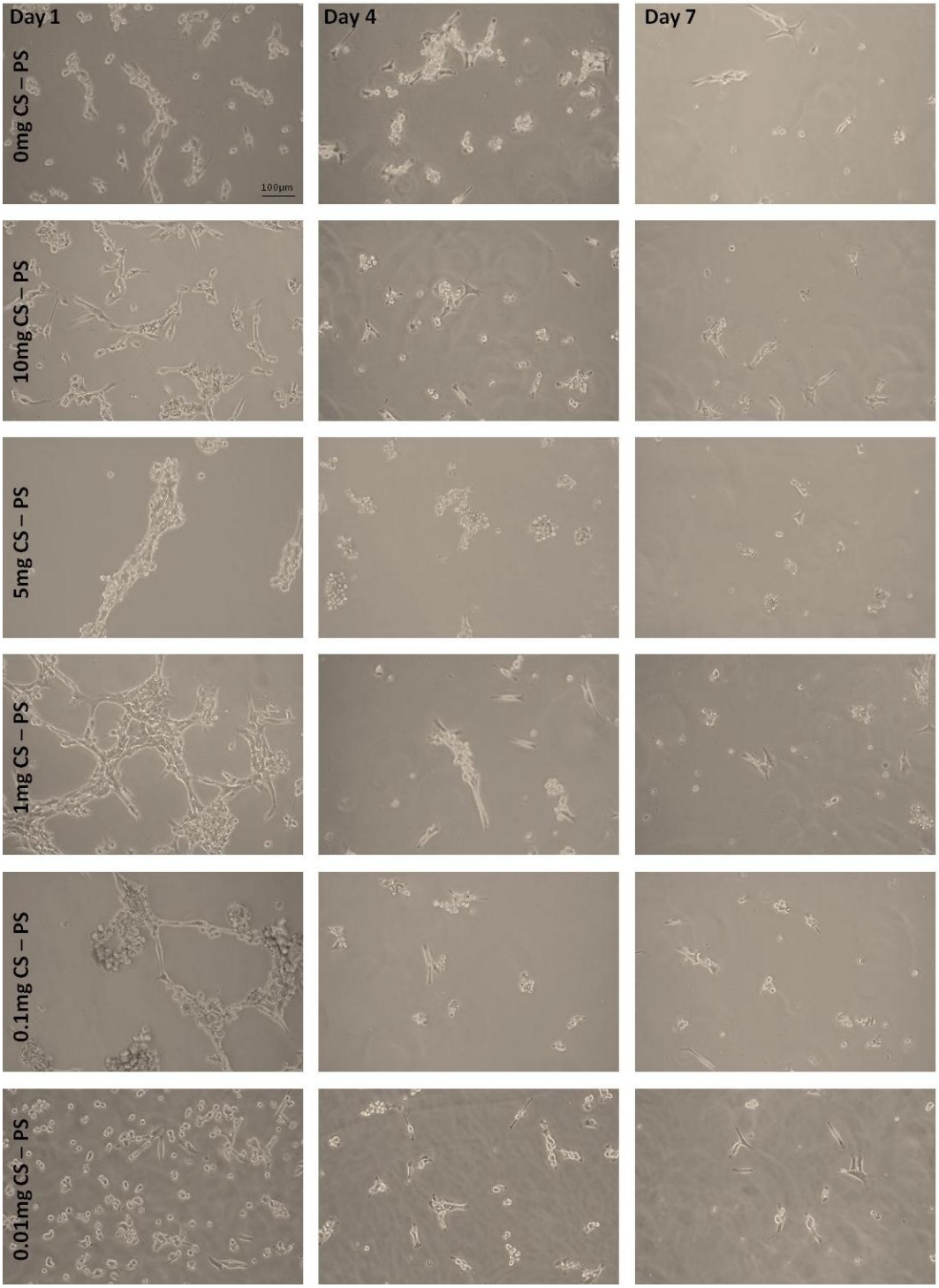

Figure 3.23: Phase contrast micrographs of cell attachment on chondroitin sulphate (CS) adsorbed onto polystyrene (PS) coverslips for 3 hour incubation at 37°C followed by a rinsing step. CS did not encourage LEC attachment regardless of concentration. This was the same response as untreated PS coverslips.

To summarise, the cellular response for HA and CS adsorbed onto PEI, TCPS and PS coatings at "3 hour incubation at 37°C followed by a rinsing step", was similar to uncoated controls, regardless of the basement substrate and GAG concentration. The higher GAG concentrations (10mg and 5mg) proved difficult to dissolve in medium prior to coating substrates, therefore were not analysed further.

3.4.2.2 3 Hour Incubation at 37°C without a Rinsing Step

To explore if more GAG could be bound to the substrates to cause an effect on the LECs attachment the study was repeated at "3 hour incubation at 37°C without a rinsing step". Similar cellular attachment and growth was observed during cell culture of HA and CS adsorbed onto TCPS and PS coatings to the previous "3 hour incubation – followed by rinsing" study, therefore micrographs are not shown.

When HA and CS were adsorbed onto PEI for "3 hour incubation at 37°C without a rinsing step" there was no cell attachment and growth on GAG adsorbed coatings, regardless of concentrations. This was similar to the control (Figure 3.24), therefore the experiment was stopped at day four as PEI in previous studies has been shown to encourage LEC attachment.

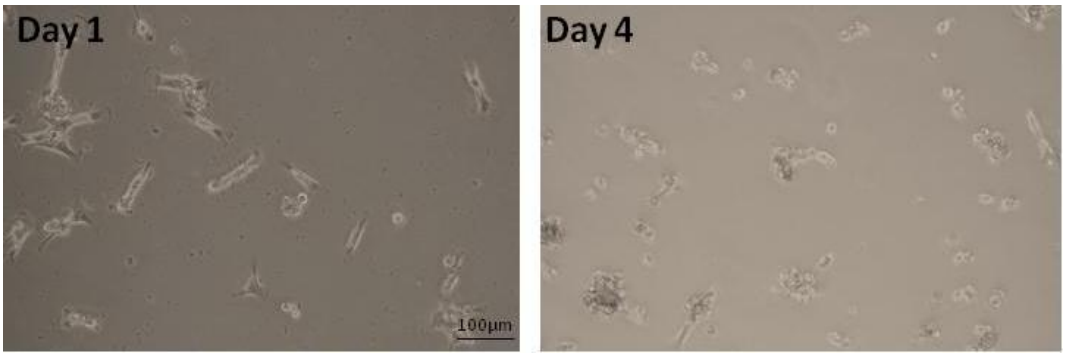

Figure 3.24: Representative phase contrast micrographs of LECs growth on polyethylenimine (PEI) base polymer in the absence of any GAG, at days 1 and 4. Cell attachment was the same for both hyaluronic acid (HA) and chondroitin sulphate (CS) concentrations and the untreated PEI control therefore the experiments were stopped at day four.

3.4.2.3 24 Hour Incubation at 37°C & 4°C without a Rinsing Step

The incubation time was increased to 24 hours to examine if a longer incubation time produced more GAG adsorption onto the substrate to produce a cellular effect. HA and CS were added to TCPS and PEI substrates for "24 hours incubation at either 37°C or 4°C without a rinsing step". Phase contrast micrographs were taken whilst in cell culture. The LEC response was similar to untreated TCPS and PEI controls regardless of GAG type, concentration and temperature (Figure 3.25).

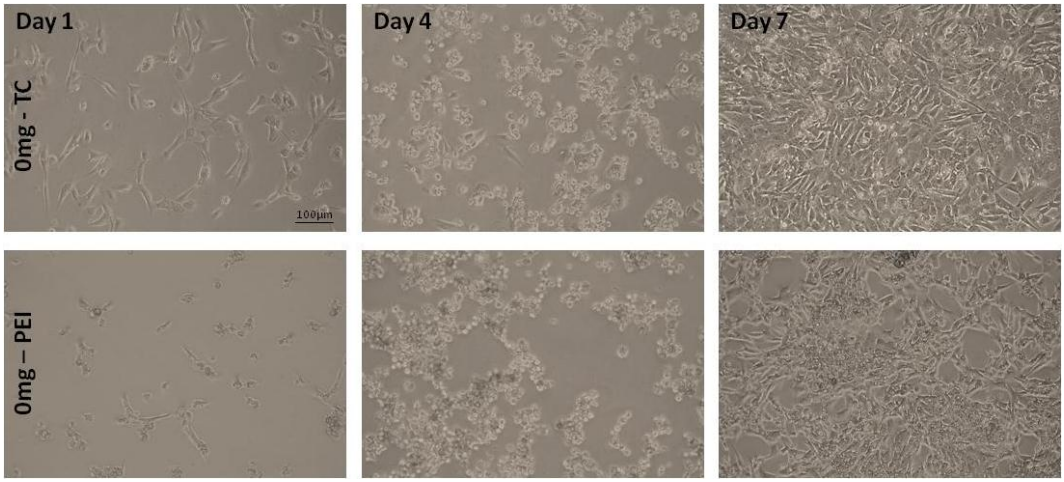

Figure 3.25: Representative phase contrast micrographs demonstrating cell attachment and growth on tissue culture polystyrene (TCPS) and polyethylenimine (PEI) controls in the absence of any GAG. Cell attachment was the same when hyaluronic acid (HA) and chondroitin sulphate (CS) were adsorbed onto TCPS and PEI for "24 hours incubation at either 37°C or 4°C without a rinsing step".

3.4.2.4 GAG Added to Cell Culture Medium

A final method of including HA and CS in the culture medium was tested. Cells were fed every 2 – 3 days with medium containing various concentrations of either HA or CS. LECs seeded on PEI substrates in the presence of "HA or CS containing medium" had a similar response to PEI control in the absence of GAG containing medium. Cells attached and spread during the seven days in cell culture and near-confluent areas of LEC growth were observed by day 7, however there was a reduction in cell growth on 1mg/ml CS throughout the seven days in cell culture (Figure 3.26).

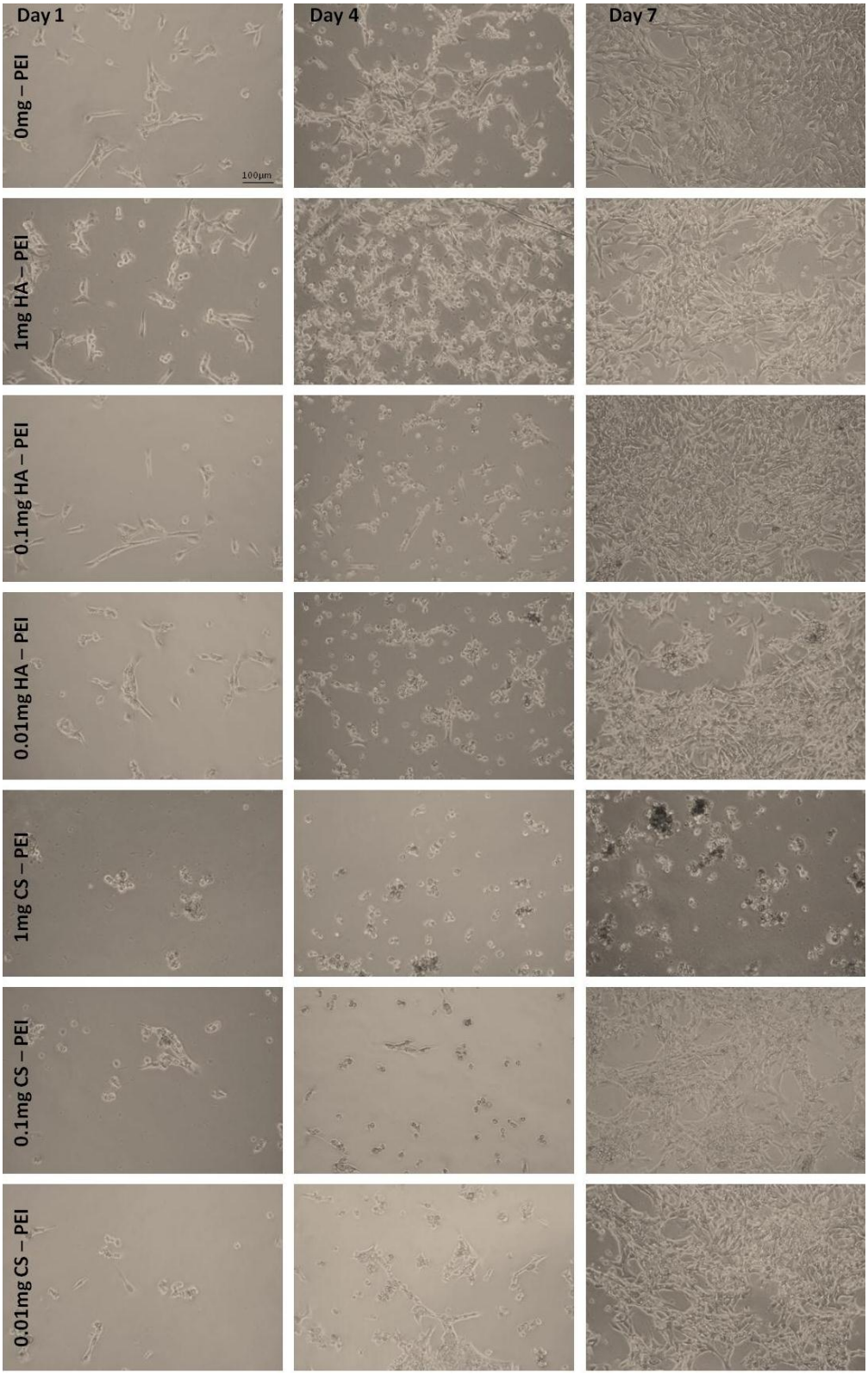

Figure 3.26: Phase contrast micrographs demonstrating LEC attachment and growth on polyethylenimine (PEI) in the presence of hyaluronic acid (HA) or chondroitin sulphate (CS) containing medium and control (PEI 0mg/ml). Some patchy growth was observed when LECs were seeded onto PEI in the presence of HA or CS containing medium compared to the control. 1mg/ml CS did not encourage cells to adhere.

Cells seeded on TCPS substrate in the presence of “HA or CS containing medium” had a reduced cell attachment and growth when compared to TCPS control (in the absence of GAG containing medium) (Figure 3.27). By day 7 LEC attachment and growth on HA and CS coatings decreased with increasing GAG concentration.

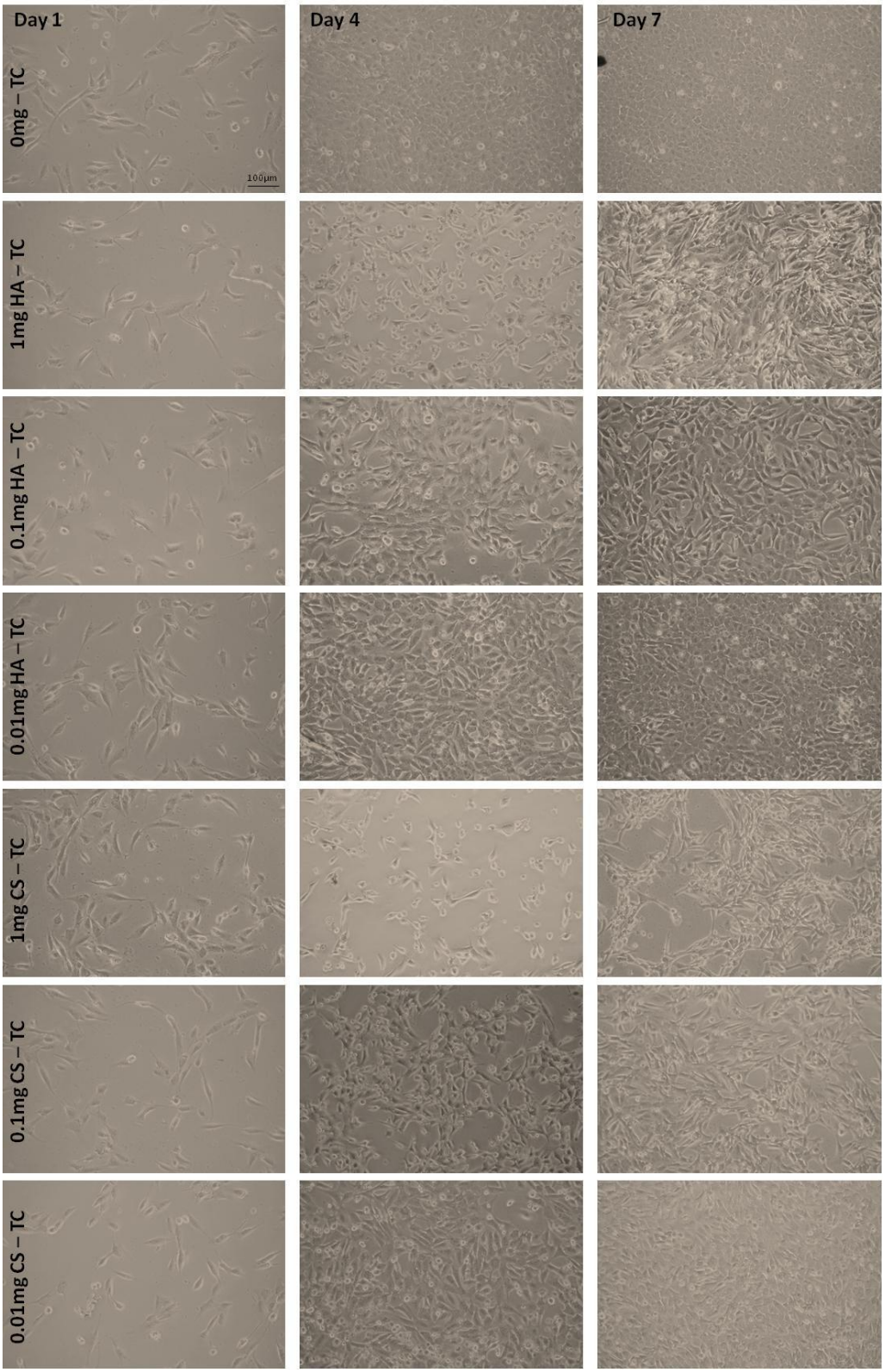

Figure 3.27: Phase contrast micrographs demonstrating LECs attachment on tissue culture polystyrene (TCPS) in the presence of hyaluronic acid (HA) or chondroitin sulphate (CS) containing medium and TCPS control (0mg/ml). Attachment and growth of cells seeded onto TCPS in the presence of HA or CS containing medium was similar to TCPS control, however the higher the concentration of GAG the less LEC attachment was observed, regardless of GAG type.

LECs seeded onto PS coverslips in the presence of "HA or CS containing medium" had a similar cellular response to PS control in the absence of GAG containing medium. PS coatings did not support cellular attachment regardless of GAG type and concentration (similar to PS control), therefore phase contrast micrographs are not shown.

3.4.2.5 Quantifying the Amount of GAG Present

All adsorbed GAG coatings were stained with toluidine blue to demonstrate the presence of adsorbed GAG to PEI, TCPS and PS substrates. Toluidine blue staining of HA and CS adsorbed onto TCPS substrates for "24 hours incubation at 37°C without a rinsing step", demonstrated little positive staining regardless of GAG concentrations (Figure 3.28).

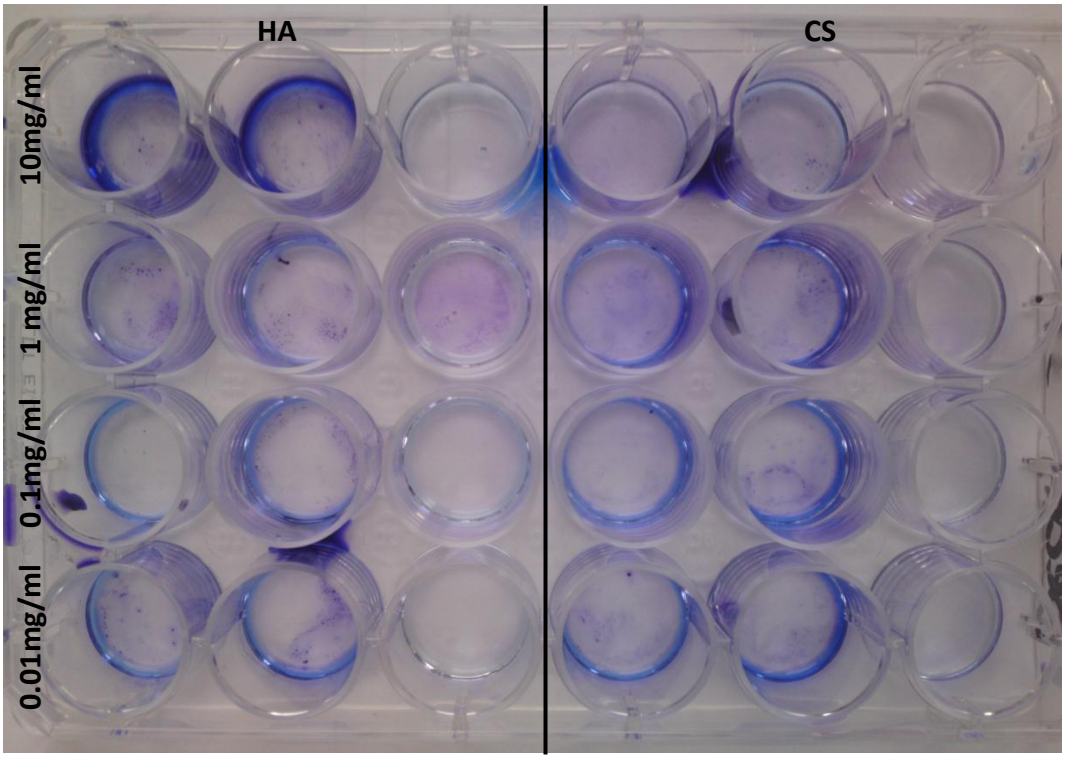

Figure 3.28: Photograph of a whole plate demonstrating toluidine blue staining of hyaluronic acid (HA) and chondroitin sulphate (CS) adsorbed onto tissue culture polystyrene (TCPS) for 24 hours at 37°C. There was little positive staining regardless of GAG. Slight toluidine blue staining was observed on higher concentrations at 10mg/ml and 1mg/ml.

Toluidine blue staining of HA and CS adsorbed onto TCPS substrates for "24 hours incubation at 4°C without a rinsing step", demonstrated slightly more toluidine blue staining present at 10mg and 1mg HA than CS, however results were inconclusive as it was not present in all the wells (Figure 3.29). Lower concentrations had no positive staining.

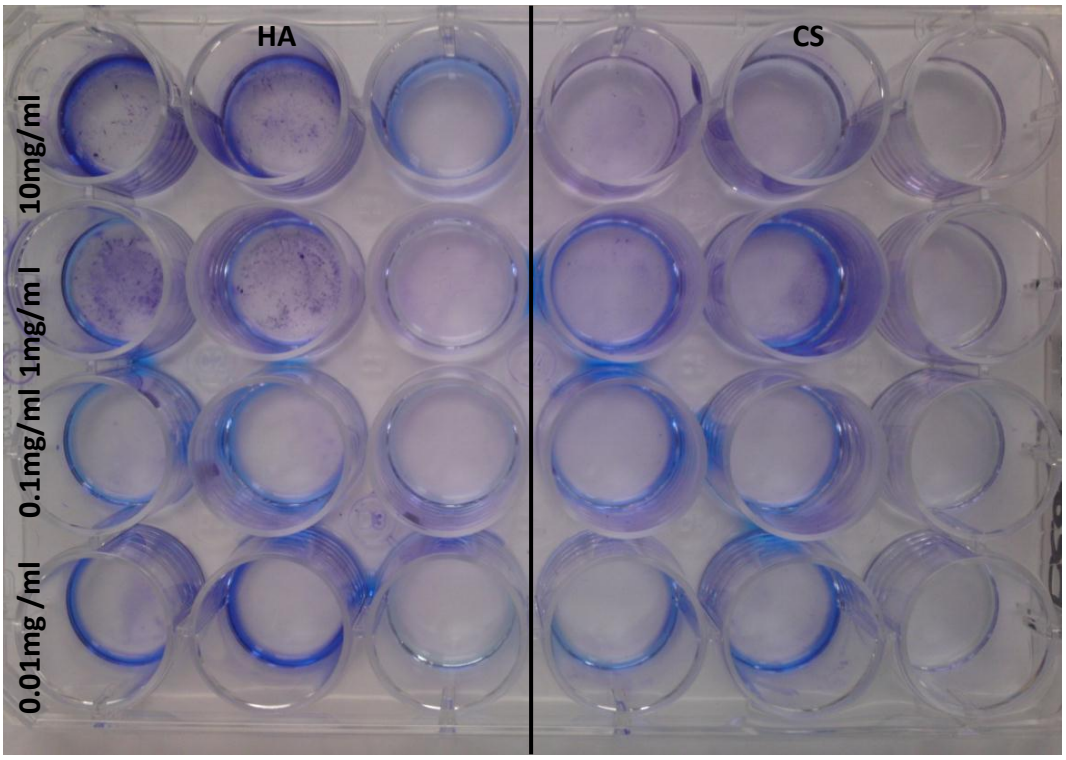

Figure 3.29: Photograph of a whole plate demonstrating toluidine blue staining of hyaluronic acid (HA) and chondroitin sulphate (CS) adsorbed onto polystyrene (TCPS) for 24 hours at 4°C. 10mg/ml and 1mg/ml HA showed a greater amount of toluidine blue staining. Other concentrations did not positively stain for the presences of GAG.

Toluidine blue did not prove successful at staining adsorbed GAG coatings regardless of method, substrate and GAG concentration, therefore toluidine blue photographs from other adsorbed GAG assays are not shown.

3.4.3 Bound GAGs Coatings

HA and CS were immobilised onto modified 13mm glass coverslips coated with amine functionality by silanisation. GAGs were bound onto the amine coatings via 1-ethyl-3-(3-dimethylaminopropyl) carbodiimide (EDC)/N-hydroxysuccinimide (NHS) reaction solution.

3.4.3.1 Cell Growth Study

N/N1003A LECs were seeded onto the bound GAG coatings for a total of seven days. Phase contrast micrographs were taken during this time of LECs seeded onto CS and HA bound coatings (Figure 3.31 and Figure 3.31 representatively).

LECs seeded onto TCPS and glass controls had typical epithelial cuboidal appearance and by day 7 a confluent monolayer was observed (Figure 3.30). Amine coated coverslips had less cell attachment than TCPS and glass controls and by day 7 a confluent monolayer was not observed. LECs seeded onto 3mg/ml and 1mg/ml bound CS coating did not encourage LECs attachment and growth, cells remained rounded in morphology during the seven days and a lot of cell debris and floating cells was produced. There was also some precipitation present from the coating. Patchy LECs growth was observed on 0.1mg/ml bound CS coating, cells that did adhere appeared epithelial in morphology.

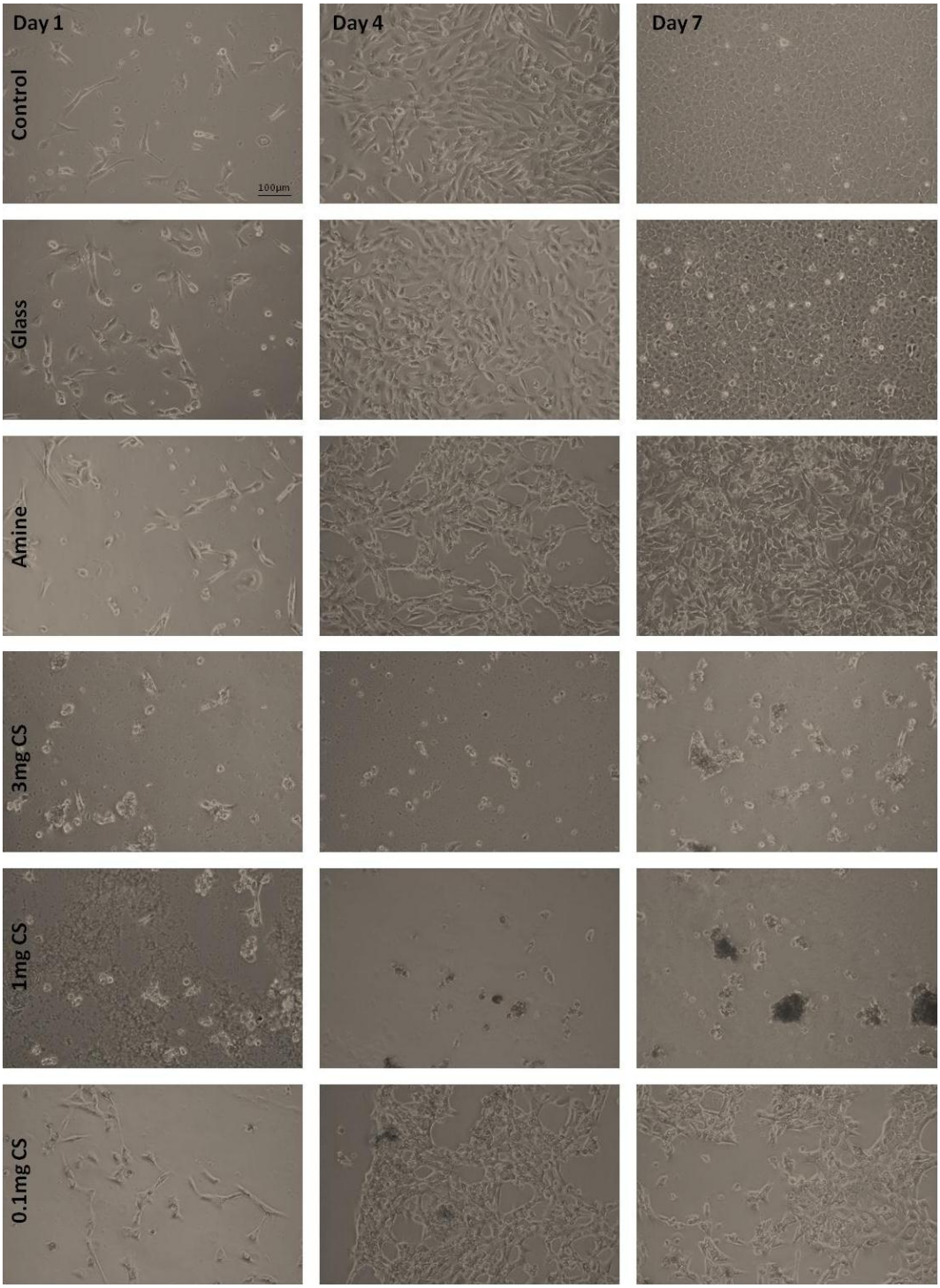

Figure 3.30: Phase contrast micrographs demonstrating cell attachment and growth on tissue culture polystyrene (TCPS) control, glass coverslips, amine coated coverslips and 3mg/ml, 1mg/ml and 0.1mg/ml of bound chondroitin sulphate (CS) on amine coated coverslips, during the 7 days in cell culture. TCPS and glass control had a similar growth pattern with LECs reaching confluency by day 7, both have a typical epithelial cuboidal appearance. 0.1mg/ml CS had patchy cell growth with some areas becoming near confluent and others areas with no cell growth. Cells appeared epithelial in morphology. 1mg/ml and 3mg/ml of bound CS did not encourage LEC attachment and growth. Instead cells appeared rounded and produced a lot of cell debris and floating cells.

LECS seeded onto 3mg/ml and 1mg/ml bound HA coating did not encourage cell attachment and growth (Figure 3.31). Patchy LEC growth was observed on 0.1mg/ml bound HA coating, similar to 0.1mg/ml CS, again cells that adhered appeared epithelial in morphology.

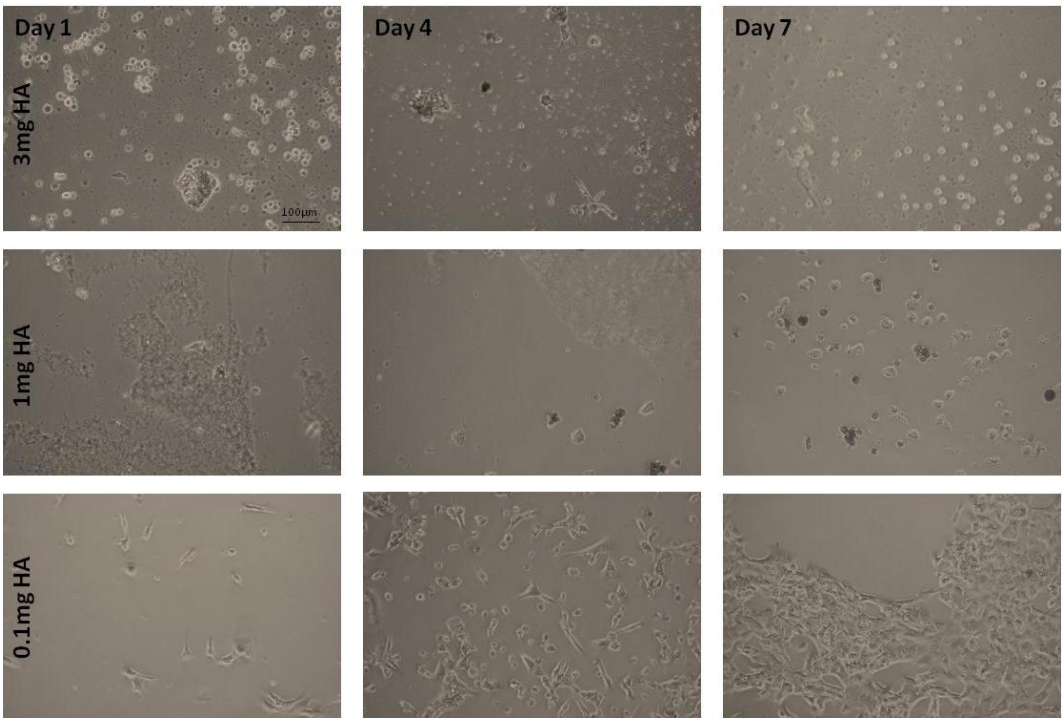

Figure 3.31: Phase contrast micrographs demonstrating cell attachment and growth on 3mg/ml, 1mg/ml and 0.1mg/ml bound hyaluronic acid (HA) on coated amine coverslips, during the 7 days in cell culture. 0.1mg/ml HA was similar to 0.1mg/ml of CS, cells grew in small patches with some areas becoming near confluent and others areas with no cell growth, and again cells appeared epithelial in morphology. 1mg/ml and 3mg/ml of bound HA did not encourage LECs attachment and growth.

On day 7 cells were fixed with methanol and stained with methylene blue for 2 minutes to grossly visualise the LECs attachment and growth. Methylene blue staining was similar for HA and CS (Figure 3.32 and Figure 3.33 representatively). Few cells were visualised on bound HA and CS at 3mg/ml and 1mg/ml. Some cell attachment was visualised on bound HA and CS at 0.1mg/ml concentration. Amine, glass and TCPS wells all had relatively confluent areas of cell growth with amine having slightly less methylene blue staining.

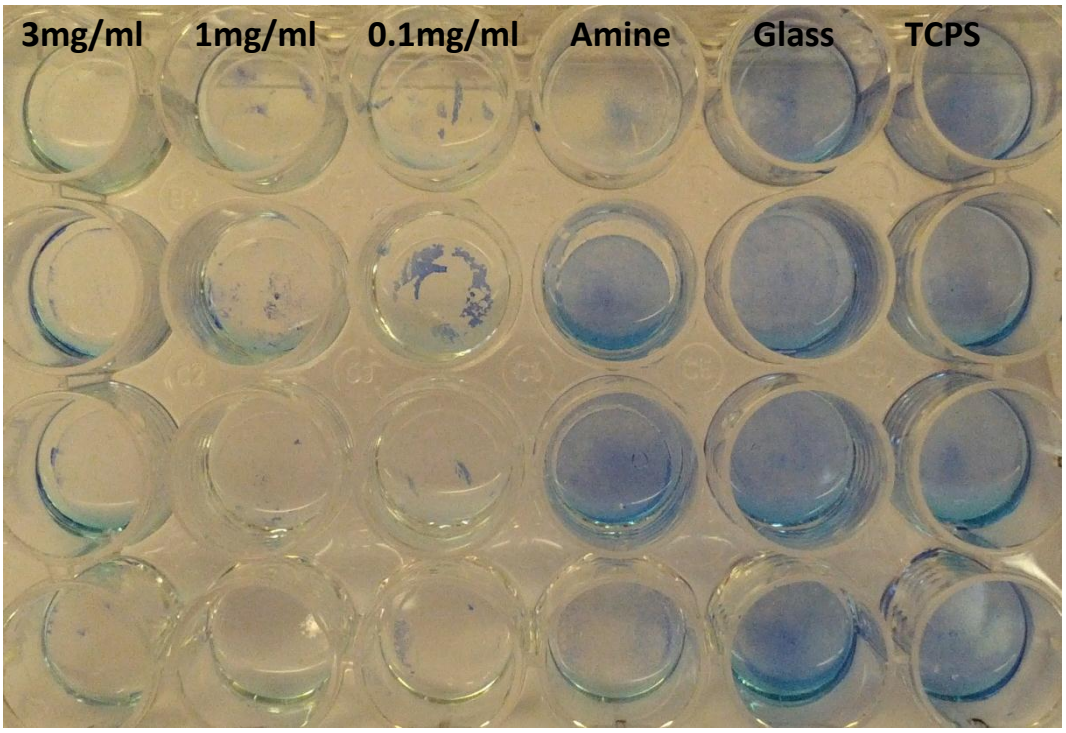

Figure 3.32: Photograph of the whole plate demonstrating methylene blue staining of LECs attached to hyaluronic acid (HA) bound to amine coated coverslips, amine coated coverslips, glass coverslips and tissue culture polystyrene (TCPS) control. Amine, glass and TCPS all have good coverage of LECs with amine having slightly less cell growth. 3mg/ml and 1mg/ml HA showed few to no cell attachment. Some dye build-up can be seen around the edges of these wells. Some methylene blue staining can be seen on 0.1mg/ml HA in small clusters.

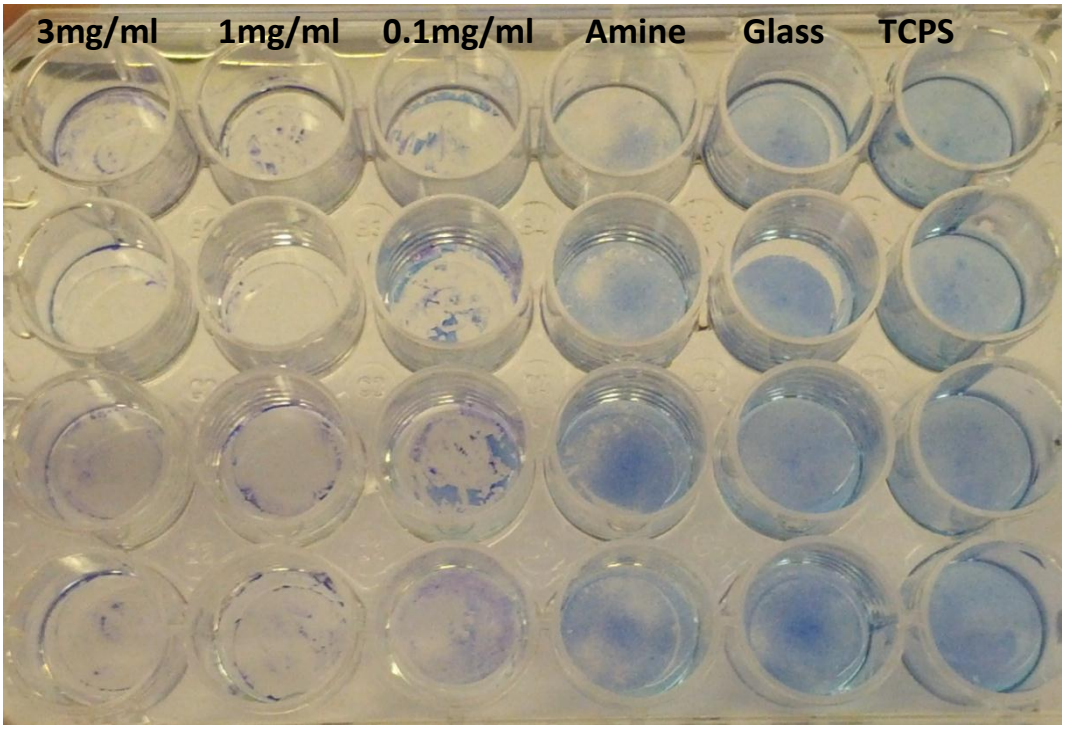

Figure 3.33: Photograph of a whole plate demonstrating methylene blue staining of LECs attached to chondroitin sulphate (CS) bound to amine coated coverslips, amine coated coverslips, glass coverslips and tissue culture polystyrene (TCPS) control. Again amine, glass and TCPS all had good coverage of LECs with amine having slightly less cell growth. 3mg/ml and 1mg/ml CS showed no cell attachment. Some dye build-up was noticeable on the CS coverslips also. Some methylene blue staining can be seen on 0.1mg/ml CS in small clusters.

3.4.3.2 Quantifying the Amount of GAG Present

To quantify if any bound GAG was present wells were again stained with toluidine blue, however the GAGs bound to the amine coated coverslips failed to stain (Figure 3.34).

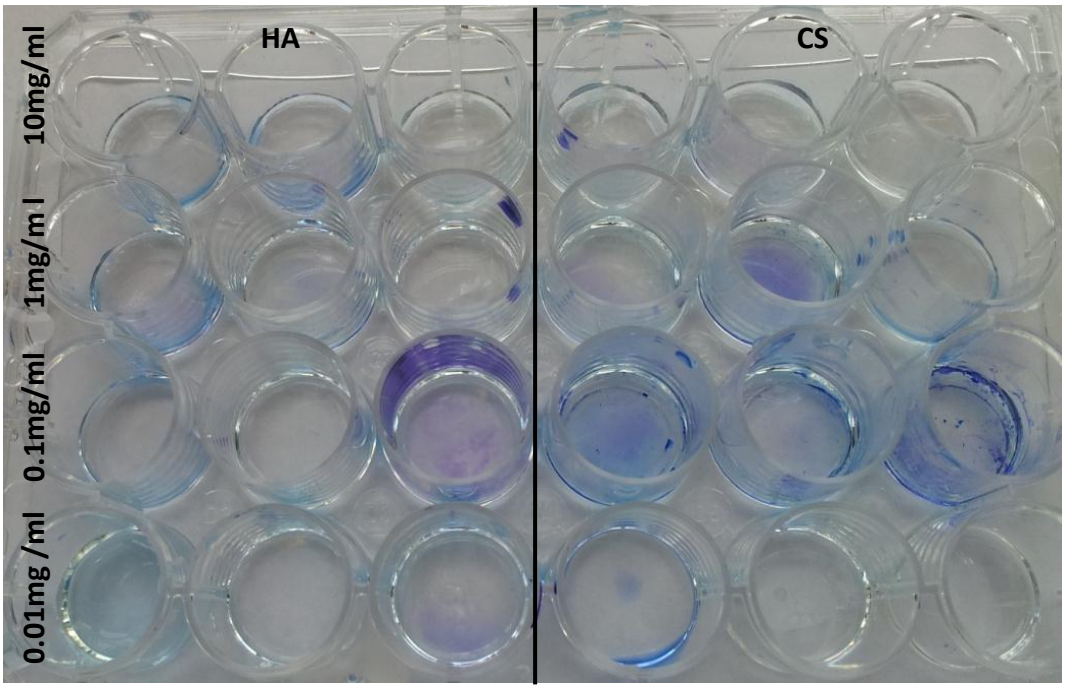

Figure 3.34: Photograph of a whole plate demonstrating toluidine blue staining of hyaluronic acid (HA) and chondroitin sulphate (CS) bound onto amine coated coverslips. Toluidine blue did not stain the bound GAG coverslips.

CA measurements were taken of bound GAG coated coverslips as an alternative to observe if any GAG was present (Figure 3.35). The CA for TCPS represents the usual substrate used in cell culture to grow LECs. Untreated glass CA was significantly more hydrophobic than TCPS. The CA increased further when glass coverslips were functionalised with amine groups, however this increase was not significant. When HA and CS were bound onto amine coated coverslips the CA decreased significantly, becoming more hydrophilic. Data was analysed using Dunnett's T3 post hoc test. The results confirmed a change in CA indicating the surface of the glass coverslips had been modified.

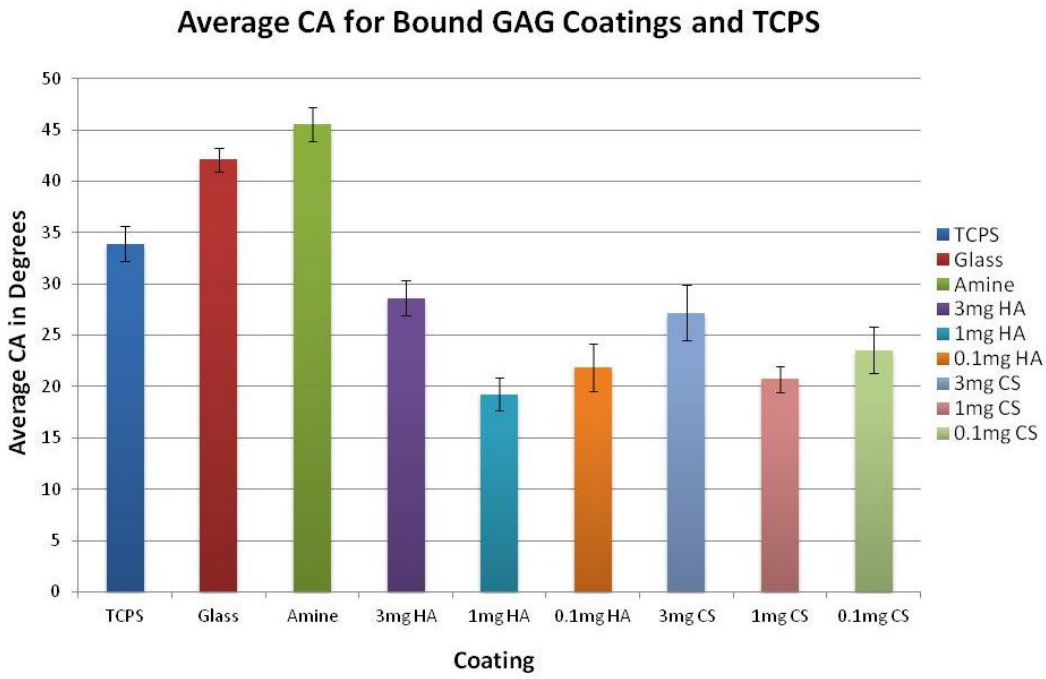

Figure 3.35: Graph demonstrating average contact angle measurements (CA) of controls (TCPS, glass and amine) and bound hyaluronic acid (HA) and chondroitin sulphate (CS) coated coverslips. Error bars equal ± 1 standard deviations. The CA of TCPS represents the usual substrate used to grow LECs in cell culture. The CA changes when the glass coverslips were coated with amine and became slightly more hydrophobic. However when HA and CS were bound onto the surface of amine coated the coverslips the CA decreased, making them more hydrophilic. The CA measurements were similar for HA and CS depending on the concentrations, 3mg/ml were more hydrophobic than 1mg/ml and 0.1mg/ml.

The CA measurement for bound GAG coatings and polymer GAG coatings provided by BioInteractions Ltd. were compared and statistically analysed using Dunnett's T3 post hoc test (Figure 3.36). Polymer HA and CS were not significantly different to 0.1mg/ml bound HA and CS. Polymer HA was also not significantly different to 3mg/ml bound CS, however the p value (0.099) was close to the significance value of 0.05. Some similarities between polymer HA and CS coatings and bound HA and CS coatings were observed.

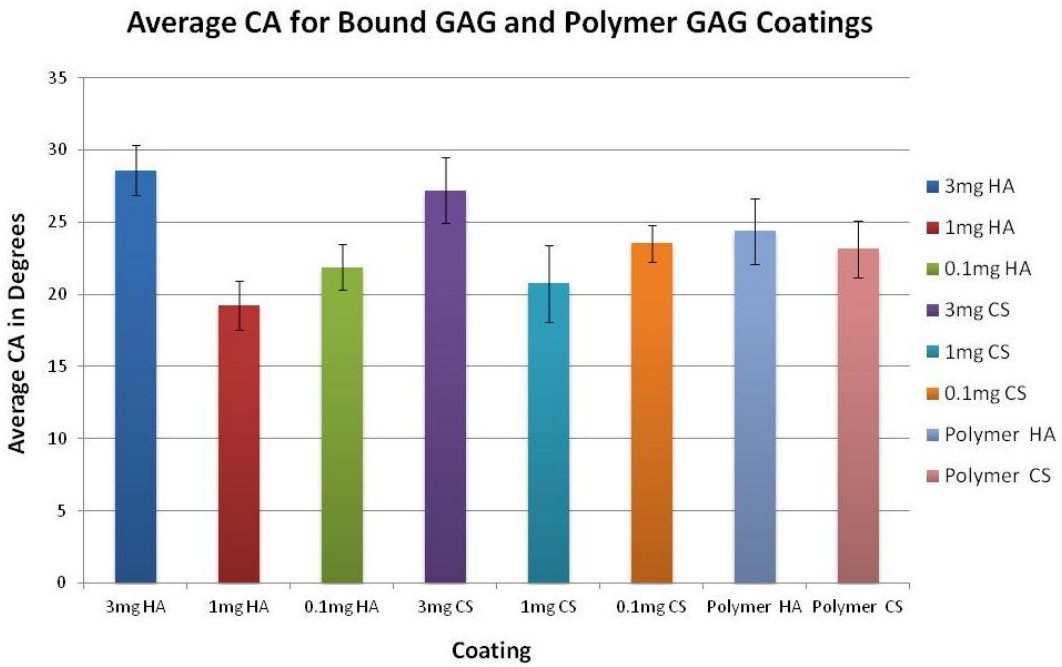

Figure 3.36: Graph demonstrating comparison of the average contact angle (CA) measurements between bound hyaluronic acid (HA) and chondroitin sulphate (CS) coating and polymer HA and CS coatings. Error bars equal ± 1 standard deviations. CA ranged from 19° - 28°. Polymer HA and CS were not significantly different from 0.1mg/ml HA and CS, indicating some correlation in CA between polymer GAG coatings and bound GAG coatings.

3.5 Zwitterionic Polymers

Six zwitterionic coatings (F-N) and three control coatings (L–N) were synthesized (Table 2-5 pg.72). Coatings were studied in cell culture for a total of seven days. The cytoxic effect of the coatings was also examined along with time lapse microscopy. Surface analyses of the coatings were performed using CA, SEM and white light interferometry.

3.5.1 Cell Growth Study

Phase contrast micrographs were taken throughout the study (Figure 3.37). LECs seeded onto TCPS wells produced a confluent monolayer by day 7, with typical epithelial morphology. Cells did not adhere to coatings F, G, and I throughout the seven days in cell culture. LECs settled and adhered to coating H and by day 7 patchy cell growth was observed.

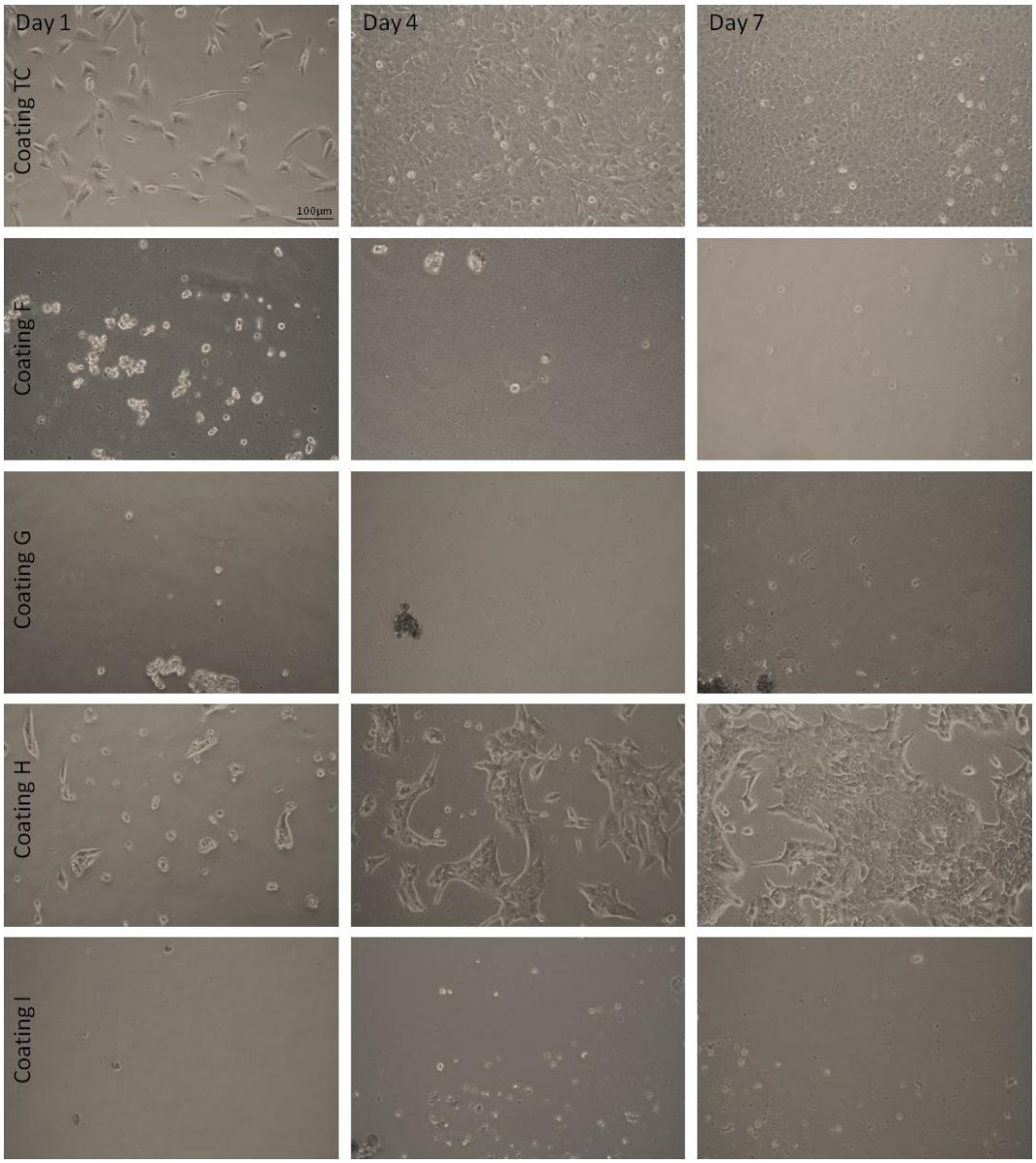

Figure 3.37: Phase contrast micrographs demonstrating LECs attachment on tissue culture polystyrene (TCPS) and zwitterionic coatings F – I (F – 90% butyl methacrylate:10% novel zwitterionic monomer, G – 80% butyl methacrylate:20% novel zwitterionic monomer, H – 70% butyl methacrylate:30% novel zwitterionic monomer and I – 58% hydroxypropyl methacrylate:31% hexyl methacrylate:11% novel zwitterionic monomer) during the 7 days in cell culture. A monolayer of cells was present by day 7 on TCPS. Coatings F, G and I behaved in a similar manner and did not support LEC attachment. Coating H supported cell attachment and confluent areas of cell attachment were observed by day 7.

Phase contrast micrographs (Figure 3.38) representative micrographs from LECs on coatings J- N throughout the seven days in culture. Coatings J, L and N were similar to

TCPS control. All three coatings supported LEC attachment and produced a monolayer of cells by day 7. Cells did not adhere to coatings K and M throughout the seven days in cell culture.

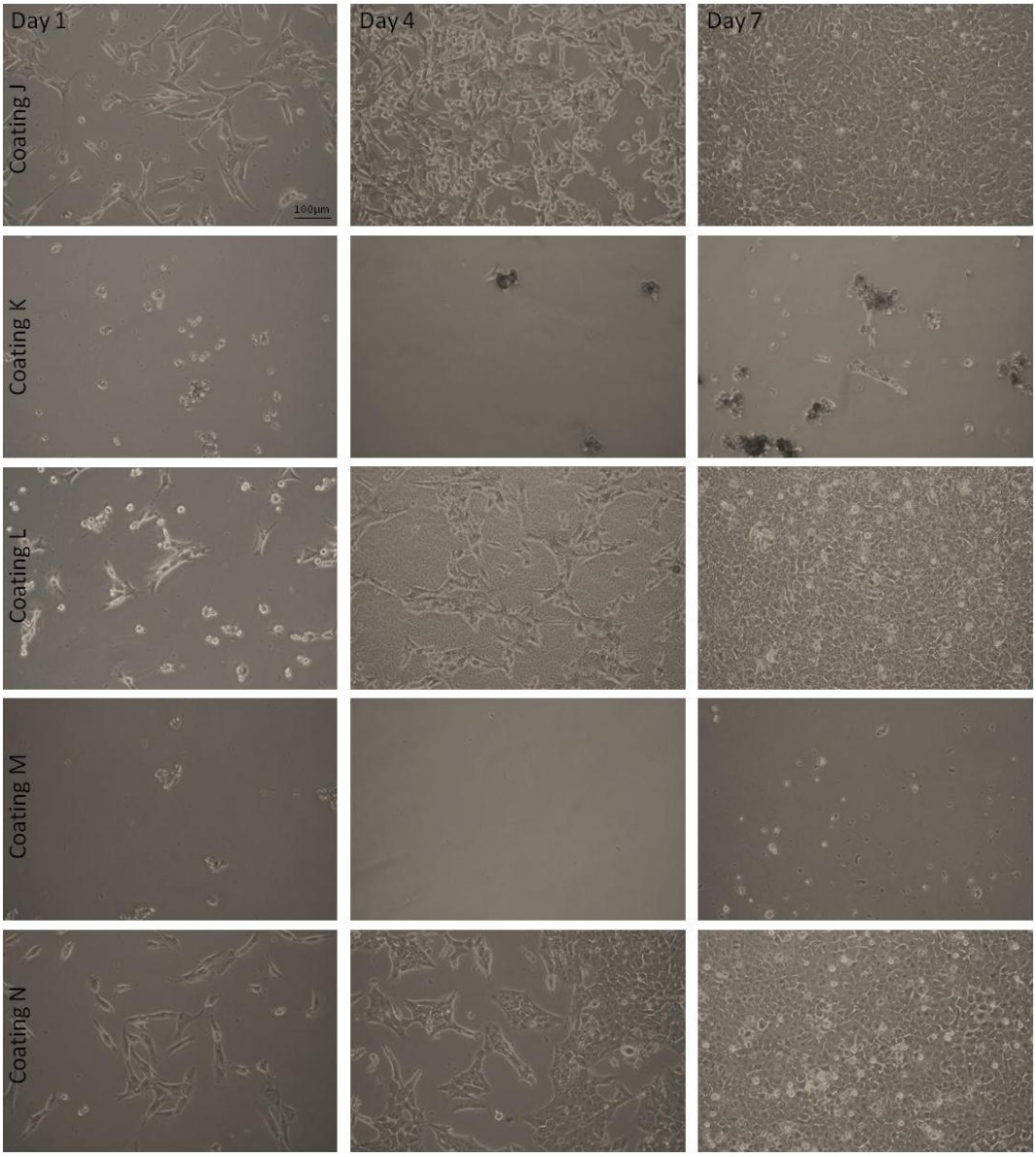

Figure 3.38: Phase contrast micrographs demonstrating LECs attachment on zwitterionic coatings J – N (J – 58% hydroxypropyl methacrylate:31% hexyl methacrylate:11% novel zwitterionic monomer, K – 50% methoxyethyl methacrylate:30% hexyl methacrylate:20% novel zwitterionic monomer, L – 100% poly (butyl methacrylate), M – 90% butyl methacrylate:10% 2-methacryloyloxyethyl - phosphorylcholine (MPC) and N – 70% butyl methacrylate:30% 2-methacryloyloxyethyl – phosphorylcholine) during the 7 days in cell culture. Cell attachment on coatings J, L and N demonstrate a similar LEC response to TCPS control. Cells did not adhere to coatings K and M throughout the seven days in cell culture.

3.5.2 Cell Staining

After each time point cells were fixed and stained with phalloidin, and DAPI. The cell nuclei were counted and the average number of cells per field of view was plotted (Figure 3.39). Coatings F, G, I, and M did not support LEC attachment or growth. Coating K had an average cell count of 22 cells/field of view or less throughout the 7 days in cell culture. On day 7 there was no significant difference between coatings F, G, I, K and M ($p>0.05$). Coatings H, J, L and N did support LEC attachment and growth to various degrees, however coating J is believed to have dissolved in the medium so will not be taken any further. There was no significant difference between coatings H, J, L and N at day 7. On day 7 no significant difference was observed between coatings J and L compared to TCPS ($p=0.55$ and $p=0.52$ respectively). This means out of the six novel zwitterionic coatings there is potentially a coating which could support the hypothesis for a monolayer of cells, coating H, and several coatings which could support the hypothesis for prohibiting cell growth, coatings F, G, and I. Dunnett's T3 post hoc test was used following one-way ANOVA.

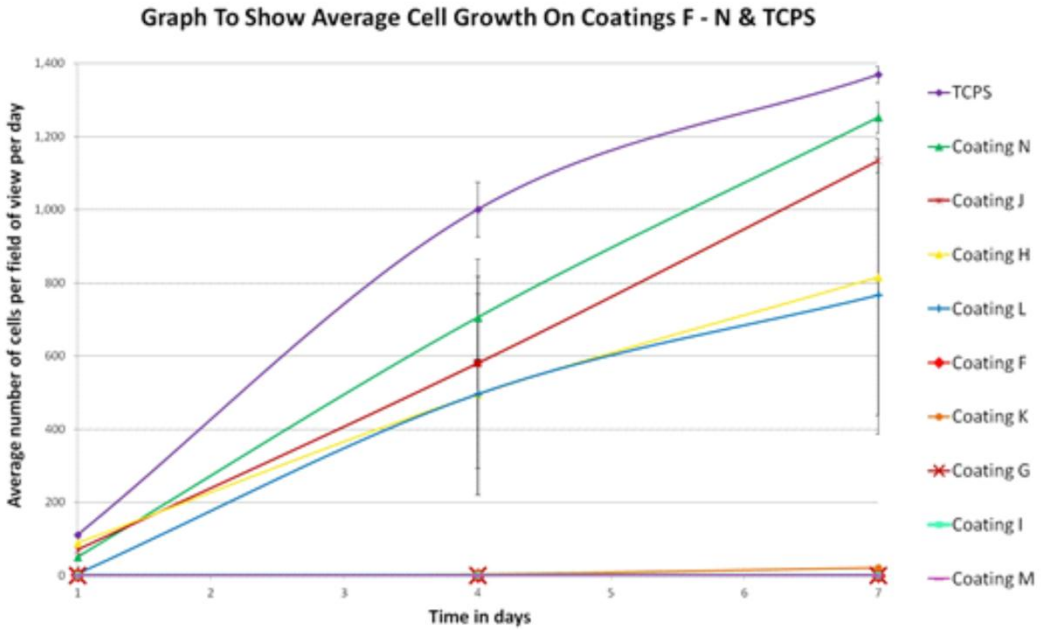

Figure 3.39: Graph demonstrating LEC attachment and growth on zwitterionic coatings F-N and control tissue culture polystyrene (TCPS) during 7 days in cell culture. Error bars equal ± 1 standard deviations. The top purple line is the control (LECs grown on TCPSP) and represents the typical growth profile for this cell line. Coatings N, J, H and L all supported cell attachment and growth to various degrees. Coating N and J had a linear profile, indicating LECs on these surfaces may carry on proliferating if they were left longer in culture. Coatings K, F, G, I and M did not support the appropriate cell binding sites required for cell attachment and growth.

3.5.3 Cytotoxic Assay

A cytotoxicity assay was performed, following BS EN ISO 10993-5:2009 using the extraction method. After LECs had been incubated in the extracted medium for 1 and 3 days the metabolic activity was measured using resazurin. The results of the cytotoxicity assay confirmed that all coatings had a similar metabolic activity and were consistent with the negative controls (blank and TCPS) (Figure 3.40). One way ANOVA was performed followed by Tukey's or Dunnett's T3 post hoc test on days 1 and 3, depending if variances were homogeneous or not, respectively. The results demonstrate the novel zwitterionic coatings had no adverse effects, as the metabolic activity was not significantly different from cells seeded onto TCPS $p<0.05$. Positive control, 5% DMSO, was significantly different and induced toxicity. The metabolic activity decreased on day 3 as the cells became confluent and less metabolically active.

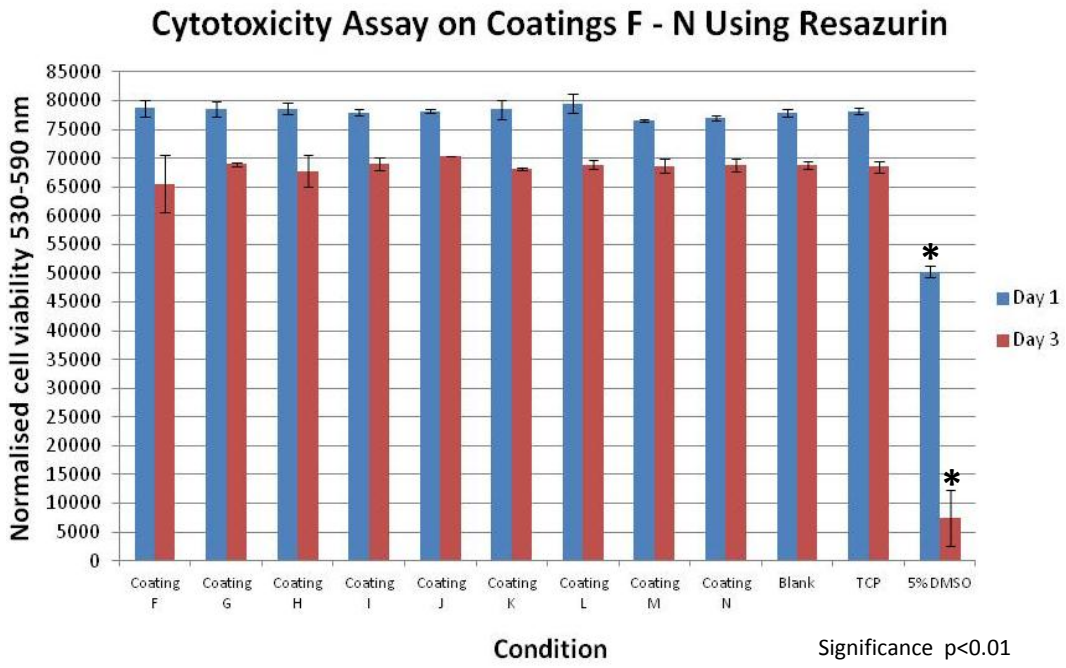

Significance $p<0.01$

Figure 3.40: Graph demonstrates cytotoxicity assay of zwitterionic coatings F–N and blank control (tissue culture polystyrene (TCPS) coverslips), negative control TCPS wells and positive control 5% DMSO. Error bars equal ± 1 standard deviations. * denote significant difference where $P<0.05$. Metabolic activity was measured using resazurin. There was no significant difference between coatings F-N & blank compared to TCPS control. 5% DMSO significantly induced cytotoxicity.

3.5.4 Toxicity Assay

LECs are adherent dependant cells, in culture they adhere to TCPS within half an hour (observed with time lapse microscopy analysis) and do not survive in the medium if they cannot settle and attach. On the majority of the coatings F-N cells did not attach during the 7 days in cell culture, instead they clumped together and died. Therefore a toxicity assay was performed to observe if unattached cells, initially seeded onto coatings F-N, could be aspirated and reseeded onto uncoated TCPS wells and attach, spread and proliferate. The results illustrate the metabolic activity increased from day 1 to day 4 across all coatings and TCPS control, indicating coatings F-N did not have a toxic effect on cell ability to attach, spread and proliferate (Figure 3.41). Coatings J and L had a lower metabolic activity than the rest of the coatings, as most cells had attached to J and L coated wells within the 2 hours and is represented by columns, original J and original L. To some extent this was the same for coating N. On day 1 there was significant difference in metabolic activity between TCPS and coatings F, J, L, N, original J, original L and original N ($p<0.05$). On day 4 coatings F, J, K, M, N, original L and original N were significantly different to TCPS ($p<0.05$).

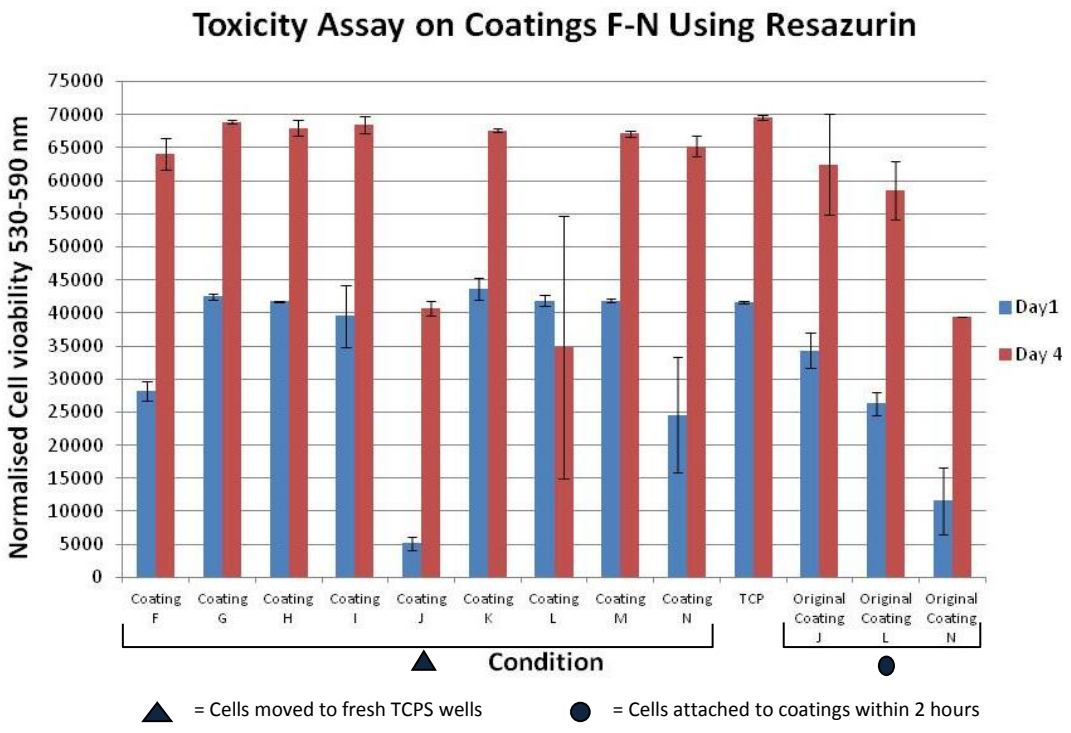

Figure 3.41: Graph demonstrates cell toxicity assay of zwitterionic coatings F – N and tissue culture polystyrene coverslips (TCPS). Error bars equal ± 1 standard deviations. Metabolic activity of LECs was measured using resazurin. On day four TCPS was significantly different to Coatings F, J, K, M, N, original L and original N ($p<0.05$).

3.5.5 Time Lapse Microscopy

The results from the time lapse microscopy were similar to the previous cell growth curve study (appendix B). Coating F did not encourage cell attachment, cells initially clumped together and did not adhere to the coating. Coating G, I, K and M all produced a similar affect. Coating H did support cell attachment to a certain degree, however cells took a while to settle and spread, approximately eight hours. By day seven small patches of cell growth in the field of view were present. Cells attached and settled onto coating J within 30 minutes to an hour. By day 7 a sub-confluent monolayer was present. Coating L encouraged cells to attach and settle within approximately an hour. LECs grew to a sub-confluent monolayer by day 7, however this was not as confluent as coating J and a lot of rounded cells were present. Coating N encouraged settlement and attachment by two hours and by day seven a confluent monolayer had formed, similar

to TCPS control. Cells settled and adhered to TCPS within 30 minutes and at day seven a fully confluent monolayer was present.

3.5.6 Surface Analysis

The wettability of coatings F-N was measured and plotted (Figure 3.42). Coating F and I were more hydrophobic (64 and 50, respectively) than the other novel zwitterionic coatings (G, H, J and K). Control coatings L and M were also had a higher CA, however the contact angle varied across all coatings from approximately 80° - 22° and were significantly different to TCPS (34°, $p<0.05$).

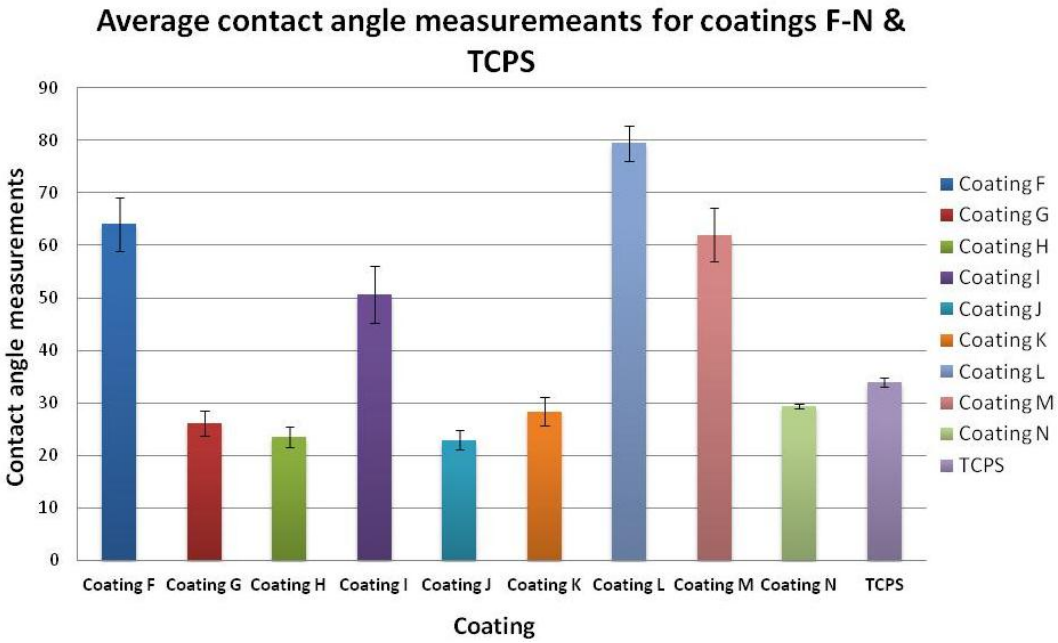

Figure 3.42: Graph demonstrates the average contact angle measurements (CA) for zwitterionic coating F-N. Error bars equal ± 1 standard deviations. CA varied across the 6 novel zwitterionic coatings (F-K). Indicating cell growth was not related to the wettability of the coating.

SEM analysis indicated most surfaces to be smooth with some having micro features and cracks (Figure 3.43). Coatings F and L both had fibrous honeycomb appearances.

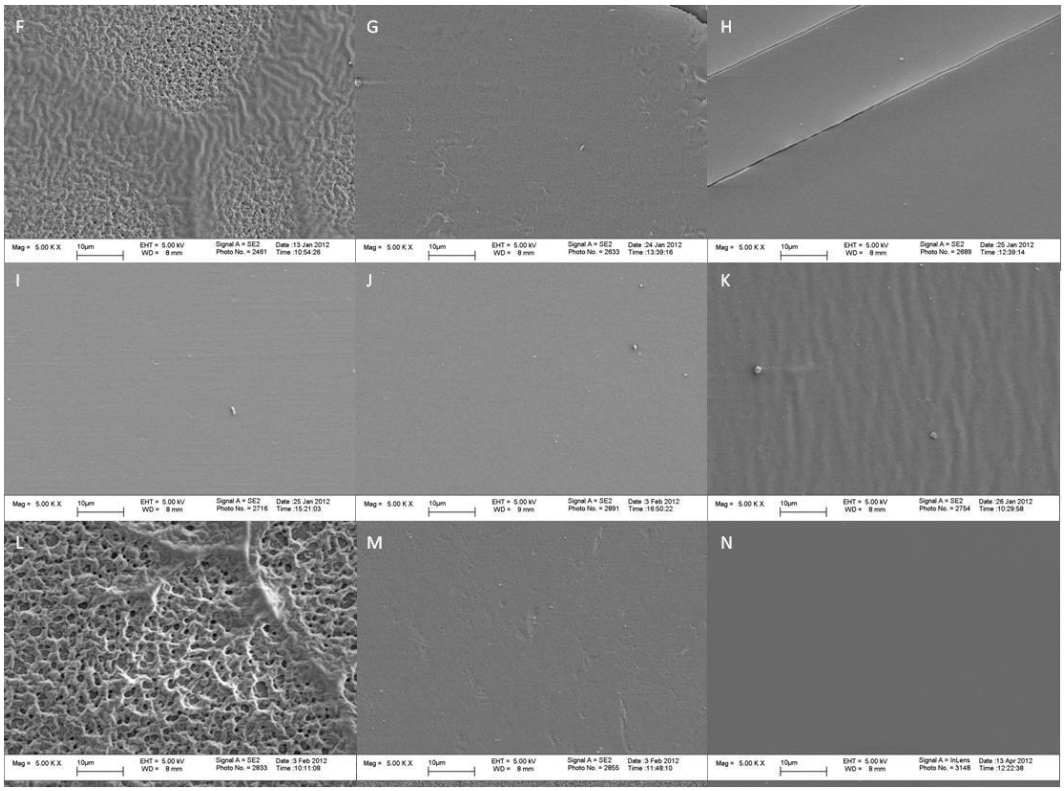

Figure 3.43: Representative scanning electron microscopy (SEM) micrographs, demonstrating zwitterionic coatings F- N. Coatings F and L had a fibrous honeycomb appearance at x 5000 magnification which may have been caused by the processing. Coatings G, H, I, J, K and M are relatively smooth apart from some cracks and ripples again believed to be artefacts of the chromium processing.

WLI results present the average surface roughness (Ra) across four areas measured at x100 magnification. All coatings apart from F (Ra 149nm) and L (Ra 378nm) had an average surface roughness of below 35nm and were not significantly different. This supports the SEM analysis (Figure 3.44). Coatings F and L were significantly different from coatings G – K & M – N and TCPS $p<0.05$, measured using one way ANOVA and Dunnett's T3 post hoc test.

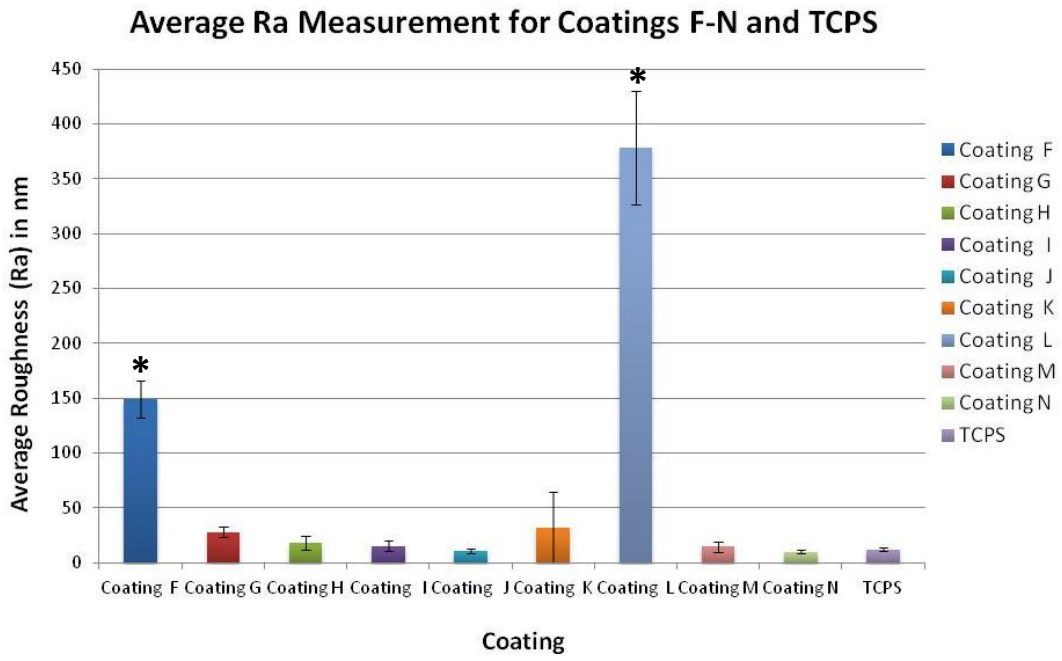

Figure 3.44: Graph represents average surface roughness values (Ra) for zwitterionic coatings F-N and tissue culture polystyrene (TCPS). Error bars equal ± 1 standard deviations. * denotes significant difference were $p<0.05$. Coatings G, H, I, J, K and M are below 35nm. Coating F (149nm) and L (378nm) had a rougher topography which was due to the fibrous topography. Coatings F and L were significantly different to all other coatings and TCPS ($p<0.05$).

3.5.7 Preliminary Bulk Materials Assay

Material F was copolymerised with pHEMA as a bulk contact lens to study the bulk material properties. PHEMA contact lenses, gold standard Acyrsof® IOLs and untreated TCPS wells were used as controls. Phase contrast micrographs were taken to monitor cell growth on substrates throughout the 7 days in cell culture (Figure 3.45). Preliminary results demonstrate LECs seeded onto TCPS control produced a confluent monolayer by

day 7 with cuboidal morphology. No cells adhered to bulk material pHEMA of material F. A large amount of LECs adhered and grew on Acrysof® IOLs, cells were observed at the edge of the IOL and in the centre and some rounded cells were also present.

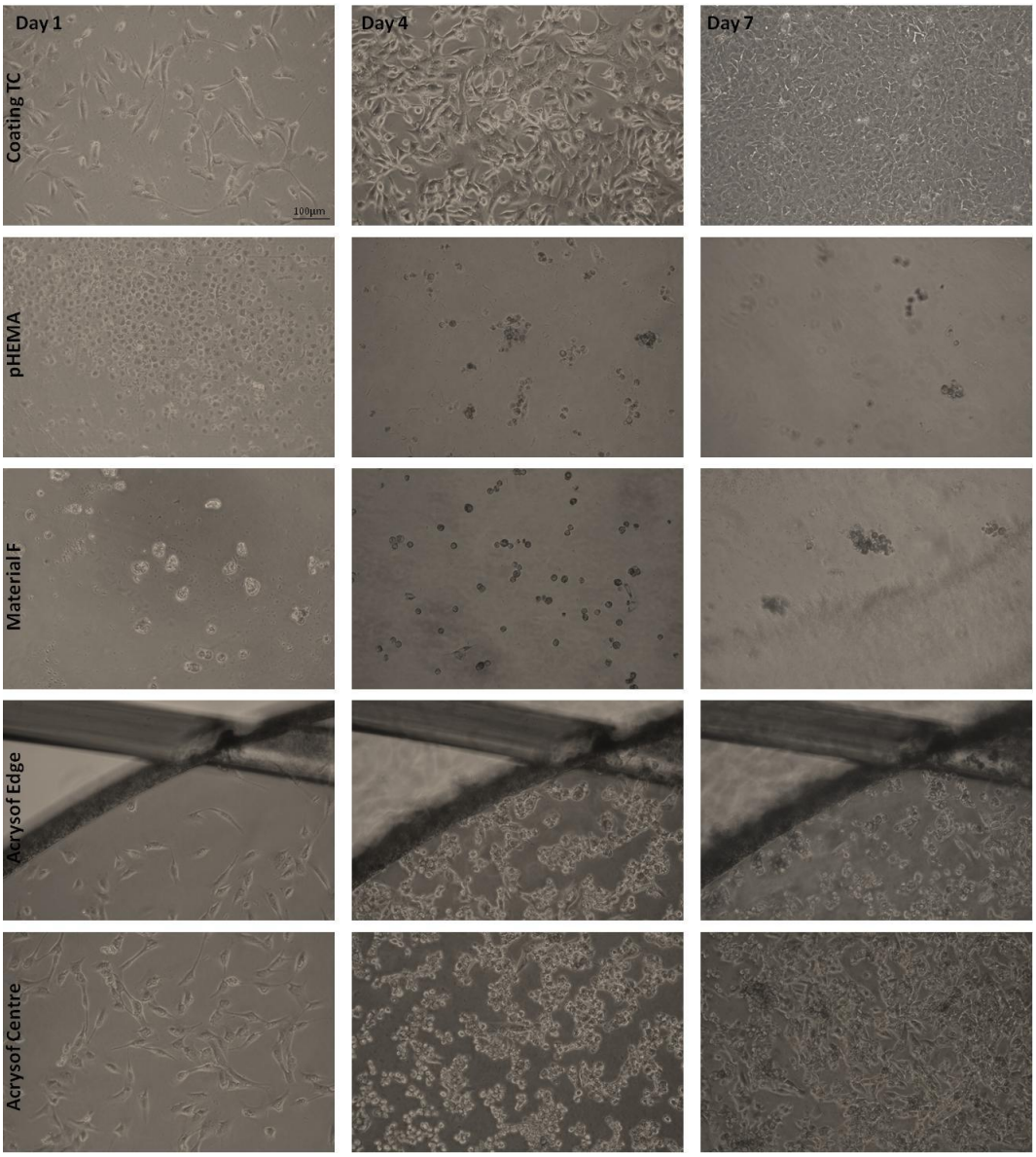

Figure 3.45: Phase contrast micrographs representative LEC attachment and growth on tissue culture polystyrene (TCPS), bulk material F, bulk material poly (hydroxyethyl methacrylate) (pHEMA) and Acrysof® IOL. Typical epithelial morphology was observed on TCPS control. Bulk material material F and pHEMA did not support LEC attachment and growth. Floating dead cells were observed on these coatings. A large proportion of LEC attachment and growth occurred on Acrysof® IOLs, cells appeared epithelial and reasonable well spread.

LECs were fixed at day 7 with methanol and stained with methylene blue. Photographs of the whole plate were taken, (Figure 3.46). Bulk materials F and bulk material pHEMA absorbed the dye. Some cell growth can be visualised on Acrysof IOLs and confluent areas can be observed on TCPS control wells.

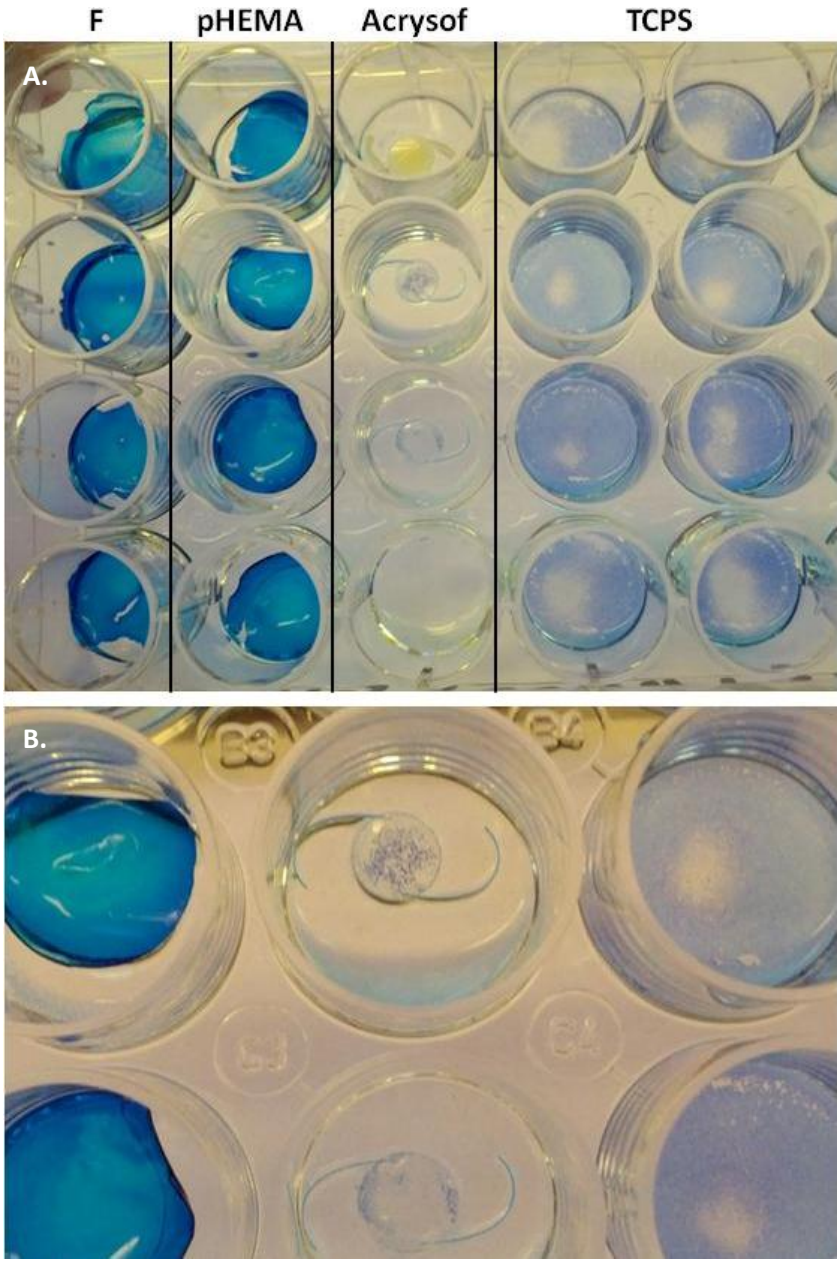

Figure 3.46: A. Photograph of the whole plate demonstrating cells stained with methylene blue on bulk material F, bulk material poly (hydroxyethyl methacrylate) (pHEMA), Acrysof® IOL and tissue culture polystyrene (TCPS). Material F and pHEMA absorbed the dye due to their hydrogel-like properties. B. Cells were visible on Acrysof® IOLs, close up photograph demonstrates cell attachment. TCPS control had a near confluent coverage of LECs at day 7.

C-Flex (Rayner) pHEMA IOL was separately tested to compare it to bulk material pHEMA provided by BioInteractions Ltd. LECs were again seeded on Acrysof® IOLs to confirm cellular response and uncoated TCPS wells were used as a control. C-Flex did not encourage LEC attachment or growth (Figure 3.47). Acrysof® IOL produced a similar cellular response to the previous study with LECs attaching and spreading throughout the duration of culture. TCPS control was confluent by day 7 with typical epithelial morphology.

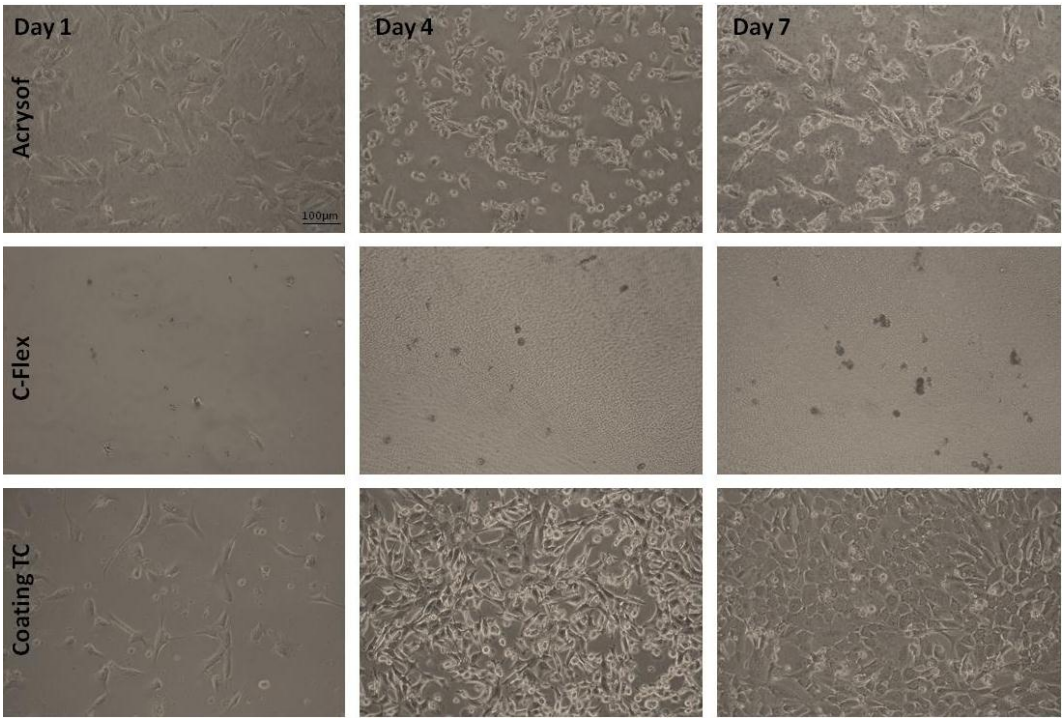

Figure 3.47: Phase contrast micrographs representative LECs attachment and growth on Acrysof® IOL, C-Flex IOL and tissue culture polystyrene (TCPS), during the 7 days in culture. A similar cellular response was seen on Acrysof IOLs to the previous study, LECs attached and spread whilst in culture. C-Flex did not enable LEC attachment or growth during the 7 days and was similar to bulk material pHEMA in the previous study. LECs seeded onto TCPS control were confluent by day 7 with typical epithelial morphology.

Methylene blue staining can be observed on Acrysof IOLs indicating LEC attachment and spreading (Figure 3.48-A and Figure 3.48-B). C-Flex IOL absorbed the dye in a similar way to the previous bulk material pHEMA due to its hydrophilic nature (Figure 3.48-C).

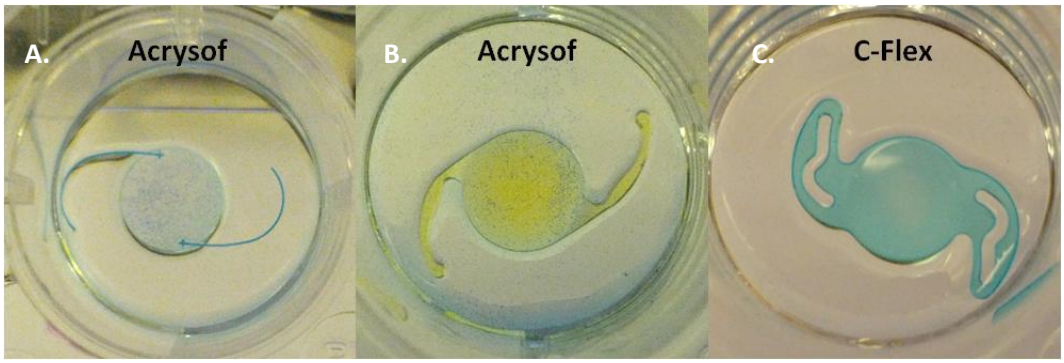

Figure 3.48: Photographs of individual wells demonstrating cells stained with methylene blue on A. Acrysof® IOL, B. Acrysof® IOL and C. C-Flex IOL. Cell attachment was observed on Acrysof® IOLs (A and B). C-Flex IOL absorbed the dye similar to bulk material pHEMA due to its hydrogel-like nature.

Confluent areas of LEC growth was observed with methylene blue on TCPS control (Figure 3.49).

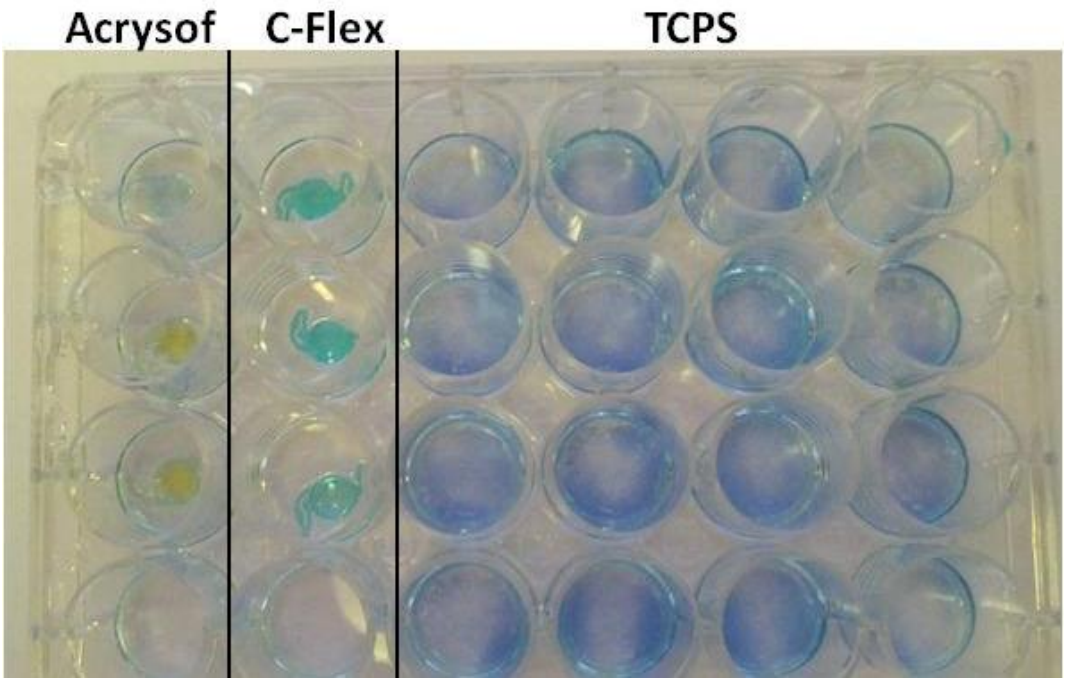

Figure 3.49: Photograph of the whole plate demonstrating methylene blue staining of, Acrysof IOL, C-Flex IOL, and tissue culture polystyrene (TCPS) control. LECs were well spread and confluent by day 7 on TCPS control.

3.6 Dedifferentiation Model and TGFβ3 Assay

A dedifferentiation model was set up to control dedifferentiation of LECs and test TGFβ3's ability to prevent or reverse the effect of dedifferentiation. This was evaluated using αSMA as a marker for dedifferentiated cells.

3.6.1 Serum Assay

Two methods for reducing the rabbit serum (RS) concentration used with N/N1003A LECs were studied, first by reducing the serum concentration from the start of the experiment or secondly seeding LECs in optimum 8% serum for either 24 or 72 hours, prior to reducing or removing the serum completely. The average number of cells per field of view for different serum concentrations at each time point was calculated and plotted (Figure 3.50). Optimum 8% serum concentration is represented by the first blue (0 hours pre-treatment), red (24 hours pre-treatment) and green (72 hours pre-treatment) bars of each time point, and represents the usual growth pattern for this cell line. By day seven all 8% RS concentrations (0 hours, 24 hours and 72 hours pre-treatment) fell within a similar range, and were not significantly different to each other. By day seven, the longer LECs were cultured in 8% RS prior to experimental conditions the greater the number of cells were counted, regardless of experimental serum concentration. Some LECs did attach in 0% serum, however cell numbers were low, regardless of whether LECs were cultured in optimum 8% serum concentration first. In 0.5% RS LECs proliferated slightly during the seven days, with increasing cell proliferation the longer the LEC had been exposed to 8% serum. A serum concentration of 2% RS encouraged cells to steadily proliferate but at a lower rate compared to the 8% control. Cells seeded in 2% RS – 72 hours pre-treatment had the highest number of cells attached by day seven, compared to all other experimental serum concentrations. When cells were treated with 2% RS – 72 hours pre-treatment cell number was significantly different ($p<0.05$) to all other experimental serum concentrations, with the exception of 2% RS – 24 hours pre-treatment. When cells were treated with 2% RS – 24 hours pre-treatment, however, cell number was also not significantly different to 0.5% RS – 72 hours pre-treatment. Due to this a serum concentration of 2% after pre-treatment with 8% RS for 72 hours was chosen for future TGFβ3 studies.

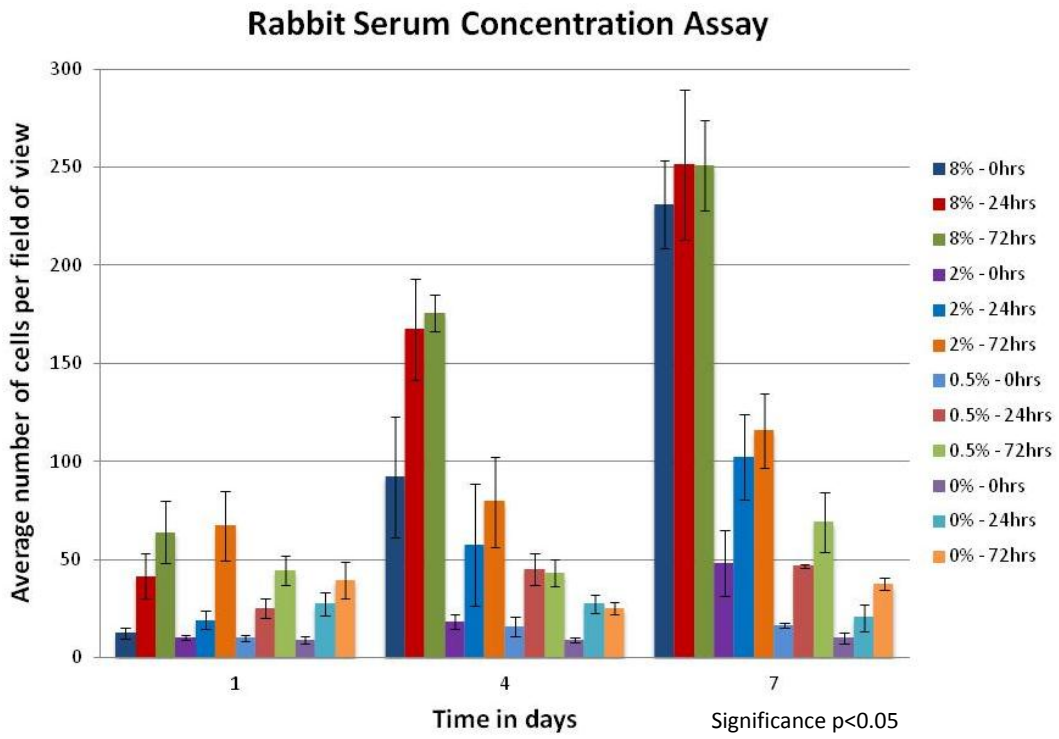

Figure 3.50: Graph presents N/N1003A LECs attachment in 8%, 2%, 0.5% and 0% rabbit serum (RS) concentrations over time, error bars are 1± standard deviation. Serum was either decreased from the start (0 hour treatment) or LECs were grown in optimum 8% serum for either 24 or 72 hours before serum starving for 24 hours then reducing the serum concentration thereafter. 8% RS represents the usual growth for these cells. The longer LECs were cultured in 8% RS prior to experimental conditions the greater the cell attachment. Some LECs did attach in 0% RS, however cell numbers were low during the 7 days, regardless of the time treated in 8% serum prior to reduction. In 0.5% RS LEC did proliferate during the 7 days but cell number on day 7 in all 0.5% RS was significantly less than 2% RS (2% - 24 and 2% - 72 hours treatment) ($p<0.05$). 2% RS concentration supported steady proliferate but at a lower rate compared to the control and LECs retained their epithelial morphology.

3.6.2 Dedifferentiation Model

The results from the dedifferentiation model show αSMA expression in green and nuclei staining in red, therefore the more green cells the more dedifferentiation (Figure 3.51). PMMA had poor cell attachment and cells did not form a monolayer therefore was not quantifiable. A small proportion of cells stained positive for αSMA when injury was induced, showing some dedifferentiation. There was however no closure of the scratch in some wells, and αSMA expression was similar to control, showing insignificant amounts of dedifferentiation. Dedifferentiation was observed in all concentrations of TGFβ2, with 10ng/ml having the most αSMA expression, therefore was chosen as a suitable model.

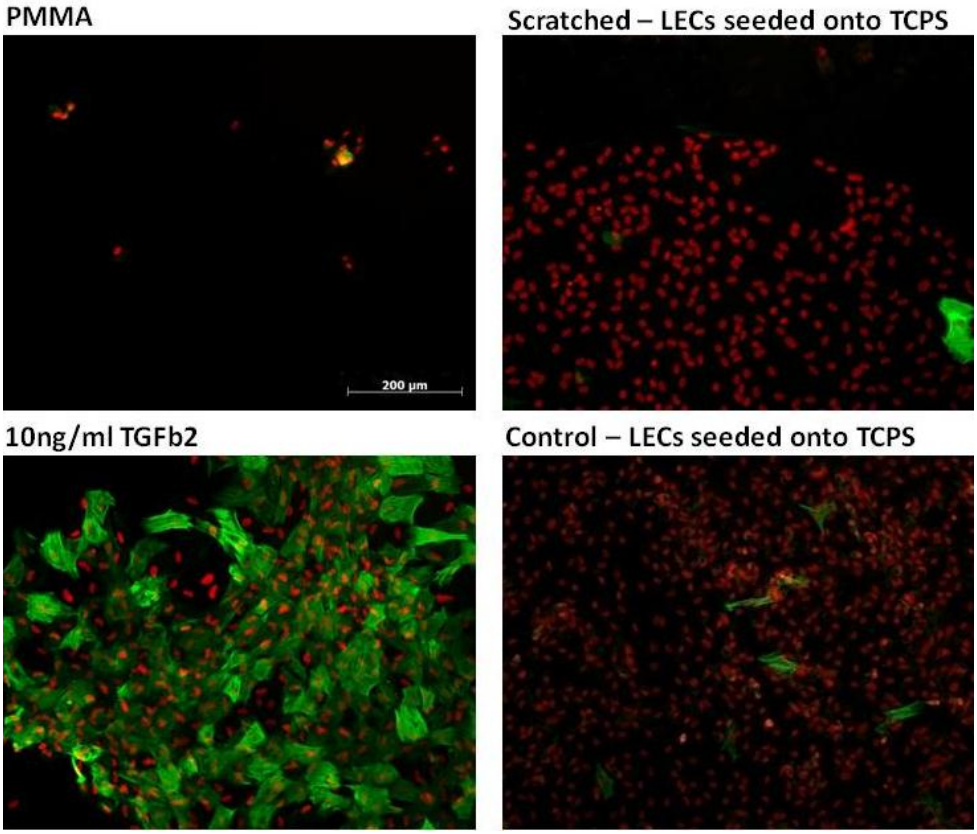

Figure 3.51: Representative fluorescent micrographs demonstrating positive expression for αSMA (green) and PI staining (red) of N/N1003A LECs seeded on poly methylmethacrylate (PMMA) substrate, seeded on tissue culture polystyrene (TCPS) then scratched with a 1ml pipette tip when confluent, seeded onto TCPS and treated with 10ng/ml TGFβ2 (pre-treated in MEME containing 8% rabbit serum (RS) for 72 hours, serum starved for 24 hours then MEME containing 2%RS with 10ng/ml TGFβ2 for 7days) and seeded onto TCPS control. PMMA had poor cell attachment and cells did not form a monolayer, there was no closure of the scratch and cells expressing αSMA were similar to TCPS control and TGFβ2 showed dedifferentiation in a dose dependant manner.

3.6.3 Optimisation

Optimisation of the dedifferentiation model was carried out on TGFβ2. The level of dedifferentiation increased in a dose dependant manner up to 6.5ng/ml (Figure 3.52). There was no difference in the level of dedifferentiation for higher doses. An optimum concentration of 5ng/ml of TGFβ2 was chosen.

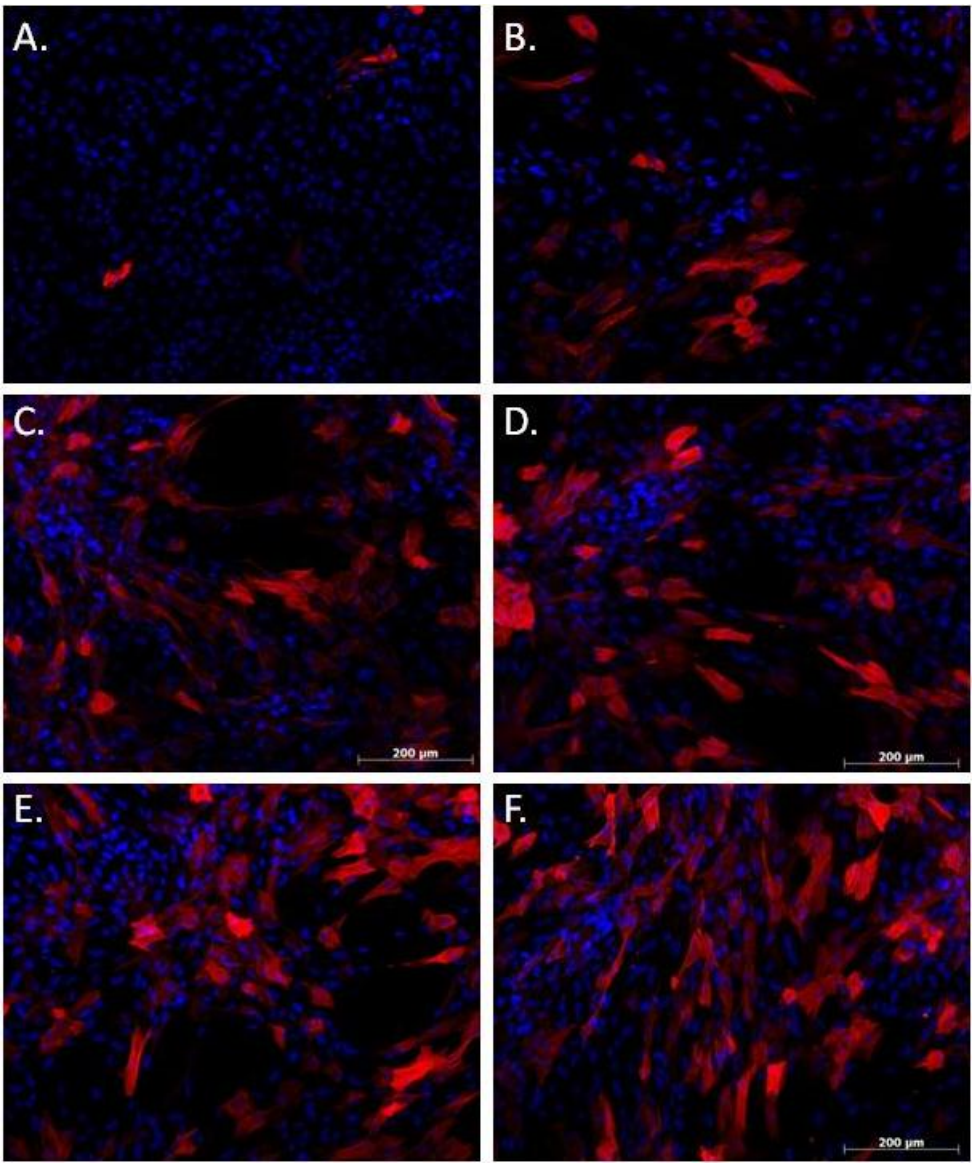

Figure 3.52: Representative fluorescent micrographs demonstrating positive expression for αSMA in a TGFβ2 dose dependent study using N/N1003A LECs at day 7. Micrographs demonstrate αSMA (red) and DAPI (blue) A. 2% serum no TGFβ2, B. 3ng/ml TG β2, C. 5ng/ml TGFβ2, D. 6.5ng/ml TGFβ2, E. 8ng/ml TGFβ2, F. 10ng/ml TGF β2. Level of dedifferentiation increased with dose of TGFβ2. All cells have been pre-treated in MEME containing 8% rabbit serum (RS) for 72 hours, serum starved for 24 hours then changed to MEME containing 2%RS with variations in TGFβ2 concentration for 7days.

3.6.4 TGFβ3 Dose Dependent Study

The influence TGFβ3 had on LEC morphology and phenotype was investigated, again cells were fluorescently stained with αSMA in red, phalloidin in green and DAPI to stain the nuclei blue (Figure 3.53).

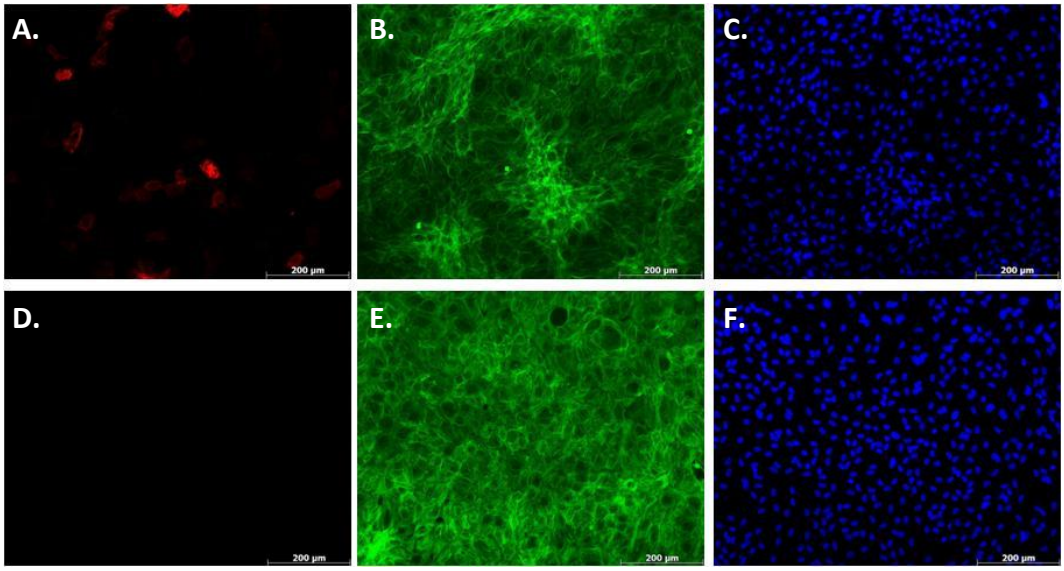

Figure 3.53: Fluorescent micrographs demonstrating positive expression for αSMA in a 10ng/ml TGFβ3 for 1 hour treatment (pre-treated in MEME containing 8% rabbit serum (RS) for 72 hours, serum starved for 24 hours then grown with MEME containing 2%RS with 10ng/ml for 1 hour followed by MEME 2%RS for 4 days) and untreated LEC control (D, E and F), day 4. αSMA (red), phalloidin (green) and DAPI (blue). Micrographs demonstrate some positive expression of αSMA in LECs that were treated with 10ng/ml TGFβ3 (A), and no positive expression in untreated control LECs (D) (this was not the case in all incidences). Cytoskeleton staining of TGFβ3 LECs (B) appears to have some cuboidal morphology similarities with untreated control (E), however more unorganised actin fibres were present in small areas when LEC were treated with TGFβ3. Nuclei staining demonstrated cells were attached and distributed well in both treated (C) and untreated (F) LECs at day 4.

Dedifferentiation was semi-quantitatively analysed by measuring the area of αSMA staining as a percentage of the total field of view, this was achieved by programming a macro on ImageJ. TGFβ3 did dedifferentiate LECs to a certain extent (Figure 3.54) at all concentrations and time exposures, however to a lesser extent when compared to how much dedifferentiation was caused by TGFβ2 (approximately 40%). When 10ng and 10pg of TGFβ3 was added for 1 and 24 hours it gave a similar percentage of

dedifferentiation to the control (approximately 2%), which was LECs with no TGFβ3 (Figure 3.54).

There was a significant difference in the amount of dedifferentiation caused between TGFβ2 and 100pg/ml at 1 hour time exposure, 1ng/ml in cell culture medium and 2%. The other concentrations and time exposures of TGFβ3 were not significantly different to TGFβ2.

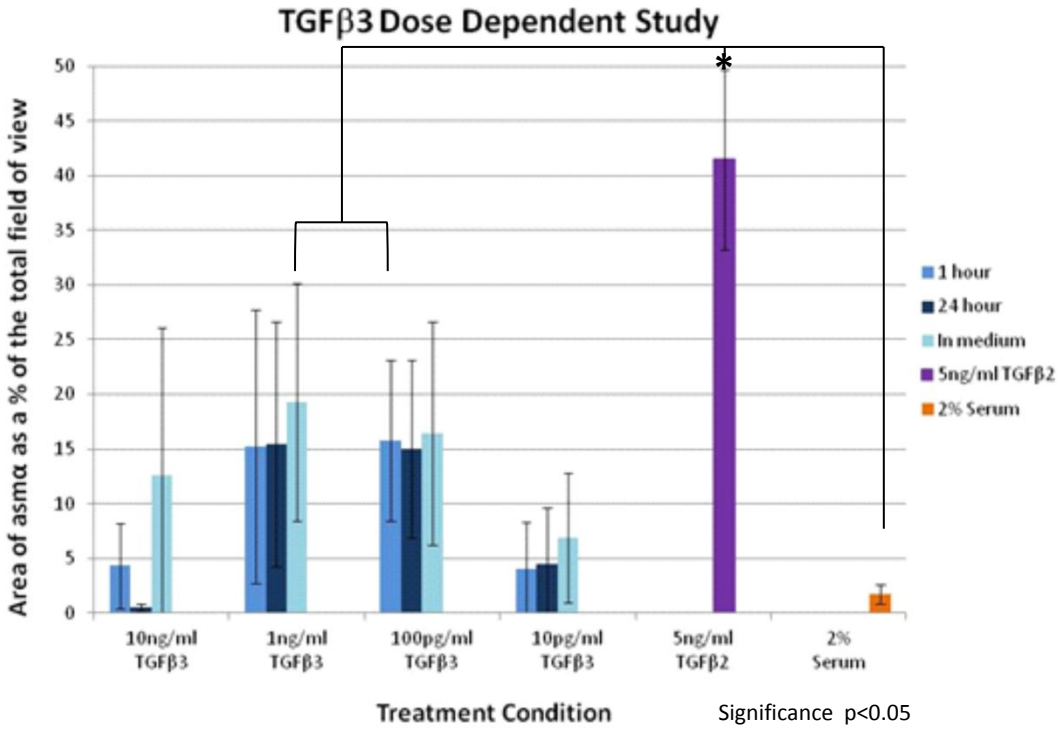

Figure 3.54: Graph demonstrating the percentage area of dedifferentiation quantified by αSMA expression in various TGFβ3 concentrations and time exposures, 5ng/ml TGFβ2 and untreated control (2 % rabbit serum (RS)). Error bars equal ± 1 standard deviations. * denote significant difference were p<0.05. 5ng/ml TGFβ2 was significantly different to all TGFβ3 concentrations and 2% RS control. With the exception of 1ng/ml TGFβ3 in medium and 100pg/ml TGFβ3 at 1 hour time exposure all other concentrations were not significant different compared to 2% RS control (p>0.05).

3.6.5 Dedifferentiation Model with TGFβ3

Once 5ng/ml TGFβ2 was established as a dedifferentiation model and the effect TGFβ3 had on LECs had been investigated, the dedifferentiation model and TGFβ3 were studied in conjunction with each other to examine TGFβ3s effect on reversing or preventing dedifferentiation.

3.6.5.1 TGFβ3's Ability to Reverse Dedifferentiation

N/N1003A LECs were pre-treated in the reduced serum procedure before changing to experimental conditions. LECs were dedifferentiated with 5ng/ml TGFβ2 followed by treatment with TGFβ3 (at the same concentrations and time exposures as previously studied) to reverse the effects of dedifferentiation. Dedifferentiation was evaluated in the same way as before (explained in section 3.6.4). The results indicate TGFβ3 had little effect at reversing dedifferentiation (Figure 3.55). Due to the high standard deviations of TGFβ3 at all concentration and time exposure averages fell within a similar range to the control, 5ng/ml TGFβ2. Cells treated with 2% serum had less than 5% area of dedifferentiation. LECs treated pre-treated with 10ng/ml at 1 hour time exposure, 1ng/ml at 1 hour time exposure, 100pg/ml at 24 hour time exposure, and 2% were significantly different to dedifferentiation levels of TGFβ2. Untreated control dedifferentiation levels (2% serum) were significantly different to all TGFβ3 concentrations and time exposures and TGFβ2 with the exception from 1ng/ml and 100pg/ml in medium (analysed using Dunnett's T3).

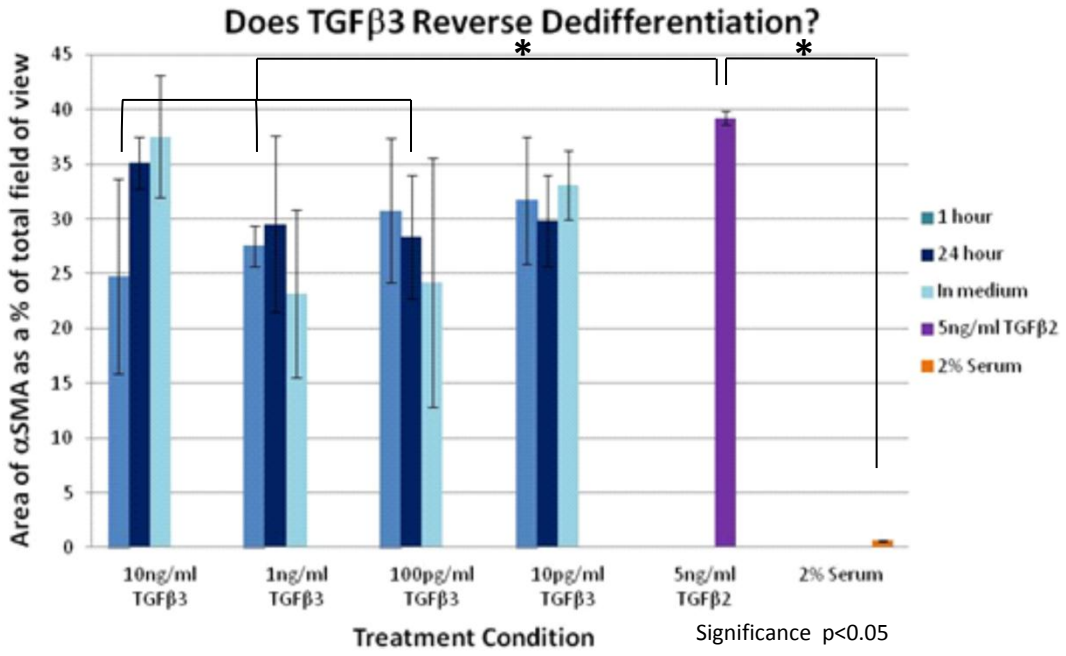

Figure 3.55: Graph to show TGFβ3 ability at reversing dedifferentiation. The percentage area of αSMA dedifferentiation was quantified by αSMA expression in LECs treated with 5ng/ml TGFβ2 for 4 days followed by various concentrations and time exposures of TGFβ3, 5ng/ml TGFβ2 and untreated control (2% serum) for 4 days. Error bars equal ± 1 standard deviations. * denote significant difference where p<0.05. There was only a small decrease in the level of dedifferentiation when dedifferentiated cells were treated with TGFβ3 regardless of dose and time exposures. The percentage area of dedifferentiation for all treatments fell within a similar range to TGFβ2 control. LECs treated with 2% serum (control) showed less than 5% area of dedifferentiation.

3.6.5.2 TGFβ3's Ability to Prevent Dedifferentiation

N/N1003A LECs were pre-treated with various concentration and time exposures of TGFβ3 then treated with 5ng/ml TGFβ2 to dedifferentiate cells to examine if TGFβ3 could prevent the effects of dedifferentiation. Cells were evaluated in the same way as before (explained in section 3.6.4). There was a reduction in the level of dedifferentiation when cells were pre-treated with TGFβ3 prior to treatment with TGFβ2, at all concentrations and time exposures (Figure 3.56), however the level of dedifferentiation caused by 5ng/ml TGFβ2 was also reduced when compared to previous studies (Figure 3.55). When cells were treated with 2% serum in the absence of any TGFβ the dedifferentiation level was fewer than 5%. There was no significant difference

from cells treated with TGFβ2 followed by TGFβ3 when compared to control TGFβ2 levels, regardless of TGFβ3 concentration and time exposure ($p>0.05$). In addition there was no significant difference between cells treated with TGFβ2 followed by TGFβ3 when compared to control 2% levels, with the exception of 10ng/ml for 24 hours time exposure (analysed using Dunnett's T3).

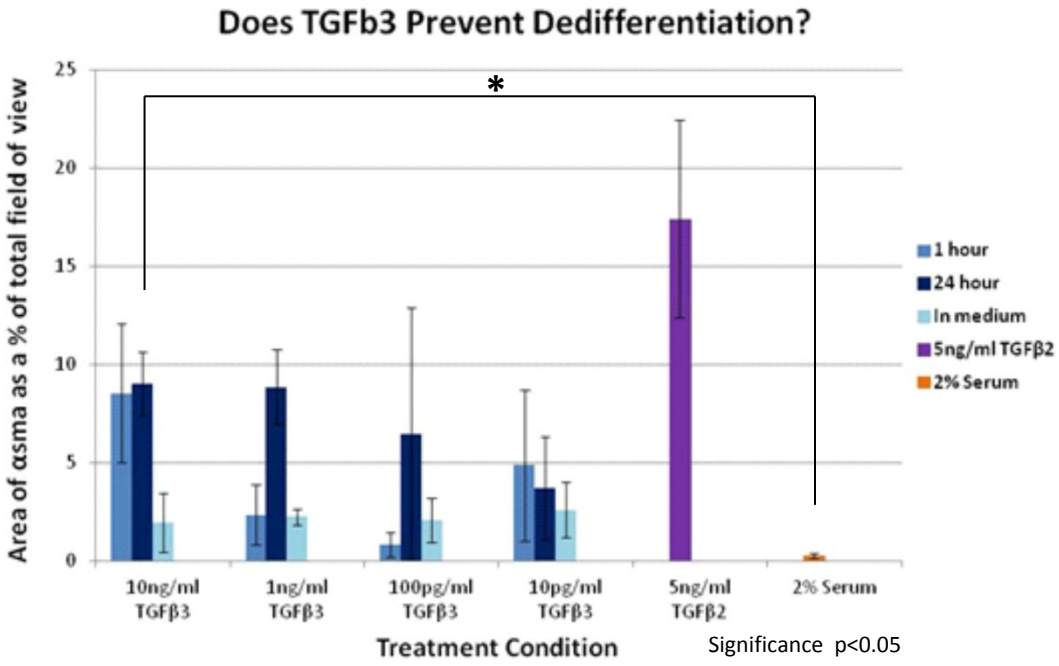

Figure 3.56: Graph demonstrating dedifferentiation prevention by TGFβ3 assay. The percentage area of αSMA dedifferentiation was quantified by αSMA expression in LECs treated with 5ng/ml for 4 days followed by various concentrations and time exposures of TGFβ3 for 4 days, 5ng/ml TGFβ2 and untreated control (2% serum). Error bars equal ± 1 standard deviations. * denote significant difference where $p<0.05$. There was a reduction in the level of dedifferentiation when cells were pre-treated with TGFβ3, regardless of dose or time exposure. The percentage area of dedifferentiation for all TGFβ3 treatments fell within a similar range. Cells treated with 2% serum showed less than 5% area of dedifferentiation.

3.6.6 Flow Cytometry

Flow cytometry was evaluated as a method for quantifying the expression of αSMA in LECs incubated with 5ng/ml TGFβ2 or control LECs (no TGFβ2). All LECs were gated to the same level based on the auto fluorescence of control, unstained cells. Control unstained LECs had a low level intensity peak indicating some auto fluorescence, this was similar to unstained LECs incubated with 5ng/ml TGFβ2 (Figure 3.57-A and Figure 3.57-B respectively). When primary negative mouse IgG antibody and Alexa Fluor 488 secondary were added to control LECs and LECs incubated with 5ng/ml TGFβ2 (Figure 3.57-C and Figure 3.57-D) a defined peak was observed in similar area and a higher level of fluorescence occurred, meaning that the IgG caused some non-specific background stain. When primary αSMA and Alexa Fluor 488 secondary antibodies were added to control LECs some positive expression was present (Figure 3.57-E). This was expected as a small population of LECs naturally dedifferentiate whilst in culture. When LECs were incubated with 5ng/ml TGFβ2 were stained with primary αSMA and secondary antibodies there was a higher increase of positive αSMA expression (Figure 3.57-F). The histogram (Figure 3.57-F), had a wider spread meaning LECs were stained to different intensities, with some cells being brighter than others.

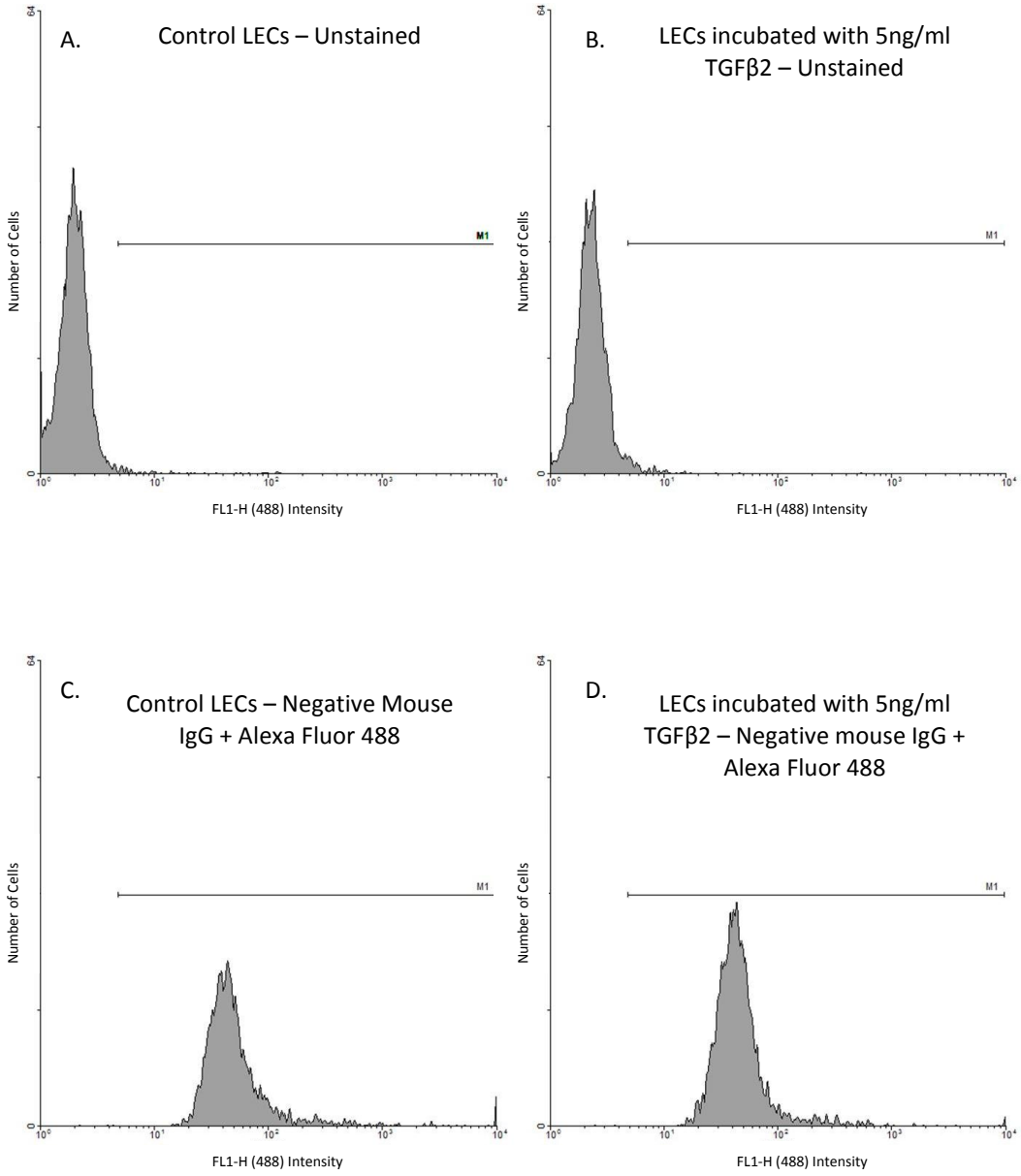

Figure 3.57: Histographs demonstrate αSMA expression measured by flow cytometry in: A. Control LECs – Unstained, B. LECs incubated with 5ng/ml TGFβ2 – Unstained, C. Control LECs – Negative IgG + Alexa Fluor 488 and D. LECs incubated with 5ng/ml TGFβ2 – Negative IgG + Alexa Fluor 488. When controls LECs and LECs incubated with 5ng/ml TGFβ2 were either unstained or stained with negative IgG a similar fluorescence peak was observed.

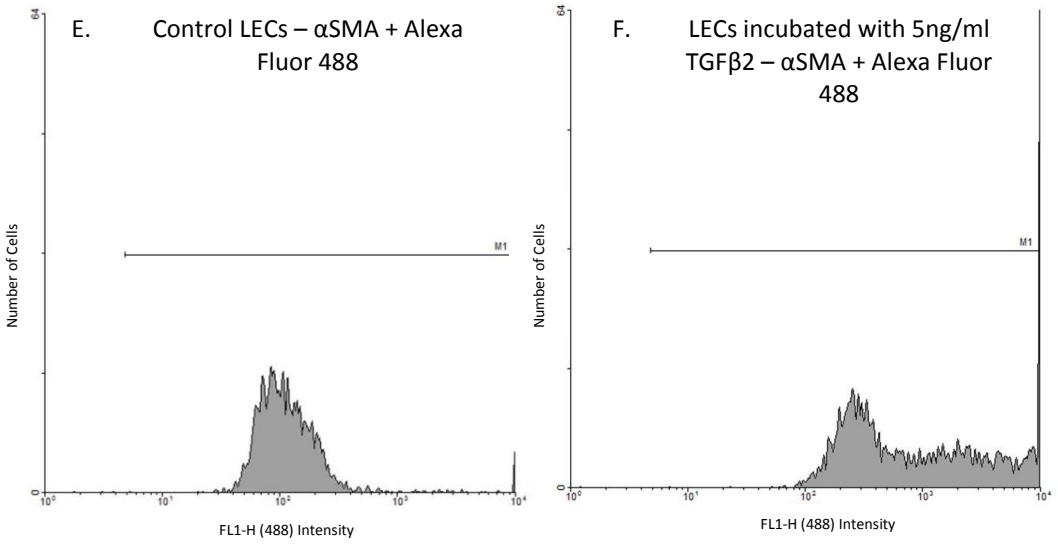

Figure 3.58: Histographs demonstrate αSMA expression measured by flow cytometry (continued) in: E. Control LECs – αSMA + Alexa Fluor 488 and F. LECs incubated with 5ng/ml TGFβ2 – αSMA + Alexa Fluor 488. LECs incubated with 5ng/ml TGFβ2 had a high positive expression of αSMA with a wider spread of intensity (F) compared to control LECs (E).

The geometric mean was calculated from the forward and side scatter, to represent fluorescently stained cells and a bar chart of the geometric mean was plotted. There was a high increase in positive αSMA expression in LECs incubated with 5ng/ml TGFβ2 when they were stain with primary αSMA and Alexa Fluor 488 secondary antibodies, demonstrating that flow cytometry was a valid way of measuring αSMA expression within N/N1003A LECs (Figure 3.59).

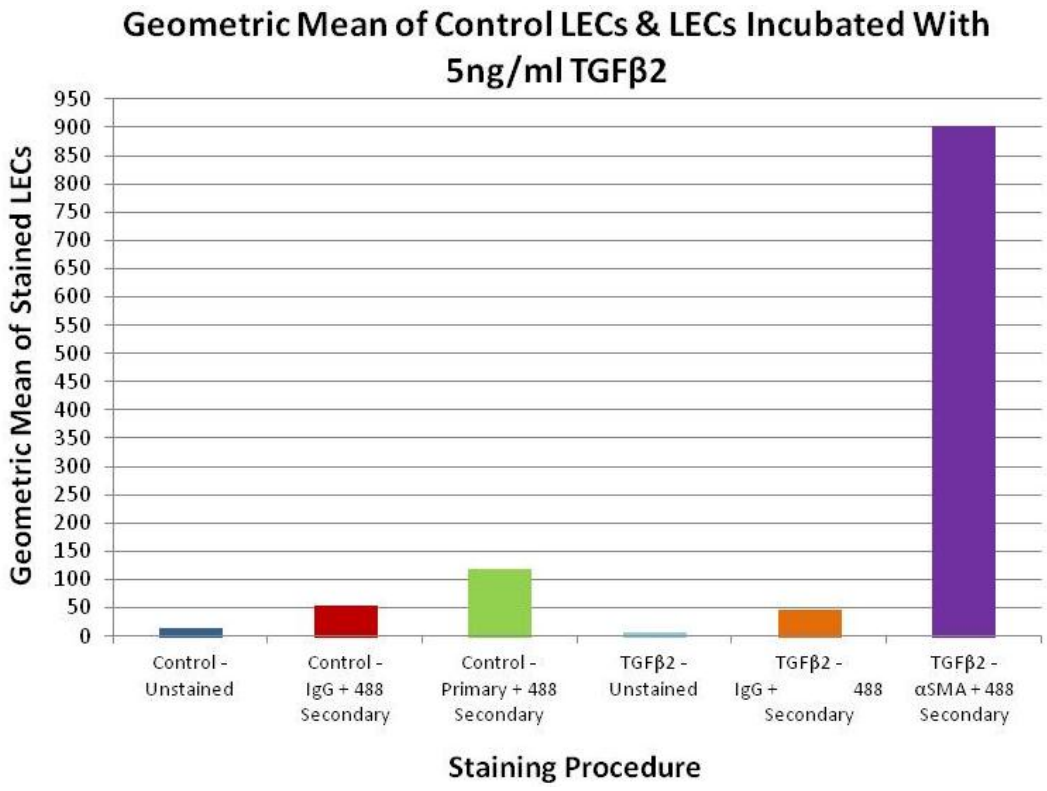

Figure 3.59: Graph demonstrating the geometric mean detection of αSMA fluorescence in control LECs and LECs incubated with 5ng/ml TGFβ2. Unstained control and unstained LECs incubated with 5ng/ml TGFβ2 had little auto fluorescence. When IgG control and Alexa Fluor 488 secondary were added to control LECS and LECs incubated with 5ng/ml TGFβ2 a slight increase in florescence was observed. Control LECs stained with primary αSMA antibody and Alexa Fluor 488 secondary showed positive expression of αSMA. However when LECs were incubated with 5ng/ml TGFβ2 and stained with primary αSMA antibody and Alexa Fluor 488 secondary there was a 7-fold increase in the amount of fluorescence.

3.6.7 PCR Assay

Real time PCR was performed on B3's LECs, using extracellular matrix adhesions PCR arrays. LECs were either incubated with TGFβ3, TGFβ2, a combination of TGFβ3 and TGFβ2 or LECs incubated with no TGFβ present (control LECs). Each test sample was compared to a "control" sample (Table 3-3). LECs incubated with TGFβ3 and TGFβ2 were compared to control LECs sample. LECs incubated with TGFβ3 followed by TGFβ2 were compared to three different control samples. Firstly test sample 1.TGFβ3_TGFβ2 was compared to TGFβ3, test sample 2.TGFβ3_TGFβ2 was compared to TGFβ2 and test sample 3.TGFβ3_TGFβ2 was compared to control LECs.

Table 3-3: Detailing PCR test and control samples

Test #	Test Sample	Control Sample
1	TGFβ3	Control LECs
2	TGFβ2	Control LECs
3	1.TGFβ3_TGFβ2	TGFβ3
4	2.TGFβ3_TGFβ2	TGFβ2
5	3.TGFβ3_TGFβ2	Control LECs

Table demonstrates test samples and control samples used to analyse PCR array plates.

A shortened list of genes that were up or down regulated was created (Table 3-4). TGFβ3 up-regulated fibronectin 1 (FN1). TGFβ2 and test sample 1.TGFβ3_TGFβ2, mainly up-regulated gene expression. Test sample 2.TGFβ3_TGFβ2 down-regulated gene expression, and test sample 3.TGFβ3_TGFβ2, did a combination of up and down regulating gene expression within B3 LECs. A group of the collagen, integrin and thrombospondin family genes were up and down regulate across the various test samples. Two matrix metallopeptidase (MMP) and two laminin (LAM) genes were expressed, in addition the amount of fibronectin expression varied across test samples. These genes could all have a role to play within PCO.

Table 3-4: Demonstrating gene expression observed in B3 LECs when treated with various combinations of TGFβ3, TGFβ2, TGFβ3 followed by TGFβ2 and untreated LECs

Genes	TGFβ3-LECs	TGFβ2-LECs	1. TGFβ3_TGFβ2 – TGFβ3	2. TGFβ3_TGFβ2 – TGFβ2	3. TGFβ3_TGFβ2 – LECs
ADAMTS1	0	0	-2.69	-2.47	-2.78
COL14A1	0	-2.83	0	0	-2.52
COL16A1	0	3.31	2.37	0	2.76
COL1A1	0	2.73	0	0	0
COL4A2	0	2.29	0	0	0
COL5A1	0	3.36	0	0	2.14
COL6A1	0	2.17	0	0	0
COL6A2	0	3.83	3.08	0	4.30
COL7A1	0	4.65	2.35	0	3.52
COL8A1	0	0	0	0	-3.33
CTGF	0	2.64	0	0	2.40
FN1	2.12	4.34	0	0	2.82
HAS1	0	0	0	0	-5.29
ITGA3	0	0	0	-2.19	0
ITGA5	0	2.05	0	0	0
ITGA6	0	0	-2.03	-2.24	-2.66
ITGA7	0	3.48	2.45	0	2.88
ITGB3	0	2.58	0	-2.32	0
ITGB5	0	2.60	0	0	0
LAMB3	0	0	0	-2.57	-2.26
LAMC1	0	0	0	-3.23	-2.30
MMP14	0	8.62	2.27	-2.33	3.70
MMP2	0	3.50	2.32	0	3.45
SPARC	0	2.07	0	0	2.11
SPG7	0	2.31	0	0	0
THBS1	0	0	0	-2.38	0
TGFBI	0	3.29	2.40	0	3.72
THBS2	0	0	2.13	0	2.21
THBS3	0	0	2.54	0	0

Gene expression showed a group of collagens (COL), Integrins (ITG) and thrombospondins (THBS) were up and down regulated dependent upon treatment. Along with several other genes that may be associated with PCO, such as matrix metallopeptidases (MMP), laminins (LAM) and fibronectin (FN1).

4. Discussion

The aim of this work was to evaluate surface coatings for potential intraocular lenses (IOLs), and the influence these coatings had on the postoperative scar reaction involved between residual lens epithelial cells (LECs) and the IOL surface.

Sight is said to be our most dominant sense [169]. Cataracts are characterised by an opacification of the natural lens and render millions of people blind worldwide [43, 47]. This blindness can be corrected by a simple ophthalmic operation [2, 31]. During cataract surgery the natural lens is removed, leaving the capsular bag in situ. A polymer IOL is inserted inside this capsular bag to replace the natural lens. The most common postoperative complication after implantation of this IOL is a type of scarring, known as posterior capsule opacification (PCO), which requires a second operation. PCO is associated with capsular contraction and wrinkling, which distorts the light path [25, 52, 60]. The clinical burden of PCO causes a significant cost factor on the health care system, and treatment is not necessarily available in developing countries. This means the patient's vision becomes compromised once again and the quality of life deteriorates, therefore efforts are needed to alleviate the problem of PCO.

It is widely known that material properties such as the surface chemistry, wettability and roughness can affect the cellular response [170-173]. One method that has been investigated to alleviate PCO is surface modification of IOLs to tailor the cellular response [9, 46, 84, 174-175]. This could be achieved by modifying a surface to enable attachment of a LEC monolayer that maintains an epithelial phenotype. Several groups have studied the effect of changing surface chemistry with the addition of various functional groups such as amine, carboxyl, and hydroxyl groups onto surfaces to encourage cell attachment in various cell types, including kidney epithelial, keratinocytes and retinal pigment epithelial cells [124, 176-177]. The cellular response could also be controlled by incorporating extracellular matrix (ECM) molecules such as glycosaminoglycan [9, 139, 178].

BioInteractions Ltd. are a manufacturer of innovative biomaterials that are designed to minimise the human host response. They specialise in the covalent binding of functional groups to biomaterial surfaces via a layer-by-layer technique, to tailor surface coatings of stents and catheters with non-thrombogenic properties [159, 179]. This PhD project has investigated various coatings for the potential use of new IOLs. The surface charge and functional groups present on coatings has been varied to encourage a monolayer of LEC growth and maintain their epithelial morphology, or to inhibit LEC growth and migration. Coatings have been produced and analysed in terms of their wettability, topography and evaluated in cell culture using established LEC lines.

4.1 Material Coatings and Techniques

Seeding primary human LECs onto the various coatings tested may be beneficial as it would be a more representative model [180]. Methods for harvest primary human LECs from donor eyes were evaluated, however these techniques produced only small populations of LECs. Donor age and time of cell extraction after post mortem time can affect the viability of the cells [181]. The average age for donor eyes is typically over 50 and the time taken from post-mortem to tissue culture was typically between 24 – 48 hours. This could explain the low cell viability that was observed [181]. In addition primary cells typically have a low growth ability and limited life span [180]. This relates to clinical observations with variations in PCO rates and age. Moisseiev et al reported PCO occurred in 47% of patients over the age of 40 and in 70% of patients under the age of 40 [182]. In addition it is known children suffer from severe PCO and capsulotomy is widely performed at time of IOL implantation to avoid future PCO, however this can lead to further complications [183-184]. This suggests there is an association between PCO rate and age, and the need for variations in treatment method. Due to this primary cell cultures were not taken further and cell lines were used for subsequent experiments.

4.2 Anticoagulation Polymers Coatings – 1 and 2

The coatings provided by BioInteractions Ltd. were designed as non-thrombogenic coatings for cardiovascular applications. They have been shown to minimise protein adsorption and platelet activation in vivo. It was hypothesised that these coatings could have a role in prohibiting cell attachment and growth on IOLs following cataract surgery, therefore these coatings were evaluated in cell culture as a starting point for this project. Coatings were synthesised on a poly ethylamine (PEI) base polymer containing functional groups of heparin (HEP) sulphates and sulfonates and poly ethylene glycol (PEG), with the aim of reducing the initial protein and cell adhesion on the biomaterial surface. HEP has extensively been used for its anticoagulation properties. Sulphate and sulfonate groups are negative charged which aim to repel cell attachment and PEG is highly hydrophilic which aims to minimise the interaction between the coating and the biological environment [109, 159, 179, 185].

Fewer LECs were attached to coatings 001, 004 and pHEMA than TCPS control. LECs that did attach onto these coatings were either rounded or elongated, showing a difference in morphology compared to cells adhered to TCPS wells. Some cells initially attached to the pHEMA coating, at later time points the cells had become rounded. This may have been due to the hydrogel-like material properties changing whilst in cell culture. PHEMA coating was received dry and was not rehydrated prior to seeding cells, therefore the coating may have absorbed a high amount of water whilst in cell culture, causing the coating to swell and disrupt attached cells. This coating may have benefited from being rehydrated after synthesis. Alternatively this coating could have been rehydrated prior to seeding LECs. Some defects were observed around the edge of coating 004, especially on the coated coverslips at later time points.

Due to their hydrogel-like nature, all three coatings absorbed methylene blue dye, making it difficult to visualise the cells. Cells that were present on the coatings prior to fixing appeared to have been washed off during the fixation and staining process, indicating cells were not strongly adhered to the surfaces. As mentioned previously (0) cell binding is dependent upon the protein layer at the surface interface [7]. These proteins are made of mobile chains of amino acids that can change in orientation, and

enable cellular binding when specific sequences of amino acids are present in the correct orientation [7]. The removal of the weakly attached cells during washing may be the result of an unfavourable 3-D structure of the proteins, and thus amino acids, at the coating interface, preventing cell attachment. Cells, therefore, could not settle and attach to the surface of the coating as the required cell binding sites were no longer available due to the folding of the protein. Changes in the chemistry of a material can affect this protein conformation and thus the amino acid sequence, resulting in variations in the cellular response across the various coatings [3]. A live/dead assay showed the majority of cells on coatings 001, 004 and pHEMA were dead, however this does not necessarily indicate that the coatings were toxic, it is most likely the cells could not adhere to the coating therefore died as LECs are anchorage-dependent cells. The methylene blue staining results showed LECs adhered and grew on the TCPS wells in the presence of coated coverslips, this supports the hypothesis that these coatings did not leach toxic materials into the medium.

The decision was made to synthesise coatings directly onto TCPS wells for all future cell work, as some coated coverslips had noticeable imperfections when observed under the microscope. In addition, multi-well plates were easy to use in cell culture and it was thought a better homogeneity of coating could be achieved. Two slight variations to coating 001 (coatings 002 and 003) were also evaluated. Coating 002 was cross-linked with glutaraldehyde, meaning the coating was more stable and PEG groups were less mobile. Coating 003 had a total of five water-based layers, with the aim of incorporating more functional groups.

More cells seemed to adhere to coating 001 in wells than in the previous study on coverslips, this may have been due to the coating procedure producing a more uniform coating. The cell attachment and growth on coatings 001 and 002 were similar ($p=0.15$) with 002 having a higher incidence of cell attachment when cells were counted, however both coatings had large standard deviations due to heterogeneous growth. The cross-linking agent utilised in coating 002 may have fixed the polymer in a set orientation. This may have caused protein adsorption that displayed more of the necessary amino acid sequences required for cellular attachment, compared to coating

001. Coatings 001 and 002 had a wettability, 68° and 62° respectively. Coating 003 had few, if any, cells attached during the 14 days in cell culture. This may be attributed to the series of water based layers increasing the number of functional groups, such as hydrophilic PEG molecules, present on the surface. This in turn may have affected the coatings wettability (35°). Coating 003 was significantly more hydrophilic than coatings 001 and 002 ($p<0.01$). Scanning electron microscopy (SEM) analysis showed all three coatings to be featureless which is promising for future use as IOL coatings, as they should not scatter light and indicates the coatings were uniform. In future work this along with other light transmission properties (for example, refraction and transmission) would be evaluated. This also implies the varied cellular response seen in cell culture was not correlated to surface topography. It is therefore believed that these differences are in relation to the surface chemistry and the presence of more functional groups on the surface. Tognetto et al compared variations in cell response on pHEMA based IOLs manufactured with different methacrylate copolymers in vivo. Results illustrated variations in the amount and type of cells attached, indicating cell attachment was dependant on material chemistry [89].

To summarise, this study demonstrated coating 004 and pHEMA did not support cell attachment, however the physical integrity of coating 004 was questionable. Complications arose with coatings 001 and 002: the coatings neither prohibited cell attachment nor enabled the growth of a LEC monolayer, therefore they did not support either hypothesis. Coating 003 did not support LEC attachment or growth.

Prior to experimentation on pre existing BioInteractions Ltd. coatings, LEC phenotype of FHL124 cell line was characterised, and cell culture conditions (seeding density and serum concentration) were optimised. It is important LEC growth on coatings and TCPS control surfaces retain their epithelial morphology and phenotype. Cytokeratin is a structural protein within the cytoskeleton. This intermediate filament is often used as an epithelial cell marker [186-187]. FHL124 LECs were stained with pan cytokeratin, clone C11. Positive expression of cytokeratin was observed following immunofluorescent staining. Cells also had a cobblestone morphology typical of epithelial cells [162-163], visualised by F-actin fibre staining using phalloidin.

As LEC attachment and growth was routinely monitored throughout various cell culture studies, a reliable method to count cells and an optimum seeding density were required. Although a haemocytometer offers quick and easy analysis of cell number it proved to be an unsuitable method of counting cells, due to the low cell numbers at early time points. Therefore it was deemed to be more accurate to fix, stain and micrograph cells. A seeding density of $1x10^4/cm^2$ provided both an exponential and stationary growth phase for analysis [180] within a convenient 7 day period.

The protein concentration required to retain proliferation and epithelial morphology was also evaluated prior to coating analysis. Serum present in cell cultures can add variability, induce contamination and also affect reproducibility from in vitro to in vivo, therefore the minimum amount of serum required for cells to retain typical morphology and proliferation should be used in cultures [188]. A serum concentration of 5% FCS was chosen to be the optimum level to culture FHL124 LECs, as this was the lowest serum concentration to encourage typical proliferation and morphology.

This optimisation process gives confidence that the cell response seen in this study was due to the surface coatings of 001, 002, 003, 004 and pHEMA, rather than inappropriate cell culture conditions.

4.3 GAG Coatings

Coatings 001, 002, 003 and 004 contained various amounts of HEP. HEP is a highly negatively charged glycosaminoglycan (GAG) and was added to these coatings as a non-thrombogenic molecule. HEP has widely been used in the coatings of vascular prostheses such as, stents, catheters, vascular grafts and heart valves [179, 189-190]. It has been shown to prevent platelet adhesion and reduce restenosis of stents, and also has been administered as a drug for its anti-thrombogenic properties to prevent clotting [190-191]. GAGs interact with the extra cellular matrix (ECM), proteins and cells. They are also known to manipulate cell behaviours such as proliferation, migration and adhesion [126, 128-129], therefore the addition of other GAG molecules was investigated. Hyaluronic acid (HA) is used in cataract surgery as the viscoelastic material injected between the cornea and the lens in the anterior chamber to allow surgeons room to operate [2]. HA is produced during embryonic development to provide space for new cells to grow [126], and has currently been used across multiple biological fields for its cell adhesion and proliferation properties [138, 178, 192]. Chondroitin sulphate (CS) has also been investigated for its potential to encourage cell adhesion and proliferation of stem cells [139]. It was hypothesised that by altering the amount of HEP, HA and CS present on a surface the LEC response could be controlled, either by encouraging a monolayer of cells to adhere or by prohibiting cell growth entirely.

GAG-modified polymer coatings were provided by BioInteractions Ltd. HEP polymer coatings inhibited most cell attachment compared to HA and CS modified coatings. The cell attachment and growth on HA and HEP polymer coatings was significantly different ($p=0.03$) at day 14. This statistical difference was only observed as 0 cells/field of view were present on all micrographs of HEP coatings, and HA had a mean of 2 cells/field of view on day 14. Therefore this difference is considered negligible. Cell attachment was heterogeneous on both HA and CS, with areas of no cell attachment and areas of concentrated growth. This sporadic growth resulted in large standard deviations. Variations in growth patterns were observed when polymer GAG coatings were examined using time lapse analysis in cell culture. LECs were seeding onto HEP, HA and CS coated wells in the same method as the previous study. HEP polymer coatings enabled a large amount of cells to attach during the 14 days in cell culture. Cells

appeared elongated and not typical of epithelial morphology. A mean of 1076 cells/field of view were counted on HEP coatings compared to 967 cells/field of view on TCPS control. HA polymer coating had a mean of 375 cells/field of view and CS polymer coatings had a mean of 80 cells/field of view. This result is in opposition to the previous studies, the cause of this is unknown. One hypothesis may be due to insufficient coating process in this particular batch or degradation of the coatings. This study would be repeated if materials and resources had allowed.

SEM analysis for all GAG polymers showed featureless coatings, at 5000x magnification (micron scale). Surface roughness analysis was measured using white light interferometry (WLI), results demonstrated TCPS and CS to be significantly different from HEP and HA, however this difference was only 2nm. This difference in nanometre height is not believed to be associated with the cellular response, as it has been reported a change in the range of 10s of nanometres is required in order to observe a change in cell attachment [193-195].

Various methods to adsorb HA and CS onto substrates were evaluated, however little difference in cell attachment was observed between these adsorbed GAG substrates and controls (substrates in the absences of absorbed HA or CS). Toluidine blue staining was used as a method to stain for the presence of GAGs [196]. Although this is commonly used no positive toluidine blue staining was observed on the adsorbed GAG substrates. It was, therefore, concluded that GAGs were not successfully adsorbed onto base substrates.

Covalent binding was considered as an alternative for depositing GAGs onto a surface. It was hypothesised that utilising the carboxyl groups present at the end of HA and CS molecules would be a more reliable method for binding the GAGs onto amine coated surfaces. Toluidine blue was again unsuccessful at confirming the presence of bound GAG, an alternative method for staining for the presence of GAGs is safranin O dye [139]. When covalently bound GAG coatings were immobilised onto their basement substrates the contact angle decreased, confirming surface modification and the presence of GAGs. The same decease was seen when GAG polymer coatings (provided

by BioInteractions Ltd.) were added onto PEI base substrates (Figure 3.36). Contact angle measurements for bound GAG coatings and GAG polymer coatings fell within a similar range (20 – 28°), however a difference was seen in the cellular response. Whilst CS polymer coating provided by BioInteractions Ltd. supported patchy LEC growth, higher concentrations of bound CS coating (3mg/ml and 1mg/ml) did not support LEC attachment or growth, suggesting CS was orientated differently when covalently bound onto the amine base surfaces. The base substrate layer could have also influenced the outermost GAG layer. HA did not encourage cellular attachment in either polymer coatings provided by BioInteractions Ltd. or the covalently bound GAG coatings. The same cellular responses was observed by D'Sa et al when B3 LECs were seeded onto HA coatings immobilised on plasma treated surfaces [9]. Uygun et al observed the opposite cellular attachment response with mesenchymal stem cells [139]. Orlidge et al examined attachment and proliferation of several cell types on HA and HEP coatings and reported that cell attachment and growth were dependant on cell type [178]. This Indicates cellular response to GAG coatings may be cell type dependant. The cell response on the covalently bound GAG coatings was somewhat dose dependent. At the lowest concentration of 0.1mg/ml of CS and HA few small patches of cell attachment and proliferation were observed. As the dose increased cell attachment decreased [9, 178]. Therefore covalent binding of higher concentrations of HA and CS to amine functionalised surfaces could be developed further as coatings to prohibit cell attachment on IOLs.

To summarise, variations in the cell attachment and growth were observed depending on the GAG type and method utilised for depositing GAGs onto a surface. This study has demonstrated that it is difficult to attach sufficient amount of GAGs to surfaces to have a significant influence on the cellular response. The data suggested that covalent binding of GAG could be a possible route to prohibit LEC attachment and growth on IOLs, thus future work in this area could be justified

As mentioned previously it is important to characterise cell phenotype, therefore prior to the use of N/N1003A LECs in this study various cytokeratin antibodies were used to test epithelial expression, however none of the cytokeratins tested proved successful in

staining N/N1003A LECs. It should be noted that no references could be found in which cytokeratin was used as an epithelial marker to stain N/N1003A LECs. Crystallins have previously been used to characterise LEC phenotype [160-166]. Reddan et al outlined the transformation of rabbit LECs into the N/N1003A LEC line, alpha A- and alpha B-crystallins were used as a method for characterising LEC phenotype [162]. When Krausz et al repeated this characterisation, however, alpha A-crystallin was not detected in N/N1003A LECs [166]. Similar results were found by Meakin et al and Wang et al, in both N/N1003A and B3 LECs [160, 197]. Whilst alpha A-crystallin has been shown to diminish with cell maturity and is generally not present past passage 10, alpha B-crystallin remains present as cells are passaged (until at least passage 26). This was shown by Flemming et al in the B3 LECs [198]. Based on this N/N1003A LECs were stained for alpha B-crystallin and positive expression of alpha B-crystallin was immunofluorescently visualised. This demonstrates the LEC used in this study were of epithelial origin.

4.4 Zwitterionic Polymers

The charge on a surface can affect cellular attachment and growth [123, 172]. GAGs are negatively charged macro-molecules [127, 137]. In addition to how these negatively charged ECM molecules interact with LEC attachment, positively and negatively charged coatings with zwitterionic character were examined. A zwitterionic molecule is a neutral entity that contains both positive and negative charges. Several authors have reported their beneficial use to prevent adsorption of specific protein and cell attachment on surfaces [199-200]. It has previously been reported that changing the ratio of phosphorylcholine in a polymer can improve haemocompatibility [201-202]. Ueda et al demonstrated that protein adsorption deceased with increasing amounts of 2-methacryloyloxyethyl phosphorylcholine (MPC) molecules in a copolymer [201]. These observations led to the advent of MPC being introduced into contact lenses [203]. Cell attachment has also been shown to be reduced on an IOL functionalised with MPC. Cell attachment and migration beneath the IOL was monitored when the IOL was placed on a collagen IV membrane (imitating the capsular bag). MPC-coated IOLs had reduced cell attachment compared to non-coated IOLs [204]. It was therefore hypothesised that by changing the amount of zwitterionic molecule present in a surface the cellular response could be controlled by preventing LEC attachment and growth. The cells used in this study were N/N1003A LECs.

Varying amounts of cell attachment were observed on the six novel zwitterionic polymers that differed in ratios between 10% to 30% zwitterionic compound copolymerised with acrylic-based monomer(s). Following investigation of the surface properties it was concluded these results were more likely due to the chemistry of the surface coatings, rather than the surface properties such as wettability and roughness.

With the exception of coating J, which contained 20% zwitterionic compound, coatings with 10 – 20% of zwitterionic compound in general did not support cell attachment. It was assumed that proteins did not adsorb onto the surface of these zwitterionic coatings in the correct confirmation to provide the necessary amino acid sequence to facilitate integrin binding and cell attachment. Coating K (20% novel zwitterionic monomer) had an average cell number of 22/field of view with the majority of

micrographs having 0 cells attached. The cell attachment observed on coating K may be due to different acrylic-based monomers (methoxyethyl methacrylate and hexyl methacrylate) used in polymerisation. It has been shown that the cellular response can be affected by the copolymer used in polymerisation (for example, butyl methacrylate and hexyl methacrylate), or the basement substrate [201, 205]. Coating J also was copolymerised with 20% zwitterionic monomer, however the coating was aqueous based and dissolved in solution, therefore the cellular response on coating J was believed to be a result of cells attached to the basement substrate, which was TCPS wells, rather than the coating. When zwitterionic monomer content was increased to 30% a change in cell attachment was observed. Coating H, containing 30% zwitterionic monomer, was orientated to have appropriate cell binding site available for N/N1003A cell attachment and growth. An Internal control, containing 30% MPC (coating N), similar to coating H also encouraged cell attachment, suggesting a higher zwitterionic component ratio in the copolymer may change the cellular response.

To investigate if the cellular response was in relation to the surface properties and chemistry and not the toxicity of the coatings, a cytotoxicity test was performed following guidelines in ISO:10993-5:2009 [206]. The metabolic activity of cells seeded onto the six zwitterionic coatings was not significantly different from cells seeded onto TCPS wells, regardless of zwitterionic ratio and acrylic monomer. This indicates the coatings were not cytotoxic to the cells and the cellular response must be the result of the surface chemistry.

As LECs are adherent dependent, cell death will occur if they cannot settle and attach to a surface. The majority of coatings did not support cell attachment, therefore a second toxicity test was conducted (Figure 3.41). This investigated cell attachment and spreading on TCPS after cells had been in contact with zwitterionic and internal control coatings for two hours. Two hours was chosen as it was a sufficient length of time for LECs to settle and attach to TCPS which typically occurs between 20 – 30 minutes, this was observed via time lapse microscopy. A longer time period prior to seeding cells onto a surface may result in cell distress and changes in cell behaviour. Some zwitterionic and internal control coatings had a chemistry that supported cell

attachment. This meant that LECs initially attached to the coated wells within the first two hours, prior to the remaining unattached cells being aspirated and re-seeded in fresh TCPS wells. This resulted in a lower number of cells attaching and proliferating across both plates, resulting in a lower metabolic activity. This was the case for 20% zwitterionic coatings (J), and internal controls, 100% poly butyl methacrylate and 70% butyl methacrylate:30%MPC (L and N respectively), however these variations in metabolic activity were not due to toxicity of the coatings. No significant difference was seen for coating L on day 4, even though the mean metabolic activity level was approximately half of the metabolic activity level for the control TCPS wells. This may be due to the variability of cells metabolic activity in one well which resulted in a large standard deviation. The metabolic activity of cells aspirated from 20% zwitterionic coating (K) and internal control 10% MPC coating (M) and reseeded onto fresh TCPS wells looked similar to TCPS control on day 4, however there was a significant difference when compared to TCPS control. This was probably due to the metabolic activity of cells on these coatings having smaller standard deviations, compared to the metabolic activity of cells on other coatings, meaning there was less variation in the data. The metabolic activity levels of cells aspirated from 10% zwitterionic coating (F) and reseeded onto fresh TCPS wells was significantly lower than TCPS control, at days 1 and 4. The cause of this is unknown, perhaps not all medium/cell solution was aspirated from the original coated wells.

Surface analysis showed variations in contact angle, topography and surface roughness across zwitterionic coatings and internal controls. The contact angle varied from approximately 80° to 22° and no correlation between wettability and cell attachment was observed. The substrate used in cell culture to maintain a monolayer of LEC growth was TCPS and had a contact angle of approximately 34°. This was significantly different to all other zwitterionic coatings and butyl methacrylate controls. A contact angle of approximately 80° (100% poly (butyl methacrylate – coating L) and a contact angle of 29° (70% butyl methacrylate:30%MPC – coating N) both enabled cell attachment. In addition coatings with a similar contact angle resulted in different cellular responses. The contact angle of coatings containing 70% butyl methacrylate:30%MPC (N) was not significantly different to 20% zwitterionic coating (K), however 70% butyl

methacrylate:30%MPC supported LECs attachment. This was not the case for the 20% zwitterionic coating (K). Similar a contact angle of 64° and 62° (coatings F and M respectively) did not enable the appropriate binding sites required for cell attachment. Likewise, a similar contact angle of 26° and 28° (coating G and K respectively) did not support LEC attachment. The contact angle of these two groups was significantly different from each other yet the same cell response was observed, supporting the conclusion that there was no clear link between wettability and cell attachment.

Coatings F and L had a fibrous honey comb appearance when the topography of the zwitterionic coatings were analysed using SEM. Some similar micro features were present on 20% zwitterionic coating (G) and 10% MPC coating (M). Cracks were also apparent in 30% zwitterionic coating (H) and ripples in the Y-axis of the image were present on 20% zwitterionic (K) at x5000 magnification (micron scale). These features have been attributed to the drying and processing of these coatings prior to SEM analysis. In future work surface topography would be examined via a method where additional processing steps are not required, for example atomic force microscopy (AFM). This would mean samples could be examined in the same state they are used in cell culture, in addition the topography of wet samples can be examined which may be beneficial to hydrogel-like substrates. This method could also be used to inspect cell attachment to the coatings. SEM analysis showed coatings I, J and N to be featureless at x5000 magnification (micron scale). There was also no significant difference in surface roughness between these coatings, however both the contact angle and the cellular response varied dramatically. This indicates there is no link between topography and cell attachment and growth for these coatings.

Coatings containing 90% butyl methacrylate:10%zwitterionic compound (F) and 100% poly butyl methacrylate (L) had a similar fibrous topography viewed using the SEM, this may be due to the high percentage of butyl methacrylate. This was not observed, however, in coating M which equally had 90% butyl methacrylate, indicating the chemistry of coating M when copolymerised with MPC may affect the topography. The contact angle for coatings F and L varied from approximately 64° - 79° respectively, and gave opposite cellular responses, with coating F not supporting LEC attachment and

growth. In addition the average surface roughness for coatings F and L was 149nm and 378nm respectively, these validate micrographs from SEM analysis. Analysis of coatings F and L may appear to indicate there is a relation between surface topography, wettability and cell attachment. Based on the results from all other zwitterionic and MPC coatings, however, it is clear this is not the case. As coatings with opposite properties, i.e. smooth and more hydrophilic coatings also enable the attachment of a LEC monolayer.

It would be advantageous to market an IOL as a bulk material as it would be more robust and easier to manipulate than coated IOLs, therefore following cell culture assays it was proposed that one or two coatings would be synthesised as bulk materials. 10% novel zwitterionic monomer was copolymerised with pHEMA and synthesised as a bulk contact lens as IOL moulds were not available. Bulk 10% zwitterionic:pHEMA (material F) was compared to pHEMA control contact lenses, TCPS wells and the gold standard, Acrysof® IOLs, and, at a later experiment time point, pHEMA IOLs (C-Flex). No cell attachment was observed on bulk material F, bulk material pHEMA and C-Flex IOLs. LECs adhered to Acrysof® IOLs: cells were observed at the edge of the IOL and in the centre, however some were rounded. None of the pHEMA based materials enabled cell attachment and all absorbed methylene blue dye due to the hydrogel like properties. This preliminary study demonstrated the difference in cell attachment and growth between a hydrophobic acrylic (Acrysof® IOLs) and a hydrophilic acrylic (pHEMA contact lenses, bulk 10% zwitterionic:pHEMA and C-Flex IOLs).

4.5 Dedifferentiation Model and TGFβ3 Assay

An alternative approach to reduce the incidence of PCO could be to control relevant cytokine release or activity following cataract surgery. Transforming growth factor beta-2 (TGFβ2) is secreted postoperatively by LECs as part of the natural wound healing response, which is known to cause dedifferentiation of LECs leading to PCO [147]. In addition the material used for IOLs can influence this wound healing response [52]. Therefore a possible route to eliminate the effect TGFβ2 had on LECs was investigated. The future aim was to apply a coating that could "mop up" the secreted TGFβ2 or neutralise its effect.

TGFβ3 is associated with wound healing and is currently being investigated in several studies to reduce scar tissue in the skin [153, 156-157, 207]. Jusitva™ is a pharmaceutical agent containing TGFβ3 aimed at reducing scarring in skin. Successful results from phase I and II clinical trials have been reported [157]. There is, therefore, the possibility for its use elsewhere in the body to reduce scarring. It was hypothesised if TGFβ3 was applied inside the capsular bag postoperatively or available on an IOL coating, it could potentially decrease scarring, and the number of dedifferentiation cells within the lens capsule. The aim of this study was to establish a model to evaluate dedifferentiation of LECs and the possibility to reduce it with the addition of TGFβ3. αSMA was selected as a suitable marker for dedifferentiated LECs [208-214]. This provided a tool to evaluate the potential of TGFβ3 to prevent or reverse dedifferentiation.

As serum is known to contain growth factors a serum concentration growth curve was performed on N/N1003A LECs prior the use of TGFβ3 in cell culture, to investigate the lowest serum concentration that could retain proliferation and typical morphological appearance. Wormstone et al have previously grown primary capsular explants in serum and protein free medium for up to 28 days, however LEC were grown inside the capsular bag on their basement membrane [215]. Capsular bags have also been harvested in serum free medium but with the addition of TGFβ2 [67]. Wormstone et al also examined TGFβ2 signalling in LECs. LECs were cultured in 5% serum for 3 days and serum starved for 2 days before exposure to experimental conditions for 24 hours.

Experimental conditions were medium supplemented with various growth factors including TGFβ2 [147]. Marcantonio et al used a similar method when studying the influence of TGFβ2 on α5β1 integrin. Cells were cultured in 5% serum until confluent, serum starved for 24 hours, then changed to experimental medium for a further 24 hours. Experimental medium was again serum free with the addition of various growth factors [216]. Based on the literature two methods were studied. Firstly by reducing the serum concentration from the start of the experiment or secondly seeding LECs in optimum 8% RS for either, 24 or 72 hours then serum starving for 24 hours prior to experimental conditions. The first method of reducing serum concentration from the start resulted in significantly less cell attachment compared to the second method of seeding cells in optimum 8% rabbit serum (RS) for 24 and 72 hours. Morphological changes were observed when serum was reduced from 8% RS to 0%. LECs appeared to decrease in size and round up, this may have been due to withdrawing the proteins and growth factors required to maintain typical growth and epithelial morphology. Pre-treatment with 8% RS for 72 hours then reducing serum to 2% RS provided the appropriate culture conditions needed to retain epithelial morphology and proliferation, a similar technique has widely been used in cell culture when evaluated growth factors or cell signalling pathways [67, 147, 215-216].

Three potential dedifferentiation models were evaluated, seeding LECs onto poly(methyl methacrylate) (PMMA) substrate, scratching a confluent monolayer of LECs and treating LECs with various concentrations of TGFβ2. A PMMA model was investigated as this material has been shown to induce contraction in LECs and PCO in vivo [50, 52]. This was a simple method using a substrate to examine dedifferentiation, however the time needed for PMMA to cause dedifferentiation in vitro is not known. Cells may need to be cultured for a long time given how long dedifferentiation takes to occur in vivo. The scratch model was examined to replicate the physical injury caused to LECs during phacoemulsification and clean up of residual LECs [60, 217]. This was a quick method using a 1ml tip to create a scratch through the centre of a monolayer, however this may be difficult to replicate on material coatings provided by BioInteractions Ltd. Depending upon the number of layers and how the coating has been applied the scratch could inevitably cause damage to the coating. LECs were maintained in medium containing

various concentrations of TGFβ2 (MEME, 2% RS) due to its association with scarring and PCO. In normal aqueous TGFβ2 is between 1 – 2ng/ml, and in eyes with cataracts it is increased to 3 – 4ng/ml [218-220]. As the level of TGFβ2 is increased postoperatively this model tries to mimic the natural environment, however the influence of TGFβ2 on LECs may vary from in vivo to in vitro. A dedifferentiation model using 5ng/ml TGFβ2 was chosen as it is clinically relevant.

TGFβ3 did dedifferentiate LECs to some extent regardless of time exposure or concentration, which was not expected. When TGFβ3 was studied in conjunction with the dedifferentiation model TGFβ3 seemed to have little effect at reversing already dedifferentiated LECs, regardless of time exposure and concentration. A higher dose of TGFβ3 may have been more effective. Wormstone et al observed long term fibrotic response up to 28 days quantified by αSMA expression when LECs had been treated with TGFβ2 for a short time period [74]. Indicating TGFβ3 was not sufficient at reversing TGFβ2 long lasting fibrotic response.

TGFβ3 seemed to offer some protection against dedifferentiation when added prior to dedifferentiating LECs. This was observed by a reduction in the level of dedifferentiation at all TGFβ3 concentrations and time exposures, when compared to the amount of dedifferentiation caused by TGFβ2. The level of dedifferentiation caused by TGFβ2, however, was reduced by approximately 22% when compared to the level of dedifferentiation caused in the previous study. One reason to explain this may be due to the short shelf life of TGFβ2 meaning optimum dedifferentiation did not occur. To validate this result the study would be repeated with fresh TGFβ2 to examine if the decrease in dedifferentiation after pre-treatment with TGFβ3 was still present. The results seen in this study could also be correlated to the results observed in the phase III clinical trial using “Juvista”. The primary and secondary end points were not met therefore the trial was stopped and funding was withdrawn [158]. The failure to meet the end points placed doubt on “Juvista” ability to reverse scarring, however this leads to more questions as to what is happening at the gene level in association with wound healing.

As the method for analysing dedifferentiation was semi quantitative, flow cytometry was evaluated for its potential to provide a quantitative method to evaluate LEC expression of αSMA. This method has previously been used to obtain quantitative data for reliable cell labelling expression [221]. Positive expression of αSMA labelled cells was apparent when LECs were incubated with 5ng/ml of TGFβ2. The histogram had a wide spread meaning some cells were stained more intensely than others. This reflects what was observed immunocytochemically in earlier studies and verifies flow cytometry as a method for quantifying αSMA expression. This method could have proved a more quantifiable method for examining the dedifferentiation model in conjunctions with TGFβ3. If more time was available the dedifferentiation study would have been repeated using flow cytometry as a quantitative method for examining dedifferentiation levels.

To examine if there was a difference in gene expression between un-dedifferentiated LECs, dedifferentiated LECs (TGFβ2) and LECs incubated with TGFβ3 polymerase chain reaction (PCR) was performed. As gene arrays were specific to human species, B3 human LEC line was used in this study. B3 LECs were characterised with pan cytokeratin, clone C11, prior to use. Each test sample was compared to a control sample (Table 3-3). If the expression of a gene was low in both the control and test sample the result was not evaluated further, due to question of reliability of the gene expression. If more time and resources had allowed this would have been repeated to validate these results.

TGFβ is associated with induction of dedifferentiation and detected by αSMA expression in several cell types throughout the body [24, 57, 74, 222]. TGFβ2 has been shown to increase the expression of collagen and fibronectin [59]. Fibronectin is associated with contraction and scarring [24, 52]. Fibronectin was up-regulated by a fold increase of 4.3 when LECs incubated with TGFβ2 were compared to untreated LECs (control LECs). Additionally, a fold increase of 2.1 was observed when LECs incubated with TGFβ3 were compared to untreated LECs (control LECs). The up-regulation of fibronectin may be directly correlated to the positive αSMA expression observed immunocytochemically, and could be a possible reason for the unexpected αSMA staining seen in LECs treated with TGFβ3. In addition LECs incubated with TGFβ2 had a higher up regulation of

fibronectin and therefore a higher expression of αSMA staining. When cells were incubated with TGFβ3 prior to dedifferentiation with TGFβ2 a similar fold increase to LECs incubated with TGFβ3 alone (2.8 and 2.1 respectively) was observed. This may indicate TGFβ3 offers some protective properties against up-regulation of fibronectin, and thus dedifferentiation. This may validate αSMA expression quantified by the previous immunocytochemistry study.

Matrix metallopeptidase are a family of enzymes involved in ECM degradation [223]. TGFβ2 treatment up-regulated the expression of matrix metallopeptidase 14 (MMP14, a member of the MMP membrane bound sub-family) by an 8.6 fold-increase when compared to control LECs. Hodgkins et al observed MMP14 had the highest expression in LECs when screening the entire MMP family [224]. MMP14 is associated with the activation of MMP2 [223-225]. MMP2 was also observed when LECs were incubated with TGFβ2 compared to untreated LECs (control LECs) but not when cells were incubated with TGFβ3. Richiert and Ireland also did not see any MMP2 expression in chick LECs unless they were incubated with TGFβ2 [226]. Eldred et al also demonstrated MMP-14 and MMP-2 were up-regulated in FHL124 LECs incubated with TGFβ2. In addition TGFβ2 induced capsular wrinkling was reduced in the presence of a MMP2 inhibitor. Suggesting that MMP-2 plays an important role in capsular wrinkling seen in PCO [225]. The true involvement with MMP14 and MMP2 in terms of dedifferentiation in relation to PCO is not fully understood therefore the results observed here would need to be examined further.

Several In vivo and in vitro studies have illustrated the presence of collagen expressed by dedifferentiated LECs [24, 102, 227-228]. Saika et al observed deposition of collagen types I, III, IV, V, and VI, on the capsular bag after implantation of an IOL [227-228]. These specific collagen genes were observed in the PCR results when LECs were incubated with TGFβ2. Several integrin genes were up and down regulated across treatments. Integrins β5 and integrin α5 were both up-regulated when LECs were incubated with TGFβ2, also shown by Dawes et al [59]. Dawes et al and Marcantonio et al have examined α5β1 integrin (a receptor for fibronectin) expression in LECs [24, 59-

60, 216]. The role integrins plays on dedifferentiation could therefore be examined further.

This technique was used as a method to highlight genes that may be of interest, the understanding of these results would require further detailed work. If more time and resources had allowed this would be repeated to validate the results. Specific genes such as fibronectin 1, MMP14, MMP2, groups of collagens and groups of integrins would be examined further by several techniques including PCR, enzyme-linked immunosorbent assay (ELISA) and western blotting.

As we know reducing the incidence of PCO is a multi and cross disciplinary process, the up and down regulation of these genes should be related to IOL material. In future work a more iterative process for screening potential IOL materials could be the combination of examining materials in cell culture, via surface analysis, and the expression of these genes. This may lead us one step closer to understanding the complexity of scarring in PCO, and a possible route to prevention of this disease.

5. Conclusions

Investigations were carried out on an array of surfaces designed to control the LEC attachment and growth response, to reduce the incidence of PCO. The following conclusions were drawn:

1. Pre-existing BioInteractions Ltd. coatings
    a. Coating 001 and 002 were not suitable as IOL coatings as they did not support either hypothesis, to prevent cellular attachment or to enable the growth of a LEC monolayer.
    b. Coating 003 supported the hypothesis to prevent cell attachment and growth and was further analysed in terms of its GAG properties.
    c. Further work was not conducted on coating 004 as there were concerns over the coatings integrity.
2. GAG coatings
    a. On average HEP and HA coatings prevented cellular attachment, and whilst some cells attached to CS it did not enable the growth of a LEC monolayer. There were, however, inconsistencies with these cellular responses, therefore future work would be required to confirm HEP's and HA's ability to prevent cellular attachment.
    b. Adsorbed GAGs did not successfully attach to the base substrate. Which resulted in no noticeable cellular difference from control coatings to HA and CS adsorbed coatings.
    c. HA and CS were successfully covalently bound onto amine coated glass coverslips. Covalently bound GAG coatings, at higher concentrations (3mg/ml and 1mg/ml), did not provide the correct binding sites for LECs to attach and grow. These could be appropriate coatings to prevent LEC attachment and growth, thus reducing the incidence of scarring and the postoperative fibrotic response. Further work using a capsule bag model could be investigated [229].

3. Zwitterionic coatings
    a. The ratio of zwitterionic:monomer can be varied to control the cellular response.
    b. Zwitterionic coating proved non-cytotoxic following ISO:10993-5:2009 protocol.
    c. There was no clear link between wettability and cellular attachment. In addition there was no correlation between surface roughness and the cellular response. Therefore it was concluded that the cellular response seen on the zwitterionic coatings was the result of surface chemistry.
    d. The confirmation of the protein adlayer on novel zwitterionic bulk material F may not have presented appropriate binding sites required for cellular attachment, therefore LECs did not settle and attach on this material. This material could possibly be synthesised as an IOL bulk material to prevent cell attachment. Future work examining the bulk material properties and protein adsorption could be investigated.
4. Dedifferentiation
    a. The effect TGFβ2 has on dedifferentiating LECs is a problem associated with PCO. A model for successfully dedifferentiated LECs using 5ng/ml TGFβ2 was developed.
    b. TGFβ3 had little effect at reversing dedifferentiation, however, it may offer some protection against dedifferentiation, although this would need to be examined further.
    c. The regulation of collagens, integrins, matrix metallopeptidase and fibronectin 1 gene expression differed in dedifferentiated and un-dedifferentiated LECs. These genes play important roles with cell attachment, proliferation, scarring and fibrosis within PCO. In future work these genes should be explored further in terms of their expression profile with IOL material. This could inevitable lead to tailoring a material to provide optimum gene expression, to achieve a monolayer of LEC growth retaining epithelial phenotype, or prohibiting LEC growth, alleviating the incidence of PCO.

6. Appendices

Appendix – A

Glycosaminoglycan time lapse microscopy of N/N1003A LECs seeded onto GAG polymer coatings (heparin, hyaluronic acid and chondroitin sulphate). Please find the CD attached, folder name is GAG time lapse sub-folders are named according to coatings.

Appendix – B

Zwitterionic time lapse microscopy of N/N1003A LECs seeded onto zwitterionic coatings (F-J) and methacryloyloxyethyl phosphorylcholine controls (L-N). Please find the CD attached, folder name is zwitterionic time lapse sub-folders are named according to coatings.

Appendix – C

PCR Array Catalogue #: PAHS-013

Position	Symbol	Description	RefSeq ID
A01	ADAMTS1	ADAM metallopeptidase with thrombospondin type 1 motif, 1	NM_006988
A02	ADAMTS13	ADAM metallopeptidase with thrombospondin type 1 motif, 13	NM_139025
A03	ADAMTS8	ADAM metallopeptidase with thrombospondin type 1 motif, 8	NM_007037
A04	CD44	CD44 molecule (Indian blood group)	NM_000610
A05	CDH1	Cadherin 1, type 1, E-cadherin (epithelial)	NM_004360
A06	CNTN1	Contactin 1	NM_001843
A07	COL11A1	Collagen, type XI, alpha 1	NM_080629
A08	COL12A1	Collagen, type XII, alpha 1	NM_004370
A09	COL14A1	Collagen, type XIV, alpha 1	NM_021110
A10	COL15A1	Collagen, type XV, alpha 1	NM_001855
A11	COL16A1	Collagen, type XVI, alpha 1	NM_001856
A12	COL1A1	Collagen, type I, alpha 1	NM_000088
B01	COL4A2	Collagen, type IV, alpha 2	NM_001846
B02	COL5A1	Collagen, type V, alpha 1	NM_000093
B03	COL6A1	Collagen, type VI, alpha 1	NM_001848
B04	COL6A2	Collagen, type VI, alpha 2	NM_001849
B05	COL7A1	Collagen, type VII, alpha 1	NM_000094
B06	COL8A1	Collagen, type VIII, alpha 1	NM_001850
B07	VCAN	Versican	NM_004385
B08	CTGF	Connective tissue growth factor	NM_001901
B09	CTNNA1	Catenin (cadherin-associated protein), alpha 1, 102kDa	NM_001903
B10	CTNNB1	Catenin (cadherin-associated protein), beta 1, 88kDa	NM_001904
B11	CTNND1	Catenin (cadherin-associated protein), delta 1	NM_001331
B12	CTNND2	Catenin (cadherin-associated protein), delta 2 (neural plakophilin-related arm-repeat protein)	NM_001332
C01	ECM1	Extracellular matrix protein 1	NM_004425
C02	FN1	Fibronectin 1	NM_002026
C03	HAS1	Hyaluronan synthase 1	M_001523
C04	ICAM1	Intercellular adhesion molecule 1	NM_000201
C05	ITGA1	Integrin, alpha 1	NM_181501
C06	ITGA2	Integrin, alpha 2 (CD49B, alpha 2 subunit of VLA-2 receptor)	NM_002203
C07	ITGA3	Integrin, alpha 3 (antigen CD49C, alpha 3 subunit of VLA-3 receptor)	NM_002204
C08	ITGA4	Integrin, alpha 4 (antigen CD49D, alpha 4 subunit of VLA-4 receptor)	NM_000885
C09	ITGA5	Integrin, alpha 5 (fibronectin receptor, alpha polypeptide)	NM_002205
C10	ITGA6	Integrin, alpha 6	NM_000210

C11	ITGA7	Integrin, alpha 7	NM_002206
C12	ITGA8	Integrin, alpha 8	NM_003638
D01	ITGAL	Integrin, alpha L (antigen CD11A (p180), lymphocyte function-associated antigen 1; alpha polypeptide)	NM_002209
D02	ITGAM	Integrin, alpha M (complement component 3 receptor 3 subunit)	NM_000632
D03	ITGAV	Integrin, alpha V (vitronectin receptor, alpha polypeptide, antigen CD51)	NM_002210
D04	ITGB1	Integrin, beta 1 (fibronectin receptor, beta polypeptide, antigen CD29 includes MDF2, MSK12)	NM_002211
D05	ITGB2	Integrin, beta 2 (complement component 3 receptor 3 and 4 subunit)	NM_000211
D06	ITGB3	Integrin, beta 3 (platelet glycoprotein IIIa, antigen CD61)	NM_000212
D07	ITGB4	Integrin, beta 4	NM_000213
D08	ITGB5	Integrin, beta 5	NM_002213
D09	KAL1	Kallmann syndrome 1 sequence	NM_000216
D10	LAMA1	Laminin, alpha 1	NM_005559
D11	LAMA2	Laminin, alpha 2	NM_000426
D12	LAMA3	Laminin, alpha 3	NM_000227
E01	LAMB1	Laminin, beta 1	NM_002291
E02	LAMB3	Laminin, beta 3	NM_000228
E03	LAMC1	Laminin, gamma 1 (formerly LAMB2)	NM_002293
E04	MMP1	Matrix metallopeptidase 1 (interstitial collagenase)	NM_002421
E05	MMP10	Matrix metallopeptidase 10 (stromelysin 2)	NM_002425
E06	MMP11	Matrix metallopeptidase 11 (stromelysin 3)	NM_005940
E07	MMP12	Matrix metallopeptidase 12 (macrophage elastase)	NM_002426
E08	MMP13	Matrix metallopeptidase 13 (collagenase 3)	NM_002427
E09	MMP14	Matrix metallopeptidase 14 (membrane-inserted)	NM_004995
E10	MMP15	Matrix metallopeptidase 15 (membrane-inserted)	NM_002428
E11	MMP16	Matrix metallopeptidase 16 (membrane-inserted)	NM_005941
E12	MMP2	Matrix metallopeptidase 2 (gelatinase A, 72kDa gelatinase, 72kDa type IV collagenase)	NM_004530
F01	MMP3	Matrix metallopeptidase 3 (stromelysin 1, progelatinase)	NM_002422
F02	MMP7	Matrix metallopeptidase 7 (matrilysin, uterine)	NM_002423
F03	MMP8	Matrix metallopeptidase 8 (neutrophil collagenase)	NM_002424
F04	MMP9	Matrix metallopeptidase 9 (gelatinase B, 92kDa gelatinase, 92kDa type IV collagenase)	NM_004994
F05	NCAM1	Neural cell adhesion molecule 1	NM_000615
F06	PECAM1	Platelet/endothelial cell adhesion molecule	NM_000442
F07	SELE	Selectin E	NM_000450
F08	SELL	Selectin L	NM_000655
F09	SELP	Selectin P (granule membrane protein 140kDa, antigen CD62)	NM_003005
F10	SGCE	Sarcoglycan, epsilon	NM_003919
F11	SPARC	Secreted protein, acidic, cysteine-rich (osteonectin)	NM_003118
F12	SPG7	Spastic paraplegia 7 (pure and complicated autosomal recessive)	NM_003119
G01	SPP1	Secreted phosphoprotein 1	NM_000582
G02	TGFBI	Transforming growth factor, beta-induced, 68kDa	NM_000358

G03	THBS1	Thrombospondin 1	NM_003246
G04	THBS2	Thrombospondin 2	NM_003247
G05	THBS3	Thrombospondin 3	NM_007112
G06	TIMP1	TIMP metallopeptidase inhibitor 1	NM_003254
G07	TIMP2	TIMP metallopeptidase inhibitor 2	NM_003255
G08	TIMP3	TIMP metallopeptidase inhibitor 3	NM_000362
G09	CLEC3B	C-type lectin domain family 3, member B	NM_003278
G10	TNC	Tenascin C	NM_002160
G11	VCAM1	Vascular cell adhesion molecule 1	NM_001078
G12	VTN	Vitronectin	NM_000638
H01	B2M	Beta-2-microglobulin	NM_004048
H02	HPRT1	Hypoxanthine phosphoribosyltransferase 1	NM_000194
H03	RPL13A	Ribosomal protein L13a	NM_012423
H04	GAPDH	Glyceraldehyde-3-phosphate dehydrogenase	NM_002046
H05	ACTB	Actin, beta	NM_001101
H06	HGDC	Human Genomic DNA Contamination	SA_00105
H07	RTC	Reverse Transcription Control	SA_00104
H08	RTC	Reverse Transcription Control	SA_00104
H09	RTC	Reverse Transcription Control	SA_00104
H10	PPC	Positive PCR Control	SA_00103
H11	PPC	Positive PCR Control	SA_00103
H12	PPC	Positive PCR Control	SA_00103

7. References

1. Williams, D.F., ed. Definitions in Biomaterials. first ed. Progress in Biomedical Engineering. Vol. 4. 1987, Elsevier Science Publishers: Amsterdam.
2. Williams, R.L. and Wong, D., Ophthalmic biomaterials, in Biomedical Materials, R. Narayan, Editor. 2009, Springer: New York. p. 327-348.
3. Keselowsky, B.G., et al., Surface chemistry modulates fibronectin conformation and directs integrin binding and specificity to control cell adhesion. Journal of Biomedical Materials Research - Part A, 2003. 66A(2): p. 247-259.
4. D'Sa, R.A., et al., Protein adhesion and cell response on atmospheric pressure dielectric barrier discharge-modified polymer surfaces. Acta Biomaterialia, 2010. 6(7): p. 2609-2620.
5. Johnston, R.L., et al., In vitro protein adsorption to 2 intraocular lens materials. Journal of Cataract and Refractive Surgery, 1999. 25(8): p. 1109-1115.
6. Schakenraad, J.M. and Busscher, H.J., Cell-polymer interactions: The influence of protein adsorption. Colloids and Surfaces, 1989. 42(2): p. 331-343.
7. Eskin, S.G., et al., Some background concepts, in Biomaterials Science: An Introduction to Materials in Medicine, B.D. Ratner, et al., Editors. 2004, Elsevier Academic Press: London. p. 237-292.
8. Vroman, L., Effect of adsorbed proteins on the wettability of hydrophilic and hydrophobic solids. Nature, 1962. 196(4853): p. 476-477.
9. D'Sa, R.A., et al., Inhibition of lens epithelial cell growth via immobilisation of hyaluronic acid on atmospheric pressure plasma modified polystyrene. Soft Matter, 2011. 7(2): p. 608-617.
10. Lombardo, M., et al., Analysis of intraocular lens surface adhesiveness by atomic force microscopy. Journal of Cataract and Refractive Surgery, 2009. 35(7): p. 1266-1272.
11. Cole, M.A., et al., Stimuli-responsive interfaces and systems for the control of protein–surface and cell–surface interactions. Biomaterials, 2009. 30(9): p. 1827-1850.
12. Aplin, A.E., et al., Signal transduction and signal modulation by cell adhesion receptors: The role of integrins, cadherins, immunoglobulin-cell adhesion molecules, and selectins. Pharmacological Reviews, 1998. 50(2): p. 197-264.
13. Ma, Z., et al., Surface modification and property analysis of biomedical polymers used for tissue engineering. Colloids and Surfaces B: Biointerfaces, 2007. 60(2): p. 137-157.
14. Grinnell, F. and Feld, M.K., Fibronectin adsorption on hydrophilic and hydrophobic surfaces detected by antibody binding and analyzed during cell adhesion in serum-containing medium. Journal of Biological Chemistry, 1982. 257(9): p. 4888-4893.
15. Underwood, P.A., et al., Effects of polystyrene surface chemistry on the biological activity of solid phase fibronectin and vitronectin, analysed with monoclonal antibodies. Journal of Cell Science, 1993. 104(3): p. 793-803.
16. Lhoest, J.B., et al., Fibronectin adsorption, conformation, and orientation on polystyrene substrates studied by radiolabeling, XPS, and ToF SIMS. Journal of Biomedical Materials Research, 1998. 41(1): p. 95-103.

17. Bron, A.J., et al., The cornea and sclera, in Wolff's Anatomy of The Eye and Orbit. 1997, Chapman and Hall: London. p. 233-278.
18. Martini, F.H., Fundamentals of Anatomy and Physiology. 2001, Pentice Hall: New Jersey. p. 538 - 557.
19. Grierson, I., The Eye Book. 2000, Liverpool University Press: Liverpool.
20. Kauffman, P.L., Accomdation and presbyopia: Neuromuscular and biophysical aspects, in Adler's Physiology of the Eye, W.H. Hart, Editor. 1992, Mosby-Year Book Inc: USA. p. 391-411.
21. Kearns V, et al., Ophthalmic applications of biomaterials in regenerative medicine, in Biomaterials and Stem Cells in Regenerative Medicine, M. Ramalingam, S. Ramakrishna, and S. Best, Editors. 2012, CRC Press. p. 185-218.
22. Gayton, J.L., et al., Interlenticular opacification: Clinicopathological correlation of a complication of posterior chamber piggyback intraocular lenses. Journal of Cataract and Refractive Surgery, 2000. 26(3): p. 330-336.
23. Davson, H., The lens, in Physiology of The Eye, H. Davson, Editor. 1980, Churchill Livingstone: London. p. 139-202.
24. De Longh, R.U., et al., Transforming growth factor-β-induced epithelial-mesenchymal transition in the lens: A model for cataract formation. Cells Tissues Organs, 2005. 179(1-2): p. 43-55.
25. Apple, D.J., et al., Posterior capsule opacification. Survey of Ophthalmology, 1992. 37(2): p. 73-116.
26. Mann, I., The lens, in Development of The Human Eye. 1969, Grunge and Stratton Inc: New York. p. 46-67.
27. Harding, J.J., et al., Men have heavier lenses than women of the same age. Experimental Eye Research, 1977. 25: p. 651.
28. Bron, A.J., et al., The lens and zonules, in Wolff's Anatomy of The Eye and Orbit. 1997, Chapman and Hall: London. p. 411-442.
29. Davson, H., Accomodation, in Physiology of The Eye. 1980, Churchill Livingstone: London. p. 767-782.
30. Refojo, M.F., Ophthalmic applications, in Biomaterials Science: An Introduction to Materials in Medicine, B.D. Ratner, et al., Editors. 2004, Elsevier Academic Press: London. p. 583-591.
31. Patel, A.S., Introduction to optics of the eye, cataracts, and intraocular lens implants, in Biomaterials Science: An Introduction to Materials in Medicine, B.D. Ratner, et al., Editors. 2004, Elsevier Academic Press: London. p. 591-602.
32. Zigman, S., The role of sunlight in human cataract formation. Survey of Ophthalmology, 1983. 27(5): p. 317-326.
33. Wu, R., et al., Smoking, socioeconomic factors, and age-related cataract: The Singapore Malay eye study. Archives of Ophthalmology, 2010. 128(8): p. 1029-1035.
34. Kanthan, G.L., et al., Alcohol consumption and the long-term incidence of cataract and cataract surgery: The blue mountains eye study. American Journal of Ophthalmology, 2010. 150(3): p. 434-440.
35. West, S.K. and Valmadrid, C.T., Epidemiology of risk factors for age-related cataract. Survey of Ophthalmology, 1995. 39(4): p. 323-334.
36. Allen, L.T., et al., Surface-induced changes in protein adsorption and implications for cellular phenotypic responses to surface interaction. Biomaterials, 2006. 27(16): p. 3096-3108.

37. Patterson, C.A. and Delamere, N.A., The lens, in Adler's Physiology of The Eye, W.H. Hart, Editor. 1992, Mosby-Year Book Inc: USA. p. 348-390.
38. Costello, M.J., et al., Ultrastructural analysis of damage to nuclear fiber cell membranes in advanced age-related cataracts from India. Experimental Eye Research, 2008. 87(2): p. 147-158.
39. Andley, U.P., Crystallins in the eye: Function and pathology. Progress in Retinal and Eye Research, 2007. 26(1): p. 78-98.
40. Jedziniak, J.A., et al., The concentration and localization of heavy molecular weight aggregates in aging normal and cataractous human lenses. Experimental Eye Research, 1975. 20(4): p. 367-369.
41. National Eye Institute, A hypermature age-related cortico-nuclear cataract with a brunescent (brown) nucleus. 2012, National Eye Institute, National Institutes of Health, Ref#: EDA13: http://www.nei.nih.gov/photo/keyword.asp?conditions=Cataract&narrow=Photo.
42. Minassian, D.C., et al., The deficit in cataract surgery in England and Wales and the escalating problem of visual impairment: epidemiological modelling of the population dynamics of cataract. British Journal of Ophthalmology, 2000. 84(1): p. 4-8.
43. Taylor, H., Cataract: How much surgery do we have to do? British Journal of Ophthalmology, 2000. 84(1): p. 1-2.
44. Pascolini, D. and Mariotti, S.P., Global estimates of visual impairment: 2010. British Journal of Ophthalmology, 2011. 96(5): p. 614-618.
45. The Royal College of Ophthalmologists. Cataract surgery guidelines. 2005 [cited 2010 14/04/10]; Available from: http://www.rcophth.ac.uk/docs/publications/CataractSurgeryGuidelinesMarch2005Updated.pdf.
46. Yuen, C., et al., Modification of the surface properties of a lens material to influence posterior capsule opacification. Clinical and Experimental Ophthalmology, 2006. 34(1): p. 568-574.
47. Resnikoff, S., et al., Policy and practice, global data on visual impairment in the year 2002. Bulletin of the World Health Organisation, 2004. 82(11): p. 844-851.
48. Peng, Q., et al., Surgical prevention of posterior capsule opacification: Part 2: Enhancement of cortical cleanup by focusing on hydrodissection. Journal of Cataract and Refractive Surgery, 2000. 26(2): p. 188-197.
49. Healthwise Inc. Phacoemulification for cataract surgery. 2011 [cited 2012 30/04/2012]; Available from: http://www.emedicinehealth.com/script/main/art.asp?articlekey=138867&ref=129647.
50. Hollick, E.J., et al., Lens epithelial cell regression on the posterior capsule with different intraocular lens materials. British Journal of Ophthalmology, 1998. 82(10): p. 1182 -1188.
51. Williams, R.L. and Kearns, V.R., Drug-device combination products for ocular applications, in Drug-Device Combination Products: Delivery Technologies and Applications, A. Lewis, Editor. 2010, Woodhead Publishing Limited: Cambridge. p. 311-340.

52. Saika, S., Relationship between posterior capsule opacification and intraocular lens biocompatibility. Progress in Retinal and Eye Research, 2004. 23(3): p. 283-305.
53. Tripathi, R.C., Growth factors in the aqueous humor and their therapeutic implications in glaucoma and anterior segment disorders of the human eye. Drug Development Research, 1991. 22(1): p. 1-23.
54. Ohta, K., et al., IL-6 antagonizes TGF-β and abolishes immune privilege in eyes with endotoxin-Induced uveitis. Investigative Ophthalmology and Visual Science, 2000. 41(9): p. 2591-2599.
55. Cousins, S.W., et al., Identification of transforming growth factor-β as an immunosuppressive factor in aqueous humor. Investigative Ophthalmology and Visual Science, 1991. 32(8): p. 2201-2211.
56. Wormstone, I.M., et al., TGF-β2-induced matrix modification and cell transdifferentiation in the human lens capsular bag. Investigative Ophthalmology and Visual Science, 2002. 43(7): p. 2301-2308.
57. Hales, A.M., et al., TGFβ1 induces lens cells to accumulate α-smooth muscle actin, a marker for subcapsular cataracts. Current Eye Research, 1994. 13(12): p. 885-890.
58. Hales, A.M., et al., Susceptibility to TGFβ2-induced cataract increases with aging in the rat. Investigative Ophthalmology and Visual Science, 2000. 41(11): p. 3544-3551.
59. Dawes, L.J., et al., TGFβ-induced contraction is not promoted by fibronectin-fibronectin receptor interaction or α-SMA expression. Investigative Ophthalmology and Visual Science, 2008. 49(2): p. 650-661.
60. Wormstone, I.M., et al., Posterior capsule opacification. Experimental Eye Research, 2009. 88(2): p. 257-269.
61. Matsushima, H., et al., Preventing secondary cataract and anterior capsule contraction by modification of intraocular lenses. Expert Review of Medical Devices, 2008. 5(2): p. 197-207.
62. Abela-Formanek, C., et al., Uveal and capsular biocompatibility of hydrophilic acrylic, hydrophobic acrylic, and silicone intraocular lenses. Journal of Cataract and Refractive Surgery, 2002. 28(1): p. 50-61.
63. Dewey, S., Posterior capsule opacification. Current Opinion in Ophthalmology, 2006. 17(1): p. 45-53.
64. Ohadi, C., et al., Posterior capsule opacification. Current Opinion in Ophthalmology, 1991. 2(1): p. 46-52.
65. Schaumberg, D.A., et al., A systematic overview of the incidence of posterior capsule opacification. Opthalmology, 1998. 105(7): p. 1213-1221.
66. Boureau, C., et al., Cost of cataract surgery after implantation of three intraocular lenses. Clinical Ophthalmology, 2009. 3(1): p. 277-285.
67. Awasthi, N., et al., Posterior capsular opacification: A problem reduced but not yet eradicated. Archives of Ophthalmology, 2009. 127(4): p. 555-562.
68. Apple, D.J., et al., Eradication of posterior capsule opacification: Documentation of a marked decrease in Nd:YAG laser posterior capsulotomy rates noted in an analysis of 5416 pseudophakic human eyes obtained postmortem. Ophthalmology, 2001. 108(3): p. 505-518.
69. Aslam, T.M., et al., Use of Nd:YAG laser capsulotomy. Survey of Ophthalmology, 2003. 48(6): p. 594-612.

70. Trivedi, R.H., et al., Post cataract-intraocular lens (IOL) surgery opacification. Nature, 2002. 16(1): p. 217 - 241.
71. Tetz, M.R. and Nimsgern, C., Posterior capsule opacification part 2: Clinical findings. Journal of Cataract and Refractive Surgery, 1999. 25(12): p. 1662-1674.
72. Pandey, S., et al., Posterior capsule opacification: A review of the aetiopathogenesis, experimental and clinical studies and factors for prevention. Indian Journal of Ophthalmology, 2004. 52(2): p. 99-112.
73. Hales, A.M., et al., Estrogen protects lenses against cataract induced by transforming growth factor-beta (TGF-β). The Journal of Experimental Medicine, 1997. 185(2): p. 273 - 280.
74. Wormstone, I.M., et al., Short-term exposure to transforming growth factor-β induces long-term fibrotic responses. Experimental Eye Research, 2006. 83(5): p. 1238-1245.
75. Dixit, N.V., et al., Outcomes of cataract surgery and intraocular lens implantation with and without intracameral triamcinolone in pediatric eyes. Journal of Cataract and Refractive Surgery, 2010. 36(9): p. 1494-1498.
76. Tan, D.T.H., et al., Randomized clinical trial of a new dexamethasone delivery system (surodex) for treatment of post-cataract surgery inflammation. Ophthalmology, 1999. 106(2): p. 223-231.
77. Tan, D.T.H., et al., Randomized clinical trial of surodex steroid drug delivery system for cataract surgery: Anterior versus posterior placement of two surodex in the eye. Ophthalmology, 2001. 108(12): p. 2172-2181.
78. Wadood, A.C., et al., Safety and efficacy of a dexamethasone anterior segment drug delivery system in patients after phacoemulsification. Journal of Cataract and Refractive Surgery, 2004. 30(4): p. 761-768.
79. Tetz, M.R., et al., Inhibition of posterior capsule opacification by an intraocular-lens-bound sustained drug delivery system: An experimental animal study and literature review. Journal of Cataract and Refractive Surgery, 1996. 22(8): p. 1070-1078.
80. Kleinmann, G., et al., Hydrophilic acrylic intraocular lens as a drug-delivery system for fourth-generation fluoroquinolones. Journal of Cataract and Refractive Surgery, 2006. 32(10): p. 1717-1721.
81. Kleinmann, G., et al., Hydrophilic acrylic intraocular lens as a drug-delivery system: Pilot study. Journal of Cataract and Refractive Surgery, 2006. 32(4): p. 652-654.
82. Kearns, V.R. and Williams, R.L., Drug delivery systems for the eye. Expert Review of Medical Devices, 2009. 6(3): p. 277-290.
83. Menzies, K.L. and Jones, L., The impact of contact angle on the biocompatibility of biomaterials. Optometry and Vision Science, 2010. 87(6): p. 387-399.
84. Yao, K., et al., Improvement of the surface biocompatibility of silicone intraocular lens by the plasma-induced tethering of phospholipid moieties. Journal of Biomedical Materials Research - Part A, 2006. 78(4): p. 684-692.
85. Schroeder, A., et al., Impact of fibronectin on surface properties of intraocular lenses. Graefe's Archive for Clinical and Experimental Ophthalmology, 2009. 247(9): p. 1277-1283.
86. Saika, S., et al., Collagenous deposits on explanted intraocular lenses. Journal of Cataract and Refractive Surgery, 1992. 18(21): p. 195 - 199.

87. Laurent, M., et al., Synthesis of types I, III and IV collagen by bovine lens epithelial cells in long-term culture. Experimental Cell Research, 1981. 134(1): p. 23-31.
88. Mullner-Eidenbock, A., et al., Cellular reaction on the anterior surface of 4 types of intraocular lenses. Joural of Cataract and Refractive Surgery, 2000. 27(5): p. 734 - 740.
89. Tognetto, D., et al., Biocompatibility of hydrophilic intraocular lenses. Joural of Cataract and Refractive Surgery, 2002. 29: p. 644 - 651.
90. Mahelkova, G., et al., Effect of culture substrate and culture conditions on lens epithelial cell proliferation and alpha-smooth muscle actin expression. Folia Biologica (Praha), 2009. 55(2): p. 66-76.
91. Nishi, O., et al., Inhibition of migrating lens epithelial cells at the capsular bend created by the rectangular optic edge of a posterior chamber intraocular lens. Ophthalmic Surgery Lasers and Imaging, 1998. 29: p. 587 - 594.
92. Oshika, T., et al., Adhesion of lens capsule to intraocular lenses of polymethylmethacrylate, silicone, and acrylic foldable materials: An experimental study. British Journal of Ophthalmology, 1998. 82: p. 549 - 553.
93. Nishi, O. and Nishi, K., Preventing posterior capsule opacification by creating a discontinuous sharp bend in the capsule. Journal of Cataract and Refractive Surgery, 1999. 25: p. 1-6.
94. Peng, Q., et al., Surgical prevention of posterior capsule opacification: Part 3: Intraocular lens optic barrier effect as a second line of defense. Journal of Cataract and Refractive Surgery, 2000. 26(2): p. 198-213.
95. Ayaki, M., et al., Lens epithelial cell migration between posterior capsule and intraocular lens with variously finished posterior optic edge and two haptic angulations. Ophthalmic Research, 2003. 35(5): p. 261-267.
96. Nishi, O., et al., Preventing lens epithelial cell migration using intraocular lenses with sharp rectangular edges. Joural of Cataract and Refractive Surgery, 2000. 26: p. 1543 - 1549.
97. Linnola, R.J., et al., Adhesion of fibronectin, vitronectin, laminin, and collagen type IV to intraocular lens materials in pseudophakic human autopsy eyes: Part 1: Histological sections. Journal of Cataract and Refractive Surgery, 2000. 26(12): p. 1792-1806.
98. Linnola, R.J., et al., Adhesion of fibronectin, vitronectin, laminin, and collagen type IV to intraocular lens materials in pseudophakic human autopsy eyes: Part 2: Explanted intraocular lenses. Journal of Cataract and Refractive Surgery, 2000. 26(12): p. 1807-1818.
99. Linnola, R.J., Sandwich theory: Bioactivity-based explanation for posterior capsule opacification. Journal of Cataract and Refractive Surgery, 1997. 23(10): p. 1539 - 1542.
100. Linnola, R.J. 'Sandwich' theory explains role of IOL design, bioactivity in PCO. 2001 June 15, 2002 [cited 2010 17/04.10]; Available from: http://www.osnsupersite.com/view.aspx?rid=13359.
101. Linnola, R.J., et al., Adhesion of soluble fibronectin, vitronectin, and collagen type IV to intraocular lens materials. Journal of Cataract and Refractive Surgery, 2003. 29(1): p. 146-152.
102. Saika, S., et al., Extracellular matrix on intraocular lenses. Experimental Eye Research, 1995. 61(6): p. 713-721.

103. Gauthier, L., et al., Neodymium:YAG laser rates after bilateral implantation of hydrophobic or hydrophilic multifocal intraocular lenses: Twenty-four month retrospective comparative study. Journal of Cataract and Refractive Surgery, 2010. 36(7): p. 1195-1200.
104. Fujimoto, K., et al., Four-year experience with a silicone refractive multifocal intraocular lens. Journal of Cataract and Refractive Surgery, 2010. 36(8): p. 1330-1335.
105. Lin, L., et al., Modification of hydrophobic acrylic intraocular lens with poly(ethylene glycol) by atmospheric pressure glow discharge: A facile approach. Applied Surface Science, 2010. 256(24): p. 7354-7364.
106. Gierek-Ciaciura, S., et al., A comparative clinical study of the visual results between three types of multifocal lenses. Graefe's Archive for Clinical and Experimental Ophthalmology, 2010. 248(1): p. 133-140.
107. Packer, M., Multifocal intraocular lens technology: Biomaterial, optical design and review of clinical outcomes. Expert Review of Ophthalmology, 2011. 6(4): p. 437-448.
108. Olson, R.J., et al., New intraocular lens technology. American Journal of Ophthalmology, 2005. 140(4): p. 709-716.
109. Rhodes, A., et al., Surface modification of biomaterials by covalent binding of poly(ethylene gycol) (PEG), in Surface Modifications of Biomaterials, R.L. Willaims, Editor. 2011, Woodhead Publishing Limited: Cambridge. p. 39-77.
110. Danion, A., et al., Fabrication and characterization of contact lenses bearing surface-immobilized layers of intact liposomes. Journal of Biomedical Materials Research - Part A, 2007. 82(1): p. 41-51.
111. Wang, P., et al., Surface modification of poly(tetrafluoroethylene) films via grafting of poly(ethylene glycol) for reduction in protein adsorption. Journal of Biomaterials Science, Polymer Edition, 2000. 11(2): p. 169-186.
112. Lee, J.H., et al., Plasma protein adsorption and platelet adhesion onto comb-like PEO gradient surfaces. Journal of Biomedical Materials Research, 1997. 34(1): p. 105-114.
113. Chen, Y., et al., Surface modification of polyaniline film by grafting of poly(ethylene glycol) for reduction in protein adsorption and platelet adhesion. Synthetic Metals, 2000. 110(1): p. 47-55.
114. Kim, M.K., et al., Effect of poly(ethylene glycol) graft polymerization of poly(methyl methacrylate) on cell adhesion: In vitro and in vivo study. Journal of Cataract and Refractive Surgery, 2001. 27(5): p. 766-774.
115. Patel, S., et al., Control of cell adhesion on poly(methyl methacrylate). Biomaterials, 2006. 27(14): p. 2890-2897.
116. Khan, F., et al., Versatile biocompatible polymer hydrogels: Scaffolds for cell growth. Angewandte Chemie - International Edition, 2009. 48(5): p. 978-982.
117. Kuo, Y.C. and Ku, I.N., Application of polyethyleneimine-modified scaffolds to the regeneration of cartilaginous tissue. Biotechnology Progress, 2009. 25(5): p. 1459-1467.
118. Lakard, S., et al., Adhesion and proliferation of cells on new polymers modified biomaterials. Bioelectrochemistry, 2004. 62(1): p. 19-27.
119. Vancha, A.R., et al., Use of polyethyleneimine polymer in cell culture as attachment factor and lipofection enhancer. BioMed Central Biotechnology, 2004. 4(23).

120. Wertz, C.F. and Santore, M.M., Effect of surface hydrophobicity on adsorption and relaxation kinetics of albumin and fibrinogen: Single-species and competitive behavior. Langmuir, 2001. 17(10): p. 3006-3016.
121. Sigal, G.B., et al., Effect of surface wettability on the adsorption of proteins and detergents. Journal of the American Chemical Society, 1998. 120(14): p. 3464-3473.
122. Lee, M.H., et al., The effect of non-specific interactions on cellular adhesion using model surfaces. Biomaterials, 2005. 26(14): p. 1721-1730.
123. Lee, J.H., et al., Cell behaviour on polymer surfaces with different functional groups. Biomaterials, 1994. 15(9): p. 705-711.
124. Kearns, V., et al., Plasma polymer coatings to aid retinal pigment epithelial growth for transplantation in the treatment of age related macular degeneration. Journal of Materials Science: Materials in Medicine, 2012. 23(8): p. 2013-2021.
125. Brooks, S.A., et al., Species-specific and unusual types of glycoprotein glycosylation, in Functional and Molecular Glycobiology, P. Dines, Editor. 2002, BIOS Scientific Publishers Limited: Oxford. p. 129-156.
126. Brooks, S.A., et al., Glycoconjugates of the extracellular matrix of animals, in Functional and Molecular Glycobiology, P. Dines, Editor. 2002, BIOS Scientific Publishers Limited: Oxford. p. 157-174.
127. Yannas, I.V., Natural materials, in Biomaterials Science: An Introduction to Materials in Medicine, B.D. Ratner, et al., Editors. 2004, Elsevier Academic Press: London. p. 127-136.
128. Comper, W.D. and Laurent, T.C., Physiological function of connective tissue polysaccharides. Physiological Reviews, 1978. 58(1): p. 255-315.
129. Furnus, C.C., et al., The hyaluronic acid receptor (CD44) is expressed in bovine oocytes and early stage embryos. Theriogenology, 2003. 60(9): p. 1633-1644.
130. Laurent, U.B.G., Hyaluronate in aqueous humour. Experimental Eye Research, 1981. 33(2): p. 147-155.
131. Price, R.D., et al., Hyaluronic acid: The scientific and clinical evidence. Journal of Plastic, Reconstructive & Aesthetic Surgery, 2007. 60(10): p. 1110-1119.
132. Stern, R., Hyaluronan catabolism: A new metabolic pathway. European Journal of Cell Biology, 2004. 83(7): p. 317-325.
133. Henry, C.B.S. and Duling, B.R., Permeation of the luminal capillary glycocalyx is determined by hyaluronan. American Journal of Physiology - Heart and Circulatory Physiology, 1999. 277(2 Pt-2): p. 508-514.
134. Engström-Laurent, A. Changes in hyaluronan concentration in tissues and body fluids in disease states. in Ciba Foundatioin Symposium 143: The Biology of Hyaluronan. 1988. London: John Wiley & Sons Ltd.
135. Winkler, J., et al., Quantitative distribution of glycosaminoglycans in young and senile (cataractous) anterior lens capsules. Experimental Eye Research, 2001. 72(3): p. 311-318.
136. Murugesan, S., et al., Immobilization of heparin: Approaches and applications. Current Topics In Medicinal Chemistry, 2008. 8(2): p. 80-100.
137. Heng, B.C., et al., Adhesion, proliferation, and gene expression profile of human umbilical vein endothelial cells cultured on bilayered polyelectrolyte coatings composed of glycosaminoglycans. Biointerphases, 2010. 5(3): p. 53-62.

138. Attia, J., et al., Evaluation of adhesion, proliferation, and functional differentiation of dermal fibroblasts on glycosaminoglycan-coated polysulfone membranes. Tissue Engineering Part A, 2008. 14(10): p. 1687-1697.
139. Uygun, B.E., et al., Effects of immobilized glycosaminoglycans on the proliferation and differentiation of mesenchymal stem cells. Tissue Engineering Part A, 2009. 15(11): p. 3499-3512.
140. Liu, J., et al., Induction of cataract-like changes in rat lens epithelial explants by transforming growth factor beta. Investigative Ophthalmology and Visual Science, 1994. 35(2): p. 388-401.
141. Hales, A.M., et al., Cataract induction in lenses cultured with transforming growth factor-β. Investigative Ophthalmology and Visual Science, 1995. 36(8): p. 1709-1713.
142. De Longh, R.U., et al., TGFβ receptor expression in lens: implications for differentiation and cataractogenesis. Experimental Eye Research, 2001. 72(6): p. 649-659.
143. Hao, J., et al., TGF-β3: A promising growth factor in engineered organogenesis. Expert Opinion on Biological Therapy, 2008. 8(10): p. 1485-1493.
144. Gordon-Thomson, C., et al., Differential cataractogenic potency of TGF-β1, -β2, and -β3 and their expression in the postnatal rat eye. Investigative Ophthalmology and Visual Science, 1998. 39(8): p. 1399-1409.
145. Lovicu, F.J., et al., TGFβ induces morphological and molecular changes similar to human anterior subcapsular cataract. British Journal of Ophthalmology, 2002. 86(2): p. 220-226.
146. Wormstone, I.M., Posterior capsule opacification: A cell biological perspective. Experimental Eye Research, 2002. 74(3): p. 337-347.
147. Wormstone, I.M., et al., Characterisation of TGF-β2 signalling and function in a human lens cell line. Experimental Eye Research, 2004. 78(3): p. 705-714.
148. Gato, A., et al., TGF-β3-induced chondroitin sulphate proteoglycan mediates palatal shelf adhesion. Developmental Biology, 2002. 250(2): p. 393-405.
149. Kaartinen, V., et al., Abnormal lung development and cleft palate in mice lacking TGF-β3 indicates defects of epithelial-mesenchymal interaction. Nature Genetics, 1995. 11(4): p. 415-421.
150. Proetzel, G., et al., Transforming growth factor-β3 is required for secondary palate fusion. Nature Genetics, 1995. 11(4): p. 409-414.
151. Martínez-Álvarez, C., et al., Medial edge epithelial cell fate during palatal fusion. Developmental Biology, 2000. 220(2): p. 343-357.
152. Brunet. C, et al., Inhibition of TGF-β3 (but not TGF-β1 or TGF-β2) activity prevents normal mouse embryonic palate fusion. International Journal of Developmental Biology, 1995. 39: p. 345-355.
153. Cowin, A.J., et al., Expression of TGF-β and its receptors in murine fetal and adult dermal wounds. European Journal of Dermatology, 2001. 11(5): p. 424-431.
154. Border, W.A. and Noble, N.A., Transforming growth factor-β in tissue fibrosis. New England Journal of Medicine, 1994. 331(19): p. 1286-1292.
155. Kim, A., et al., Growth factor regulation of corneal keratocyte differentiation and migration in compressed collagen matrices. Investigative Ophthalmology and Visual Science, 2010. 51(2): p. 864-875.

156. Shah, M., et al., Neutralisation of TGF-β1 and TGF-β2 or exogenous addition of TGF-β3 to cutaneous rat wounds reduces scarring. Journal of Cell Science, 1995. 108(3): p. 985-1002.
157. Occleston, N.L., et al., Prevention and reduction of scarring in the skin by Transforming Growth Factor beta 3 (TGF-β3): From laboratory discovery to clinical pharmaceutical. Journal of Biomaterials Science Polymer Edition, 2008. 19(8): p. 1047-1063.
158. Renovo Group plc. Justiva european phase 3 trail results. 2011 [cited 2011 01/06/2011]; Available from: http://www.renovo.com/en/news/juvista-eu-phase-3-trial-results.
159. BioInteractions Ltd. Astute™ advanced heparin coating technical. 2009 [cited 2010 30/04/2010]; Available from: http://www.biointeractions.com/pdfs/astute_technical.pdf.
160. Wang-Su, S.T., et al., Proteome analysis of lens epithelia, fibers, and the HLE B-3 cell line. Investigative Ophthalmology and Visual Science, 2003. 44(11): p. 4829-4836.
161. McAvoy, J.W., Cell division, cell elongation and distribution of α-, β- and γ-crystallins in the rat lens. Journal of Embryology and Experimental Morphology, 1978. 44: p. 149-165.
162. Reddan, J.R., et al., Retention of lens specificity in long-term cultures of diploid rabbit lens epithelial cells. Differentiation, 1986. 33(2): p. 168-174.
163. Andley, U.P., et al., Propagation and immortalization of human lens epithelial cells in culture. Investigative Ophthalmology and Visual Science, 1994. 35(7): p. 3094-3102.
164. Piatigorsky, J., Lens differentiation in vertebrates. Differentiation, 1981. 19(1-3): p. 134-153.
165. Vermorken, A.J.M. and Bloemendal, H., α-Crystallin polypeptides as markers of lens cell differentiation. Nature, 1978. 271(5647): p. 779-781.
166. Krausz, E., et al., Expression of crystallins, Pax6, Filensin, CP49, MIP, and MP20 in lens-derived cell lines. Investigative Ophthalmology and Visual Science, 1996. 37(10): p. 2120-2128.
167. Sax, C.M., et al., Analysis of α-crystallin expression in cultured mouse and rabbit lens cells. Experimental Eye Research, 1995. 61(1): p. 125-127.
168. Andley, U.P., et al., Enhanced prostaglandin synthesis after ultraviolet-B exposure modulates DNA synthesis of lens epithelial cells and lowers intraocular pressure in vivo. Investigative Ophthalmology and Visual Science, 1996. 37(1): p. 142-153.
169. Pu, F.R., et al., Effects of plasma treated PET and PTFE on expression of adhesion molecules by human endothelial cells in vitro. Biomaterials, 2002. 23(11): p. 2411-2428.
170. Arima, Y. and Iwata, H., Effect of wettability and surface functional groups on protein adsorption and cell adhesion using well-defined mixed self-assembled monolayers. Biomaterials, 2007. 28(20): p. 3074-3082.
171. D'Sa, R.A., et al., Protein adhesion and cell response on atmospheric pressure dielectric barrier discharge-modified polymer surfaces. Acta Biomaterialia, 2010. 6(7): p. 2609-2620.

172. Khatua, D., et al., Influence of charge densities of randomly sulfonated polystyrene surfaces on cell attachment and proliferation. Journal of Nanoscience and Nanotechnology, 2011. 11(5): p. 4227-4230.
173. Ratner, B.D., Correlation, surfaces and biomaterials science, in Biomaterials Science: An Introduction to Materials in Medicine, B.D. Ratner, et al., Editors. 2004, Elsevier Academic Press: London. p. 765-771.
174. D'Sa, R.A., et al., Lens epithelial cell response to atmospheric pressure plasma modified poly(methylmethacrylate) surfaces. Journal of Materials Science: Materials in Medicine, 2010. 21(5): p. 1703-1712.
175. Lundvall, A., et al., Effect of 3-piece AcrySof and downsized heparin-surface-modified poly(methyl methacrylate) intraocular lenses in infant rabbit eyes. Journal of Cataract and Refractive Surgery, 2003. 29(1): p. 159-163.
176. France, R.M., et al., Attachment of human keratinocytes to plasma co-polymers of acrylic acid/octa-1,7-diene and allyl amine/octa-1,7-diene. Journal of Materials Chemistry, 1998. 8(1): p. 37-42.
177. Jacchetti, E., et al., Biomimetic poly(amidoamine) hydrogels as synthetic materials for cell culture. Journal of Nanobiotechnology, 2008. 6(14): p. 14-28.
178. Orlidge, A. and D'Amore, P.A., Cell specific effects of glycosaminoglycans on the attachment and proliferation of vascular wall components. Microvascular Research, 1986. 31(1): p. 41-53.
179. BioInteractions Ltd. Astute™ advanced heparin coating overview. 2009 [cited 2010 30/04/2010]; Available from: http://www.biointeractions.com/pdfs/astute_overview.pdf.
180. Philippeos, C., et al., Introduction to cell culture, in Human Cell Culture Protocols, Methods in Moecular Biology, R.R. Mitry and R.D. Hughes, Editors. 2011, Springer Science and Business Media LLC. p. 1-13.
181. Tassin, J., et al., Human lens cells have an in vitro proliferative capacity inversely proportional to the donor age. Experimental Cell Research, 1979. 123(2): p. 388-392.
182. Moisseiev, J., et al., Long-term study of the prevalence of capsular opacification following extracapsular cataract extraction. Journal of Cataract and Refractive Surgery, 1989. 15(5): p. 531-533.
183. Stager, D.R.J., et al., Long-term rates of PCO following small incision foldable acrylic intraocular lens implantation in children. Journal of Pediatric Ophthalmology and Strabismus, 2002. 39(2): p. 73-76.
184. Grieshaber, M.C., et al., Posterior vertical capsulotomy with optic entrapment of the intraocular lens in congenital cataracts—prevention of capsule opacification. Journal of Cataract and Refractive Surgery, 2005. 31(5): p. 886-894.
185. Jung, J., et al., A cell-repellent sulfonated PEG comb-like polymer for highly resolved cell micropatterns. Journal of Biomaterials Science, Polymer Edition, 2008. 19(2): p. 161-173.
186. Sun, T.T., et al., Keratin cytoskeletons in epithelial cells of internal organs. Proceedings of the National Academy of Sciences of the United States of America, 1979. 76(6): p. 2813-2817.
187. Pitz, S. and Moll, R., Intermediate-filament expression in ocular tissue. Progress in Retinal and Eye Research, 2002. 21(2): p. 241-262.

188. Huang, X.-D., et al., Uveal and capsular biocompatibility of an intraocular lens with a hydrophilic anterior surface and a hydrophobic posterior surface. Journal of Cataract and Refractive Surgery, 2010. 36(2): p. 290-298.
189. Zhao, X. and Courtney, J.M., Surface modificaition of biomaterials by heperinisation to improve blood compatibility, in Surface Modifications of Biomaterials, R.L. Willaims, Editor. 2011, Woodhead Publishing Limited: Cambridge. p. 56-77.
190. Sefton, M.V. and Gemmell, C.H., Nonthrombogenic treatments and strategies, in Biomaterials Science: An Introduction to Materials in Medicine, B.D. Ratner, et al., Editors. 2004, Elsevier Academic Press: London. p. 456-469.
191. Hildebrandt, P., Glycosaminoglycans-all round talents in coating technology. Biomedizinische Technik, 2002. 47 Suppl 1 Pt 1: p. 476-478.
192. Marson, A., et al., Development of a microtiter plate-based glycosaminoglycan array for the investigation of glycosaminoglycan-protein interactions. Glycobiology, 2009. 19(12): p. 1537-1546.
193. Dalby, M.J., et al., In vitro reaction of endothelial cells to polymer demixed nanotopography. Biomaterials, 2002. 23(14): p. 2945-2954.
194. Dalby, M.J., et al., Nonadhesive nanotopography: Fibroblast response to poly(n-butyl methacrylate)-poly(styrene) demixed surface features. Journal of Biomedical Materials Research - Part A, 2003. 67(3): p. 1025-1032.
195. Kearns, V., et al., Biomaterials surface topography to cellular response: Technologies, cell techniques and biomedical applications, in Surface Modifications of Biomaterials, R.L. Willaims, Editor. 2011, Woodhead Publishing Limited: Cambridge. p. 169-204.
196. D'Ilario, L., et al., Insight into the heparin-toluidine blue (C.I. basic blue 17) interaction. Dyes and Pigments, 2008. 80(3): p. 343-348.
197. Meakin, S.O., et al., A rabbit lens epithelial cell line supports expression of an exogenous crystallin gene characteristic of lens fiber cell differentiation. Experimental Eye Research, 1989. 48(1): p. 131-137.
198. Fleming, T.P., et al., Expression of growth control and differentiation genes in human lens epithelial cells with extended life span. Investigative Ophthalmology and Visual Science, 1998. 39(8): p. 1387-1398.
199. Zhang, J., et al., Chemical modification of cellulose membranes with sulfo ammonium zwitterionic vinyl monomer to improve hemocompatibility. Colloids and Surfaces B: Biointerfaces, 2003. 30(3): p. 249-257.
200. Zhang, Z., et al., Zwitterionic hydrogels: An in vivo implantation study. Journal of Biomaterials Science, Polymer Edition, 2009. 20(13): p. 1845-1859.
201. Ueda, T., et al., Perparation of 2-methacryloyloxyethyl phosphorylcholine copolymers with alkyl methacrylates and their blood compatibility. Polymer Journal (Maruzen), 1992. 24(11): p. 1259-1269.
202. Xu, J., et al., Ozone-induced grafting phosphorylcholine polymer onto silicone film grafting 2-methacryloyloxyethyl phosphorylcholine onto silicone film to improve hemocompatibility. Colloids and Surfaces B: Biointerfaces, 2003. 30(3): p. 215-223.
203. Li, L. and Xin, Z., Surface-hydrophilic and protein-resistant tris(trimethylsiloxy)-3-methacryloxypropylsilane-containing polymer by the introduction of phosphorylcholine groups. Colloids and Surfaces A: Physicochemical and Engineering Aspects, 2011. 384(1–3): p. 713-719.

204. Okajima, Y., et al., Effect of surface coating an acrylic intraocular lens with poly(2-methacryloyloxyethyl phosphorylcholine) polymer on lens epithelial cell line behavior. Journal of Cataract and Refractive Surgery, 2006. 32(4): p. 666-671.
205. Zhang, S.F., et al., Physical and biological properties of compound membranes incorporating a copolymer with a phosphorylcholine head group. Biomaterials, 1998. 19(7-9): p. 691-700.
206. British Standards Institution, ISO 10993-5 Biological evaluation of medical devices, in Tests for in vitro cytotoxicity. 2009, British Standards Institution. p. 46.
207. O'Kane, S. and Ferguson, M.W.J., Transforming growth factor βs and wound healing. International Journal of Biochemistry and Cell Biology, 1997. 29(1): p. 63-78.
208. Matsushima, H., et al., Analysis of cytoskeletal proteins in posterior capsule opacification after implantation of acrylic and hydrogel intraocular lenses. Journal of Cataract and Refractive Surgery, 2004. 30(1): p. 187-194.
209. Colitz, C.M.H., et al., Histologic and immunohistochemical characterization of lens capsular plaques in dogs with cataracts. American Journal of Veterinary Research, 2000. 61(2): p. 139-143.
210. Saika, S., et al., Osteopontin: A component of matrix in capsular opacification and subcapsular cataract. Investigative Ophthalmology and Visual Science, 2003. 44(4): p. 1622-1628.
211. Srinivasan, Y., et al., Lens-specific expression of transforming growth factor β1 in transgenic mice causes anterior subcapsular cataracts. Journal of Clinical Investigation, 1998. 101(3): p. 625–634.
212. Saika, S., et al., Loss of osteopontin perturbs the epithelial-mesenchymal transition in an injured mouse lens epithelium. Laboratory Investigation, 2007. 87(2): p. 130-138.
213. Yadav, U.C.S., et al., Prevention of posterior capsular opacification through aldose reductase inhibition. Investigative Ophthalmology and Visual Science, 2009. 50(2): p. 752-759.
214. Gerardi, J.G., et al., Immunohistochemical analysis of lens epithelial-derived membranes following cataract extraction in the dog. Veterinary Ophthalmology, 1999. 2: p. 163 - 168.
215. Wormstone, I.M., et al., Human lens epithelial cell proliferation in a protein-free medium. Investigative Ophthalmology and Visual Science, 1997. 38(2): p. 396-404.
216. Marcantonio, J.M. and Reddan, J.R., TGFβ2 influences α5-β1 integrin distribution in human lens cells. Experimental Eye Research, 2004. 79(3): p. 437-442.
217. Saika, S., et al., Response of lens epithelial cells to injury: Role of lumican in epithelial-mesenchymal transition. Investigative Ophthalmology and Visual Science, 2003. 44(5): p. 2094-2102.
218. Jampel, H.D., et al., Transforming growth factor-beta in human aqueous humor. Current Eye Research, 1990. 9(10): p. 963-969.
219. Wallentin, N., et al., Effect of cataract surgery on aqueous TGF-β and lens epithelial cell proliferation. Investigative Ophthalmology and Visual Science, 1998. 39(8): p. 1410-1418.

220. Tripathi, R.C., et al., Aqueous humor in glaucomatous eyes contains an increased level of TGF-β2. Experimental Eye Research, 1994. 59(6): p. 723-728.
221. Mach, W.J., et al., Flow cytometry and laser scanning cytometry, a comparison of techniques. Journal of Clinical Monitoring and Computing, 2010. 24(4): p. 251-259.
222. Bissell, D.M., Chronic liver injury, TGF-β, and cancer. Experimental and Molecular Medicine, 2001. 33(4): p. 179-190.
223. Esparza, J., et al., Fibronectin upregulates gelatinase B (MMP-9) and induces coordinated expression of Gelatinase A (MMP-2) and its activator MT1-MMP (MMP-14) by human T lymphocyte cell lines. A process repressed through RAS/MAP kinase signaling pathways. Blood, 1999. 94(8): p. 2754-2766.
224. Hodgkinson, L.M., et al., MMP and TIMP expression in quiescent, dividing, and differentiating human lens cells. Investigative Ophthalmology and Visual Science, 2007. 48(9): p. 4192-4199.
225. Eldred, J.A., et al., MMP2 activity is critical for TGFβ2-induced matrix contraction—Implications for fibrosis. Investigative Ophthalmology and Visual Science, 2012. 53(7): p. 4085-4098.
226. Richiert, D.M. and Ireland, M.E., Matrix metalloproteinase secretion is stimulated by TGF-β in cultured lens epithelial cells. Current Eye Research, 1999. 19(3): p. 269-275.
227. Saika, S., et al., Immunolocalization of prolyl 4-hydroxylase subunits, α-smooth muscle actin, and extracellular matrix components in human lens capsules with lens implants. Experimental Eye Research, 1998. 66(3): p. 283-294.
228. Saika, S., et al., Immunohistochemical identification of proteoglycan types in fibrotic human capsules with intraocular lens implants. Japanese Journal of Ophthalmology, 1998. 42(5): p. 368-372.
229. Dawes, L.J., et al., A fully human in vitro capsular bag model to permit intraocular lens evaluation. Investigative Ophthalmology and Visual Science, 2012. 53(1): p. 23-29.